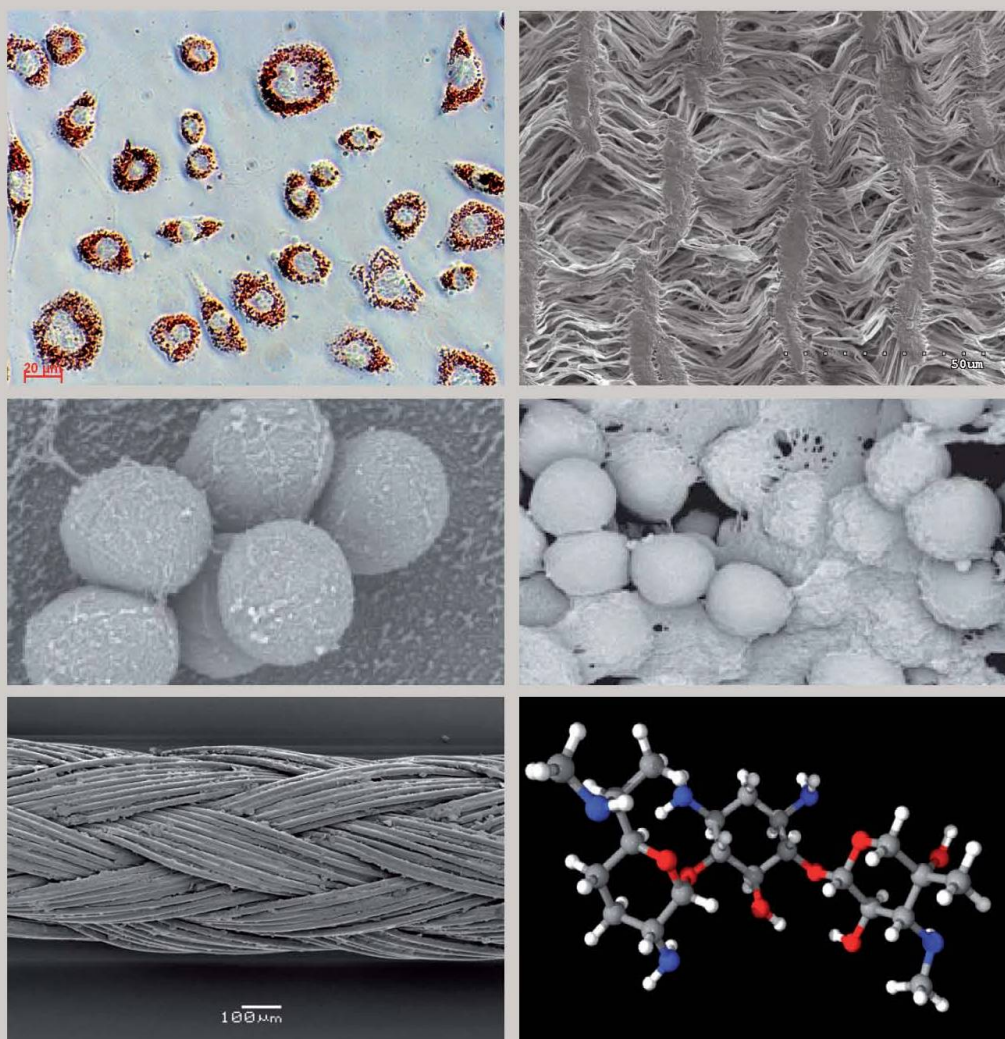


Infected Biomaterials

New Strategies For Local Anti-Infective Treatment



Dissertation
zur Erlangung des Doktorgrades der Fakultät für
Chemie und Pharmazie der Ludwig-Maximilians-Universität
München

Infected Biomaterials
New Strategies For Local Anti-Infective Treatment

Florian Matl

aus München

2008

Bibliografische Information der Deutschen Nationalbibliothek

Die Deutsche Nationalbibliothek verzeichnet diese Publikation in der Deutschen Nationalbibliografie; detaillierte bibliografische Daten sind im Internet über <http://dnb.ddb.de> abrufbar.

1. Aufl. - Göttingen : Cuvillier, 2009

Zugl.: München, Univ., Diss., 2008

978-3-86727-871-3

Erklärung

Diese Dissertation wurde im Sinne von § 13 Abs. 4 der Promotionsordnung vom 29. Januar 1998 von Herrn Prof. Dr. Dr. Axel Stemberger vom Institut für Experimentelle Onkologie betreut und von Herrn Prof. Dr. Wolfgang Frieß von der Fakultät für Chemie und Pharmazie vertreten.

Ehrenwörtliche Versicherung

Diese Dissertation wurde selbständig, ohne unerlaubte Hilfe erarbeitet.

München, am 25.07.08

Dissertation eingereicht am 25.07.08

1. Gutachter: Prof. Dr. Dr. A. Stemberger

2. Gutachter: Prof. Dr. W. Frieß

Mündliche Prüfung am: 29.09.08

© CUVILLIER VERLAG, Göttingen 2009

Nonnenstieg 8, 37075 Göttingen

Telefon: 0551-54724-0

Telefax: 0551-54724-21

www.cuvillier.de

Alle Rechte vorbehalten. Ohne ausdrückliche Genehmigung des Verlages ist es nicht gestattet, das Buch oder Teile daraus auf fotomechanischem Weg (Fotokopie, Mikrokopie) zu vervielfältigen.

1. Auflage, 2009

Gedruckt auf säurefreiem Papier

978-3-86727-871-3

Acknowledgements

The presented thesis was written at the Institute of Medical Engineering at the Technical University of Munich and at the Department of Pharmacy, Pharmaceutical Technology and Biopharmaceutics at the Ludwig-Maximilians-University in Munich under supervision of Prof. Dr. Dr. Axel Stemberger and Prof. Dr. Wolfgang Friess.

First of all I want to express my gratefulness to Prof. Dr. Dr. Axel W. Stemberger for the possibility to be part of his research group and especially for his scientific guidance, professional input and fruitful discussions throughout my work. I very much appreciate that he offered me the opportunity to stay in Texas for a scientific project for three months and to take part in many conferences throughout Europe. Thank you for the fantastic working climate that made it a pleasure to be part of your group.

My special thanks go to Prof. Dr. Wolfgang Friess, who guided me through the pharmaceutical part of my work with great engagement and supported me whenever questions came up. Thank you for giving me the possibility to be part of your group and to write my thesis at the Pharmaceutical Department at the Ludwig-Maximilians University Munich. It has been a pleasure to work with you.

I want to thank Prof. Dr. Gross from the University of North Texas, USA for the outstanding time in Denton, the tremendous support he gave me personally as well as professionally. It was a great time for me – thank you very much.

Many thanks to Prof. Dr. Gerhard Winter for his enthusiastic and dedicated leadership of the chair of Pharmaceutical Technology and Biopharmaceutics.

Special thanks go to my colleague Dipl.-Ing. Andreas Obermeier who shared most of the time here at the IMETUM with me. Without his active support in setting up the experimental constructions as well as organizing and planning things, this work would not have been possible. Thanks for our fruitful and personal discussions and the fantastic working climate.

Many thanks to Katharina Seiffe, Julia Zlotnyk, Simone Repmann and Teissa Köhler who did a great job during their student time in our working group. It was a pleasure to work with you.

Special thanks to Tobias Pirzer for his parents and great support in all questions concerning computer programs used for this thesis.

Thanks to Tiffany Kinney for reviewing parts of my thesis and Jochen Mayer for his cooperation in the neuroscience project.

Thanks to Prof. Dr. Frank Böckler, Dr. Olga Mykhaylyk and Chemicell in Berlin for their advice and contributions to the magnetic drug targeting project.

The microbiological investigations would not have been possible without the tremendous help of Ms V. Vatou, Institute for Medical Microbiology at the Klinikum rechts der Isar, Technical University, Munich – many thanks to you.

Many thanks go to Dipl. Phys. W. Kraus and Dipl.-Ing. H. Stephan for their engagement, and the entire staff of the Neue Magnetodyn GmbH for their professional support and for providing the equipment.

Special thanks to the entire staff of the Pharmaceutical Technology and Biopharmaceutics as well as my colleagues at the IMETUM especially Susanne Schnell-Witteczek and Ursula Hopfner for their professional support and the others for all the enjoyable dinners and night sessions we had. We had a wonderful time together.

Furthermore I would like to thank the ITEM GmbH for the providing of laboratory space for carrying out the series of bacteriological experiments and, in particular, Mr J. Hintermeier for his very kind support.

My aunt Dr. Ingrid Hofmann and my uncle Dr. Hans Hofmann for their support at the beginning of this thesis. Thank you very much.

My parents, my sister Saskia and my brother Mark and Corinna, I want to thank you all for the support and the encouragement you gave me in all the years.

For mom and dad

List of Abbreviations

a.c.	Alternating current
AHL	Acylated Homoserine Lactone
ATCC [®]	American Type Culture Collection
cfu	Colony-forming units
CP	Chlorhexidine dipalmitate
CL	Chlorhexidine dilaurate
d.c.	Direct current
DG	Diglyceride
EF	Electric field
EMF	Electro-magnetic field
EMF+ ind. EF	Electro-magnetic field with additional a.c. electrical field
ePTFE	Expanded PTFE
ICR	Ion-Cyclotron-Resonance
MIC	Minimal inhibitory concentration
MRSA	Methicillin-resistant <i>Staphylococcus aureus</i>
OH	Octenidine hydrochloride
PDLLA	Poly(D,L)lactide
PET	Polyethyleneterephthalate
PTFE	Polytetrafluoroethylene
RIP	RNA III Inhibiting Peptide
TA	Tocopherole acetate
TG	Triglyceride
TRAP	Target of RNA III-Activating Peptide
USPIO	Ultra-small superparamagnetic iron oxide

Table of Contents

Chapter 1

Introduction and Objectives of the Thesis

1	INTRODUCTION	2
2	BIOMATERIALS	3
2.1	VASCULAR GRAFTS	3
2.2	SUTURES	6
3	INFECTIONS.....	7
3.1	POST-OPERATIVE INFECTIONS	8
3.2	POST-OPERATIVE INFECTIONS IN VASCULAR SURGERY.....	8
3.2.1	<i>Pathogenesis of post-operative infections after vascular reconstructive interventions.....</i>	<i>9</i>
3.2.2	<i>Time point of vascular graft infections</i>	<i>10</i>
3.2.3	<i>Localisation of vascular graft infections</i>	<i>10</i>
3.2.4	<i>Infection risk of different grafts</i>	<i>11</i>
3.2.5	<i>Diagnosis of infectious complications after vascular reconstructive interventions.....</i>	<i>11</i>
3.2.6	<i>Bacteriology of septic complications in vascular grafts.....</i>	<i>12</i>
3.2.7	<i>Sutures in infected areas.....</i>	<i>12</i>
3.3	NEURONAL INFECTIONS	13
3.4	MEDICAL DEVICE INFECTIONS.....	13
3.5	BIOFILMS	14
3.5.1	<i>Bacterial adhesion to surfaces.....</i>	<i>14</i>
3.5.2	<i>Biofilm formation.....</i>	<i>15</i>
3.5.3	<i>Strategies of biofilm prevention.....</i>	<i>16</i>
3.6	THERAPEUTIC METHODS	17
3.6.1	<i>New tactics in surgery and local wound management.....</i>	<i>17</i>
3.6.2	<i>Antiseptics in wound care.....</i>	<i>18</i>
3.6.3	<i>Antibiotics in wound care.....</i>	<i>18</i>
3.6.4	<i>Prosthesis explantation.....</i>	<i>19</i>
3.7	IMPLANTS AS DRUG DELIVERY SYSTEMS	19
3.8	BIOCOMPATIBILITY	20
3.9	HAEMOCOMPATIBILITY	20
3.10	NEW APPROACHES FOR PROTECTION OF BIOMATERIAL INFECTIONS	21
3.10.1	<i>Electro-magnetic field influence</i>	<i>21</i>
3.10.2	<i>Antimicrobial coatings.....</i>	<i>23</i>
3.10.3	<i>Magnetic drug targeting systems</i>	<i>23</i>
3.10.4	<i>Neuronal networks.....</i>	<i>24</i>
4	CONCLUSIONS	27
5	OBJECTIVES OF THE THESIS.....	28
6	FIGURE CAPTIONS	30
7	REFERENCES.....	31

Chapter 2

New anti-infective coatings of medical implants based on lipid-like drug carriers

1	INTRODUCTION	38
2	MATERIALS AND METHODS	39
2.1	MEDICAL IMPLANT	39
2.2	THE ANTI-INFECTIVE COATING.....	39
2.2.1	<i>Drug carriers</i>	<i>39</i>
2.2.2	<i>PDLLA</i>	<i>39</i>
2.2.3	<i>Softisan® 649.....</i>	<i>39</i>
2.2.4	<i>Dynasan® 118.....</i>	<i>40</i>
2.2.5	<i>Tocopherol acetate.....</i>	<i>40</i>
2.2.6	<i>Antibiotics</i>	<i>40</i>
2.3	COATING PROCESS	40
2.4	PARTICLE SIZE	41
2.5	MORPHOLOGICAL ANALYSIS-SEM	41
2.6	ANTIBIOTIC RELEASE	41
2.7	TEST BACTERIUM.....	42
2.7.1	<i>Growth curve.....</i>	<i>42</i>
2.7.2	<i>Antibacterial characteristics</i>	<i>42</i>
2.7.3	<i>Adhesion of viable bacteria and antimicrobial potency after 24 hours elution</i>	<i>43</i>
2.8	CELL CULTURE	43
2.9	IN VITRO CYTOTOXICITY STUDIES	43
2.10	HAEMOCOMPATIBILITY STUDIES.....	44
3	RESULTS.....	45
3.1	MORPHOLOGICAL ANALYSIS.....	45
3.2	ANTIBIOTIC RELEASE	45
3.3	ANTIBACTERIAL CHARACTERISTICS.....	47
3.3.1	<i>Adhesion of viable bacteria and antimicrobial potency after 24 hours elution</i>	<i>48</i>
3.4	IN VITRO CYTOTOXICITY STUDIES	49
3.5	HAEMOCOMPATIBILITY STUDIES.....	50
3.5.1	<i>Monoclonal enzyme immunoassay for plasma F_{1+2} values.....</i>	<i>50</i>
3.6	AMIDOLYTIC SUBSTRATE ASSAY FOR FACTOR XIIIA-LIKE ACTIVITY	50
3.6.1	<i>Thromboelastography</i>	<i>50</i>
3.6.2	<i>Complement C3a-desArg ELISA.....</i>	<i>51</i>
4	DISCUSSION.....	51
5	CONCLUSIONS.....	53
6	ACKNOWLEDGEMENTS	53
7	FIGURE AND TABLE CAPTIONS.....	54
8	REFERENCES	55

Chapter 3

New anti-infective coatings of surgical sutures based on a combination of antiseptics and fatty acids

1	INTRODUCTION	58
2	MATERIALS AND METHODS	58
2.1	MEDICAL IMPLANT	58
2.2	THE ANTI-INFECTIVE COATING.....	59
2.3	MORPHOLOGICAL ANALYSIS-SEM	59
2.4	DRUG RELEASE	59
2.5	TEST BACTERIUM.....	60
2.5.1	<i>Antibacterial characteristics</i>	<i>60</i>
2.5.2	<i>Adhesion of viable bacteria and antimicrobial potency after 24 hours elution</i>	<i>60</i>
2.6	CELL CULTURE	61
2.7	IN VITRO CYTOTOXICITY STUDIES	61
3	RESULTS.....	62
3.1	MORPHOLOGICAL ANALYSIS.....	62
3.2	DRUG RELEASE	62
3.3	ANTIBACTERIAL CHARACTERISTICS.....	64
3.4	ADHESION OF VIABLE BACTERIA AND ANTIMICROBIAL POTENCY AFTER 24 HOURS ELUTION.....	65
3.5	IN VITRO CYTOTOXICITY STUDIES	66
4	DISCUSSION.....	67
5	CONCLUSIONS.....	69
6	ACKNOWLEDGEMENTS	69
7	FIGURE CAPTIONS.....	70
8	REFERENCES	71

Chapter 4

Growth inhibition of *Staphylococcus aureus* induced by low-frequency electric and electro-magnetic fields

1	INTRODUCTION	74
2	MATERIALS AND METHODS	75
2.1	TEST BACTERIUM.....	75
2.2	GROWTH CURVE	75
2.3	BACTERIA ON GEL-LIKE MEDIUM	76
2.4	BACTERIA IN FLUID MEDIUM.....	77
2.5	SINUSOIDAL LOW-FREQUENCY ELECTRO-MAGNETIC FIELD.....	78
2.6	ELECTROMAGNETIC FIELD COMBINED WITH AN ADDITIONAL ELECTRIC ALTERNATING FIELD	79
2.7	SINUSOIDAL ELECTRIC ALTERNATING FIELD	81
2.8	DIRECT CURRENT ELECTRIC FIELD	81
2.9	CALCULATIONS AND STATISTICAL METHODS.....	82
3	RESULTS.....	83
4	DISCUSSION.....	85
5	CONCLUSIONS.....	89
6	ACKNOWLEDGEMENTS	89
7	FIGURE AND TABLE CAPTIONS	90
8	REFERENCES	91

Chapter 5

Augmentation of antibiotic efficacy by low-frequency electric and electro-magnetic fields examining *Staphylococcus aureus*

1	INTRODUCTION	95
2	MATERIALS AND METHODS	95
2.1	TEST BACTERIUM.....	95
2.2	GROWTH CURVE	95
2.3	ANTIBIOTIC.....	96
2.4	GENTAMICIN TEST CONCENTRATION.....	96
2.5	BACTERIA ON GEL-LIKE MEDIUM	97
2.6	BACTERIA IN FLUID MEDIUM.....	97
2.7	SINUSOIDAL LOW-FREQUENCY ELECTRO-MAGNETIC FIELD.....	98
2.8	ELECTRO-MAGNETIC FIELD COMBINED WITH AN ADDITIONAL ELECTRIC ALTERNATING FIELD	101
2.9	SINUSOIDAL ELECTRIC ALTERNATING FIELD	101
2.10	DIRECT CURRENT FIELD	102
2.11	CALCULATIONS AND STATISTICAL METHODS.....	103
3	RESULTS.....	103
3.1	BACTERIA ON GEL-LIKE MEDIUM	103
3.2	BACTERIA IN FLUID MEDIUM.....	104
3.2.1	<i>Gentamicin test concentration.....</i>	<i>104</i>
3.2.2	<i>Low - frequent electromagnetic field.....</i>	<i>104</i>
3.2.3	<i>Electro-magnetic field combined with an additional electric field.....</i>	<i>107</i>
3.2.4	<i>Sinusoidal alternating electric field</i>	<i>107</i>
3.2.5	<i>Direct current field.....</i>	<i>107</i>
4	DISCUSSION.....	107
5	CONCLUSIONS.....	110
6	ACKNOWLEDGEMENTS	110
7	FIGURE AND TABLE CAPTIONS	111
8	REFERENCES	113

Chapter 6

Magnetic drug targeting for biomaterial infections

CHAPTER 6.....	115
1 INTRODUCTION.....	116
2 MATERIALS AND METHODS.....	117
2.1 NANOPARTICLES.....	117
2.2 PARTICLE SIZE AND ZETA POTENTIAL	118
2.3 DRUG LOADING.....	118
2.4 COATING TECHNOLOGY.....	119
2.5 ANTIBACTERIAL CHARACTERISTICS.....	120
2.5.1 <i>Test bacterium</i>	120
2.5.2 <i>Calibration curve</i>	120
2.5.3 <i>Antimicrobial potential</i>	120
2.5.4 <i>Pathologically relevant bacterial concentrations</i>	121
2.5.5 <i>Gentamicin efficacy</i>	121
2.6 GENTAMICIN RELEASE FROM NANOPARTICLES	121
2.7 IN VITRO CYTOTOXICITY STUDIES	122
2.7.1 <i>Cell culture</i>	122
2.7.2 <i>Ferrofluid toxicity</i>	122
2.7.3 <i>Gentamicin toxicity</i>	122
2.8 CIRCULATORY EXPERIMENTS.....	123
2.9 IRON CONTENT DETERMINATION.....	124
3 RESULTS.....	125
3.1 LOADING OF MAGNETIC NANOPARTICLES WITH GENTAMICIN	125
3.2 ANTIBACTERIAL CHARACTERISTICS.....	126
3.3 PERCENT SURFACE COVERAGE.....	128
3.4 IN VITRO CYTOTOXICITY STUDIES	128
3.5 CIRCULATORY EXPERIMENTS.....	130
4 DISCUSSION.....	132
5 CONCLUSIONS.....	135
6 ACKNOWLEDGEMENTS.....	135
7 FIGURE AND TABLE CAPTIONS.....	136
8 REFERENCES	137

Chapter 7

Functional neurotoxicity of individual antibiotics investigated with mammalian neuronal networks grown on microelectrode neuroarray

1	INTRODUCTION.....	141
2	MATERIALS AND METHODS	142
2.1	COMPOUNDS	142
2.2	MICROELECTRODE ARRAYS (MEAs).....	142
2.3	CELL CULTURE	143
2.4	EXPERIMENTAL SETUP	146
2.4.1	Recording station.....	146
2.4.2	Chamber Setup	146
2.4.3	Data recording	148
2.4.4	Data analysis	149
2.4.5	Dose Response curves	150
2.5	EXPERIMENTAL DESIGN	150
3	RESULTS	151
3.1	SUPPRESSION OF ACTION POTENTIAL PRODUCTION	151
3.1.1	Dose-response curves	151
3.1.2	IC ₅₀ Determination	152
3.2	BURST PARAMETER.....	156
3.3	DROP OUT OF INDIVIDUAL CELLS	158
3.3.1	Bursting neurons.....	158
3.3.2	Active neurons	158
3.3.3	Active neurons versus bursting neurons.....	159
4	DISCUSSION	160
5	CONCLUSIONS	161
6	ACKNOWLEDGEMENTS	162
7	APPENDIX.....	163
7.1	ACTIVITY PATTERN OF ANTIBIOTICS	163
7.1.1	Penicillin G.....	163
7.1.2	Penicillin G/Streptomycin.....	165
7.1.3	Streptomycin	166
7.1.4	Gentamicin.....	168
7.1.5	Vancomycin	169
8	FIGURE AND TABLE CAPTIONS	171
9	REFERENCES.....	174

Chapter 8

SUMMARY OF THE THESIS	175
------------------------------------	------------

Chapter 1

Introduction and Objectives of the Thesis

Abstract

In the general introduction the classification for medical applied biomaterials with the focus on vascular grafts and surgical sutures is discussed. The complex process of infection in particular post-operative infections, neuronal infections and medical device-associated infections are highlighted. Biofilm formation on the surface of biomaterials and the associated increase of antibiotic and host immune resistance is a challenge for patients and physicians. Graft explantation and the pre-, peri and postoperative administration of antibiotics and antiseptics is the common procedure for implant infection therapy. The utilization of devices as drug delivery systems is described. Furthermore biocompatible and haemocompatible requirements for devices are specified. Various new approaches for the prevention and on demand therapy of implant infections are presented in Chapter 1.

Keywords: Biomaterials, vascular grafts, surgical sutures, biofilm, infection

1 Introduction

In 1986 the European Society for Biomaterials, realizing that terms in this very interdisciplinary field of science are often being confused, organized a congress with the aim of harmonizing the terminology of “Definitions in Biomaterials”. According to these definitions, a **prosthesis** is a device that “replaces, in part or in whole, the function of one of the organs of the body”. An **implant** is named as “any medical device made from one or more materials that is intentionally placed within the body, either totally or partially buried beneath an epithelial surface”. A **biomaterial** is defined as a “non-viable material, used in a medical device, intended to interact with biological systems” (107).

Biomaterials have accompanied human life since early civilizations. While the Mayan people used nacre teeth from sea shells in 600 A.D. (76), an iron dental implant four hundred years later was found in a corpse dated 200 A.D. in Europe (22). Particular sutures were manufactured and applied for thousands of years (1).

A reasonable chronological classification of modern biomaterials is the allocation into first-generation, second-generation and third-generation biomaterials. The declared goal of all developed biomaterials of the first-generation during the 1960s and 1970s was to “achieve a suitable combination of physical properties to match those of the replaced tissue with a minimal toxic response in the host” (47). The requirements for the second-generation during the 1980s and 1990s shifted from a bioinert tissue response to “instead producing bioactive components that could elicit a controlled action and reaction in the physiological environment” (49). This new mindset to utilize the biomaterial rather than to hide it, opened up new vistas in the interaction of foreign material with the biological system of the host. The compositions of a great variety of bioactive glasses, ceramics or glass ceramics reached clinical use in the mid-1980s in orthopaedic and dental applications. Bioactive glasses (composed of Na_2O - CaO - P_2O_5 - SiO_2) for instance were demonstrated to cause a sequence of 11 reaction steps in the creation of a strong bond between tissue and biomaterial surface finally resulting in a formation of new bone (46). The development of resorbable biomaterials with a defined chemical breakdown and resorption marked another progress in this second-generation of biomaterials. This innovation solves the interface problem, as the regenerating tissue replaces the foreign material and provides a basis for the application of controlled-release drug delivery systems. Biodegradable sutures consisting of a composition of polylactide and polyglycolic acid as well as resorbable screws or fracture plates became an important pillar in wound management and orthopaedic treatment (43).

However the irrevocable success of first and second generation biomaterials cannot hide the fact that the clinical application of bioinert, bioactive and resorbable biomaterials is connected with many problems. The endurance for instance of skeletal prostheses and artificial heart valves is limited to 10 to 25 years (50, 89, 109) and already small improvements of failure rates require an enormous financial and experimental effort (50). This limitation, based on the fact that synthetic materials, in contrast to living tissues, can never respond to changing physiological loads or biochemical stimuli, has directed the focus of interest toward a more biological solution for a new generation of biomaterials.

The declared aim of third-generation biomaterials is the stimulation of specific cellular responses at the molecular level. The originally separately considered approaches of bioactive materials and resorbable materials have been combined and transferred to the cellular level. The inducement of cell proliferation, differentiation or gene activation in order to stimulate tissue regeneration is the target of third-generation resorbable materials such as polymers, alloys or bioactive glasses (48). Thereby two concepts are tracked, the *tissue engineering* and *in situ tissue regeneration*. For *tissue engineering*, biomaterial surfaces are modified outside the body with cellular networks imitating naturally occurring tissue and implanted into the patient. The scaffolds are resorbed and replaced by a fully functionalized host tissue.

For *in situ tissue regeneration*, biomaterials are thought to release biological active drugs like for example growth factors to stimulate tissue regeneration inside the body.

However coming along with innovations and new ideas in the field of biomaterials, it is obvious that only an effective cooperation between the different disciplines of science and a yielding dialogue between physicians, engineers and natural scientists will not only result in fruitful concepts but also in realizable products for future implants and will help patients to regain a better quality of life.

2 Biomaterials

2.1 Vascular grafts

Biomaterials applied in the cardiovascular system, the so-called cardiovascular medical devices, play a key role in the life-saving treatment of patients. Particularly the enhancement of survival, besides an improvement of quality of life, makes them unique among all other medical devices. Cardiovascular medical devices include a broad spectrum of devices from heart valves,

pacemakers, implantable cardioverter-defibrillators, cardiac assist and replacement devices to the area of stents and vascular grafts.

Reconstructive vascular surgery dates back to the nineteenth century when the first animal experiments were carried out testing different sewing techniques and vascular replacements using aluminium, silver, glass or Lucite[®] tubes (9, 62). These experiments paved the way for the first surgical intervention in a human being in 1897 by the american surgeon John B. Murphy who redissected a traumatized femoralis segment and reconstructed the vessel via a special sewing technique (9).

In contemporary vascular surgery, the application of autogenous, allogeneous, xenogeneous or alloplastic vascular replacements is standard practice. The accidental observation of a pseudointima formation around a silk suture gave the impulse to develop vascular grafts out of alloplastic material (104). The requirement of biological indifference and porosity led to the invention of a pool of different biocompatible alloplastic grafts consisting of materials like Nylon[®], Orlon[®], Ivalon[®], Marlex[®], Teflon[®] and Dacron[®] (24, 106).

Teflon[®] (Polytetrafluoroethylene) and Dacron[®] (Polyethylenterephthalate) showed the most suitable and superior properties (42) and represent the gold standard of synthetic vascular grafts nowadays. Variations of the texture (knitted or woven) and unilateral or bilateral velour trimming, as well as crimping and the invention of expanded PTFE (ePTFE), improved the physiological characteristics of alloplastic grafts (27). While Dacron[®] prostheses are more commonly used for “larger vessel applications”, Teflon[®] grafts are preferred to bypass “smaller vessels” (up to 4 mm diameter) leaving the decision of size to the surgeon’s discretion (76). Before application, porous alloplastic Dacron[®] grafts are impregnated with connective tissue proteins or preclotted with the patient’s blood in order to reduce blood loss, aid clotting and stimulate tissue ingrowth.

After implantation the inner surface of a vascular graft becomes covered with a so-called pseudointima developed from the interaction of plasma proteins, in particular fibrinogen, and thrombocytes aggregating into a platelet-fibrin layer. A neointima is formed when endothelial cells cover this layer (Figure 1). This desirable as nonthrombogenic formation of a neointima is unfortunately limited to a small area adjacent to the anastomosis, nevertheless efforts are being made in the area of tissue engineering to find solutions (72).

From the outside, the surrounding connective tissue encapsulates the vascular graft within normal tissue and develops a foreign-body reaction. The exterior surface is mantled with giant cells covered by a mixture of collagen, fibroblasts, extracellular and cellular tissue elements as well as blood vessels (76).

The great advantages of alloplastic vascular grafts such as short operation times, availability of each required size and large numbers as well as facile operation techniques, are overshadowed by several unsatisfying observations. The short-term and long-term patency is dependant on the size of interposition, the graft diameter and the flow resistance in such a way that an increase in interposition size and a decrease of vessel diameter, associated with an increase in resistance to flow, leads to a decrease in both the short-term and long-term patency rates. Five to ten years patency rates of 90 % for grafts used for aortofemoral bypass are reduced to 50 % for small vascular grafts (< 8 mm diameter) (17). The common most frequently occurring complications of vascular grafts are thrombosis, thromboembolism, periprosthetic fluid collection, pseudoaneurysm, intima hyperplasia, structural degeneration and infection. The problem of infection of PTFE grafts will be elaborated in chapter 3.2.

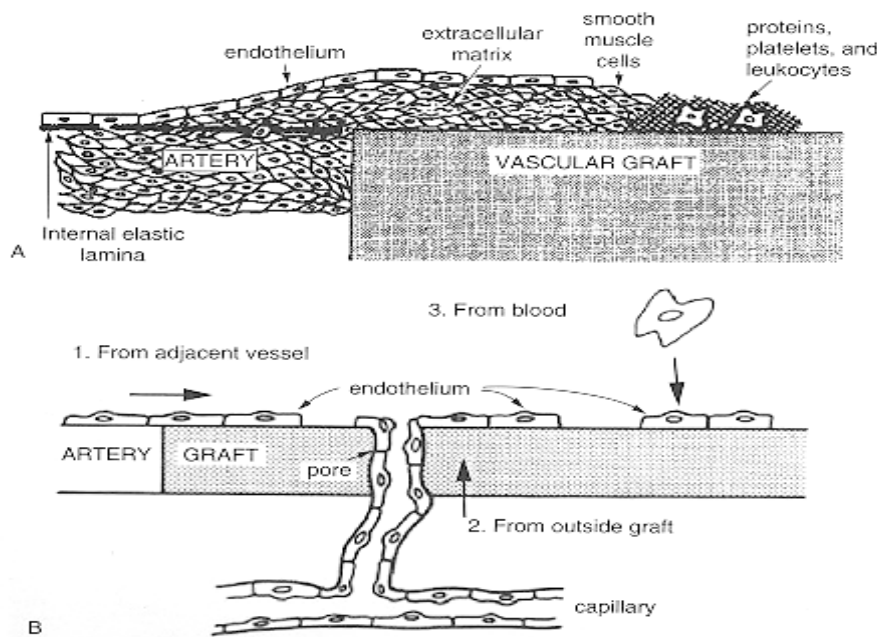


Figure 1. Vascular graft healing. A) Pannus formation, smooth muscle cells migrate from the media to the intima of the adjacent artery and proliferate on the graft surface. B) Possible sources of endothelium on the blood-contacting surface of the vascular graft (76).

2.2 Sutures

Sutures are known to be one of the oldest applied biomaterials in human history traceably appearing for the first time in 32000 B.C. (16). Several developments and acquired knowledge about polymers, sterilization, toxicology, immunology and inflammation or biodegradation lead to an array of modern suture forms which shall be highlighted in the following.

Sutures can be described by three different characteristics – the material (synthetic or natural), absorption profile (absorbable or nonabsorbable) and fiber construction (monofilament or multifilament). Materials with natural origin are based on plant or animal fibers of cellulose or protein structure, for instance catgut or silk spun whereas synthetic sutures are made of metal or polymers like PET, PTFE and those based on α -hydroxy acids. The original borderline between nonabsorbable and absorbable sutures associated with the property to maintain mechanical strength for more than 2 months (94) has been obliterated since the time period of mechanical strength was enhanced up to one year for newly developed sutures (15, 40). The profile of mechanical strength loss is an important parameter for the choice of the right suture as it is an effective support during wound-healing process. Sutures of natural origin degrade enzymatically, whereas the absorption of synthetic sutures is predominantly caused by hydrolysis (4, 13, 80) and enzymes are presumed to play more of a role in degradation and elimination of hydrolysis by-products (80).

The basis of the fabrication of sutures as monofilaments or multifilaments is the requirement for an adequate suppleness. Materials with a high tensile modulus are more likely manufactured into a multifilament suture. The tensile modulus range for the fabrication of a monofilament is at about 500 kpsi or less. Multifilament braids are generally coated to increase the tissue lubricity (76).

The most common suture types on the market are absorbable synthetic sutures which represent almost 42 % of total suture usage worldwide (76). The five different cyclic monomers, glycolide (GA), L-lactide (LLA), ϵ -caprolactone (CL), p-dioxane (DO) and trimethylene carbonate (TMC), mark the basic building blocks for absorbable polymers.

This broad range of different types of suture material demonstrates that the selection of the right suture material depends on several parameters, such as the tissue type or the surgeons preference (97). Multifilament sutures for instance provide a higher comfort for knotting technique, however the fabrication is complex. They have to be coated in order to minimize tissue trauma, and the danger of bacterial colonization and the risk of infection, due to the so-called “wicking “, can not be trivialized (36).

3 Infections

Pus bonum et laudabile – This expression in medicine of the nineteenth century reflects the involuntary togetherness of surgical intervention and infection in former times. Infection was even considered as part of the normal wound healing process as the alternatives – wound phlegmons or gangrenes – led to a predetermined death of the patient. The history of wound management is linked to the care of infection and goes back to the Egyptians who realized that a suppurating wound needed drainage (25). However mismanagement over hundreds of years of introducing substances into wounds to encourage suppuration must have added to the risk of infection and killed many patients (90). The introduction of personal hygiene, for instance the simple act of hand washing, and the discovery and knowledge of asepsis and antisepsis marked an important advance in infection prevention and treatment. At the beginning of the twentieth century antiseptic surgery was replaced by aseptic techniques. The simultaneous discovery of antibiotics and their targeted application during and after the Second World War resulted in better infection handling and prophylaxis care (29).

The immune response of the body is the natural guard to prevent infection. It is classified into the specific (recognition of antigens) and the non-specific (not directed against specific antigens). The physical and chemical environment of the body surface presents the major barrier for microorganisms. When this host defence is modified, opportunists, normally considered to be harmless, become pathogenic. This depression of host defences is caused by systemic factors like shock, immunosuppression and poor nutrition or local factors like ischaemia, trauma, or implantation of prosthetic grafts. Primary pathogens unite a number of attributes which allow them to enter the host, multiply *in vivo*, interfere with the host defence mechanisms, and cause damage to the host and are therefore dangerous in case of a depressed host defence.

The dimension of infection is determined by the size of the inoculum of microorganisms and the degree of pathogenicity. It is not only a high risk for the patient to delay healing after operation or tissue damage, but also of economical interest of hospitals, to prevent and treat infections as effectively as possible. The unchecked application of antibiotics has resulted in an increase of resistance and emergency. Particular nosocomial infections have recently become a great challenge for infection treatment.

3.1 Post-operative infections

In a formative clinical study in 1980, where over 60,000 post-operative wounds were analysed in a time period of 10 years for occurrence and their etiopathogenesis, Cruse et al. demonstrated a total post-operative infection rate of 4.7 % (23). In order to determine such infection rates more precisely, it is unavoidable to classify the conditions under those which the operations are performed. There are four categories, which lead as expected to different infection rates. If the operative intervention is elective under sterile conditions without opening contaminated hollow organs like in heart, vascular, orthopaedic, respiratory, intestinal or urogenital surgery, the intervention is characterized as *clean intervention*. Other categories are *clean-contaminated*, *contaminated* and *infected*. *Clean interventions* represent 75 % of all operations. The infection occurrence in *clean interventions* is widely dependent on exogenous factors. The duration of preoperative hospitalisation for instance increases the infection risk from 1.2 % for a one day of hospital inhabitation up to 3.4 % for a hospital stay of two weeks. A second exogenous influence is the duration of the surgical intervention itself. Because of a higher risk of bacterial contamination, as well as a decreased resistance of the operation field and a weakening of the patient the infection risk rises hourly from 1.3 % up to 4 %. The time point of operations also plays an important role in the risk management of operations. Operation performed after midnight showed twice as high infections rates than day time interventions. A last important fact which influences the risk of infection is the age and therefore the actual condition of the patient. Infection risk, averaging 1.5 % for a 20 year old patient, increases up to 3.2 % for patients older than 66 years of age (23).

3.2 Post-operative infections in vascular surgery

The invention and application of synthetic biomaterials for graft replacements present a boon and bane in vascular surgery. Post-operative infections give rise to an unexpected challenge for surgeons as severe complications can result in amputations and death. In order to react in an appropriate and therapeutically sensible way, it is important to classify graft infections under specific characterizations. In 1972, Szilagyi et al. published a classification of different grades of graft infections predominantly under morphological aspects (95). The differentiation between superficial and deep graft infection is essential for the prognosis and therapy. Especially the stadium of a deep infection, subdivided by Koning and van Dongen, with an involvement of the implant actively threatens extremity or life of patients (57). Under consideration of the

application of modern alloplastic grafts, a subdivision into deep graft infections after Zühlke and Harnoss copes with present conditions (111). It has been recognized that the localisation of infection as well as the local complications are of decisive importance for therapy.

The infection rate for vascular reconstructive interventions is influenced by many parameters such as intra-operative contamination, the stadium of pathogenesis, the localization and dimension of the intervention, the operation technique, used prosthetic material and infection prophylactic regimen. Different clinical studies demonstrate that deep post-operative wound healing disorders average from about 1.2 % to 6 % (74). A pronounced tendency of a higher infectious sensitivity of alloplastic grafts in comparison to autogenous grafts is stated in several studies (110), however the comparison of different patient groups must be viewed critically.

3.2.1 Pathogenesis of post-operative infections after vascular reconstructive interventions

In general, during every graft reconstructive intervention, independent of the applied operation technique or used graft material, post-operative infection can occur. Thereby the virulence of the pathogen as well as the constitution of host immune defence determine the ability of microorganism to cause infection. Fry and Lindenauer demonstrated that the quantity and intensity of bacterial contamination in the operation wound are the key parameters to induce infection in each performed graft reconstruction in animal experiments independent of the type of operation (31). Thereby infection can be caused by the patient himself through locoregional ways, for instance the surgical margin of the operation wound and haematogene factors like intra-operative concomitant infection of the patient in the area of the urogenital tract. The constitution of the host immune defence can be influenced by exogenous factors like intensive therapy or blood loss and endogenous factors like age or comorbidity of the patient.

Bacterial infection is abetted through the structure of allografts and their initiated reactions inside the host. The porous architecture of Teflon[®] grafts or the fibrin network of pre-clotted knitted Dacron[®] prostheses enables pathogens to immigrate into areas where the host immune cells can not follow. Through unspecific foreign body reactions, pathogens can be activated which promotes infection. The ability of pathogens to adhere to the implant surface depends on the type and structure of bacteria, the ability to secrete mucus, the endurance and point in time of contamination and the physical and chemical characteristics of the graft. In a comparative study, a significantly higher affinity of enterobacteria to Dacron[®] grafts was demonstrated by Sugerman. In in vitro experiments, the lowest adherence of *Staphylococcus aureus* was assessed

at PTFE grafts followed by umbilical-venious prostheses and Dacron[®] grafts. This specific behaviour of pathogens leads to different infection rates for different vascular grafts (7, 8). In chapter 3.5 the mechanism of bacterial adherence to surfaces and biofilm formation is further discussed.

3.2.2 Time point of vascular graft infections

In patients with implants, infection can occur at any point in time. In general, the differentiation between early and late manifestations can be made, whereas the limitation of four weeks induced by operation for early infections by Vollmar makes sense (103). An estimated 60 % of all graft infections after reconstructive graft intervention manifest between one and four weeks. Late graft infections can be observed after more than seven years. The integration of the biomaterial into the host plays a key role in infection occurrence. Only in fully integrated vascular grafts, a haematogene and lymphogene perfusion is the precondition for host defence mechanism assured. After integration, late manifestations can only occur as consequences of an incompletely developed neointima, injuries such as punctuations, or as so-called dormant infections. Thereby an intraoperative bacterial contamination persists over a longer time period in the perivascular tissue of the implant and becomes clinically relevant months or years later. Symptoms of early infections are characterized by abscess development, bleeding or purulent secretion through the operation wound, and are mostly manifested in the groin. Late manifestations are predominantly abdominally localized and cause fever, shivering or septic complications.

3.2.3 Localisation of vascular graft infections

The probability of post-operative infectious complications is dependant on the location of the intervention. The axillo-femorale bypass shows the highest infection risk at 4.7 %, whereas at the carotids an infection risk of only 0.5 % is quoted. In general the natural pathogenic flora, the possibility of complicated surgery and a nominal amount of stress because of a minimization of graft stress as well as the selection between autogenous and allogeneous grafts can influence the probability of graft infection.

3.2.4 Infection risk of different grafts

Different types of vascular grafts - autografts, xenografts and allografts - demonstrate a different infection risk. Autografts show the lowest rate of deep infections in clinical studies. Depending on the location, rates of infection were between 0.2 % for thrombarteric excision or patchplastic and 0.5 % for a graft reconstruction with an autogenic vein (81). In the last ten years a total infection rate of 1.36 % for autogenic vein replacement and, as consequence of deep infections, an amputation rate of 54 % and a lethality of 20 % was observed. The application of xenografts is widely obsolete because of the decisive disadvantage of being dissolved. Allografts represent the most infection susceptible graft, resulting in hardly avoidable intra-operative contamination. Simultaneously the immune defence is suppressed as a consequence of insufficient perfusion and capillarization. This is also the reason for the bad prospects of antibiotic treatment. According to Vollmar, risks for deep infections average at 2.6 % which is almost double that of the occurrence for autogenic grafts (102). Within allografts a slight tendency for a lower incidence of infection for knitted, primary non-sealing Dacron-Velour prostheses is presumed (105), however this could not be significantly proven. In fact in a study by Lorentzen no advantages of individual materials could be demonstrated (66).

3.2.5 Diagnosis of infectious complications after vascular reconstructive interventions

Every patient with an implanted alloplastic graft bears the risk of implant infection. The reason can be a transitoric bacteriaemie, an incomplete or through shear force damaged pseudointima. Different types of diagnosis are used when there is a hint of graft infection. Clinical inspections of the operation scars for signs of inflammatory processes or the opening of the wound in the early post-operative stage, provide further evidence of a possible infection. Sonography, x-ray diagnostic, computer tomography, magnetic resonance tomography, szintigraphy, wound smear and blood cultures provide insight into possible vascular graft infections. The modern diagnostic possibilities, the acknowledgement of symptoms, and the omnipresent possibility of infection should be deep-seated in the consciousness of surgeons.

3.2.6 Bacteriology of septic complications in vascular grafts

There is a broad spectrum of pathogens responsible for vascular implant infection. *Staphylococcus aureus* unquestionably represents the most frequently occurring pathogen in mono and mixed infections. In 1962 Javid showed that *S. aureus* can be assessed in every infection after graft reconstructive interventions (52). In an overview of five clinical studies Bunt et al. demonstrated the average occurrence of *S. aureus* at 43 %, followed by *S. albus* and *E. coli* each at 14 % (12). However, there is a detectable downward tendency in the appearance of *S. aureus* to 25 % and a simultaneous increase of *S. albus*. Comparing early and late manifestations, high virulent pathogens like *S. aureus*, *E. coli* or *P. aeruginosa* can mostly be found within the first month whereas gram-negative germs are often detected in later manifestations. Particularly coagulase-negative staphylococci such as *S. epidermidis* play a certain role in later manifestations. A possible answer may be the low virulence of this pathogen and the endurance to establish an infection against host immune response.

3.2.7 Sutures in infected areas

In general the requirements for surgical sutures used for vascular reconstruction are the same as for vascular grafts. In several studies, synthetic monofilic non-resorbable sutures (Polypropylene) have proven their value (44, 82). However in traumatology, paediatric and septic surgery, the application of suture material may result in complications. Particularly, in the application to infected areas there is a risk of a non healing infection (100). Sandmann and Schmitz-Rixen demonstrated that non-resorbable sutures lead to an additional and permanent foreign body reaction and can obstruct infection healing (83, 88). The requirements for a suture material in infected areas is therefore a predictable, but enhanced and reproducible loss of tensile strength, a smooth surface, no capillarity, a minimum of induced tissue reaction and good management by the surgeon. In many areas of surgery, medium-term monofilic resorbable suture materials have replaced the non-resorbable ones. Giessler demonstrated that resorbable sutures are particularly suited for healing anastomoses (33). The reconstruction with respect to anatomic layers of artery walls and a healing promotion between two blunt vessels are only two of several advantages of resorbable suture materials.

3.3 Neuronal infections

Neuronal infections like bacterial meningitis, pathogen caused meningoencephalitis, brain abscess, neuroborreliosis or neurosyphilis require antibiotic therapy. For neuro-surgical interventions the additional antibiotic prophylaxis is a common method for pre-operative treatment. The choice of applied antibiotics is geared to the diagnosed bacterial species and covers the broad spectrum of available antibiotics. Most applied antibiotics show sufficient infection protection, however in some cases for instance inflammatory meningitis therapy failure is not uncommon as a consequence of pathogen - or resistance change during therapy. Insufficient penetration into the liquor can also be considered as a reason for therapeutic failure. Therefore an adequate effective high drug level in devitalized brain tissue or in the area of inserted implants and foreign bodies like dura mater replacement, or fibrin glue has to be assured. The local application of antibiotics (intrathecal or intraventricular) for instance 10 mg to 50 mg vancomycin i. th. for infections caused by staphylococci is indicated in complicated neuronal infections. Applied antibiotic concentrations are mostly based on clinical experience. The systematic investigation of the influence of antibiotics on neuronal tissue, particularly the dose response and functional toxicity of antibiotics, is of basic interest in the area of neuronal infections and may improve antibiotic therapy.

3.4 Medical device infections

The “classic” device-related infection observed by surgeons for the first time could not be explained properly, as it did not seem to follow a logical pattern. In many cases symptoms caused by medical device-related infections showed up almost immediately, sometimes months or years after device implantation, inflammation was bordered locally in the area of medical device or spread systemically. To get to the bottom of these observations a glance over the fence to environmental microbiology was very helpful. In this scientific area Costerton et al. developed and articulated the theory of the biofilm concept in 1978 (20). Four years later Tom Marrie introduced this concept into medical microbiology (69). The theory is based on the assumption that bacteria grow in matrix-enclosed communities adhered to surfaces in nutrient-deprived ecosystems (21). In medicine this assumption was soon confirmed by observations made by scanning and transmission electron microscopy investigating hundreds of failed medical devices (76). The highest bacterial colonization appeared in intrauterine contraceptives and dental devices. The sealable way of introducing pathogens to the normally sterile environment is the

channel from the skin to the device. Common environmental and skin pathogens like staphylococci are the most frequently detected germs in device-related infection. Large and complicated operations also enhance the risk of pathogenic manifestation on the implant surface. A surface colonization however, does not automatically lead to infection. In many cases the pathogenic change of surrounding tissue causes a loosening or detachment of the implant and therefore the loss of function (51). Symptoms may not be elicited immediately as only the release of planktonic cells and toxins from the biofilm community causes an inflammatory response. Furthermore a biofilm formation protects bacterial cells from both humoral and cell-mediated immunity (61).

The constitution of the patient therefore does not influence the occurrence of device-related infections since the key event is the discharge of single bacterial cells from the community. Only released pathogens can be antagonized by the immune response or applied antibiotics leading to the alleviation of symptoms, however the infection itself persists and the fear of severe and life-threatening consequences always looms over the patient.

3.5 Biofilms

3.5.1 Bacterial adhesion to surfaces

Wild natural bacteria are necessary to study adhesion of pathogens on the surface of biomaterials as lab-adapted strains do not reproduce conditions inside the body. The DLVO theory constituted by van Loodsrecht et al. in 1990 is based on the comparison of bacterial cells with smooth colloid particles that interact with a surface as a result of an electrostatic attraction (99). However several studies showed that this theory is of limited application in terms of bacterial adhesion as the bacterial cells are not smooth-surfaced particles. The surface is rather covered by hydrophobic exopolysaccharide and sometimes a highly structured protein shell. There are different mechanisms of adherence ranging from utilization of flagella or pili to the point of producing windrows of cells (58). In general, pathogens show reversible and irreversible patterns of adherence (70), meaning that bacterial cells are able to adhere to the surface as well as to detach and leave the area again before attaching irreversibly and initiating the process of biofilm formation. Physical properties of the biomaterial surface seem to play an inferior role for adherence procedure as several studies have demonstrated. Pathogens seem to adhere equally well to hydrophilic and hydrophobic, and to rough as well as to smooth surfaces (68, 91) even in systems with very a high shear flow rate (14). Scientists are still searching for new solutions.

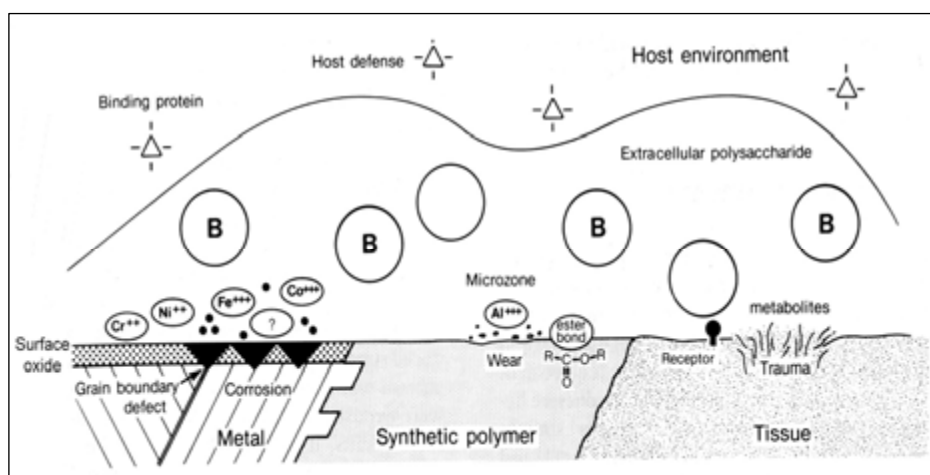


Figure 2. Interaction between pathogens, tissue and implant (37).

3.5.2 Biofilm formation

The irreversible attachment of bacterial cells at a biomaterial surface is accompanied by a genetic switch which implicates a phenotypic change, in some cases up to 70 % (84). The phenotype of planktonic cells of *Pseudomonas aeruginosa* for instance, shows a higher agreement with planktonic cells of other species in the same genus than their biofilm counterparts (85). The production of exopolysaccharides by up-regulated genes is thereby one of the first activities of the bacterial cell with a differing phenotype (84, 93). These exopolysaccharides attach the cell irreversibly to the biomaterial surface and form the matrix of the biofilm. Binary fission or further attachment increases the number of phenotypically modified bacterial cells on the biomaterial surface resulting in a community of matrix and bacterial colonies of varying shape. These entities are separated by open water channels and water moves through these complex microcolonies in a convective pattern. A balance between multiplication and detachment of planktonic cells adjusts. Approximately one week after the initiation of colonization, a stable community structure has formed and can remain so for years. Observed resistance to antibiotics or to uptake by phagocytes can also be attributed to the upregulation of genes, as for example the gene *fnt C* is responsible for antibiotic resistance of staphylococcal species. The clinical consequence is that antibiotics can be used for treating acute infection occurrence caused by planktonic cells, but not for biofilm clearance. Biofilm-covered devices therefore have to be removed in many cases by surgery.

The complex structure and organization of these bacterial microcolonies lead to the conclusion that pathogens within these entities are able to communicate with each other via signals like

hormones or pheromones. The assumption of this so-called quorum sensing was first confirmed in 1998 by Davis et al. who demonstrated that biofilm formation in *Pseudomonas aeruginosa* is controlled by an acylated homoserine lactone (AHL) quorum sensing signal. This AHL signal is only one of many signals which control the organization of pathogens in biofilm communities.

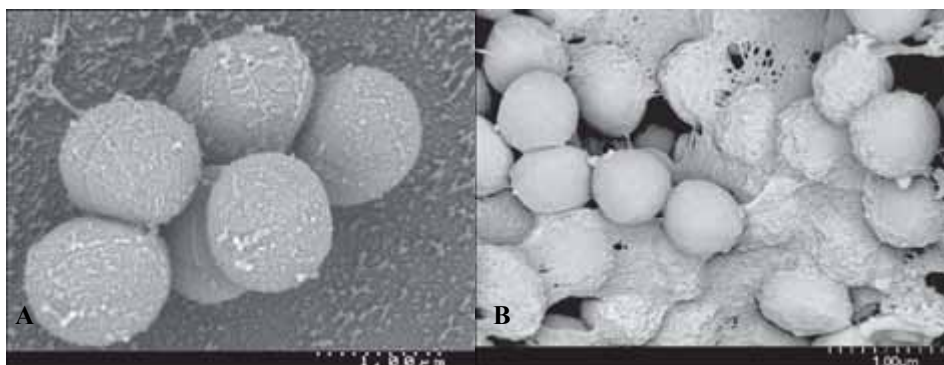


Figure 3. *Staphylococcus aureus* accumulation A) without B) with slime production (41).

3.5.3 Strategies of biofilm prevention

The most common way to prevent biofilm formation on medical devices is the incorporation of antibiotics into surface material in order to kill incoming planktonic cells before they can adhere and start biofilm formation. After complicated and longer operations, in particular, device-related infections can occur because skin and environmental bacteria have enough time to adhere and initiate biofilm formation. An antibiotic-modified surface is therefore a helpful and established strategy. The problem is that after the initial drug release, which guarantees effective protection against planktonic bacteria for a short period of time, the delivered sublethal antibiotic concentrations after months or years as well as the application of highly specialized drugs like ciprofloxacin can cause resistant strains. A switch to multitarget antiseptics like chlorhexidine has improved the situation, however, most are not approved yet for systemic use in humans. Another method of resolution is the development of intelligent coatings mimicking skin consisting of a self-assembled surface layer that contains molecules loaded into an underlying plastic. The advantage is the delivery of antimicrobial drugs in controlled impulses by ultrasonic waves post-operatively or any time preliminary signs of device-related infection show up. Other studies show that the application of ultrasonic energy itself (71, 77) or weak direct current fields (19) are promising strategies to render pathogens susceptible to antimicrobial agents.

A more focused method to prevent biofilm formation is the utilization of biofilm signal blockers, for instance the RNA III-inhibiting peptide (RIP) analogue blocking the target of RNA III-activating protein (TRAP) receptor in gram-positives or brominated furanones targeted on the acylated homoserine lactone (AHL) system of gram-negative bacteria (6). This method is based on the idea to inhibit the genetic switch between planktonic cells and their biofilm counterparts and is derived from observations of plants that protect themselves from biofilm colonization by the use of signal blockers (92). This lock of pathogens in the planktonic phenotype makes them susceptible to conventional antibiotic therapy.

The new development from Westaim Biomedical Inc. for burn bandages uses a galvanic combination between silver and copper along with a simultaneous release system of silver and copper ions. This may have an effect on pathogen adhesion, biofilm formation and susceptibility to antibiotics. The synthesis of different concepts may be the best way for the development of new antimicrobial devices or so-called antifouling materials.

3.6 Therapeutic methods

3.6.1 New tactics in surgery and local wound management

Wound management is based on knowledge of the wound healing process. This process proceeds in four stages, the inflammatory phase, followed by the resorptive, the proliferative and the reparative phase (64). Within the inflammatory phase, the wound can be opened and inflammation can be battled through surgical cleaning and if necessary local application of antibiotic or antiseptic agents. Additionally the systemic application of antibiotics is recommended in order to prevent recontamination of the vascular graft in revision surgery. In the resorptive phase, the surgical cleaning of the wound, bandage changing, and removal of necrotic tissue provide the basis for the later replenishment of the wound in the proliferative phase. A necessary prerequisite in starting wound healing is the physical and enzymatic wound cleaning. The following reparative phase leads to a completely closed wound which may result in a scar. The application of different dressings with and without drugs, like autogenous skin transplants or poly-urethane dressings, may prevent wound re-infection. The management of an infected wound after vascular graft infection differs from wound management in other areas of surgery due to the fact that spread of infection from the wound to the vascular graft may lead to severe complications like sepsis, sometimes with lethal consequences for the patient. An early diagnosis of infection is therefore as important as the correct classification into superficial or deep, as well

as into early and late manifestation. The probability of limiting infection and avoiding severe complications is higher when surgical intervention and the appropriate therapy is performed quickly.

3.6.2 Antiseptics in wound care

Antiseptics are predominantly applied for external use and sterilization of instruments or surfaces. The application of antiseptics in open wound management is regarded sceptically as they are inactivated by body fluids or pus (34, 75). Different types of antiseptics are used for skin preparation and instrument cleaning in surgery and wound management. These drugs are not approved for i.v. administration. Particular hypochlorite solutions are controversially discussed as the doubtless bactericidal effect is accompanied by a clear toxicity to healing tissue. Nevertheless their use is historically widespread for skin grafting. Povidone-iodine, a polyvinylpyrrolidone iodophor presented with a detergent as Betadine, is used as a topical antimicrobial for skin preparation or hand-washing (63). It should be used with caution in open wounds as it may have an effect on thyroid function when absorbed as well as a delay on healing (28, 101). Due to side reactions concerning fibrin formulation, application of fibrin glue and betadine is a contraindication. Chlorhexidine is known to have a prolonged broad spectrum of activity against gram-positive and gram-negative pathogens and has been demonstrated to have superior antimicrobial effectiveness compared with other antiseptics (73). Another advantage is its smaller interaction with body fluids and the fact that it is not absorbed through intact skin. Although the evidence of antimicrobial activity of hydrogen peroxide is missing (11), it is widely used as wound irrigant. Though toxicity to fibroblasts has been proven when properly used, it does not appear to interfere with healing (65).

3.6.3 Antibiotics in wound care

Antibiotics in wound management are applied as prophylactic therapy as well as for diagnosed infections. The choice of resorbable and non-resorbable antibiotics is empirical and defined by drug approval (60, 96). The parenteral application (i.v. or i.m.) is often preferred to achieve necessary peak levels. The duration of antibiotic treatment differs between prophylactic application and therapeutic demand. Furthermore the application has to be oriented to biological resistance of the diagnosed pathogen and application has to be focused on the patient. In the

following, the most commonly proven antibiotics in wound care are briefly described. Penicillins are the first choice for streptococcal or clostridial wound infections, however their narrow spectrum of activity, the risk of sensitivity and a short half life limit their application for internal use only. The combination with clavulanic acid in newer formulations prevents agents from β -lactamase degradation. The cephalosporines are used in general prophylaxis and therapy of broadband infections. Because of their higher potency, third generation agents like cefotaxime are applied, usually in combination, in serious infections. This enhanced potency, however, is limited to a narrowed spectrum. Aminoglycosides like gentamicin are effective against staphylococci and aerobic gram-negative bacilli and safe for prophylactic therapy with a prolonged post-antibiotic effect. In high risk patients, side effects like renal and oto-toxicity can be avoided by close drug monitoring. Tetracyclines and sulphonamides play an inferior role in wound infection management and are used for special indications like abdominal or colorectal surgery. To avoid resistance, the responsible application of antibiotics and the compliance of hygienic guidelines in hospital is still of high priority.

3.6.4 Prosthesis explantation

Implants and infected biomaterials for instance an infected vascular prosthesis need surgical excision. Notable are involvement of the pseudo-intima by infection, danger of rupture, incidence of distale septic emboli or a septic thrombosis. The surgical intervention covers the exposure and excision of prosthesis and suture material, follow-up resection of the vessel wall and the occlusion of the vessel by suture or the maintenance of the vessel axis with the help of an interponat. In primary operations long term results are focused upon, whereas in secondary reconstructions in an infected area life maintenance and infection palliation are the main targets. Therefore, autogenic material is the gold standard, however in consideration of the danger of rupture in autogenic graft, the application of alloplastic material like Dacron® or Teflon® as bypass graft in non infected areas is also common (98). In vessel lesions alloplastic grafts are only used in the case of emergency, as for instance when a patient's life is threatened.

3.7 Implants as drug delivery systems

Biomaterials have altered modern medicine and improved life of patients. Strategies to utilize the artificial surfaces of biomaterials for local drug delivery are developed to improve tissue compatibility, control infection, prevent thrombogenicity and improve tissue integration. These

artificial surfaces can also be utilized to locally insert defined drug delivery systems (DDS) that release drugs in a controlled manner. These DDS are commonly used to maintain low blood plasma levels for a long period of time below the therapeutic index as well as to obtain high local drug concentrations in the area of the device. An approved technology in orthopaedic and trauma surgery is the anti-infective coating of osteosynthesis material for the prevention of biofilm colonization. In device coatings drugs are often dispersed in biodegradable matrix systems as for instance poly(lactic acid) or poly(lactic-co-glycolic acid). These polymers play a decisive role among biodegradable drug delivery systems as they are hydrolysed to the natural metabolites L-lactide acid and glycolic acid (45). In thick coatings the erosion of poly(L-lactic acid) follows four steps beginning at the outer perimeter of the device and gradually moving into the interior, thereby releasing the incorporated drug and preventing the device for instance from a possible bacterial colonization.

3.8 Biocompatibility

The biocompatibility of a medical device is defined as the tolerance between the implant and the organism and can be subdivided into structure compatibility and surface compatibility (108). Structure compatibility is characterized by mechanical adaptation of the implant to the recipient tissue with the aim to take structure properties of the biological system. Surface compatibility means an adaptation of the chemical, physical, biological and morphological properties of the implant surface to the recipient tissue. The surface structure of an implant is the key to improved biocompatibility as the body is confronted with this surface and responds with inflammatory or allergic reactions in case of a limited compatibility. It is the subject of an entire scientific field to improve biocompatibility. For the clinical application of new materials or surface modifications, like device coatings, evidence of safety for the patient has to be investigated according to ISO (DIN) standards.

3.9 Haemocompatibility

The implantation of artificial surfaces like cardiovascular medical devices and the blood contact initiate haemostatic mechanisms originally designed to arrest bleeding from injured blood vessels. This haemostatic process involves a complex system of reactions between the biomaterial surface, thrombocytes, coagulation and the complement system as well as the

fibrinolytic system. It is the task of biomaterial engineers to assure that this interaction between activation and inhibition systems on the biomaterial surface is balanced in a way that blood flow in the circulation is maintained and the danger of thrombosis or exaggerated inflammatory response is minimized. Many interactions of participating cells and proteins with artificial surfaces, including polymer coatings as drug delivery systems have not yet been defined and it is difficult to standardize haemocompatibility requirements for biomaterials. Increased haemostatic procedures still limit the utilizability of many cardiovascular devices and require the system application of anticoagulants such as heparin or coumarines (76).

3.10 New approaches for protection of biomaterial infections

3.10.1 Electro-magnetic field influence

The Magnetodyn[®] procedure is based on the influence of electro-magnetic fields on bone healing and infection palliation (Figure 4). The non-invasive magnetic-field therapy is clinically applied in case of loosening of prostheses and non-union in the fracture zone. The involved body parts are inserted in a magnetic field coil and exposed to a low-frequency sinusoidal magnetic field.

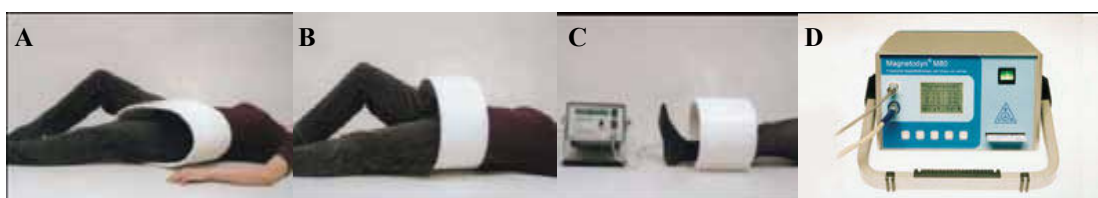


**Figure 4. Extracorporeal magnetic-field coils of the Magnetodyn[®] procedure.
A) pelvis and thorax B) hip and shoulder C) extremities D) medical device M80**

(Source: Neue Magnetodyn GmbH)

A frequency in the range of 0 Hz up to 20 Hz, a magnetic flux density of 0.5-10 mT, and the wave form of the signal can be adjusted individually. The invasive magnetic-field therapy is performed in the same way with the difference that via implanted secondary coils, an additional electro-magnetic field is induced over the fracture gap (Figure 5). This additional field has a considerably stronger electric field part and can extend over larger fracture areas. A sinusoidal current, similar to the "leakage current" of a condenser, flows over the cross-sectional area of the fracture. Investigations of the therapeutic benefit of the invasive Magnetodyn[®] procedure in the treatment of avascular defects and pseudo arthrosis in association with bone transplants

demonstrate superior healing rates (5, 59, 86, 87). The possible mechanisms of the influence of low frequency electro-magnetic fields on biological systems are based on different theories which are the object of several studies. The radical pair effect constitutes the generation of free radicals during high-energy photonic or electro-magnetic irradiation in biological systems. These free radicals can damage cell membranes or modify ionic channel conductivity. However the energy of low-frequency systems used in the Magnetodyn[®] therapy with frequencies between 10 and 30 Hz are too weak to result in radical formation. Although the energy is not sufficient for stimulation, quantum electrodynamics predicts magnetic effects in the case that resonant stimulation conditions occur simultaneously.

The mechanism of the ion-cyclotron resonance (ICR) constitutes that the Lorentz force effects ions and ion-protein complexes because of their intrinsic movements and their charges within a static magnetic field. This diverts the ions from circular orbits and causes a precession movement, according to Larmor (32). The resonant stimulation is the stimulation of a biological system by electro-magnetic fields of defined orbital frequency. The resonance frequency for Ca^{2+} ions is in the range of extremely low-frequency fields like those used in the Magnetodyn[®] procedure which could be a possible explanation for a bactericidal effect.

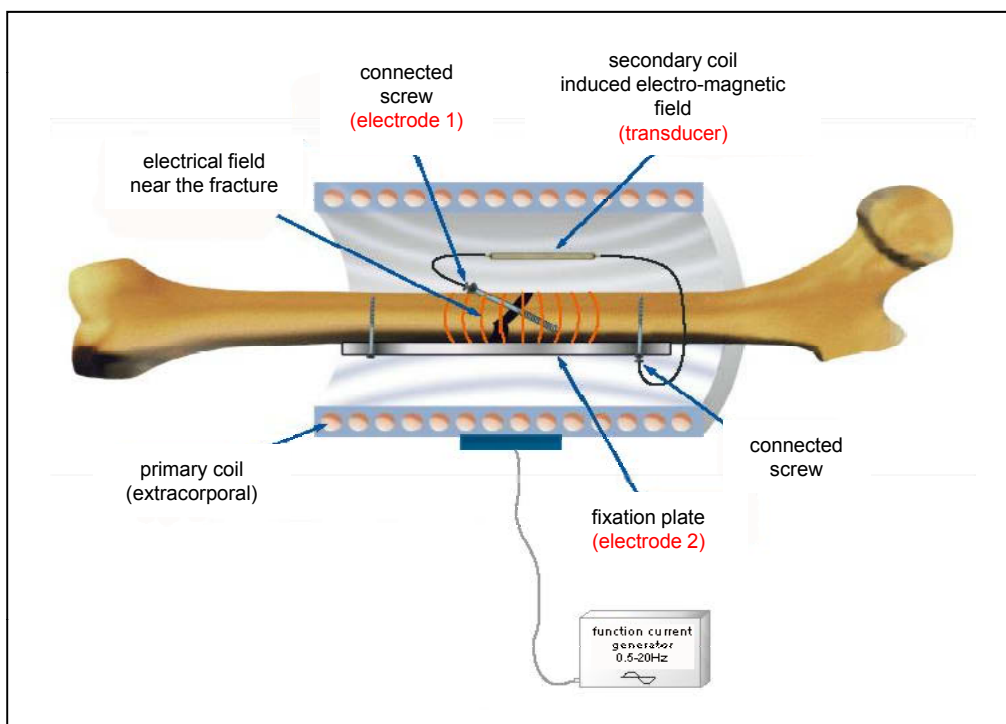


Figure 5. Principle of the invasive Magnetodyn[®] procedure.
(Source: Neue Magnetodyn GmbH)

3.10.2 Antimicrobial coatings

Biofilm formations and haemostatic reactions on the surface of allografts lead to the modification of graft surfaces. For the improvement of physical and mechanical properties and the adaptability to the target vessel Intervascular[®] has developed a polyester vascular graft coated with collagen (InterGard Knitted UltraThin[®]). SEALPTFE[®] is a gelatine coating of PTFE provided by VASCUTEK[®] with the advantage that gelatine closes the branch canals and bleeding is stopped quickly. In order to avoid the formation of thrombi, an antithrombotic lumen surface was developed by JOTEC[®] (FlowLine Biopore[®] Heparin). The lumen surface of this ePTFE prosthesis is coated with a synthetic protein where heparin is attached via covalent bonds and ionic interactions. VASCUTEK[®] offers a system of rifampicin powder that can be used for preoperative graft coating in order to avoid adherence of bacterial cells. An antimicrobial coating for vascular grafts is provided by Intervascular[®], Intergard[®] is a polyester graft coated with a combination of collagen and silver and claims to be effective against post-operative infections. In the area of surgical sutures, Vicryl[®] Plus (Ethicon[®]), an absorbable synthetic braided suture is antimicrobially coated with triclosan. This technology represents the current development to predominantly focus on the equipment of biomaterial surfaces with drug release systems consisting of antibiotics or antiseptics incorporated in drug carriers in order to prevent bacterial colonization of medical devices like PTFE grafts or surgical sutures.

3.10.3 Magnetic drug targeting systems

Nanotechnology will play a decisive role in future technology for many areas such as medicine, material science and electronics. A combination of thin polymer layers at the nanoscale and inorganic hybrid materials, for instance, can prevent energy-saving organic illuminating diodes from faster aging. Many membranes in solar cells and facilities for water treatment to filter nanoparticles consist of nano structures. In building services engineering, barrier layers at the nanoscale are used for vacuum isolation panels.

In medicine, nanotechnology opens up new possibilities as all important life processes in human cells happen at the nanoscale. Structures and customized particles of less than 100 nm in size are gaining interest in different medical disciplines. Ferries at the nanoscale are designed to carry molecules, genetic material, and drugs, selectively and well-dosed to diseased cells. This targeted drug transport especially raises hope in chemotherapy where only diseased cells should be destroyed. Different methods to direct nanoparticles to their targets are practical such as the

equipment with antibodies, sugars, enzymes and tensides which serve as identification molecules or enable the docking at the target cell via receptors. Polyethylene glycol coated particles in a range of 500 nm, for instance, still penetrate the mucous membrane, although the common opinion supposes that penetration can be performed only by particles in the range of a nanometer. Nanoparticles consisting of iron oxide (Fe_3O_4), better known as *ultra-small superparamagnetic iron oxides (USPIO)*, are only one type of a wide range of different nanoparticle materials like stealth liposomes or polybutylcyanoacrylat particles. These USPIOs usually consist of the iron core and an organic shell like dextrans or fatty acids and are formulated as suspensions. A big advantage of those so called ferrofluids is the already proven biocompatibility as they are in clinical use as x-ray contrast agent. A second advantage is that these nanoparticles can be magnetized through an external magnetic field and concentrated after intra-venous or intra-arterial injection in the target tissue where a controlled release of the specific drug is desirable. This technique known as magnetic drug targeting has been successfully applied in several in vitro and in vivo studies for cancer treatment (2, 3). The first clinical approach in human patients was performed with epirubicin-loaded ferrofluids for advanced and unsuccessfully pre-treated cancers or sarcomas and opened the way for further clinical experiments (67). In consideration of this successful new concept in chemotherapy the switch to apply magnetic drug targeting in alternative indications by using different drugs seems to be a more than logical development.

3.10.4 Neuronal networks

Neural mechanisms are based on activities at the cellular and molecular level, however only the interaction between sub - and suprathreshold electrophysiological signals of neuronal networks determine perception and behaviour (26, 30). A good structural organization of such neuronal groups is a basic requirement for a system where transient information calls for a fast response. However the structural complexity of vertebral nervous systems becomes obvious in several observations. Even stable adult nervous systems show constant changes in their physical structure (53, 55) as well as in synaptic weights (10). Glasser showed that a specific morphology of neuronal circuits does not always predict specific electric properties (35). In consideration of these challenges simplified systems are unavoidable in order to gain a better insight of neuronal interaction.

Slice preparations (56) and invertebrate preparations have been established experimental systems (18), however most investigations have focused on input/output relationships which are informative about network responses but do not provide information about how responses are formed.

An alternative and advanced development describes the cultivation of mammalian neuronal networks on beds of photoetched microelectrodes. The first recording of spike potentials with photoetched microelectrode surfaces was described by Gross et al. in 1977 and is nowadays a routine method for monitoring internal dynamics of mammalian networks (38, 39).

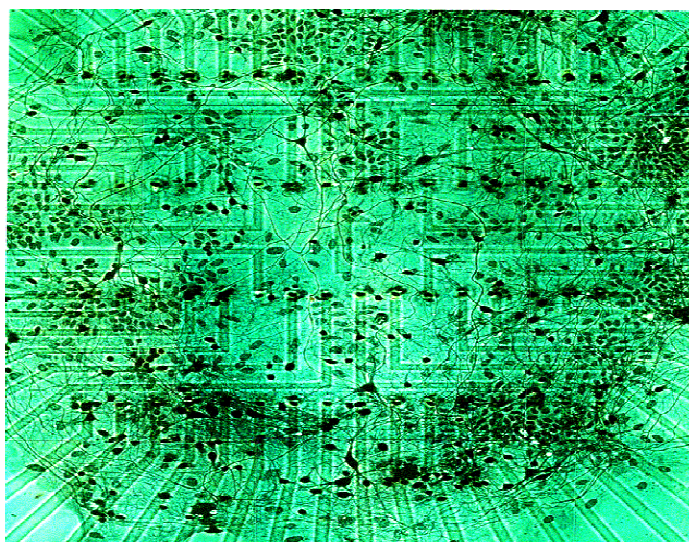


Figure 6. Mammalian frontal cortex networks cultivated on microelectrode neuroarray (CNNS archives).

This monitoring of spike activity from visible cells makes it possible to simultaneously gather statistical temporal and spatial data, as well as to select high signal-to-noise ratio of representative spike activity. Several applications are conceivable. The electrical stimulation of networks (79) as well as optical measurements of ionic fluxes in the living state in monolayer networks (54) or the development of tissue based biosensors can be performed. Disease models like epilepsy can be established as cultures are maintained in specific states of activity for long periods of time without signs of excitotoxicity (78).

An interesting application field for pharmacological studies is the screening of compounds. In the focus is the question how networks react to certain agents and the investigation of acclimatization effects, and receptor – agent interactions. Functional compound toxicity of novel agents can be studied, and generated dose response data are helpful markers for further studies in

animal models. The combination of all these applications shed light into the inner life of neuronal networks and enables the extraction of general principles of the organization of neuronal networks.

4 Conclusions

Various approaches to prevent and treat device-associated infections are part of our research activities. The development of biodegradable drug delivery systems on the surface of biomaterials highlight the most important requirements for an effective as well as biocompatible anti-infective equipment of implants such as PTFE grafts and surgical sutures for the prevention of post-operative infection.

The application of low-frequency electromagnetic fields to *S. aureus* cultures corroborated observations of infection palliation in clinical situations of bone infections during magnetic field therapy and could be used for new developments in the treatment of biomaterial associated infections.

A new perspective in the on demand treatment of vascular graft infection is presented in the development of biomaterial oriented magnetic drug targeting systems. With the help of a strong external magnetic field, drug-functionalized nanoparticles are concentrated at the surface of infected grafts ensuring high drug levels to destroy biofilm embedded pathogens.

The utilization of mammalian neuronal networks on microelectrode neuroarray will provide new concepts regarding the functional toxicity of antibiotics locally applied with resorbable and non-resorbable implants during brain surgery.

5 Objectives of the thesis

The key events in biomaterial-associated infection are the pathogen adherence on the surface of biomaterials and the subsequent biofilm formation coming along with a genetic switch and a change of the planktonic phenotype of pathogens into the biofilm phenotype. This genetic switch of pathogens leads to an increased antibiotic and host defence resistance which is the major problem for a successful clinical treatment. The most frequently occurring pathogens in biomaterial-associated infection belong to *S. aureus* and *S. epidermidis*.

The concept of this thesis was to find new ways to prevent post-operative medical device-associated infections and new perspectives for the on demand treatment of already manifested medical device-associated infections.

For post-operative device protection our intention was to develop individual biodegradable drug delivery systems on the surface of PTFE prostheses based on lipid-like drug carriers like PDLLA, tocopherol acetate, a diglyceride (Softisan[®]) and a triglyceride (Dynasan[®]) with incorporated antibiotics like gentamicin and teicoplanin. The in vitro investigation and comparison of drug release, anti-infective characters, biocompatibility and haemocompatibility highlighted the most important requirements for effective as well as compatible anti-infective coatings of vascular grafts (Chapter 2).

A second project for the prevention of post-operative infection presented the antimicrobial equipment of synthetic absorbable PGA surgical sutures with biodegradable drug delivery systems based on a combination of antiseptics like chlorhexidine or octenidine and fatty acids like palmitic acid and lauric acid. In vitro investigations for drug release, anti-infective characters and biocompatibility were performed and checked for realization (Chapter 3).

For the on demand therapy of already existing device-associated infections various methods of resolution were taken into consideration.

Clinical observations of bone infection palliation during magnetic field therapy gave reason to study the influence of low-frequency electromagnetic fields on *S. aureus* growth in vitro (Chapter 4).

Furthermore we tried to increase antibiotic susceptibility of *S. aureus* by the application of low-frequency electromagnetic fields in presence of an aminoglycoside. These data are the fundament for further investigations about the influence of low-frequency electromagnetic fields on susceptibility of pathogens with increased antibiotic resistance in biofilms (Chapter 5).

A further study for the on demand therapy of device-associated infections focused on the establishment of a magnetic drug targeting system to accumulate high antibiotic concentrations

on the surface of vascular grafts. The development and characterization of gentamicin coated ultra-small superparamagnetic iron oxides and the establishment of a circulatory model to imitate blood flow were in the focus of this investigation (Chapter 6).

In a cooperation of the Technical University of Munich and the University of North Texas, the functional neurotoxicity of locally applied drugs in neurosurgery was investigated with mammalian neuronal networks grown on microelectrode neuroarray. Our intention therefore was to study the local application of antibiotics in combination with biomaterials used in brain surgery to predict functional neurotoxicity (Chapter 7).

In summary the main objectives of the thesis were:

1. The anti-infective equipment and characterization of PTFE grafts for the prevention of post-operative infection.
2. The anti-infective equipment and characterization of PGA surgical sutures for the prevention of post-operative infection.
3. The elucidation of the influence of low-frequency electromagnetic fields on *Staphylococcus aureus* growth in order to corroborate clinical observations about bone infection palliation during magnetic field therapy.
4. The investigation of the influence of low-frequency electromagnetic fields on antibiotic susceptibility of *Staphylococcus aureus*.
5. The development and characterization of anti-infective coated ultra-small superparamagnetic iron oxides and the establishment of a magnetic drug targeting system for biomaterial infections.
6. The study of functional neurotoxicity of individual antibiotics investigated with mammalian neuronal networks grown on microelectrode neuroarrays.

6 Figure Captions

Figure 1. Vascular graft healing. A) Pannus formation, smooth muscle cells migrate from the media to the intima of the adjacent artery and proliferate on the graft surface. B) Possible sources of endothelium on the blood-contacting surface of the vascular graft.

Figure 2. Interaction between pathogens, tissue and implant.

Figure 3. Staphylococcus aureus accumulation A) without B) with slime production.

Figure 4. Extracorporeal magnetic-field coils of the Magnetodyn[®] procedure.

Figure 5. Principle of the invasive Magnetodyn[®] procedure.

Figure 6. Mammalian frontal cortex networks cultivated on microelectrode neuroarrays.

7 References

1. 1983. NATNEWS **20**:15-7.
2. **Alexiou, C., W. Arnold, R. J. Klein, F. G. Parak, P. Hulin, C. Bergemann, W. Erhardt, S. Wagenpfeil, and A. S. Lubbe.** 2000. Locoregional cancer treatment with magnetic drug targeting. *Cancer Res* **60**:6641-8.
3. **Alexiou, C., R. Jurgons, R. Schmid, A. Hilpert, C. Bergemann, F. Parak, and H. Iro.** 2005. In vitro and in vivo investigations of targeted chemotherapy with magnetic nanoparticles. *Journal of Magnetism and Magnetic Materials* **293**:389-393.
4. **Ali, S. A., S. P. Zhong, P. J. Doherty, and D. F. Williams.** 1993. Mechanisms of polymer degradation in implantable devices. I. Poly(caprolactone). *Biomaterials* **14**:648-56.
5. **Ascherl, R., F. Lechner, and G. Blumel.** 1985. Electrical stimulation of low frequency range in cases of pseudarthroses. Survey of 350 cases. *Reconstr Surg Traumatol* **19**:106-12.
6. **Balaban, N., Y. Gov, A. Bitler, and J. R. Boelaert.** 2003. Prevention of *Staphylococcus aureus* biofilm on dialysis catheters and adherence to human cells. *Kidney International* **63**:340-345.
7. **Bandyk, D. F.** 1991. Prosthetic infections due to bacterial biofilms: clinical and experimental observations. *J Vasc Surg* **13**:757-8.
8. **Bandyk, D. F.** 1985. Vascular graft infection: Epidemiology, bacteriology and pathogenesis., p. 471-485. *In* V. M. Bernhard, Towne, J.B. (ed.), *Complications in vascular surgery*. Grune and Stratton, Orlando.
9. **Barker, W. F.** 1988. A century's worth of arterial sutures. *Ann Vasc Surg* **2**:85-91.
10. **Bliss, T. V., and T. Lomo.** 1973. Long-lasting potentiation of synaptic transmission in the dentate area of the anaesthetized rabbit following stimulation of the perforant path. *J Physiol* **232**:331-56.
11. **Brennan, S. S., and D. J. Leaper.** 1985. The effect of antiseptics on the healing wound: a study using the rabbit ear chamber. *Br J Surg* **72**:780-2.
12. **Bunt, T. J.** 1983. Synthetic vascular graft infections. I. Graft infections. *Surgery* **93**:733-46.
13. **Capperauld, I. B., T.E.** 1984. *Sutures and dessings., Wound Healing for Surgeons*, Eastbourne, UK.
14. **Characklis, W. G.** 2003. Biofilm processes, p. 195-231. *In* W. G. Characklis, Marshall, K.C. (ed.), *Biofilms*. John Wiley and Sons, New York.
15. **Chu, C. C.** 1997. Classification and general characteristics of suture materials.
16. **Chu, C. C.** 1991. Recent advancements in suture fibers for wound closure. *ACS Symp. Ser. High-Tech Fibrous Mater.*:167-211.
17. **Clagett, G. P.** 2002. What's new in vascular surgery. *J Am Coll Surg* **194**:165-201.
18. **Cohen, A. H., Rossignol, S., Grillner, S.** 1988. *Neural Control of Rythmic Movements in Vertebrates*. Miley, New York.
19. **Costerton, J. W., B. Ellis, K. Lam, F. Johnson, and A. E. Khoury.** 1994. Mechanism of Electrical Enhancement of Efficacy of Antibiotics in Killing Biofilm Bacteria. *Antimicrobial Agents and Chemotherapy* **38**:2803-2809.
20. **Costerton, J. W., G. G. Geesey, and K. J. Cheng.** 1978. How Bacteria Stick. *Scientific American* **238**:86-&.
21. **Costerton, J. W., P. S. Stewart, and E. P. Greenberg.** 1999. Bacterial biofilms: A common cause of persistent infections. *Science* **284**:1318-1322.
22. **Crubezy, E., P. Murail, L. Girard, and J. P. Bernadou.** 1998. False teeth of the Roman world. *Nature* **391**:29.

-
23. **Cruse, P.** 1980. The epidemiology of wound infection. *Surg Clin North Am* **60**:27-40.
 24. **Deterlin, R. A., Bhonslay, S.B.** 1955. An evaluation of synthetic materials and fabrics suitable for blood vessels replacement. *surgery* **38**:71-76.
 25. **Ebbell, B.** 1937. The Ebers papyrus. The greatest Egyptian medical document. Oxford University Press, Oxford.
 26. **Edelman, G. M.** 1987. Neural Darwinism. Basic Books Inc., New York.
 27. **Edwards, W. S.** 1962. hemically treated Nylon tubes as arterial grafts. *Surgery* **38**:61-67.
 28. **Faddis, D., D. Daniel, and J. Boyer.** 1977. Tissue toxicity of antiseptic solutions. A study of rabbit articular and periarticular tissues. *J Trauma* **17**:895-7.
 29. **Fraenkel, G. J.** 1998. Penicillin at the beginning. *Ann Diagn Pathol* **2**:422-4.
 30. **Freeman, W. J.** 1994. Neural networks and chaos. *J Theor Biol* **171**:13-8.
 31. **Fry, W. J., and Lindenau.Sm.** 1967. Infection Complicating Use of Plastic Arterialimplants. *Archives of Surgery* **94**:600-&.
 32. **Galland, P., and A. Pazur.** 2005. Magnetoreception in plants. *J Plant Res* **118**:371-89.
 33. **Giessler, R.** 1980. [Anastomosis-aneurysms following synthetic vascular replacement]. *Chirurg* **51**:14-8.
 34. **Gilmore, O. J.** 1977. A reappraisal of the use of antiseptics in surgical practice. *Ann R Coll Surg Engl* **59**:93-103.
 35. **Glasser, S.** 1977. Computer reconstruction and passive modeling of identified nerve cells in the lobster stomatogastric ganglion. University of California, San diego.
 36. **Grigg, T. R., F. R. Liewehr, W. R. Patton, T. B. Buxton, and J. C. McPherson.** 2004. Effect of the wicking behavior of multifilament sutures. *J Endod* **30**:649-52.
 37. **Gristina, A. G.** 1994. Implant failure and the immuno-incompetent fibro-inflammatory zone. *Clin Orthop Relat Res* **298**:106-18.
 38. **Gross, G. W., B. K. Rhoades, H. M. Azzazy, and M. C. Wu.** 1995. The use of neuronal networks on multielectrode arrays as biosensors. *Biosens Bioelectron* **10**:553-67.
 39. **Gross, G. W., E. Rieske, G. W. Kreutzberg, and A. Meyer.** 1977. A new fixed-array multi-microelectrode system designed for long-term monitoring of extracellular single unit neuronal activity in vitro. *Neuroscience Letters* **6**:101-105.
 40. **Guttman, B., Guttman, H.** 1994. Polymeric Biomaterials, New York.
 41. **Harris, L. G., and R. G. Richards.** 2006. Staphylococci and implant surfaces: a review. *Injury* **37 Suppl 2**:S3-14.
 42. **Harrison, J. H.** 1958. Synthetic materials as vascular prostheses. A comparative study in small vessles of Nylon, Dacron, Orlon, Ivalon, Sponge and Teflon. *Am J Surg* **35**:3-9.
 43. **Hastings, G., Ducheyne, P.** 1984. Eds. *Macromolecular Biomaterials (CRC Press, Boca Raton, FL, 1984)*.
 44. **Heberer, G., Dongen van, R.J.A.M.** 1987. *Gefäßchirurgie, Kirschnersche allgemeine und spezielle Operationslehre.* Springer Verlag, Berlin, Heidelberg, New York.
 45. **Heller, J.** 1984. Biodegradable polymers in controlled drug delivery. *Crit Rev Ther Drug Carrier Syst* **1**:39-90.
 46. **Hench, L. L.** 1998. Bioceramics. *Journal of the American Ceramic Society* **81**:1705-1728.
 47. **Hench, L. L.** 1980. Biomaterials. *Science* **208**:826-31.
 48. **Hench, L. L., and J. M. Polak.** 2002. Third-Generation Biomedical Materials 10.1126/science.1067404. *Science* **295**:1014-1017.
 49. **Hench, L. L., and J. Wilson.** 1984. Surface-active biomaterials. *Science* **226**:630-6.
 50. **Hench, L. L., Wilson, J.** 1996. Clinical Performance of Skeletal Prostheses, vol. chaps. 13 and 15.

51. **Hyde, J. A. J., R. O. Darouiche, and J. W. Costerton.** 1998. Strategies for prophylaxis against prosthetic valve endocarditis: A review article. *Journal of Heart Valve Disease* **7**:316-326.
52. **Javid, H., O. C. Julian, W. S. Dye, and J. A. Hunter.** 1962. Complications of Abdominal Aortic Grafts. *Archives of Surgery* **85**:650-662.
53. **Jenkins, W. M., M. M. Merzenich, M. T. Ochs, T. Allard, and E. Guic-Robles.** 1990. Functional reorganization of primary somatosensory cortex in adult owl monkeys after behaviorally controlled tactile stimulation. *J Neurophysiol* **63**:82-104.
54. **Jimbo, Y. R., H.P.C., Kawana, A.** 1992. Presented at the Proc. 14th Conf.
55. **Kaas, J. H.** 1991. Plasticity of sensory and motor maps in adult mammals. *Annu Rev Neurosci* **14**:137-67.
56. **Kettenmann, H. G., R.** 1992. *Practical Electrophysiological Methods*. Wiley-Liss, New York.
57. **Koning, K., Barwegen, G.M.H., Berge Henegouven van, D.P.** 1980. Die Behandlung von Infektionen nach arteriellen Gefäßrekonstruktionen. *Angio* **4**:269-75.
58. **Korber, D. R., Lawrence, J.R., Lappin-Scott, H.M., Costerton, J.W.** 1995. Growth of microorganisms on surfaces., p. 15-45. *In* H. M. Lappin-Scott, Costerton, J.W. (ed.), *Microbial Biofilms*. Cambridge University Press, Cambridge UK.
59. **Kraus, W.** 1984. [Magnetic field therapy and magnetically induced electrostimulation in orthopedics]. *Orthopade* **13**:78-92.
60. **Leaper, D. J., Pritchett, C.J.** 1989. Prophylactic antibiotics in general surgical practice. *Curr. Pract. in Surg.* **1**:178-84.
61. **Leid, J. G., M. E. Shirliff, J. W. Costerton, and P. Stoodley.** 2002. Human leukocytes adhere to, penetrate, and respond to *Staphylococcus aureus* biofilms. *Infection and Immunity* **70**:6339-6345.
62. **Leriche, R.** 1956. [Jaboulay and experimental researches on vascular sutures, grafts and shunts.]. *Lyon Chir* **51**:21-3.
63. **Lilly, H. A., E. J. Lowbury, and M. D. Wilkins.** 1979. Limits to progressive reduction of resident skin bacteria by disinfection. *J Clin Pathol* **32**:382-5.
64. **Lindner, J. H., P.** 1983. Zur Morphologie und Biochemie der Wundheilung: Eine Übersicht. *Haemostasiologie* **1**:8-40.
65. **Lineaweaver, W., R. Howard, D. Soucy, S. McMorris, J. Freeman, C. Crain, J. Robertson, and T. Rumley.** 1985. Topical antimicrobial toxicity. *Arch Surg* **120**:267-70.
66. **Lorentzen, J. E., O. M. Nielsen, H. Arendrup, H. H. Kimose, S. Bille, J. Andersen, C. H. Jensen, F. Jacobsen, and O. C. Roder.** 1985. Vascular graft infection: an analysis of sixty-two graft infections in 2411 consecutively implanted synthetic vascular grafts. *Surgery* **98**:81-6.
67. **Lubbe, A. S., C. Bergemann, H. Riess, F. Schriever, P. Reichardt, K. Possinger, M. Matthias, B. Dorken, F. Herrmann, R. Gurtler, P. Hohenberger, N. Haas, R. Sohr, B. Sander, A. J. Lemke, D. Ohlendorf, W. Huhnt, and D. Huhn.** 1996. Clinical experiences with magnetic drug targeting: a phase I study with 4'-epidoxorubicin in 14 patients with advanced solid tumors. *Cancer Res* **56**:4686-93.
68. **Marrie, T. J., and J. W. Costerton.** 1984. Scanning and Transmission Electron-Microscopy of Insitu Bacterial-Colonization of Intravenous and Intraarterial Catheters. *Journal of Clinical Microbiology* **19**:687-693.
69. **Marrie, T. J., J. Nelligan, and J. W. Costerton.** 1982. A Scanning and Transmission Electron-Microscopic Study of an Infected Endocardial Pacemaker Lead. *Circulation* **66**:1339-1341.

-
70. **Marshall, K. C., R. Stout, and R. Mitchell.** 1971. Selective Sorption of Bacteria from Seawater. *Canadian Journal of Microbiology* **17**:1413-&.
 71. **Nelson, J. L., B. L. Roeder, J. C. Carmen, F. Roloff, and W. G. Pitt.** 2002. Ultrasonically activated chemotherapeutic drug delivery in a rat model. *Cancer Research* **62**:7280-7283.
 72. **Perea, H., J. Aigner, J. T. Heverhagen, U. Hopfner, and E. Wintermantel.** 2007. Vascular tissue engineering with magnetic nanoparticles: seeing deeper. *J Tissue Eng Regen Med* **1**:318-21.
 73. **Peterson, A. F., A. Rosenberg, and S. D. Alatary.** 1978. Comparative evaluation of surgical scrub preparations. *Surg Gynecol Obstet* **146**:63-5.
 74. **Pircher, W., Kessler, B., Rühland, D., Stegemann, B.** 1979/1980. Infektionen in der rekonstruktiven Gefäßchirurgie. *Chir Praxis* **26**:593 -600.
 75. **Pollock, A. V., and M. Evans.** 1975. Povidone-iodine for the control of surgical wound infection: a controlled clinical trial against topical cephaloridine. *Br J Surg* **62**:292-4.
 76. **Ratner, B. D., Hoffman, A.S., Schoen, F.J., Lemons, J.E.** 2004. *Biomaterials Science*. Elsevier Academic Press.
 77. **Rediske, A. M., W. C. Hymas, R. Wilkinson, and W. G. Pitt.** 1998. Ultrasonic enhancement of antibiotic action on several species of bacteria. *Journal of General and Applied Microbiology* **44**:283-288.
 78. **Rhoades, B. K., Gross, G.W.** 1991. The effects of extracellular potassium on epileptiform burst dynamics in cultured monolayer networks. *Soc. Neurosci. (Abstr.)* **17**.
 79. **Rhoades, B. K., Gross, G.W.** 1992. Patterned electrical stimulation of cultured neuronal networks on multielectrode plates. *Soc. Neurosci. (Abstr.)* **18**.
 80. **Salthouse, T. N., and B. F. Matlaga.** 1976. Polyglactin 910 suture absorption and the role of cellular enzymes. *Surg Gynecol Obstet* **142**:544-50.
 81. **Sandmann, W., and K. Kremer.** 1983. Material Problems in Vascular-Surgery. *Chirurg* **54**:433-443.
 82. **Sandmann, W., Staskiewicz, w., Wildeshaus, K.H., Lenz, W., Peronneau, P.** 1979. Gefäßnähte mit resorbierbarem Nahtmaterial: Röntgenologische, hämodynamische, licht- und elektronenmikroskopische Befunde. *Langenbecks Arch Chir (Suppl) Chir Forum* **79**:1-6.
 83. **Sandmann, W., Torsello, G., Kaschner, A., Lindemann, A., Lenz, G.** 1982. Experimentelle Ergebnisse und klinische Erfahrungen mit PGS-Fäden in der Arterienchirurgie., p. 70-80. *In* A. Thiede, Hamelmann, H., (ed.), *Moderne Nahtmaterialien und Nahttechniken in der Chirurgie*. Springer Verlag, Berlin, Heidelberg, New York.
 84. **Sauer, K., and A. K. Camper.** 2001. Characterization of phenotypic changes in *Pseudomonas putida* in response to surface-associated growth. *Journal of Bacteriology* **183**:6579-6589.
 85. **Sauer, K., A. K. Camper, G. D. Ehrlich, J. W. Costerton, and D. G. Davies.** 2002. *Pseudomonas aeruginosa* displays multiple phenotypes during development as a biofilm. *Journal of Bacteriology* **184**:1140-1154.
 86. **Schmelzeisen, H.** 1979. [Infected pseudoarthrosis of the tibial shaft - clinical study of 252 cases]. *Hefte Unfallheilkd* **138**:167-8.
 87. **Schmit-Neuerburg, K. P., K. M. Sturmer, H. Kehr, D. Ullrich, and H. Hirche.** 1980. [The influence of alternating current on the incorporation of autologous cancellous bone grafts in experimental nonunions (author's transl)]. *Unfallheilkunde* **83**:195-201.
 88. **Schmitzrixen, T., S. Horsch, B. Klein, and H. Pichlmaier.** 1984. Experiments in Animals in Vascular-Surgery with a New Single-Strand Absorbable Suture Material. *Langenbecks Archiv Fur Chirurgie* **362**:53-60.

89. **Schoen, F. J., Levy, R.J., Piehler, H.R.** 1992. *J. Soc. Cardiovasc. Pathol.* **1**.
90. **Semmelweis, I. P.** 1974. A corner of history. Ignaz Philipp Semmelweis. *Prev Med* **3**:574-80.
91. **Sottile, F. D., T. J. Marrie, D. S. Prough, C. D. Hobgood, D. J. Gower, L. X. Webb, J. W. Costerton, and A. G. Gristina.** 1986. Nosocomial Pulmonary Infection - Possible Etiologic Significance of Bacterial Adhesion to Endotracheal-Tubes. *Critical Care Medicine* **14**:265-270.
92. **Stoodley, P., K. Sauer, D. G. Davies, and J. W. Costerton.** 2002. Biofilms as complex differentiated communities. *Annual Review of Microbiology* **56**:187-209.
93. **Svensater, G., J. Welin, J. C. Wilkins, D. Beighton, and I. R. Hamilton.** 2001. Protein expression by planktonic and biofilm cells of *Streptococcus mutans*. *Fems Microbiology Letters* **205**:139-146.
94. **Swanson, N. A., and T. A. Tromovitch.** 1982. Suture materials, 1980s: properties, uses, and abuses. *Int J Dermatol* **21**:373-8.
95. **Szilagyi, D. E., Vrandeci.Mp, R. F. Smith, and J. P. Elliott.** 1972. Infection in Arterial Reconstruction with Synthetic Grafts. *Annals of Surgery* **176**:321-&.
96. **Taylor, E. W.** 1992. General principles of antibiotic prophylaxis. *In* E. W. Taylor (ed.), *Infection in surgical practice*. Oxford University Press, Oxford.
97. **Thiede, A., U. Dietz, and S. Debus.** 2002. [Clinical application--suture materials]. *Kongressbd Dtsch Ges Chir Kongr* **119**:276-82.
98. **Trout, H. H., L. Kozloff, and J. M. Giordano.** 1984. Priority of Revascularization in Patients with Graft Enteric Fistulas, Infected Arteries, or Infected Arterial Prostheses. *Annals of Surgery* **199**:669-683.
99. **van Loosdrecht, M. C., W. Norde, and A. J. Zehnder.** 1990. Physical chemical description of bacterial adhesion. *J Biomater Appl* **5**:91-106.
100. **Varma, S., H. L. Ferguson, H. Breen, and W. V. Lumb.** 1974. Comparison of 7 Suture Materials in Infected Wounds - Experimental Study. *Journal of Surgical Research* **17**:165-170.
101. **Viljanto, J.** 1980. Disinfection of surgical wounds without inhibition of normal wound healing. *Arch Surg* **115**:253-6.
102. **Vollmar, J., and A. Buettneristow.** 1976. Diagnostic and Clinical Aspects of Septic Complications in Vascular Surgery. *Langenbecks Archiv Fur Chirurgie* **342**:505-509.
103. **Vollmar, J. F., Hepp, W., Voss, E.U.** 1981. Das infizierte Gefäßimplantat - Entfernung oder Erhaltung? *Aktuel Chir* **16**:86-92.
104. **Vorhees, A., Jaretski, A., Blakemore, A.H.** 1952. Use of tubes constructed from Vinyon-N-cloth in bridging arterial defects. *Ann Surg* **135**:332-336.
105. **Weber, T. R., S. M. Lindenauer, T. A. Miller, C. A. Salles, S. Ramsburgh, and P. Gleich.** 1976. Focal infection of aortofemoral prostheses. *Surgery* **79**:310-2.
106. **Weselowski, S. A., Sauvage, L.R.** 1956. Comparison of the fate of Orlon mesh prosthetic replacement of the thoracic aorta and bifurcation. *Ann Surg* **143**:65-70.
107. **Williams, D. F.** 1988. Consensus and definitions in biomaterials. *Advances in biomaterials* **8**:11-16.
108. **Wintermantel, H. S.-W.** 2002. *Medizintechnik mit biokompatiblen Werkstoffen und Verfahren*. Springer-Verlag, Berlin Heidelberg New York.
109. **Wroblewski, B. M., P. A. Fleming, and P. D. Siney.** 1999. Charnley low-frictional torque arthroplasty of the hip. 20-to-30 year results. *J Bone Joint Surg Br* **81**:427-30.
110. **Yashar, J. J., A. K. Weyman, R. J. Burnard, and J. Yashar.** 1978. Survival and Limb Salvage in Patients with Infected Arterial Prostheses. *American Journal of Surgery* **135**:499-504.

111. **Zühlke, H. V., Harnoss, B.-M., Lorenz, E.P.M.** 1994. Septische Gefäßchirurgie, 2 ed. Blackwell Wissenschaft, Berlin.

Chapter 2

New anti-infective coatings of medical implants based on lipid-like drug carriers

Abstract

Objectives: Implantable devices are highly susceptible to infection and therefore a major risk in surgery. The present work presents a novel strategy to prevent formation of a biofilm on PTFE grafts.

Methods: PTFE grafts were coated with gentamicin and teicoplanin incorporated in different lipid-like carriers under aseptic conditions in a dipping process. Poly-D, L-lactic acid, tocopherol acetate, the diglyceride Softisan[®] 649 and the triglyceride Dynasan[®] 118 were used as drug carriers. Drug release kinetics, anti-infective characteristics, biocompatibility and haemocompatibility of developed coatings were studied.

Results: All coatings showed an initial drug burst followed by a low continuous drug release over 96 hours. The dimension of release kinetics depended on the carrier used. All coated prostheses reduced bacterial growth even beyond pathologically relevant concentrations drastically over 24 hours. Different cytotoxic levels could be observed bringing up tocopherol acetate as the most promising biocompatible carrier. A possible reason for the highly cytotoxic effect of Softisan[®] 649 could be assessed by demonstrating incorporated lipids in the cell soma with the oil red O staining. The performance of tromboelastography studies, ELISA assays and an amidolytic substrate assay could confirm haemocompatibility of individual coatings.

Conclusions: The development and in vitro studies of described biodegradable drug delivery systems highlight the most important requirements for an effective as well as compatible anti-infective equipment of PTFE grafts. Through continuous local release, high drug levels can be obtained at only the targeted area, physiological bacterial proliferation can completely be inhibited while at the same time biocompatibility as well as haemocompatibility can be ensured.

Keywords: Vascular graft, antimicrobial coating, drug release, biocompatibility, haemocompatibility

1 Introduction

A major risk associated with surgical placement of medical implants such as endoprotheses or vascular prostheses is their high infection rate (4, 8). This is not only of prime importance for the patient, but also presents a high financial factor for the economy (21). Synthetic vascular grafts like PTFE prostheses are easily accessible to pathogens mostly belonging to *Staphylococcus aureus* and *Staphylococcus epidermidis*. These pathogens colonize the implant by adhering to the patients own proteins located on the surface of the graft and form a biofilm (1, 14, 16, 23, 34). The formation of biofilms on biomaterials present challenging complications in the field of medical implants (2, 12, 24, 28, 30). In a biofilm bacteria are well protected from the host immune defence. An increase in antibiotic resistance is the consequence (6, 8, 35), even high local concentrations of antibiotics do not completely eradicate bacteria in biofilms (8, 10). It is therefore of high importance to prevent bacterial adhesion on vascular grafts (7). This can be achieved by antibiotic surface coatings.

There have been several approaches to equip vascular grafts with anti-infective agents to avoid bacterial colonization. Different antimicrobial agents have been used (3, 5) as well as different ways to bind those drugs on the surface of a PTFE prostheses.

A common method used to bind hydrophilic drugs on the lipophilic surface of PTFE grafts is the use of surfactant-mediated agents e.g. benzalkonium chloride (15, 18) or tridodecylmethylammonium chloride (17). Another way of drug binding is the incorporation of drugs in biodegradable polymer carriers (13).

The present work presents new lipid-based formulations to incorporate antibiotics for anti-infective graft equipment. Through local release, high drug levels can be attained at only the targeted area and a pathogenic colonization of the graft can be avoided. PTFE grafts were coated with lipophilic agents like Poly-D,L-lactic acid (PDLLA), tocopherol acetate, the diglyceride Softisan[®] 649 and the triglyceride Dynasan[®] 118 as carriers for gentamicin and teicoplanin. An overall in vitro study assessing release kinetics as well as cytotoxicity, anti-infective characters and haemocompatibility of the corresponding coatings was examined.

2 Materials and Methods

2.1 Medical implant

Commercially available PTFE grafts of 6 mm diameter (Alpha Graft[®] PTFE, Alpha Research Deutschland GmbH, Berlin, Germany) were studied. Sterile grafts were cut into 1 cm length under aseptic conditions in a laminar airflow. The average weight of four 1 cm samples was assessed by weighing each sample three times as weight standards are more accurate than length measurements.

2.2 The anti-infective coating

2.2.1 Drug carriers

A defined mass of each of the following drug carriers was weighed out in a glass vial.

2.2.2 PDLA

Resomer R203H purchased from Boehringer Ingelheim (Ingelheim, Germany) is a polymer of PDLA of 29,000 Da molecular weight. It is a racemic mixture of D- and L-enantiomers of lactic acid and is well studied as a biodegradable coating for medical implants.

2.2.3 Softisan[®] 649

Softisan[®] 649 (Sasol Germany GmbH, Witten, Germany) is a partial ester of diglycerin containing medium chain fatty acids, isostearic acid, stearic acid 12-hydroxystearic acid and adipic acid. It can be sterilized by heat and has a stable viscosity from 25 °C to 75 °C similar to that of lanolin. In the following it is termed as DG for diglyceride.

2.2.4 Dynasan[®] 118

Dynasan[®] 118 (Sasol Germany GmbH, Witten, Germany) is a tristearin and is often used in the pharmaceutical and cosmetic industry as adjuvants in preparations. Its melting range according to SOP 0540 (Sasol Germany GmbH, Witten, Germany) is 70 °C to 74 °C and it is stable against oxidation. In the following it is termed as TG for triglyceride.

2.2.5 Tocopherol acetate

Tocopherol acetate (Sigma-Aldrich AG, Deisenhofen, Germany) is termed as TA.

2.2.6 Antibiotics

Gentamicin sulfate (Fa. Heraeus, Holding GmbH, Hanau, Germany) and teicoplanin (Fa. Heraeus, Holding GmbH, Hanau, Germany) were lyophilized and suspended in chloroform (Sigma-Aldrich AG, Deisenhofen, Germany) in case of PDLLA, DG and TG and in 99 % ethanol (Sigma-Aldrich AG, Deisenhofen, Germany) in case of TA at a concentration of 22.9 mg/mL. To decrease the particle size, suspensions were homogenized for five minutes (Hand homogenizer, Sartorius AG, Göttingen, Germany). The resulting suspension was added to the drug carriers building up a drug concentration of ten percent.

2.3 Coating process

Four different drug carriers were used for incorporating gentamicin sulfate as well as teicoplanin in a concentration of ten percent. The implants were coated by two dip-coating procedures ensuring a regular polymer coating and are termed in the following as drug-carrier-coated PTFE prostheses. Dip-coating procedure was carried out in sterile sealable glass vials in presence of a magnetic stir bar on a magnetic stirrer (IKA, RET basic IKAMAG[®]) for 5 min following a drying period of 5 min between both coating procedures. All coating steps were carried out under aseptic conditions in a laminar air-flow hood. For cytotoxicity tests, grafts were additionally coated with the drug carriers without drug in the same way and are termed in the following as carrier-coated PTFE prostheses. The weight of each coating as well as the amount of incorporated drug was assessed by weight difference of PTFE grafts before and after the coating procedure. As the surface of PTFE prostheses is not

plane and regular and shows many pores, the thickness of individual coatings could not be reliably determined. In order to control reproducibility of the quantity of coating and the drug dose per sample and to minimize mistakes caused by 1 cm samples of PTFE prostheses inexact in length, the weights of PTFE prostheses before and after coating procedure were assessed and a coating quotient was established. The coating quotient is defined as the ratio between the weight of coating and the weight of 1 cm uncoated PTFE prostheses of this individual coating process: $m_{\text{coating}} / m_{\text{PTFE prosthesis}}$. The coating quotient is termed in the following as Q_c . For each developed coating the Q_c was obtained for 10 samples.

2.4 Particle size

The median particle size of untreated drug, lyophilized drug and drug after lyophilisation in combination with homogenization was determined by a particle size meter (Zetasizer Nano SZ, Malvern Instruments, Malvern UK). Particle size after lyophilisation and homogenization averaged 15.7 μm for gentamicin and 21.1 μm for teicoplanin. These data are confirmed by SEM studies.

2.5 Morphological analysis-SEM

Coated PTFE prostheses were prepared for SEM by sputtering with Gold (BAL-TEC MED 020 coating system, Boeckeler Instruments, Arizona, USA) and examined with a high vacuum SEM (JSM 6060LV Scanning Electron Microscope, JEOL Ltd., Tokyo, Japan).

2.6 Antibiotic release

Drug release from drug-carrier-coated PTFE prostheses ($n=3$, length 1 cm, diameter 6 mm) was studied in phosphate-buffered saline (PBS) at 37 °C (pH 7.4) at 300 rpm in a Thermomixer (Fa. Eppendorf, Hamburg, Germany). The rotation was preferred to static state to simulate blood flow conditions in the vascular system. Uncoated PTFE prostheses served as control. At the time points 15 minutes, 1, 4, 8, 24, 48, 72 and 96 hours elution medium was completely changed. Sample drug solutions were assayed for gentamicin by spectroscopy. Therefore gentamicin was treated with 1.25 % aqueous ninhydrin solution at 95 °C for 15 min

and absorption was measured at 405 nm. Teicoplanin concentrations were determined by Innofluor Teicoplanin assay system (Opus Diagnostics, Fort Lee, USA).

2.7 Test bacterium

For in vitro studies a clinical isolate of *S. aureus* (strain ATCC[®] 49230) was used. The test strain was susceptible to both gentamicin (MIC 0.5 mg/l) and teicoplanin (MIC 0.25 mg/l). *S. aureus* was cultured on columbia agar plates (Becton Dickinson GmbH, Heidelberg, Germany) at 37 °C for 18 hours before testing.

2.7.1 Growth curve

In order to correlate the optical density at 600 nm (GeneQuant pro, biochrom, Cambridge, UK) of a *S. aureus* suspension with the colony forming units of the microorganism, a growth curve was recorded at different time points in Mueller-Hinton broth (No. 275730, BD Diagnostic Systems, Difco[™], Heidelberg, Germany) at 37 °C. A logarithmic regression curve with the formula $OD=0.0741 \ln(cfu)-0.2066$ and a correlation coefficient of 0.91 resulted.

2.7.2 Antibacterial characteristics

In order to assess antibiotic efficacy at pathologically relevant concentrations (11), bacterial suspensions with 1×10^2 , 1×10^3 , 1×10^4 cfu/ml were prepared and incubated with 1 cm of drug-carrier-coated prostheses for 24 hours at 37 °C. 1 ml of each sample was added to 9 ml of Mueller-Hinton broth and incubated for another 24 hours at 37 °C. The optical density of the obtained suspensions and colony forming units on blood agar plates were determined for each sample and reference.

In order to investigate the antimicrobial potential of drug-carrier-coated grafts, a hundredfold concentration of the commonly observed pathological concentration (1×10^4 cfu/ml) was chosen. Aseptically drug-carrier-coated PTFE prostheses (n=3, length 1 cm) as well as sterile uncoated PTFE prostheses as reference were added to 50 ml of *S. aureus* suspensions (2×10^6 cfu/ml) and the optical density was measured at defined time intervals.

2.7.3 Adhesion of viable bacteria and antimicrobial potency after 24 hours elution

After incubation of drug-carrier-coated PTFE prostheses in a suspension of *S. aureus* (2×10^6 cfu/ml) for 24 hours, prostheses were removed and washed twice with isotonic NaCl. To determine the quantity of germs adsorbed, washed prostheses were placed into an ultrasonic bath of 1 ml of isotonic NaCl for ten minutes. 100 μ l of the bacterial suspension obtained were plated on blood agar plates. For reference prostheses two dilution steps of 1 to 10 were carried out additionally expecting a high amount of adhered pathogens. Blood agar plates were incubated for 18 h at 37 °C and colony forming units were visually determined and extrapolated to the initial number of adsorbed pathogens. Uncoated reference prostheses were treated the same way.

To determine whether drug-carrier-coated prostheses still retained anti-infective characteristics after the initial drug burst, drug-carrier-coated prostheses (n=3, length 1 cm) were eluted for 24 h in phosphate-buffered saline (PBS) at 37 °C (pH 7.4) at 300 rpm in a Thermomixer and placed on bacterial lawns cultured on Mueller-HintonII-agar plates (No. 221177 BD Diagnostic System, Heidelberg, Germany).

2.8 Cell culture

Mouse connective tissue fibroblasts L929 were kindly provided by the ITEM GmbH – The Biotooling Company (Garching, Germany) and maintained in RPMI 1640 medium supplemented with 10 % fetal bovine serum, penicillin and streptomycin (100 U/ml and 0.1 mg/ml, respectively), parturicin (50 μ g/ml) and stable glutamine at 37 °C in a humidified atmosphere containing 5 % CO₂.

2.9 In vitro cytotoxicity studies

Cytotoxicity tests were carried out with L929 fibroblasts from mouse connective tissue. Developed drug-carrier-coated PTFE prostheses as well as carrier-coated PTFE prostheses were studied. In order to achieve the optimal ratio between the inner surface area of the grafts and the area of cell culture, grafts were cut into 0.33 cm pieces (n=3). Subsequently cells were cultured in 96-well microplates in presence of uncoated, carrier-coated and drug-carrier-coated PTFE prostheses were immersed in 200 μ l medium. Cells were cultured until

subconfluence, prostheses were taken out of the microplates and metabolic activity of viable cells was measured with the Roche cell proliferation reagent WST-1 (Roche Diagnostics GmbH, Mannheim, Germany).

In order to analyze the toxicity of the drugs themselves, cells were cultured in 96-well microplates in presence of different concentrations of gentamicin and teicoplanin until subconfluence followed by a Roche cell proliferation reagent WST-1 test.

For determination of fatty inclusions in the cell soma, cells were cultured in 96-well microplates in presence of coated PTFE prostheses (n=3, length 1cm) until subconfluence. Subsequently, cells were fixed with 50 % ethanol, treated with Oil Red O reagent (Sigma-Aldrich AG, Deisenhofen, Germany) for 10 minutes at 4 °C and after washing with 50 % ethanol incubated in PBS. LM-micrographs were taken from sample and reference cells.

2.10 Haemocompatibility studies

Blood tests were carried out to study thrombogenic characteristics of individual coatings. Therefore 1 cm of sample and reference grafts were incubated for eight minutes in four ml freshly drawn non anticoagulated human whole blood in 15 ml conical centrifugal tubes (Carl Roth, Karlsruhe, Germany). Incubated blood was anticoagulated with trisodium citrate as well as EDTA and plasma was generated. In order to get information about a modified coagulation different coagulation factors were determined. Citrated blood plasma was examined with an amidolytic substrate assay for factor XIIa-like activity (Unitest™ FXIIA, Unicorn Diagnostics Ltd, Kent, UK) as well as by a monoclonal enzyme immunoassay for plasma F₁₊₂ values (Enzygnost F₁₊₂ micro, Behring, Marburg, Germany). EDTA blood plasma was tested for C3a-desArg (Complement C3a-desArg ELISA, Progen Biotechnik GmbH, Heidelberg, Germany). A thromboelastography for whole blood was carried out with a roTEG Coagulation Analyser (Pentapharm GmbH, Munich, Germany) using the in-TEM® (Pentapharm GmbH, Munich, Germany) for analysing the intrinsic pathway of blood coagulation.

3 Results

3.1 Morphological analysis

Stable and regular coatings could be observed through SEM after dip-coating. All coated grafts kept their flexibility and open pores for both side penetrations (Figure 1A – D).

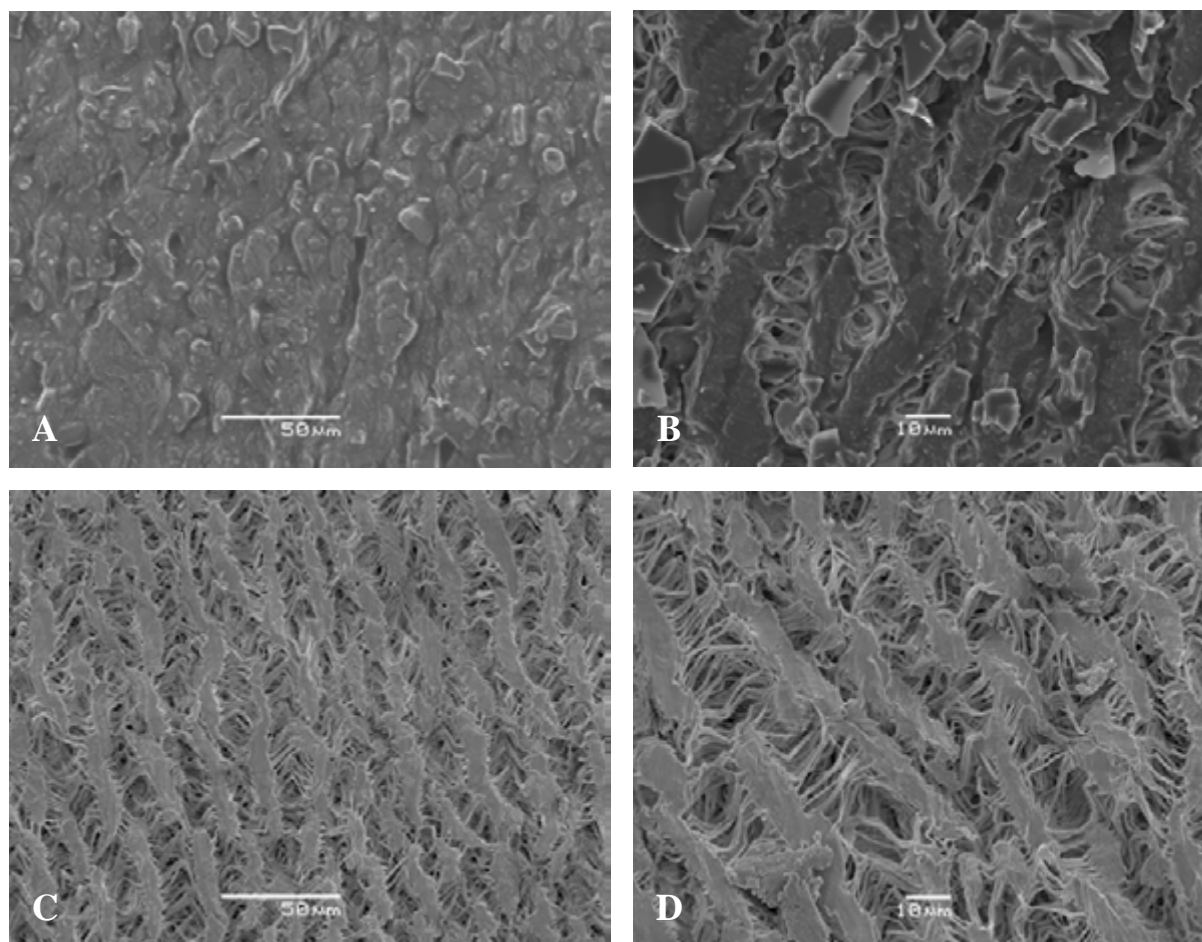


Figure 1. SEM pictures of the inner surface of a PTFE prostheses coated with gentamicin 10 % in tocopherol acetate: A) magnification 500; B) magnification 1500 and uncoated PTFE prostheses: C) magnification 500; D) magnification 1500.

3.2 Antibiotic release

The weights of used PTFE prostheses of a size of 1 cm averaged 76.80 mg and varied by more than ten percent concluding that measuring 1 cm lengths of PTFE prostheses is less accurate than weighing. Coatings consisting of PDLLA with incorporated gentamicin showed

an average Q_c of 0.52 corresponding to a coating weight of 39.94 mg relating as the following given coating weights to the average 1 cm PTFE prostheses, whereas the Q_c of coatings consisting of PDDL A with incorporated teicoplanin averaged at 0.32 corresponding to a coating weight of 24.58 mg. Tocopherol acetate based coatings showed a Q_c of 0.25 (coating weight of 19.2 mg) in case of incorporated gentamicin and 0.23 (coating weight of 17.67 mg) in case of teicoplanin. Q_c of coatings with DG averaged at 0.24 (coating weight of 18.43 mg) for incorporated gentamicin and at 0.25 (coating weight of 19.2 mg) for incorporated teicoplanin. The coatings consisting of TG with gentamicin showed a Q_c of 0.29 (coating weight of 22.72 mg) and in case of teicoplanin a Q_c of 0.31 (coating weight of 23.81 mg) (Figure 2). Reliable reproducibility of coating procedure was demonstrated with TA, DG and TG. Average Q_c of PDDL A with incorporated gentamicin is statistically different than average Q_c of PDDL A with incorporated teicoplanin.

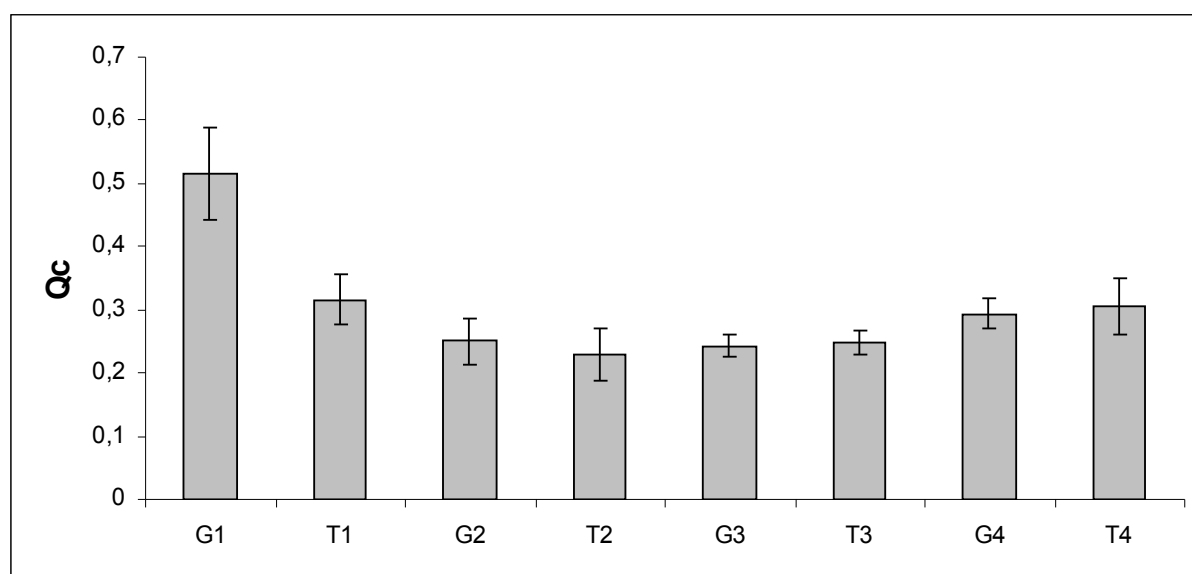


Figure 2. Individual coating quotients Q_c defined as the ratio between the weight of coating and the weight of a 1 cm uncoated PTFE prosthesis of this individual coating process: $m_{\text{coating}} / m_{\text{PTFE prosthesis}}$.

G1 \wedge = gentamicin 10 % in PDDL A, *G2* \wedge = gentamicin 10 % in tocopherol acetate, *G3* \wedge = gentamicin 10 % in Softisan[®] 649, *G4* \wedge = gentamicin 10 % in Dynasan[®] 118, *T1* \wedge = teicoplanin 10 % in PDDL A, *T2* \wedge = teicoplanin 10 % in tocopherol acetate, *T3* \wedge = teicoplanin 10 % in Softisan[®] 649, *T4* \wedge = teicoplanin 10 % in Dynasan[®] 118

To obtain information about time - dependant drug kinetics, the release rates (defined as the total amount of released drug in microgram per hour) of gentamicin/teicoplanin present in the respective carriers were plotted against time. Continuous drug release kinetics could be demonstrated over 96 hours for the four individual carriers (PDDL A, TA, DG, TG). In the first hour an initial drug burst was observed followed by a low continuous release of

gentamicin for the rest of the testing interval. The carriers TA and DG showed comparable release rates for incorporated gentamicin after 15 minutes between 2403.1 $\mu\text{g/h}$ and 2121.6 $\mu\text{g/h}$. For gentamicin in PDLLA, a much higher release rate after 15 minutes of 4528.0 $\mu\text{g/h}$ could be assessed whereas the lowest release rate of 1167.0 $\mu\text{g/h}$ was detected for gentamicin in TG. After 96 hours, release rates for all four individual carriers varied between 0.5 $\mu\text{g/h}$ in case of PDLLA and 0.1 $\mu\text{g/h}$ in case of TG.

For Teicoplanin an initial drug burst in the first hour was detected following a continuous drug release for the rest of the testing time. Release rates after 15 minutes of the four individual carriers varied between 6090.0 $\mu\text{g/h}$ for PDLLA and 1477.7 $\mu\text{g/h}$ for TA decreasing almost exponentially.

Continuous drug release over 96 hours fulfils the primary aim of developing an effective anti-infective method for post-operative protection against infection. The total amount of the drug is expected to be released as the lipid-based carrier degrades over one to six months which implies an extended protection for this period of time.

Gentamicin and teicoplanin each showed a distinct pattern of drug release using the four different lipid-based carriers. Gentamicin and teicoplanin were stable in PBS in experiments for at least 96 hours.

3.3 Antibacterial characteristics

Continuous antibiotic release for more than one day after a surgical procedure is one important aspect, but the key characteristic is the antibacterial effect. Individual coatings showed a highly effective potency against pathologically relevant *S. aureus* concentrations in a range of 10^2 to 10^4 cfu/ml. There was no difference between OD values from samples and sterile Mueller-Hinton medium. Colony growth on agar plates incubated with sample medium could not be observed with each of the individual coatings concluding a total germ eradication caused by individual coatings.

Bacterial growth in highly concentrated bacterial suspensions of 2×10^6 cfu/ml could be reduced by all developed drug-carrier-coated PTFE prostheses. In all cases using gentamicin, a pathogen reduction of over 99 % after 24 hours was observed. After 5 hours of incubation a decrease in colony forming units compared to uncoated prostheses was observed. While the number of *S. aureus* colonies in reference tubes increases in the following incubation time, drug-carrier coated samples show no additional growth. The best growth inhibition effect

after 24 hours was observed with the combination of PDLLA and gentamicin resulting in a colony reduction of 99.42 % (Table 1).

Coatings with teicoplanin showed a reduction in *S. aureus* concentration after 24 hours of at least 93.14 % with TA up to 99.43 % using PDLLA as drug carrier (Table 1). First growth inhibition effects can also be detected after 5 hours of incubation.

Type of coating	Colony reduction [%]
G1	99.42
G2	99.35
G3	99.36
G4	99.31
T1	99.43
T2	93.14
T3	99.48
T4	94.53
Uncoated PTFE prostheses	0

Table 1. *S. aureus* colony reduction of drug-carrier-coated PTFE prostheses in [%] compared to uncoated PTFE prostheses after 24 hours of incubation in *S. aureus* suspension (initial *S. aureus* concentration: 2×10^6 cfu/ml, *S. aureus* concentration after 24 hours in presence of uncoated PTFE prostheses: 5381.06×10^6 cfu/ml).

G1 ^=*gentamicin 10 % in PDLLA*, *G2* ^=*gentamicin 10 % in tocopherol acetate*, *G3* ^=*gentamicin 10 % in Softisan® 649*, *G4* ^=*gentamicin 10 % in Dynasan® 118*, *T1* ^=*teicoplanin 10 % in PDLLA*, *T2* ^=*teicoplanin 10 % in tocopherol acetate*, *T3* ^=*teicoplanin 10 % in Softisan® 649*, *T4* ^=*teicoplanin 10 % in Dynasan® 118*

3.3.1 Adhesion of viable bacteria and antimicrobial potency after 24 hours elution

Bacterial adhesion on 1 cm coated grafts after 24 hours of incubation in a *S. aureus* suspension was determined. All gentamicin and teicoplanin coatings showed a visible reduced number of adhered pathogens on the surface. The lowest number of pathogens on gentamicin coatings was observed on the surface of DG based coatings with average counts of 67 cfu whereas PDLLA based coatings showed the highest counts at an average of 5433 cfu. Reference pathogen numbers could not be assessed being far beyond visual determination building up a bacterial mat even after carrying out two dilution steps of 1 to 10 (Table 2). Inhibition zones on *S. aureus* lawns could not be detected for all four gentamicin coatings. For tested coatings with incorporated teicoplanin, the lowest number of adsorbed bacteria was

found on the surface of PDLLA based coatings at an average of 120 counts whereas TA based coatings averaged 14956 counts. Inhibition zones could not be detected for all four teicoplanin coatings.

Coating type	Averaged counts of adhered cfu
G1	5433 ± 9411
G2	1967 ± 3748
G3	67 ± 58
G4	600 ± 1039
T1	123 ± 70
T2	14956 ± 8735
T3	1450 ± 190
T4	1706 ± 1951
Uncoated PTFE prostheses	Bacterial lawn/ total coverage

Table 2. Averaged numbers of *S. aureus* colonies adsorbed on the surface of drug-carrier-coated PTFE prostheses after 24 hours of incubation in 2×10^6 cfu/ml suspension.

G1 ^= gentamicin 10 % in PDLLA, *G2* ^= gentamicin 10 % in tocopherol acetate, *G3* ^= gentamicin 10 % in Softisan® 649, *G4* ^= gentamicin 10 % in Dynasan® 118, *T1* ^= teicoplanin 10 % in PDLLA, *T2* ^= teicoplanin 10 % in tocopherol acetate, *T3* ^= teicoplanin 10 % in Softisan® 649, *T4* ^= teicoplanin 10 % in Dynasan® 118

3.4 In vitro cytotoxicity studies

The WST-1 assay shows high metabolic activity of viable cells in presence of PTFE prostheses coated with a combination of TA with 10 % teicoplanin (91 % of reference cell proliferation) followed by PDLLA (79 % of reference cell proliferation) and TG with 10 % teicoplanin (77 % of reference cell proliferation). Cells in presence of gentamicin 10 % incorporated in TA, PDLLA and TG maintain a sufficient but lower metabolic activity (32 % to 67 % of reference cell proliferation). Prostheses coated with gentamicin 10 % in DG as well as teicoplanin 10 % in DG in contrast show a very low metabolic activity concluding a higher cytotoxic potential (≤ 15 % of reference cell proliferation). The Oil Red O assay gives a possible explanation for this observation. Under the microscope, red stained lipid inclusions were only detected in cells cultured in presence of prostheses coated with DG and gentamicin respectively teicoplanin.

The WST-1 assay for pure drug carriers shows results with a similar tendency. A high cell proliferation in presence of PDLLA, TA and TG could be demonstrated whereas cells in presence of DG show a low metabolic activity and lipid inclusions.

In concentrations of 200 µg to 1000 µg per well teicoplanin showed no cytotoxic effect on mouse fibroblasts whereas gentamicin showed increased cytotoxic properties at concentrations beyond 200 µg.

3.5 Haemocompatibility studies

3.5.1 Monoclonal enzyme immunoassay for plasma F_{1+2} values

The incubation of individual drug-carrier-coated PTFE prosthesis in human blood caused the formation of a smaller degree of human prothrombin fragment F_{1+2} compared to uncoated PTFE prostheses. The concentration of F_{1+2} fragments varied between 204 pmol/l and 272 pmol/l. The range of citrated plasma for healthy adults averages from 69 pmol/l to 229 pmol/l. Uncoated PTFE prostheses however showed a much higher F_{1+2} fragment concentration at 350 pmol/l.

3.6 Amidolytic substrate assay for factor XIIa-like activity

The assessment of factor XIIa-like activity in human blood showed that all individual coatings activated factor XIIa in the same range as uncoated prostheses. Developed coatings showed a factor XIIa-like activity between 11.25 u/l and 12.06 u/l whereas uncoated PTFE prostheses caused a slightly higher factor XIIa-like activity of 13.37 u/l.

3.6.1 Thromboelastography

The roTEG coagulation study provides two important parameters the clotting time (CT) and maximal clot firmness (MCF). CT describes the time interval from the start of the measurement until initiation of clotting whereas MCF is a dimension of the firmness of a clot. All lipid-based coatings besides teicoplanin 10 % in TG showed median CT values in a range of 102.63 seconds to 146.13 seconds. The coating type of teicoplanin 10 % in TG caused a CT of 62.50 seconds similar to those of uncoated PTFE prostheses of 63.31 seconds. These data confirm results from F_{1+2} value assessment indicating a delayed blood coagulation for almost all individual coatings. MCF values of all lipid-based coatings are situated in the normal range of 53 mm to 72 mm and do not differ from uncoated PTFE values.

3.6.2 Complement C3a-desArg ELISA

The quantitative assessment of C3a-desArg showed different results depending on the used lipid-based coating. Prostheses coated with gentamicin sulfate incorporated in PDLA showed very low C3a-desArg concentrations at 189 ng/ml whereas TA with incorporated gentamicin and teicoplanin as well as DG in combination with teicoplanin activated a higher amount of C3a-desArg in a range between 406 ng/ml and 442 ng/ml. All other coatings activated C3a-desArg fragments between 241 ng/ml and 351 ng/ml whereas uncoated prostheses caused a median C3a-desArg fragment concentration of 179 ng/ml.

4 Discussion

In the present work new anti-infective surface coatings using lipid-based drug delivery systems were studied. Used PDLA, TA, DG and TG carrier give the possibility to bring hydrophilic antibiotics on the surface of hydrophobic implants building up a slow release drug delivery system independent of drug charge. Further important characteristics of individual carriers are a melting point above body temperature and the possibility of sterilization.

There is a great diversity of used antibiotics for a reasonable graft protection in literature using penicillins (18), fluoroquinolons (29) or aminoglycosides (27).

Okahara et al. (29) impregnate PTFE grafts with ofloxacin, Prahlad et al. (31) use (14)C-penicillin for antimicrobial PTFE graft protection while Modak et al. (25) claim to achieve a less toxic and less thrombogenic effect by binding antibiotics directly or in combination with a metal such as silver to the surface of a graft, however this sets a limitation both in the quantity of drug on the graft surface as well as in the development of a slow drug release system.

Another way for an anti-infective equipment of grafts is the use of cationic surfactants like benzalkonium chloride (19), but both cytotoxicity studies have demonstrated that these surfactants often used in pharmaceutical preparations as preservatives show a high cytotoxic potential in already low concentrations (9, 22) and there is a limitation of drug choice because of charge dependency. Haverich et al. (20) and Ney et al. (27) use a fibrin sealant while Moore et al. (26) developed a collagen-release system as antibiotic carrier for anti-infective graft protection, however a decreased haemocompatibility could be the consequence.

In this study the coverage of a broad spectrum of pathogens was the crucial factor for antibiotics of choice. Gentamicin was chosen as it is a basic antibiotic for treating implant

infection (33) whereas teicoplanin is clinically applied in more pronounced infections and MRSA treatment (32) which is of increasing importance for nosocomial infections.

In the present work a coating process was developed and received coated PTFE prostheses were studied in vitro for drug release, biocompatibility, anti-infective character and haemocompatibility. Reproducibility of the coating process could be ensured in case of TA, DG and TG, however coating procedure with PDLLA showed fluctuation in terms of coating weights. Developed coatings ensure a continuous drug release over 96 hours and guarantee a high local antibiotic concentration around the graft. In comparison to systemic drug application side effects for the host organism can thereby be reduced.

As gentamicin and teicoplanin do not dissolve in used organic solvents, samples were coated in drug/carrier suspensions. As a result coatings consisted of antibiotic particles which are incorporated in the polymer. An initial drug burst in the first hour of elution is the consequence as antibiotic particles from the surface of the coating dissolve rapidly after contact with elution buffer. Particles located deeper inside the lipid-based polymer will only be released after polymer degradation or diffusion through the polymer.

In pathologically relevant bacterial concentrations as demonstrated by Elek and Conen (11), developed drug-carrier coatings achieved a bacterial eradication rate of 100 %. This shows a highly effective potency against *S. aureus* colonization. Even in a concentration hundredfolds beyond maximal pathologically relevant bacterial concentration, *S. aureus* growth could highly be reduced after 24 hours by each of the developed drug-carrier coatings. Coatings with incorporated teicoplanin showed an insignificant smaller growth inhibition effect than coatings with gentamicin. Bacterial adhesion after 24 hours of incubation in a 2×10^6 cfu/ml *S. aureus* suspension could also highly be reduced by drug-carrier-coated prostheses compared to uncoated ones. Drug-carrier coatings after 24 hours of drug elution could not show inhibition zones on bacterial lawns assuming that the contact area to agar plates is too small and drug diffusion into agar medium is not as easy as in fluid media. However the antibacterial effects in fluid media are closer to physiological conditions. All coatings besides DG showed small but functionally acceptable cytotoxic levels (≤ 22.8 % cell proliferation decrease). Tests with oil red O reagent show that DG is incorporated in the cell soma which apparently leads to cell death.

Haemocompatibility of individual coatings could be confirmed by several experiments. Data of activated human prothrombin fragment F_{1+2} and FXIIa activity in plasma as well as clotting time and maximal clot firmness from roTEG tests show an even lower thrombogenic effect of individual lipid-based coatings in comparison to uncoated PTFE grafts. Increased

C3a-desArg concentrations were caused by some of the coatings, nevertheless tolerable C3a-desArg concentration limits have to be discussed.

5 Conclusions

In this study we could demonstrate the development of a drug delivery system consisting of lipid-based polymers with incorporated gentamicin and teicoplanin to locally release high drug concentrations in the area of implant infection. Developed coatings with PDLLA, tocopherol acetate and Dynasan[®] 118 as drug carriers completely inhibited the proliferation of *S. aureus* in pathologically relevant concentrations while preserving biocompatible and haemocompatible characteristics. If these results can be confirmed in vivo, developed drug delivery systems could have a high interest in vascular surgery.

6 Acknowledgements

We would like to thank V. Vatou (University Hospital, Technical University Munich, Germany) for her great assistance in microbial testing. The authors did not receive any payments or benefits from a commercial party related directly or indirectly to the subject of this article. This study was supported by the Arbeitsgemeinschaft industrieller Forschungsvereinigungen (AiF).

7 Figure and Table Captions

Figure 1. SEM pictures of the inner surface of a PTFE prostheses coated with gentamicin 10 % in tocopherol acetate and uncoated PTFE prostheses.

Figure 2. Individual coating quotients Q_c defined as the ratio between the weight of coating and the weight of a 1 cm uncoated PTFE prostheses of this individual coating process:
 $m_{\text{coating}} / m_{\text{PTFE prosthesis}}$.

Table 1. *S. aureus* colony reduction of drug-carrier-coated PTFE prostheses in [%] compared to uncoated PTFE prostheses after 24 hours of incubation in *S. aureus* suspension.

Table 2. Averaged numbers of *S. aureus* colonies adsorbed on the surface of drug-carrier-coated PTFE prostheses after 24 hours of incubation in 2×10^6 cfu/ml suspension.

8 References

1. **Barton, A. J., R. D. Sagers, and W. G. Pitt.** 1996. Bacterial adhesion to orthopedic implant polymers. *J Biomed Mater Res* **30**:403-10.
2. **Beiko, D. T., B. E. Knudsen, J. D. Watterson, and J. D. Denstedt.** 2003. Biomaterials in urology. *Curr Urol Rep* **4**:51-5.
3. **Bergamini, T. M., T. M. McCurry, J. D. Bernard, K. L. Hoeg, R. A. Corpus, B. E. James, J. C. Peyton, K. R. Brittian, and W. G. Cheadle.** 1996. Antibiotic efficacy against *Staphylococcus epidermidis* adherent to vascular grafts. *J Surg Res* **60**:3-6.
4. **Bunt, T. J.** 1983. Synthetic vascular graft infections. I. Graft infections. *Surgery* **93**:733-46.
5. **Camiade, C., P. Goldschmidt, F. Koskas, J. B. Ricco, M. Jarraya, J. Gerota, and E. Kieffer.** 2001. Optimization of the resistance of arterial allografts to infection: comparative study with synthetic prostheses. *Ann Vasc Surg* **15**:186-96.
6. **Costerton, J. W., L. Montanaro, and C. R. Arciola.** 2005. Biofilm in implant infections: its production and regulation. *Int J Artif Organs* **28**:1062-8.
7. **Darouiche, R. O.** 2001. Device-associated infections: a macroproblem that starts with microadherence. *Clin Infect Dis* **33**:1567-72.
8. **Darouiche, R. O.** 2004. Treatment of infections associated with surgical implants. *N Engl J Med* **350**:1422-9.
9. **Deutsche, T., U. Porkert, R. Reiter, T. Keck, and H. Riechelmann.** 2006. In vitro genotoxicity and cytotoxicity of benzalkonium chloride. *Toxicol In Vitro* **20**:1472-7.
10. **Dunne, W. M., Jr., E. O. Mason, Jr., and S. L. Kaplan.** 1993. Diffusion of rifampin and vancomycin through a *Staphylococcus epidermidis* biofilm. *Antimicrob Agents Chemother* **37**:2522-6.
11. **Elek, S. D., and P. E. Conen.** 1957. The virulence of *Staphylococcus pyogenes* for man; a study of the problems of wound infection. *Br J Exp Pathol* **38**:573-86.
12. **Filloux, A., and I. Vallet.** 2003. [Biofilm: set-up and organization of a bacterial community]. *Med Sci (Paris)* **19**:77-83.
13. **Gollwitzer, H., K. Ibrahim, H. Meyer, W. Mittelmeier, R. Busch, and A. Stemberger.** 2003. Antibacterial poly(D,L-lactic acid) coating of medical implants using a biodegradable drug delivery technology. *J Antimicrob Chemother* **51**:585-91.
14. **Gotz, F.** 2002. *Staphylococcus* and biofilms. *Mol Microbiol* **43**:1367-78.
15. **Greco, R. S., R. A. Harvey, P. C. Smilow, and J. V. Tesoriero.** 1982. Prevention of vascular prosthetic infection by a benzalkonium-oxacillin bonded polytetrafluoroethylene graft. *Surg Gynecol Obstet* **155**:28-32.
16. **Gristina, A. G.** 1994. Implant failure and the immuno-incompetent fibro-inflammatory zone. *Clin Orthop Relat Res*:106-18.
17. **Harvey, R. A., D. V. Alcid, and R. S. Greco.** 1982. Antibiotic bonding to polytetrafluoroethylene with tridodecylmethylammonium chloride. *Surgery* **92**:504-12.
18. **Harvey, R. A., and R. S. Greco.** 1981. The noncovalent bonding of antibiotics to a polytetrafluoroethylene-benzalkonium graft. *Ann Surg* **194**:642-7.
19. **Harvey, R. A., J. V. Tesoriero, and R. S. Greco.** 1984. Noncovalent bonding of penicillin and cefazolin to dacron. *Am J Surg* **147**:205-9.
20. **Haverich, A., S. Hirt, M. Karck, F. Siclari, and H. Wahlig.** 1992. Prevention of graft infection by bonding of gentamycin to Dacron prostheses. *J Vasc Surg* **15**:187-93.

21. **Hebert, C. K., R. E. Williams, R. S. Levy, and R. L. Barrack.** 1996. Cost of treating an infected total knee replacement. *Clin Orthop Relat Res*:140-5.
22. **Huhtala, A., P. Alajuuma, S. Burgalassi, P. Chetoni, H. Diehl, M. Engelke, M. Marselos, D. Monti, P. Pappas, M. F. Saettone, L. Salminen, M. Sotiropoulou, H. Tahti, H. Uusitalo, and M. Zorn-Kruppa.** 2003. A collaborative evaluation of the cytotoxicity of two surfactants by using the human corneal epithelial cell line and the WST-1 test. *J Ocul Pharmacol Ther* **19**:11-21.
23. **Khardori, N., and M. Yassien.** 1995. Biofilms in device-related infections. *J Ind Microbiol* **15**:141-7.
24. **Mack, D., P. Becker, I. Chatterjee, S. Dobinsky, J. K. Knobloch, G. Peters, H. Rohde, and M. Herrmann.** 2004. Mechanisms of biofilm formation in *Staphylococcus epidermidis* and *Staphylococcus aureus*: functional molecules, regulatory circuits, and adaptive responses. *Int J Med Microbiol* **294**:203-12.
25. **Modak, S. M., L. Sampath, C. L. Fox, Jr., A. Benvenisty, R. Nowygrod, and K. Reemstmau.** 1987. A new method for the direct incorporation of antibiotic in prosthetic vascular grafts. *Surg Gynecol Obstet* **164**:143-7.
26. **Moore, W. S., M. Chvapil, G. Seiffert, and K. Keown.** 1981. Development of an infection-resistant vascular prosthesis. *Arch Surg* **116**:1403-7.
27. **Ney, A. L., P. H. Kelly, D. T. Tsukayama, and M. P. Bubrick.** 1990. Fibrin glue-antibiotic suspension in the prevention of prosthetic graft infection. *J Trauma* **30**:1000-5; discussion 1005-6.
28. **O'Gara, J. P., and H. Humphreys.** 2001. *Staphylococcus epidermidis* biofilms: importance and implications. *J Med Microbiol* **50**:582-7.
29. **Okahara, K., J. Kambayashi, T. Shibuya, T. Kawasaki, M. Sakon, Y. Dohi, Y. Oka, S. Ito, and S. Miyake.** 1995. An infection-resistant PTFE vascular graft; spiral coiling of the graft with ofloxacin-bonded PTFE thread. *Eur J Vasc Endovasc Surg* **9**:408-14.
30. **Parsek, M. R., and P. K. Singh.** 2003. Bacterial biofilms: an emerging link to disease pathogenesis. *Annu Rev Microbiol* **57**:677-701.
31. **Prahlad, A., R. A. Harvey, and R. S. Greco.** 1981. Diffusion of antibiotics from a polytetrafluoroethylene-benzalkonium surface. *Am Surg* **47**:515-8.
32. **Rayner, C., and W. J. Munckhof.** 2005. Antibiotics currently used in the treatment of infections caused by *Staphylococcus aureus*. *Intern Med J* **35 Suppl 2**:S3-16.
33. **Schmidmaier, G., M. Lucke, B. Wildemann, N. P. Haas, and M. Raschke.** 2006. Prophylaxis and treatment of implant-related infections by antibiotic-coated implants: a review. *Injury* **37 Suppl 2**:S105-12.
34. **Schmitt, D. D., D. F. Bandyk, A. J. Pequet, and J. B. Towne.** 1986. Bacterial adherence to vascular prostheses. A determinant of graft infectivity. *J Vasc Surg* **3**:732-40.
35. **von Eiff, C., C. Heilmann, M. Herrmann, and G. Peters.** 1999. Basic aspects of the pathogenesis of staphylococcal polymer-associated infections. *Infection* **27 Suppl 1**:S7-10.

Chapter 3

New anti-infective coatings of surgical sutures based on a combination of antiseptics and fatty acids

Abstract

Objectives: Wound infection is a feared complication in surgery. The aim of this study was to develop new anti-infective coatings of surgical sutures and to compare the antimicrobial effectiveness and biocompatibility to the well-established Vicryl Plus®.

Methods: Synthetic absorbable PGA surgical sutures were coated with three different chlorhexidine concentrations and two different octenidine concentrations in combination with palmitic acid and lauric acid. Drug release kinetics lasting 96 hours was studied in phosphate buffered saline at 37 °C. Anti-infective characteristics were determined by measuring the change in optical density of *Staphylococcus aureus* suspensions charged with coated sutures over time. Microorganisms adsorbed at the surface of sutures were assessed on blood agar plates and coated sutures eluted for 24 hours were placed on bacterial lawns cultured on Mueller-Hinton plates to prove retained antimicrobial potency. A cell proliferation assay was performed to assess the degree of cytotoxicity. Anti-infective characteristics and biocompatibility were compared to Vicryl Plus®.

Results: A coating technology for slow-release drug delivery systems on surgical sutures could be developed. All coatings showed a continuous drug release within 96 hours. Individual chlorhexidine and octenidine coated sutures showed superior anti-infective characteristics but inferior biocompatibility in comparison to Vicryl Plus®.

Conclusions: We conclude that developed anti-infective suture coatings consisting of lipid based drug delivery systems in combination with antiseptics are highly effective against bacterial colonization in vitro, however drug doses for human use have to be adjusted to comply with biocompatibility.

Keywords: Surgical sutures, antimicrobial coating, drug delivery system, biocompatibility, fatty acids

1 Introduction

Wound infection is a feared complication in post-operative treatment leading to severe health burden for the patient and high medical costs for society (1, 3). One of the most common pathogens in wound infections is *Staphylococcus aureus* colonizing surgical implants or sutures (8, 20). It is of high importance to avoid those infections as good as possible. A new technology is the equipment of surgical sutures with antimicrobial drugs like antiseptics (11, 25). In order to fix hydrophilic agents on the surface of biomaterials, a lipophilic mediator agent is needed.

Beyond its character to equip the surface of biomaterials with hydrophilic antimicrobial agents, this mediator agent should fulfil the function of a retarded drug release in order to achieve anti-infective protection during wound healing after surgery. Furthermore the mediator agent should decrease the surface roughness and consequently reduce mechanical stress during sewing. In order to give considerations to all of these requirements, the mediator agent has to be chosen advisedly. In this work the fatty acids palmitic acid and lauric acid are used as mediator agents to build up a slow release system in anti-infective coatings on PGA sutures. The present work presents newly developed lipid-based drug delivery systems in combination with antiseptics for anti-infective suture equipment and the evaluation of drug release, anti-infective characters and biocompatibility compared to Vicryl Plus[®].

2 Materials and Methods

2.1 Medical Implant

Commercially available synthetic absorbable PGA surgical sutures (3 metric) (PGA Resorba[®], Resorba, Nürnberg, Germany) and Vicryl Plus[®] (3 metric) (Ethicon GmbH Deutschland, Norderstedt, Germany) were applied. Sterile sutures were cut into defined length (1 cm, 3 cm) under aseptic conditions in a laminar airflow and used for further experiments.

2.2 The anti-infective coating

PGA sutures were antimicrobially equipped with one type of chlorhexidine dipalmitate (CP) (Heraeus, Hanau, Germany) coating, two types of chlorhexidine dilaurate (CL1 and CL2) (Heraeus, Hanau, Germany) coatings and two types of octenidine hydrochloride (OH1 and OH2) (Dishman Pharmaceutical, NJ, USA) coatings. For octenidine hydrochloride the fatty acid palmitic acid (Carl Roth, Karlsruhe, Germany) was used as drug carrier. Within one coating type, coatings differed only in the drug weight per unit length. Methanol was used as solvent for individual coatings. Drug concentrations (w/v) in methanol differed for each coating. (CP: 2 %, CL1: 5 %, CL2: 15 %, OH1: 10 %, OH2: 21 %). In preliminary experiments the influence of ethanol and methanol as bath solvent was elucidated. During coating procedure with ethanolic solvents, a delamination of the commercial coating of the PGA Resorba[®] can occur, the application of methanol is practical in this respect. Sutures (50 cm length) were coated by a dip-coating procedure carried out in sterile sealable one neck flasks in presence of a magnetic stir bar on a magnetic stirrer (RCT basic IKAMAG[®], IKA, Staufen, Germany) at room temperature (23 °C). Therefore sutures were pulled through the coating bath within few seconds. This procedure was followed by a drying process for 24 hours under the laminar air-flow hood. Coated sutures were packed in PE bags and sterilized with ethylenoxide. Coating weights were gravimetrically determined and a standardized drug weight per unit length $\text{mass}_{\text{drug}}/\text{length}_{\text{suture}}$ (µg/cm) was assessed for each coating type.

2.3 Morphological analysis-SEM

Individual coated sutures were prepared for SEM by sputtering with gold (BAL-TEC MED 020 coating system, Boeckeler Instruments, Arizona, USA) and examined with a high vacuum SEM (JSM 6060LV Scanning Electron Microscope, JEOL Ltd., Tokyo, Japan).

2.4 Drug release

Drug release kinetics lasting 96 hours was studied in phosphate-buffered saline (PBS) at 37 °C (pH 7.4) in a thermomixer (Fa. Eppendorf, Hamburg, Germany). Therefore one thread of 1 cm length was placed in 750 µl PBS in a 1.5 ml flask (Eppendorf Cap, Fa. Eppendorf, Hamburg, Germany). Three experiments per coating type were performed. At time points 1 h, 4 h, 8 h and 24 h, 48 h, 72 h and 96 h elution medium was completely changed. Octenidine

was assessed by spectroscopic measurement at 280 nm. Chlorhexidine was assessed by derivatize with bromocresol and measuring the optical density at 410 nm.

2.5 Test bacterium

For in vitro studies a clinical isolate of *S. aureus* (strain ATCC[®] 49230) was used. The test strain was susceptible to both gentamicin (MIC 0.5 mg/l) and teicoplanin (MIC 0.25 mg/l). *S. aureus* was cultured on columbia agar plates (Becton Dickinson GmbH, Heidelberg, Germany) at 37 °C for 18 hours before testing.

2.5.1 Antibacterial characteristics

In order to assess antibiotic efficacy at pathologically relevant concentrations, *S. aureus* was resuspended in normal saline and adjusted to 1×10^8 cfu/ml by visual comparison with a 0.5 McFarland standard. Based on this stock suspension, bacterial suspensions (1 ml) with 1×10^2 , 1×10^3 , 1×10^4 cfu/ml were prepared and incubated with individual sutures (length: 3 cm, n=3) in sealed glass capillaries. Samples were incubated for 24 hours at 37 °C. 100 µl of each sample was plated on blood agar plates and incubated for 24 hours at 37 °C. Colony forming units were determined for each sample and reference. In order to investigate the maximal antimicrobial potential of coated sutures, a hundredfold concentration of the maximal pathologically relevant concentration (1×10^4 cfu/ml) was chosen. Sterile coated sutures (length: 3 cm, n=3) were added to 50 ml of *S. aureus* suspensions. The optical density was measured every 60 minutes within the first eight hours and after 24 hours again. Optical density was plotted against time. With the aid of a calibration curve, bacterial concentrations in colony forming units (cfu/ml) of sample and reference at different investigation times could be obtained. A reference was established by investigating Vicryl Plus[®] and uncoated sutures the same way.

2.5.2 Adhesion of viable bacteria and antimicrobial potency after 24 hours elution

In order to determine the number of germs adsorbed, sutures were incubated in 1×10^6 cfu/ml for 24 hours. Subsequently sutures were washed twice with NaCl and placed into an ultrasonic bath of 1 ml of isotonic NaCl for ten minutes. 100 µl of the bacterial suspension

obtained were plated on blood agar plates. For reference sutures two dilution steps of one to ten were carried out additionally expecting a high amount of adhered pathogens. Blood agar plates were incubated for 18 h at 37 °C and colony forming units were visually determined and extrapolated to the initial number of adsorbed pathogens. Sutures (length 3 cm, n=3) were eluted for 24 h in PBS at 37 °C and placed on bacterial lawns cultured on Mueller-HintonII-agar plate (BD Diagnostic System, Heidelberg, Germany). Bacterial lawns were produced by adding cultured *S. aureus* in isotonic NaCl, adjusted to 1×10^8 cfu/ml by visual comparison with a 0.5 McFarland standard.

2.6 Cell culture

Mouse connective tissue fibroblasts L929 were kindly provided by the ITEM GmbH – The Biotoooling Company (Garching, Germany) and maintained in RPMI 1640 medium supplemented with 10 % fetal bovine serum, penicillin and streptomycin (100 U/ml and 0.1 mg/ml, respectively), partricin (50 µg/ml) and stable glutamine at 37 °C in a humidified atmosphere containing 5 % CO₂.

2.7 In vitro cytotoxicity studies

Cytotoxicity tests were carried out with L929 fibroblasts from mouse connective tissue. In order to prove biocompatibility, L929 fibroblasts (IMETUM, Garching, Germany) were cultured in presence of 1 cm of individual sutures until subconfluence. To assess the degree of cytotoxicity, the Roche cell proliferation assay (Roche Diagnostics GmbH, Mannheim, Germany) was performed. The Oil Red O staining was used for detecting incorporated lipids in the cell soma.

3 Results

3.1 Morphological analysis

Coatings could be observed through SEM after dip-coating. All coated sutures kept their flexibility (Figure 1A - D).

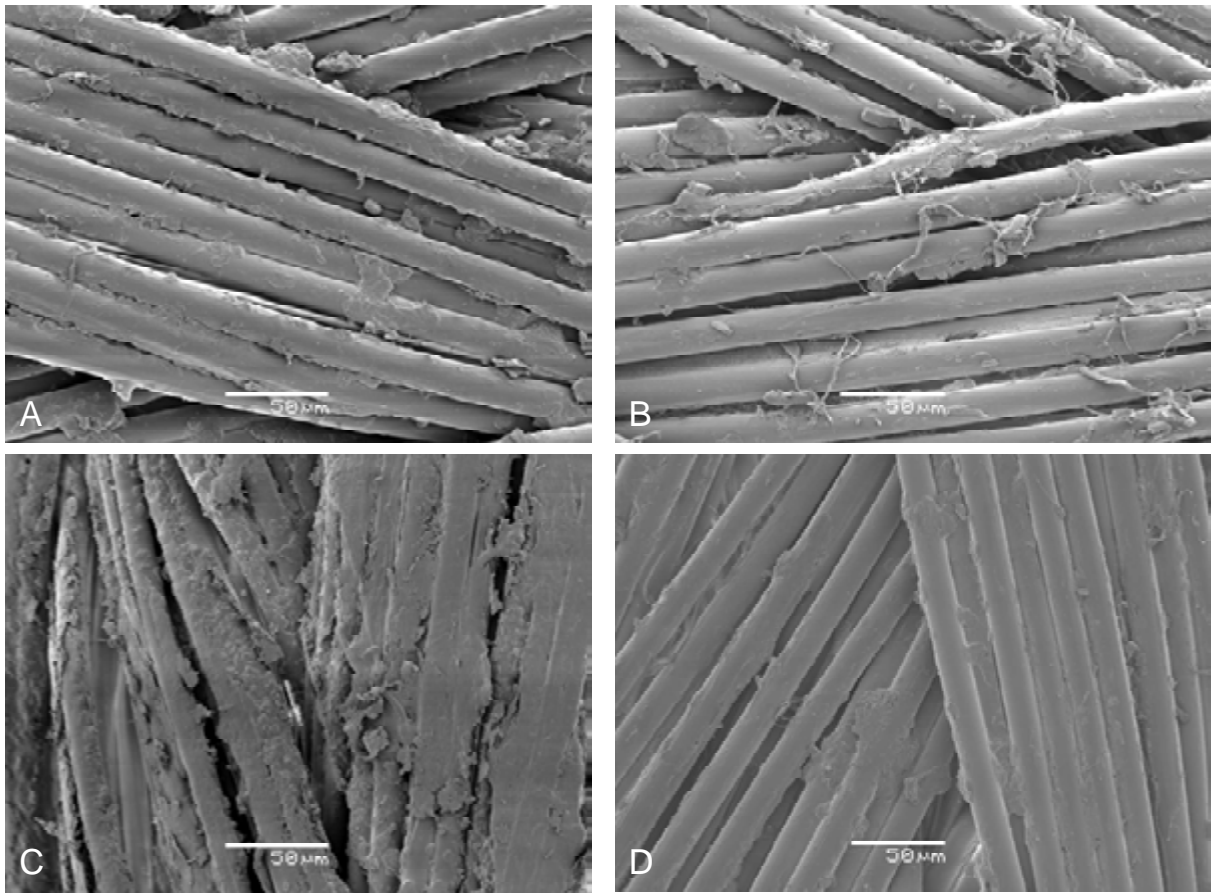


Figure 1. SEM pictures of PGA Resorba[®] sutures coated with A) chlorhexidine dipalmitate (CP) and B) octenidine hydrochloride (OH2), C) Vicryl Plus[®] and D) clinically used PGA Resorba[®] (magnification 450).

3.2 Drug release

The drug weight per unit length was assessed for the CP coating at 90 µg/cm, for CL1 at 70 µg/cm and CL2 at 190 µg/cm and for OH1 at 6 µg/cm and OH2 at 28 µg/cm (Figure 2). All developed coatings showed a continuous drug release within 96 hours. CP was released continuously within 96 hours ending up in a concentration of 4.1 µg/ml. The concentration of

CL1 was assessed at 10.4 $\mu\text{g/ml}$ after 96 hours, for CL2 concentrations of 31.1 $\mu\text{g/ml}$ within 96 hours were determined. OH1 showed a released concentration of 0.7 $\mu\text{g/ml}$ after 96 hours whereas for OH2 a concentration after 96 hours of 0.5 $\mu\text{g/ml}$ was assessed (Figure 3).

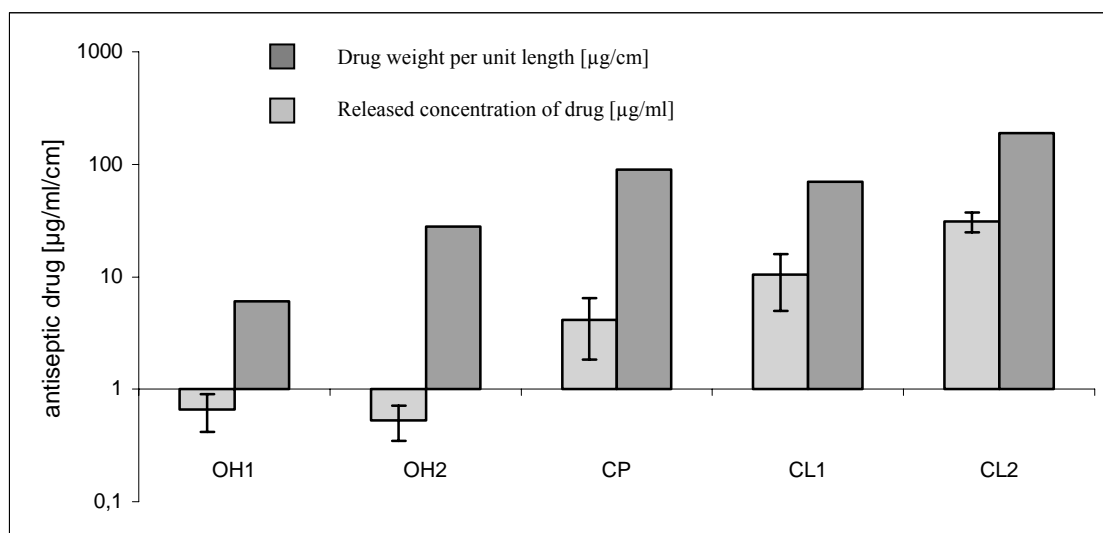


Figure 2. Released concentration of antiseptic drugs (weight/volume) from PGA sutures after 96 hours into PBS buffer, related to antiseptic drug charge (weight/unit length).

CP ^= chlorhexidine dipalmitate (90 $\mu\text{g/cm}$), CL1 ^= chlorhexidine dilaurate (70 $\mu\text{g/cm}$), CL2 ^= chlorhexidine dilaurate (190 $\mu\text{g/cm}$), OH1 ^= octenidine hydrochloride (6 $\mu\text{g/cm}$), OH2 ^= octenidine hydrochloride (28 $\mu\text{g/cm}$)

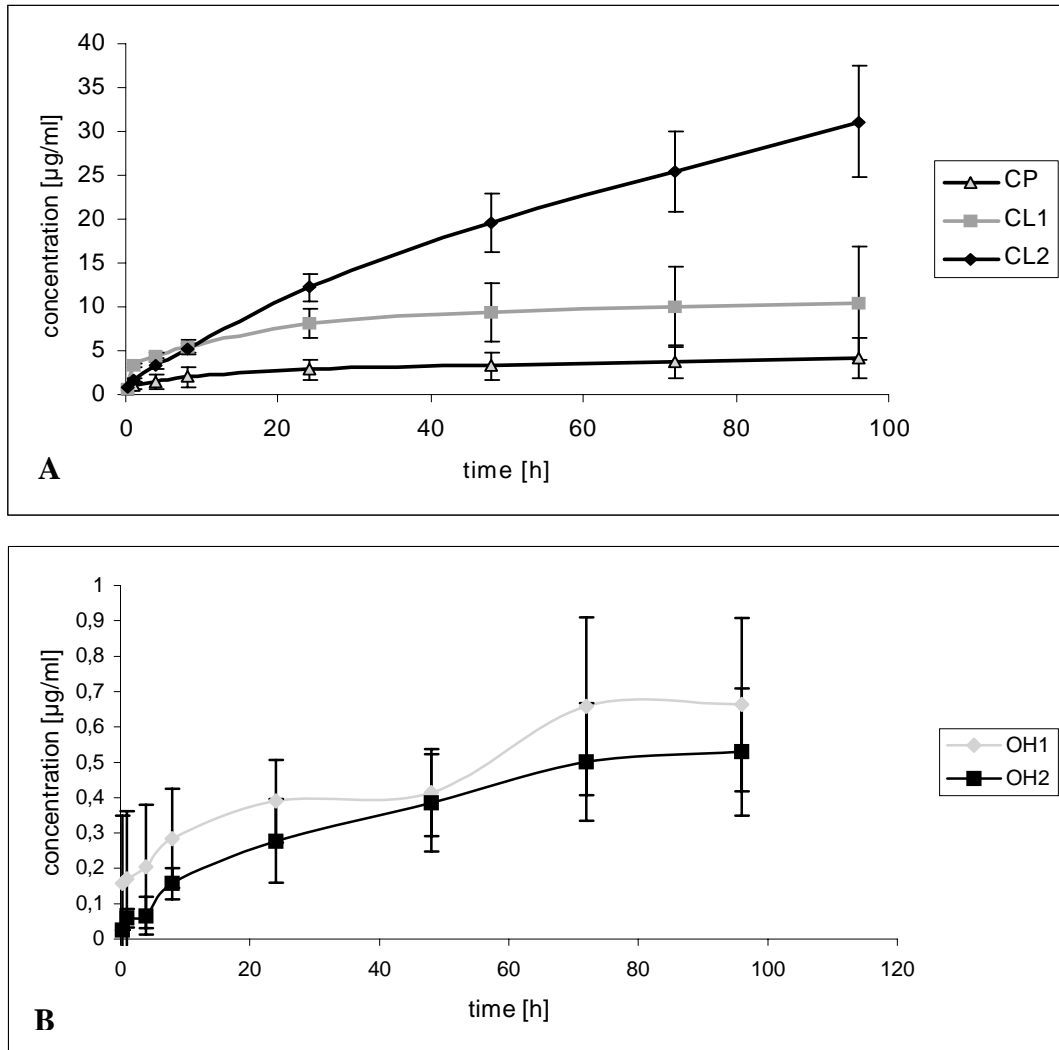


Figure 3. Elution profiles of different drugs into PBS from A) chlorhexidine coated PGA sutures and B) octenidine coated PGA sutures.

CP \wedge = chlorhexidine dipalmitate (90 $\mu\text{g}/\text{cm}$), *CL1* \wedge = chlorhexidine dilaurate (70 $\mu\text{g}/\text{cm}$), *CL2* \wedge = chlorhexidine dilaurate (190 $\mu\text{g}/\text{cm}$), *OH1* \wedge = octenidine hydrochloride (6 $\mu\text{g}/\text{cm}$), *OH2* \wedge = octenidine hydrochloride (28 $\mu\text{g}/\text{cm}$)

3.3 Antibacterial characteristics

Individual coatings showed a highly effective potency against physiological *S. aureus* concentrations in a range of 10^2 to 10^4 cfu/ml. Colony growth on agar plates incubated with sample medium could not be observed with each of the individual coatings concluding a total germ eradication caused by all tested individual coatings.

Bacterial growth in highly concentrated bacterial suspensions of 2×10^6 cfu/ml could be reduced by all developed suture coatings. CP, CL1, CL2 and OH2 coated sutures showed a cfu/ml reduction after 24 hours in comparison to uncoated reference of over 99 % whereas

OH1 coated sutures only reduced pathogen concentration in a range of 17 % after 24 hours in comparison to uncoated sutures. Vicryl Plus[®] reduced bacterial growth in a range of 34 % after 24 hours (Figure 4).

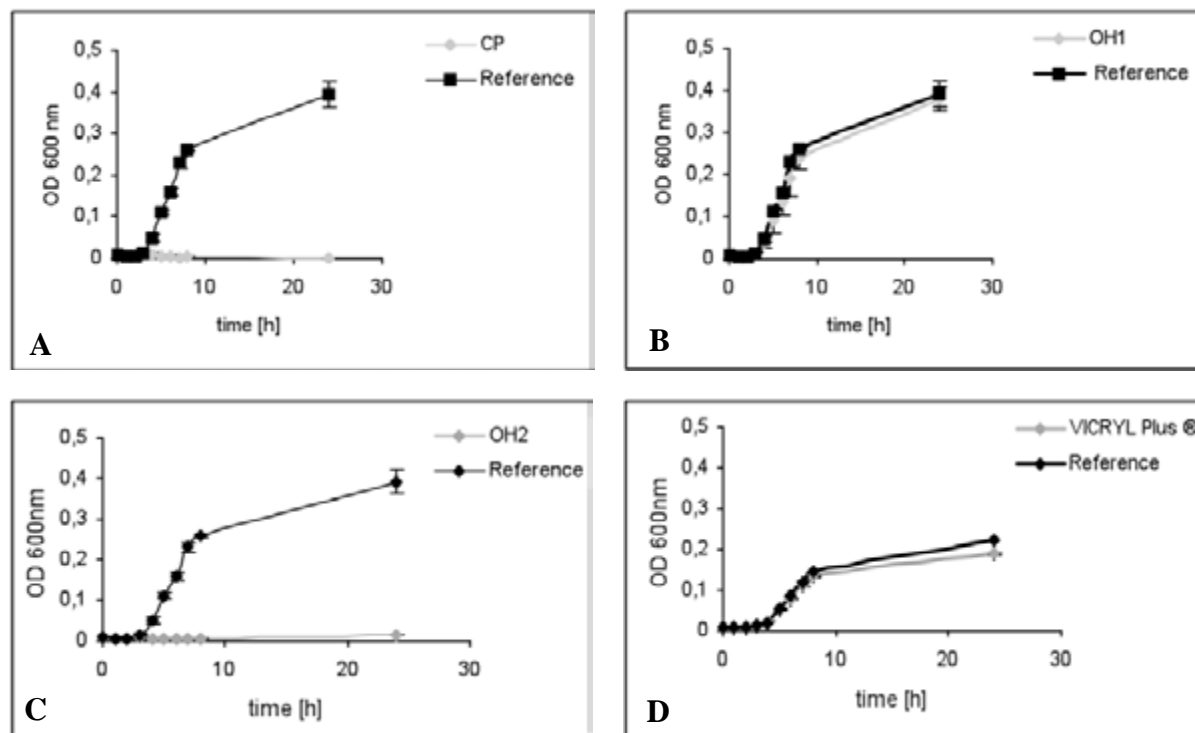


Figure 4. *S. aureus* growth cultured in sterile Mueller-Hinton broth for 24 hours in the presence of individual antimicrobially coated sutures: A) chlorhexidine dipalmitate, B) octenidine hydrochloride, C) octenidine hydrochloride, D) Vicryl Plus[®].

CP [^]= chlorhexidine dipalmitate (90 μ g/cm), CL1 [^]= chlorhexidine dilaurate (70 μ g/cm), CL2 [^]= chlorhexidine dilaurate (190 μ g/cm), OH1 [^]= octenidine hydrochloride (6 μ g/cm), OH2 [^]= octenidine hydrochloride (28 μ g/cm)

3.4 Adhesion of viable bacteria and antimicrobial potency after 24 hours elution

Bacterial adhesion on coated PGA sutures was reduced depending on the coating type. The lowest number of adhered pathogens was observed on the surface of PGA sutures coated with CL2 at an average of 5326 cfu/ml \pm 7048 cfu/ml. CP and CL1 showed adhered bacterial concentrations of 163392 cfu/ml \pm 87402 cfu/ml and 121434 cfu/ml \pm 86770 cfu/ml. Adhered bacterial concentration on the surface of OH1 and OH2 were assessed at 5772 cfu/ml \pm 2141 cfu/ml and 8214 cfu/ml \pm 11920 cfu/ml. The highest amount of adsorbed germs on coated sutures was detected on Vicryl Plus[®] suture surfaces at 273060 cfu/ml \pm 52016 cfu/ml. Uncoated reference sutures showed an average pathogen adhesion of 273948 cfu/ml \pm 35694

cfu/ml. Inhibition zones on bacterial lawns were only developed by CL2 coated sutures and Vicryl Plus[®] sutures (Figure 5).

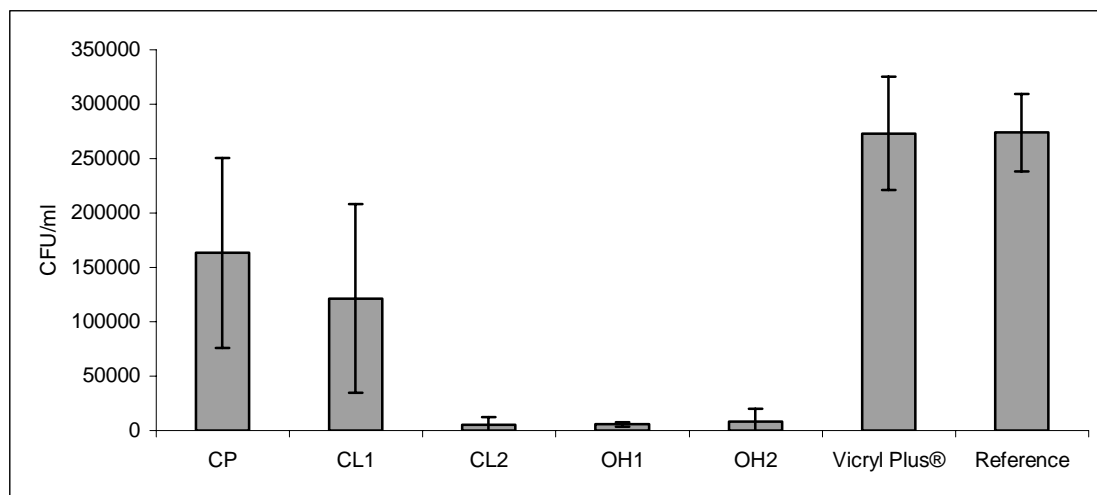


Figure 5. Numbers of *S. aureus* colonies adsorbed on the surface of coated PGA sutures after 24 hours of incubation in 2×10^6 cfu/ml suspension.

CP ^= chlorhexidine dipalmitate (90 $\mu\text{g}/\text{cm}$), *CL1* ^= chlorhexidine dilaurate (70 $\mu\text{g}/\text{cm}$), *CL2* ^= chlorhexidine dilaurate (190 $\mu\text{g}/\text{cm}$), *OH1* ^= octenidine hydrochloride (6 $\mu\text{g}/\text{cm}$), *OH2* ^= octenidine hydrochloride (28 $\mu\text{g}/\text{cm}$)

3.5 In vitro cytotoxicity studies

Cells in presence of coated sutures showed a metabolic activity in a range of 16 % and 17 % for coating types CP, CL1, OH1 and OH2 and a relative metabolic activity of 25 % for CL2 in comparison to reference. Cells in presence of Vicryl Plus[®] showed a comparable metabolic activity to uncoated sutures. The oil red O test demonstrates high amounts of fatty inclusions inside the cell soma of cells in presence of palmitic acid which is a possible reason for the high cytotoxic level of fatty acid coated sutures (Figure 6).

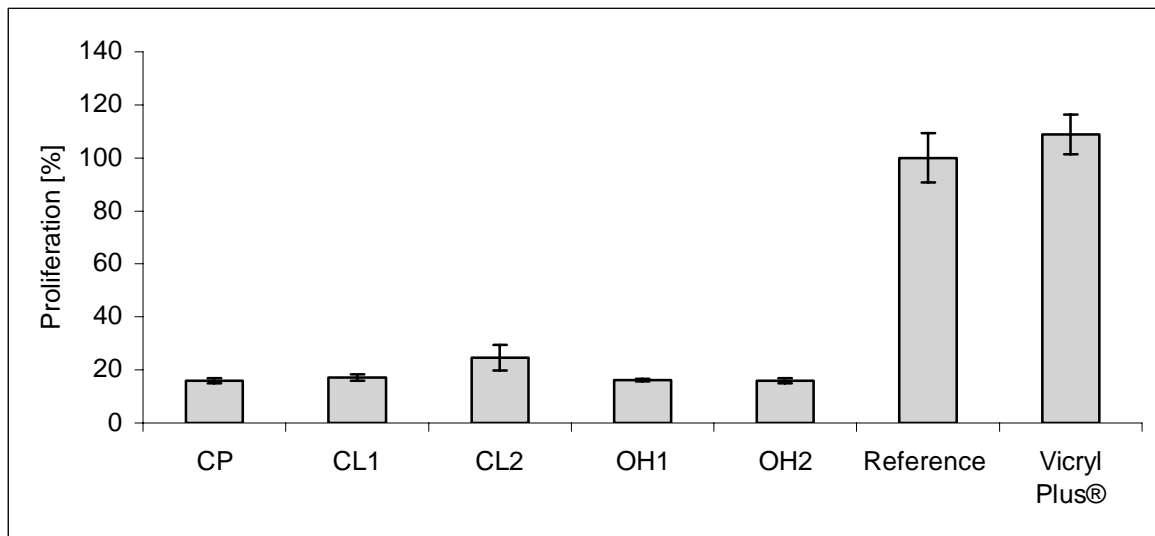


Figure 6. Metabolic activity of viable cells incubated with individual coated sutures measured with the Roche cell proliferation assay. Uncoated PGA sutures as well as Vicryl Plus® sutures served as reference.

CP ^ = chlorhexidine dipalmitate (90 µg/cm), *CL1* ^ = chlorhexidine dilaurate (70 µg/cm), *CL2* ^ = chlorhexidine dilaurate (190 µg/cm), *OH1* ^ = octenidine hydrochloride (6 µg/cm), *OH2* ^ = octenidine hydrochloride (28 µg/cm)

4 Discussion

Post-operative infections are feared complications in surgery (5). One of the most common pathogens in wound infections and implant-associated infections is *Staphylococcus aureus* colonizing foreign surfaces like surgical implants, sutures and the surrounding tissue (6, 24, 26). In presence of implants, a smaller amount of pathogens is necessary to cause infection. The formation of biofilms on biomaterials protects bacteria from host immune defence and increases antibiotic resistance so that even high local concentrations of antibiotics do not completely eradicate bacteria in biofilms (7, 10, 17). It is therefore of high importance to prevent bacteria from surface adhesion (11). A promising therapeutical approach is the anti-infective equipment of sutures in order to release locally high amounts of antimicrobial drugs (12, 13, 15, 16). Antiseptics like chlorhexidine and octenidine have shown high anti-infective efficacy in several studies about orthopaedic and dental applications however no literature is available concerning suture coatings (9, 14, 23).

In this work PGA sutures were coated with antiseptics to achieve an effective protection against bacterial colonization during wound healing. A coating technology for PGA sutures was developed and coatings were characterized by drug release, anti-infective effectiveness

and biocompatibility. Morphological analysis by SEM showed that developed anti-infective coatings are partly integrated into the multifilament structure of PGA sutures, a delamination of coatings could not be assessed macroscopically. Therefore, when applied in vivo, no delamination is expected during sewing. The evaluation by surgeons in animal experiment under standardized conditions could shed light on this regard (22).

In order to fix the used antiseptics chlorhexidine and octenidine on the suture surfaces and to build up a retarded drug release system for long-term anti-infective characters, chlorhexidine and octenidine were combined with the fatty acids palmitic acid and lauric acid. These lipid-based formulations furthermore decrease the surface roughness of sutures and consequently reduce mechanical stress during sewing. The newly developed anti-infective coatings using the antiseptics chlorhexidine and octenidine were compared to the already well established suture Vicryl Plus[®] using triclosan as anti-infective compound.

Biocompatibility as well as the anti-infective effectiveness of Vicryl Plus[®] have been corroborated in several in vitro and in vivo studies. Rothenburger et al. have evaluated a coated polyglactin 910 suture with triclosan for its antibacterial effectiveness against staphylococci (19). They report a sufficient antimicrobial effect to prevent in vitro colonization caused by *S. aureus* and *S. epidermidis*. A significant in vitro efficacy of Poliglecaprone[®] 25 suture with triclosan against several strains of bacteria was assessed by Ming et al. (18). Storch et al. studied the effect of the effect of coated polyglactin 910 suture with triclosan to tissue response and wound healing over a 28 day period on full-thickness linear wounds in the hairless guinea pig model and assessed no evidence of impedance to wound healing (21). In a review about the safety of triclosan and the biocompatibility of coated polyglactin 910 suture with triclosan, Barbolt could demonstrate the safety of this suture and triclosan for clinical use (2). However it is of fundamental importance to have a choice between different antimicrobial agents on surgical sutures primarily due to an increased pathogen resistance, but also to parameters like tissue compatibility or drug stability. Yazdankhah et al. confirmed the occurrence of triclosan resistance amongst dermal, intestinal, and environmental microorganisms of clinical relevance and assume that the widespread use of triclosan lead to the development of concomitant resistance to clinically important antimicrobials (27). The increased triclosan susceptibility of clinical isolates of MRSA assessed by Brenwald and Fraise corroborates these observations (4).

Drug release studies showed a continuous drug release within 96 hours which is a basic requirement for an effective anti-infective protection. The gap between the amount of released drug after 96 hours and the remaining drug amount on the surface of developed sutures

revealed a high potential for a long-term anti-infective protection (Figure 1). The controversial result that OH1 (6 $\mu\text{g}/\text{cm}$) released slightly more octenidine than OH2 (28 $\mu\text{g}/\text{cm}$) is obvious and needs further investigation.

A reduction of the number of adhered pathogens on the suture surface as well as the inhibition of *S. aureus* growth in suspension was assessed by all investigated coating types. All chlorhexidine and octenidine coated sutures showed superior anti-infective characteristics in comparison to the clinically well-established Vicryl Plus[®]. Biocompatibility studies revealed a higher cytotoxic potential of developed suture coatings than Vicryl Plus[®]. One possible reason for this effect is the inclusion of palmitic acid in the cell soma assessed by the Oil Red O staining. The balance between an adequate drug concentration and the biocompatibility of developed coatings is under elucidation. As the anti-infective potential is superior to Vicryl Plus[®], a drug concentration decrease is conceivable contributing to a lower cytotoxicity.

5 Conclusions

In this study we demonstrated the development of novel anti-infective suture coatings consisting of lipid based drug delivery systems in combination with antiseptics to avoid post-operative wound infections. Continuous drug release kinetics and superior anti-infective characteristics were assessed. Enhanced tissue compatibility is under development rendering these coatings of high interest in surgery.

6 Acknowledgements

We would like to thank Josef Hintermair (ITEM-GmbH, The Biotoooling Company, Garching, Germany) for his great assistance in microbial testing. The authors did not receive any payments or benefits from a commercial party related directly or indirectly to the subject of this article. This study was partly supported by the Arbeitsgemeinschaft industrieller Forschungsvereinigungen (AiF).

7 Figure Captions

Figure 1. SEM pictures of PGA Resorba[®] sutures coated with A) chlorhexidine dipalmitate (CP) and B) octenidine hydrochloride (OH2), C) Vicryl Plus[®] and D) uncoated PGA Resorba[®] (magnification 450).

Figure 2. Release concentration of drugs (weight/volume) from PGA sutures after 96 hours into PBS buffer, related to drug charge (weight/unit length).

Figure 3. Elution profiles of different drugs into PBS from A) chlorhexidine coated PGA sutures and B) octenidine coated PGA sutures.

Figure 4. *S. aureus* growth cultured in sterile Mueller-Hinton broth for 24 hours in the presence of individual antimicrobially coated sutures: A) chlorhexidine dipalmitate, B) octenidine hydrochloride, C) octenidine hydrochloride, D) Vicryl Plus[®].

Figure 5. Numbers of *S. aureus* colonies adsorbed on the surface of coated PGA sutures after 24 hours of incubation in 2×10^6 cfu/ml suspension.

Figure 6. Metabolic activity of viable cells incubated with individual coated sutures measured with the Roche cell proliferation assay. Uncoated PGA sutures as well as Vicryl Plus[®] sutures served as reference.

8 References

1. **Alfonso, J. L., S. B. Pereperez, J. M. Canoves, M. M. Martinez, I. M. Martinez, and J. M. Martin-Moreno.** 2007. Are we really seeing the total costs of surgical site infections? A Spanish study. *Wound Repair Regen* **15**:474-81.
2. **Barbolt, T. A.** 2002. Chemistry and safety of triclosan, and its use as an antimicrobial coating on Coated VICRYL* Plus Antibacterial Suture (coated polyglactin 910 suture with triclosan). *Surg Infect (Larchmt)* **3 Suppl 1**:S45-53.
3. **Barnett, T. E.** 2007. The not-so-hidden costs of surgical site infections. *Aorn J* **86**:249-58.
4. **Brenwald, N. P., and A. P. Fraise.** 2003. Triclosan resistance in methicillin-resistant *Staphylococcus aureus* (MRSA). *J Hosp Infect* **55**:141-4.
5. **Chaudhary, S. B., M. J. Vives, S. K. Basra, and M. F. Reiter.** 2007. Postoperative spinal wound infections and postprocedural diskitis. *J Spinal Cord Med* **30**:441-51.
6. **Christensen, G. D., W. A. Simpson, A. L. Bisno, and E. H. Beachey.** 1982. Adherence of slime-producing strains of *Staphylococcus epidermidis* to smooth surfaces. *Infect Immun* **37**:318-26.
7. **Costerton, J. W., L. Montanaro, and C. R. Arciola.** 2005. Biofilm in implant infections: its production and regulation. *Int J Artif Organs* **28**:1062-8.
8. **Darouiche, R. O.** 2001. Device-associated infections: a macroproblem that starts with microadherence. *Clin Infect Dis* **33**:1567-72.
9. **Darouiche, R. O., J. Farmer, C. Chaput, M. Mansouri, G. Saleh, and G. C. Landon.** 1998. Anti-infective efficacy of antiseptic-coated intramedullary nails. *J Bone Joint Surg Am* **80**:1336-40.
10. **Dunne, W. M., Jr., E. O. Mason, Jr., and S. L. Kaplan.** 1993. Diffusion of rifampin and vancomycin through a *Staphylococcus epidermidis* biofilm. *Antimicrob Agents Chemother* **37**:2522-6.
11. **Edmiston, C. E., G. R. Seabrook, M. P. Goheen, C. J. Krepel, C. P. Johnson, B. D. Lewis, K. R. Brown, and J. B. Towne.** 2006. Bacterial adherence to surgical sutures: can antibacterial-coated sutures reduce the risk of microbial contamination? *J Am Coll Surg* **203**:481-9.
12. **Gollwitzer, H., K. Ibrahim, H. Meyer, W. Mittelmeier, R. Busch, and A. Stemberger.** 2003. Antibacterial poly(D,L-lactic acid) coating of medical implants using a biodegradable drug delivery technology. *J Antimicrob Chemother* **51**:585-91.
13. **Gollwitzer, H., P. Thomas, P. Diehl, E. Steinhauser, B. Summer, S. Barnstorf, L. Gerdesmeyer, W. Mittelmeier, and A. Stemberger.** 2005. Biomechanical and allergological characteristics of a biodegradable poly(D,L-lactic acid) coating for orthopaedic implants. *J Orthop Res* **23**:802-9.
14. **Kaliche, T., J. Schierholz, U. Schlegel, T. M. Frangen, M. Koller, G. Printzen, D. Seybold, S. Klockner, G. Muhr, and S. Arens.** 2006. Effect on infection resistance of a local antiseptic and antibiotic coating on osteosynthesis implants: an in vitro and in vivo study. *J Orthop Res* **24**:1622-40.
15. **Lucke, M.** 2005. Local protection for surgical implants. *Chem Biol* **12**:958-9; discussion 1041-8.
16. **Lucke, M., G. Schmidmaier, S. Sadoni, B. Wildemann, R. Schiller, N. P. Haas, and M. Raschke.** 2003. Gentamicin coating of metallic implants reduces implant-related osteomyelitis in rats. *Bone* **32**:521-31.
17. **Mack, D., P. Becker, I. Chatterjee, S. Dobinsky, J. K. Knobloch, G. Peters, H. Rohde, and M. Herrmann.** 2004. Mechanisms of biofilm formation in *Staphylococcus epidermidis* and *Staphylococcus aureus*: functional molecules, regulatory circuits, and adaptive responses. *Int J Med Microbiol* **294**:203-12.

18. **Ming, X., S. Rothenburger, and D. Yang.** 2007. In vitro antibacterial efficacy of MONOCRYL plus antibacterial suture (Poliglecaprone 25 with triclosan). *Surg Infect (Larchmt)* **8**:201-8.
19. **Rothenburger, S., D. Spangler, S. Bhende, and D. Burkley.** 2002. In vitro antimicrobial evaluation of Coated VICRYL* Plus Antibacterial Suture (coated polyglactin 910 with triclosan) using zone of inhibition assays. *Surg Infect (Larchmt)* **3 Suppl 1**:S79-87.
20. **Schierholz, J. M., and J. Beuth.** 2001. Implant infections: a haven for opportunistic bacteria. *J Hosp Infect* **49**:87-93.
21. **Storch, M., L. C. Perry, J. M. Davidson, and J. J. Ward.** 2002. A 28-day study of the effect of Coated VICRYL* Plus Antibacterial Suture (coated polyglactin 910 suture with triclosan) on wound healing in guinea pig linear incisional skin wounds. *Surg Infect (Larchmt)* **3 Suppl 1**:S89-98.
22. **Storch, M., H. Scalzo, S. Van Lue, and G. Jacinto.** 2002. Physical and functional comparison of Coated VICRYL* Plus Antibacterial Suture (coated polyglactin 910 suture with triclosan) with Coated VICRYL* Suture (coated polyglactin 910 suture). *Surg Infect (Larchmt)* **3 Suppl 1**:S65-77.
23. **Suido, H., S. Offenbacher, and R. R. Arnold.** 1998. A clinical study of bacterial contamination of chlorhexidine-coated filaments of an interdental brush. *J Clin Dent* **9**:105-9.
24. **Visai, L., C. R. Arciola, G. Pietrocola, S. Rindi, P. Olivero, and P. Speziale.** 2007. Staphylococcus biofilm components as targets for vaccines and drugs. *Int J Artif Organs* **30**:813-9.
25. **Volenko, A. V., S. Germanovich Ch, O. P. Gurova, and R. A. Shvets.** 1994. [Kapromed - antibacterial suture material]. *Med Tekh*:32-4.
26. **von Eiff, C., C. Heilmann, M. Herrmann, and G. Peters.** 1999. Basic aspects of the pathogenesis of staphylococcal polymer-associated infections. *Infection* **27 Suppl 1**:S7-10.
27. **Yazdankhah, S. P., A. A. Scheie, E. A. Hoiby, B. T. Lunestad, E. Heir, T. O. Fotland, K. Naterstad, and H. Kruse.** 2006. Triclosan and antimicrobial resistance in bacteria: an overview. *Microb Drug Resist* **12**:83-90.

Chapter 4

Growth inhibition of *Staphylococcus aureus* induced by low-frequency electric and electro-magnetic fields

Abstract

Objectives: Magnetic field therapy is an established technique in the treatment of pseudarthrosis. In cases of osteomyelitis, palliation is also observed. This study focuses on the impact of different electric and electromagnetic fields on the growth of *Staphylococcus aureus* by in vitro technologies.

Methods: Cultures of *S. aureus* in fluid and gel-like media were exposed to a low-frequency electromagnetic field, an electromagnetic field combined with an additional electric field, a sinusoidal electric field and a static electric field.

Results: In gel-like media no significant difference between colony-forming units of exposed samples and non-exposed references was detected. In contrast, *S. aureus* concentrations in fluid media could clearly be reduced under the influence of the four different applied fields within 24 hours of experiment. The strongest effects were observed for the direct current electric field which could decrease cfu/ml of 37 %, and the low-frequency electro-magnetic field with additional induced electric alternating field with a decrease of staphylococci concentration by 36 %.

Conclusions: The effects of the electromagnetic treatment on staphylococci within fluid media are significantly higher than in gel-like media. The application of low-frequency electromagnetic fields corroborates clinical situations of bone infections during magnetic field therapy.

Keywords: Electro-magnetic field, *Staphylococcus aureus*, growth inhibition, infection, low-frequency

1 Introduction

Magnetic fields are in use in medicine, for example in the magnet resonance tomography, the magnetic stimulation of brain areas and for magnetic drug targeting. Several studies in literature attest magnetic fields a therapeutic benefit. Sharrard performed a double-blind trial of pulsed electromagnetic fields for delayed union of tibial fractures and concluded that pulsed electromagnetic fields significantly influence healing in tibial fractures with delayed union (30). Borsalino et al. reported in a double-blind treatment of 32 consecutive patients treated with femoral intertrochanteric osteotomy for hip degenerative arthritis a statistically significant difference between controls and patients treated with low-frequency pulsing electromagnetic fields (5). In a double blind study about the effect of electromagnetic fields on patients undergoing massive bone graft following bone tumor resection, Capanna et al. observed a decrease in the healing time from 9.4 months in the control group to 6.7 months in the active stimulated group when adjuvant postoperative chemotherapy was not employed (6). Trock et al. assessed pulsed electromagnetic fields the potential as an effective method of improving symptoms in patients with osteoarthritis (35). In the area of wound healing Stiller et al. assessed the clinical efficacy and safety of pulsed electromagnetic limb ulcer therapy in the healing of recalcitrant, predominantly venous leg ulcers by a portable pulsed electromagnetic field device (31).

Magnetic field therapy is often used as a therapeutic procedure to improve fracture healing (34). Heckman et al. claimed the effectiveness in the treatment of ununited fractures by noninvasive, pulsed electromagnetic fields after three months of intensive use in more than 85 % of 149 patients (16). Bassett et al. demonstrated that the surgically noninvasive, outpatient method of pulsing electromagnetic fields induce weak electric currents in bone and produced confirmed end results in 1,007 ununited fractures and 71 failed arthrodeses, worldwide (3).

The so-called Kraus-Lechner procedure is based on the interaction of low-frequency nonthermal sinusoidal electro-magnetic fields with bone and cartilage tissue and it is often applied to purely healing bone fractures of non-unions (19). Clinical observations have shown that in infected pseudarthrosis this technology improves bone healing and decreases bone infections (20, 21). Nowadays there are no data of low-frequent electromagnetic fields based on the Kraus-Lechner techniques and similar electric fields on the influence on bacterial growth. Methodical investigations of the effect of different kinds of applied fields on bacterial

growth have not been elucidated before as previous studies mostly focused on one specific electric or electromagnetic field effect.

The purpose of this study was to determine whether an application of different electric and electromagnetic fields could influence the growth of *S. aureus* since it is the main cause of bone and implant-associated infections.

2 Materials and Methods

2.1 Test bacterium

A clinical isolate of *S. aureus* (strain ATTC[®] 49230) was provided by the Institute of Clinical Microbiology (Department of Clinical Hygiene, Klinikum rechts der Isar, Munich, Germany). The germ was plated on columbia agar plates (No. 254071, BD Diagnostic Systems Heidelberg, Germany) and incubated at 37 °C for 24 hours. After 24 hours, several colonies were gathered with a sterile one-way inoculation loop, plated on a fresh agar plate and placed in an incubator at 37 °C. This procedure was repeated every other day for life maintenance and 24 hours before experimental performance.

2.2 Growth curve

In order to correlate the optical density at 600 nm of *S. aureus* suspension with the colony forming units of the microorganism, a calibration curve was recorded. A bacterial suspension was produced by resuspending about 100 colonies of *S. aureus* from columbia agar plates in 750 ml of sterile Mueller-Hinton broth (No. 275730, BD Diagnostic Systems, Difco[™], Heidelberg, Germany). The homogeneous suspension was incubated at 37 °C for 24 hours under static conditions. In time intervals of 60 minutes within the first eight hours and again after 24 hours both the optical density (GeneQuant pro, biochrom, Cambridge, UK) of obtained suspension at 600 nm was measured and different dilutions of each sample were plated on columbia agar plates. The degree of dilution was assessed in preliminary experiments and conformed to the number of obtained colony forming units visually countable.

After incubating for 24 hours at 37 °C the colony forming units were visually determined, extrapolated to the initial concentration in suspension and correlated to the measured value of optical density. This experiment was repeated three times and all values were combined as optical density values as well as cfu/ml can not be reproduced to defined values. A logarithmic regression curve with the formula $OD=0.0741 \ln(\text{cfu})-0.2066$ and a correlation coefficient of 0.91 resulted.

2.3 Bacteria on gel-like medium

Experiments on gel-like medium were performed on columbia agar plates with 5 % sheep blood. This highly nutritious medium is used for the isolation and cultivation of nonfastidious and fastidious microorganisms (10). Bacteria from columbia agar plates were resuspended in normal saline and adjusted to 1×10^8 cfu/ml by visual comparison with 0.5 McFarland standard. This suspension was diluted with normal saline to an inoculum of 1×10^3 cfu/ml. For each of the four applied electric or electromagnetic fields the same volume of the suspension was plated on seven sample and seven reference columbia agar plates. The sample plates were then exposed to one of the four applied electromagnetic fields in a sample incubator at 37 °C for 24 hours. The reference plates were placed in a reference incubator at 37 °C for 24 hours (Figure 1). These experiments were performed thrice for each of the four applied electric or electromagnetic fields.

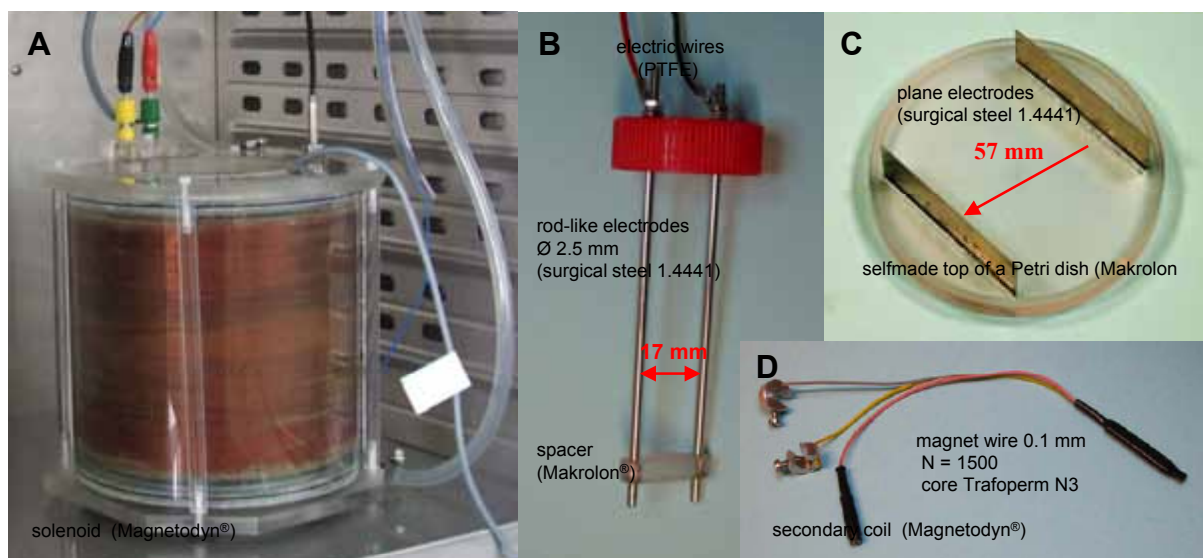


Figure 1. Experimental equipment: A) Solenoid with cooling jacket to generate a sinusoidal electromagnetic field (5 mT, 20 Hz), B) Electric field applicator with rod-like electrodes to expose bacterial suspensions, C) Electric field applicator for standard Petri dishes, D) Secondary coil to induce an additional electric field.

2.4 Bacteria in fluid medium

Staphylococcus aureus suspension was produced as already described. Eight sterile 50 ml tubes were filled with 50 ml bacterial suspension (1×10^3 cfu/ml). Four reference tubes were placed in the reference incubator. Four sample tubes were then exposed to one of the four applied electromagnetic fields in the sample incubator. Field exposure took place in the sample incubator at 37 °C within the first eight hours in respectively 40 minutes intervals following 20 minutes breaks. After this samples were then incubated at 37 °C for further 16 hours. Four references were placed in the reference incubator at 37 °C for 24 hours. In a time interval of 60 minutes within the first eight hours and again at a time point of 24 hours of incubation at 37 °C the optical density at 600 nm of bacterial suspension was measured. A bacterial growth curve of sample and reference was determined. The bacterial concentrations of sample and reference at different points in time could be compared with the aid of the calibration curve.

2.5 Sinusoidal low-frequency electro-magnetic field

A sinusoidal low-frequency electromagnetic field was generated by a solenoid (FA-P6-K, Neue Magnetodyn[®], Munich, Germany) (Figure 1A and 2A, 2C) combined with a frequency generator (M80, Neue Magnetodyn[®], Munich, Germany). This setup is clinically established as magnetic field therapy in bone fracture healing using sinusoidal frequencies between 0 and 30 Hz and magnetic flux densities between 0.5 mT and 10 mT. Test tubes containing bacteria in fluid medium as well as agar plates inoculated with bacteria were placed inside the solenoid. The solenoid was constructed in a manner that it was possible to insert seven agar plates as well as four 50 ml test tubes. A cooling system was built to prevent the solenoid from overheating by connecting a circulation water bath including a thermostat (F3, Haake, Vreden, Germany). A stable incubation temperature of the bacteria at $37\text{ }^{\circ}\text{C} \pm 0.1\text{ }^{\circ}\text{C}$ was assured by placing the coil in a sample incubator (CB150, Binder, Tuttlingen, Germany). Culture temperature was monitored by a calibrated temperature meter (VC306/K202, Conrad Electronic, Hirschau, Germany) located close to bacteria cultures and recorded online. A reference incubator was placed at 3 meter distance to the sample incubator. The stray field of the coil was measured in radial and axial direction to make sure that the reference incubator (CB150, Binder, Tuttlingen, Germany) is not influenced by the electro-magnetic stray field. By measuring the spatial distribution of the magnetic flux density inside the coil with a Gauss meter (Bell640, F.W. Bell Inc.), the homogeneity of the magnetic field was assured (Figure 3). In this experimental setup a low-frequency electro-magnetic field with a frequency of 20 Hz and a flux density of 5 mT by using a current of 1.2 A was applied. The electric field strength of the solenoid itself at a radial distance $r = 4.5\text{ cm}$ from the coil axis is about 17 mV/cm and was neglected because of its low amplitude. The geomagnetic field was measured at 60 μT .

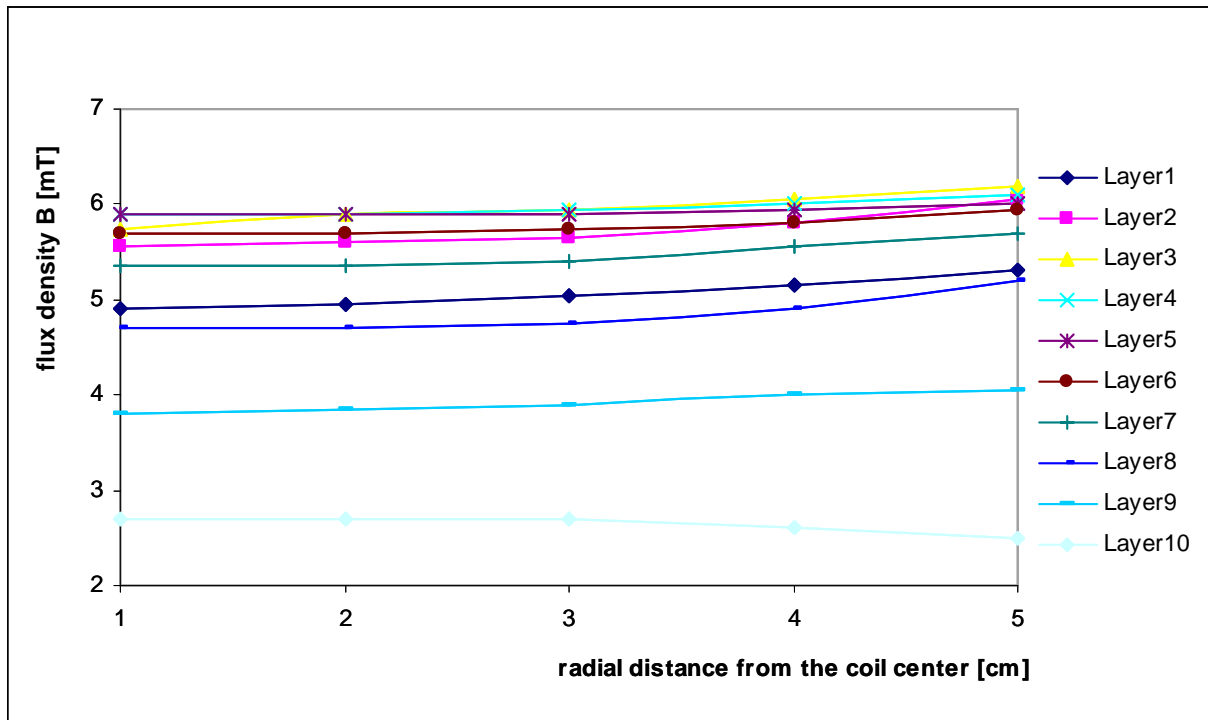


Figure 2. Spatial distribution of the magnetic flux density inside the coil - during action at 5 mT, 20 Hz - along the cross section beginning at the central axis. Measurements were carried out in each Petri dish layer to make sure that the cultures are exposed to a defined region of flux density.

2.6 Electromagnetic field combined with an additional electric alternating field

The same experimental setup as already described for low-frequency electromagnetic field was applied (2B and 2D). Additionally, secondary coils (SI-FE, Neue Magnetodyn[®], Munich, Germany) (Figure 1D) were placed inside the primary solenoid in order to establish an additional electric alternating field. Especially designed lids for standard Petri dishes were used containing two plane electrodes at a distance of 5.7 cm, which were dipping inside the agar (Figure 1C). An alternating voltage which can be gripped at the secondary coil is induced by the alternating magnetic field from the primary solenoid. An additional voltage of $0.8V_{\text{eff}}$ at 20 Hz is induced in the secondary coil running the primary coil with 20 Hz and 5 mT which results in an effective alternating electric field strength of 140 mV/cm. This homogeneous electric field is applied as an additional electric field between the electrodes across the agar medium inside the Petri dishes directed perpendicular to the magnetic field. For *S. aureus* suspensions, the secondary coils were connected to electric field applicators made of surgical steel rods placed at a distance of 1.7 cm inside the tubes attached to the lids (Figure 1B). In

this experimental setup an additional voltage of $0.8 V_{\text{eff}}$ at 20 Hz resulting in a maximal induced alternating electric field strength of 470 mV/cm by the alternating magnetic field from the primary solenoid at 5 mT and 20 Hz.

The electric field strength is the quotient of the applied voltage ($0.8 V_{\text{eff}}$) and the electrode distance (5.7 cm for gel-like medium, 1.7 cm for bacterial suspensions).

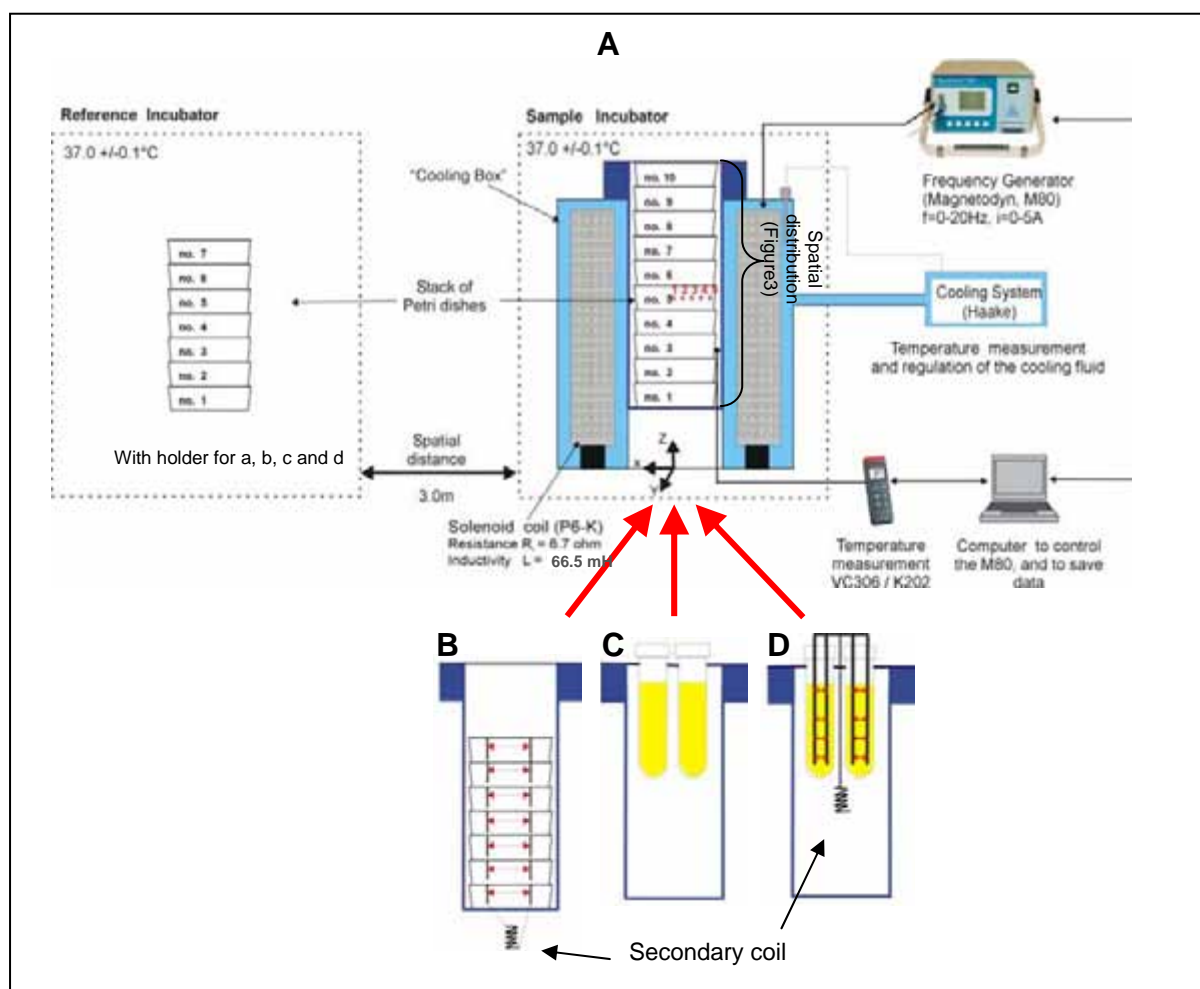


Figure 3. Scheme of experimental setups to apply low-frequency electro-magnetic fields (20 Hz, 5 mT: only Solenoid) and electro-magnetic fields with additional electric fields for *S. aureus* cultures on Mueller-HintonII agar and in suspensions. A sample incubator with A) Low-frequency electro-magnetic fields (5 mT, 20 Hz) exposed to gel-like medium and similar with B) Electro-magnetic field (5 mT, 20 Hz) combined with an additional electric field of 140 mV/cm on gel-like medium, C) Low-frequency electro-magnetic field (5 mT, 20 Hz) in fluid medium, D) Electro-magnetic field (5 mT, 20 Hz) combined with an additional electric field of 470 mV/cm in fluid medium.

2.7 Sinusoidal electric alternating field

Bacteria colonies on agar plates as well as in fluid medium were exposed to a pure sinusoidal electric field. Electric field applicators already described were connected to a frequency generator (PM 5131, Phillips, Hamburg, Germany) to apply an electric alternating field without using a primary or secondary coil. In agar plates sinusoidal voltages of $0.707 V_{\text{eff}}$ were applied which results in an electric field strength of 124 mV/cm. A sinusoidal voltage of $0.8 V_{\text{eff}}$ and a field strength with a maximum of 470 mV/cm in case of bacteria suspension were applied (Figure 1 and 4A, 4C).

2.8 Direct current electric field

A direct current field was applied by connecting the electrodes already described to a frequency generator (PM 5131, Phillips, Hamburg, Germany). Bacteria colonies on agar plates as well as in fluid medium were exposed to this field. Bacteria on agar plates were affected by a direct voltage of 1.0 V and an electric field strength of 175 mV/cm. Bacteria in fluid medium were exposed to a direct voltage of 1.0 V resulting in a maximal field strength of 470 mV/cm. For the calculation of the direct current electric field strength, the direct current voltage corresponds to the peak voltages already used (Figure 1 and 4B, 4D).

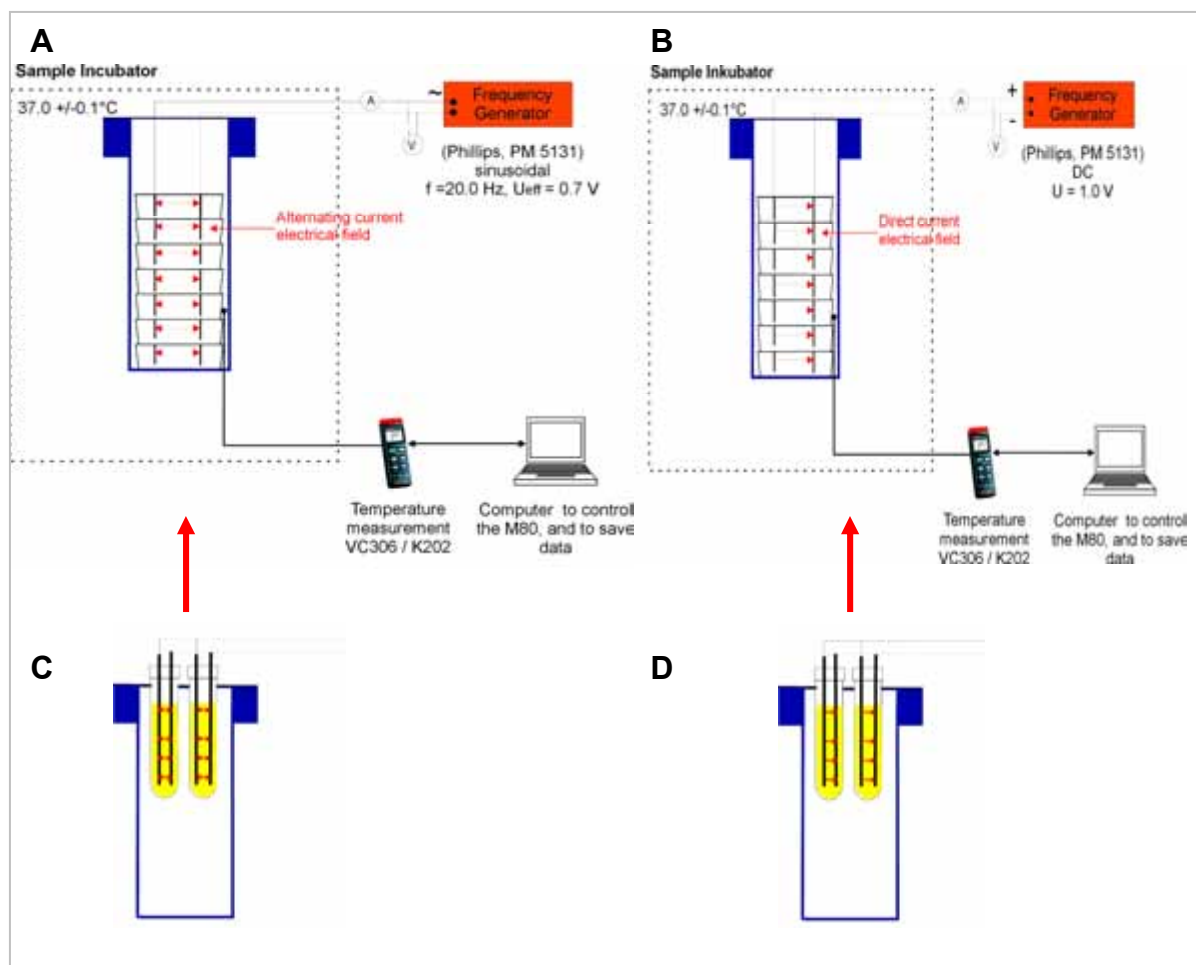


Figure 4. Scheme of experimental setups to apply sinusoidal and direct current electric fields for *S. aureus* cultures on columbia agar and Mueller-HintonII suspensions: A) Sinusoidal electric alternating field (124 mV/cm, 20 Hz) in gel-like medium, B) Direct current field of 175 mV/cm in gel-like medium, C) Sinusoidal electric alternating field (470 mV/cm, 20 Hz) in fluid medium, D) Direct current field of 588 mV/cm in fluid medium.

2.9 Calculations and statistical methods

Data from bacterial growth studies were compared for statistical significance using a two tailed student t-test with $P < 0.05$ considered significant.

3 Results

An application of the four different electromagnetic fields on *S. aureus* cultured on columbia agar plates showed no significant effect regarding the stimulation or inhibition of colony forming (Figure 5). A tendency of growth inhibition was detected by exposing the pathogen cultures to a low-frequency electromagnetic field (5 mT, 20 Hz) as well as to an electromagnetic field combined with an additional electric field (5 mT, 140 mV/cm, 20 Hz). The application of a sinusoidal electric field (124 mV/cm, 20 Hz) as well as a constant electric field (175 mV/cm) to *S. aureus* on columbia agar plates shows a weak but not statistically significantly stimulating effect of colony forming. The absolute heights of cfu differ from experiment to experiment due to various amounts of bacterial suspension used to inoculate the agar plates. However within one experimental setup the used cfu are identical for samples and references. Samples and reference can therefore be compared and the field effect evaluated.

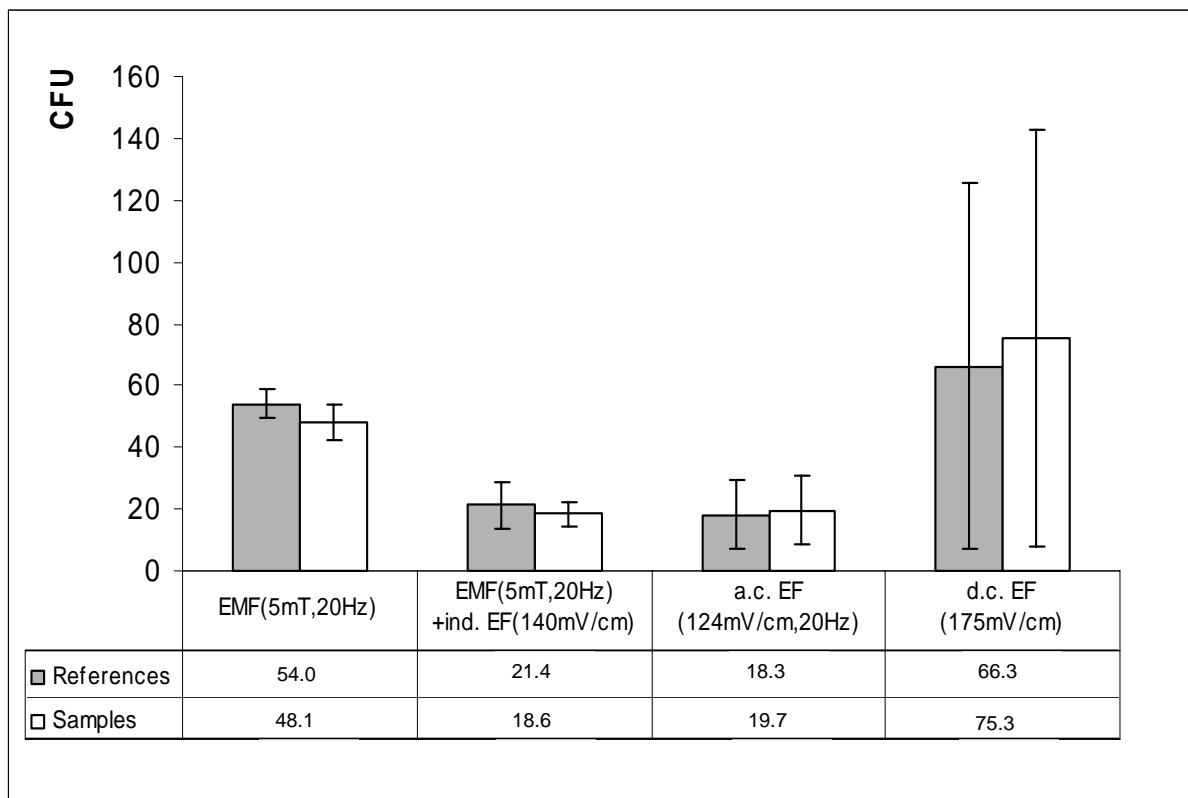


Figure 5. Gel-like medium containing *S. aureus*: Influence of electric and electro-magnetic fields on colony-forming units.

EMF ^= electromagnetic field, a.c. EF ^= alternating electrical field, d.c. EF ^= direct current electrical field, ind. EF ^= additional a.c. electrical field

In fluid medium, a faster bacterial growth compared to reference of *S. aureus* under the influence of a low-frequency electromagnetic field (5 mT, 20 Hz) within the first eight hours was observed. However, at the end of the experiment after 24 hours, bacteria concentration in low-frequency electromagnetic sample showed a significantly lower cfu/ml than in the reference. A significant microorganism concentration reduction of 29 % could be demonstrated under the influence of the applied low-frequency electromagnetic field (Figure 6A).

Treatment of *S. aureus* in fluid medium with an electromagnetic field (5 mT, 20 Hz) combined with an additional electric field (470 mV/cm) showed during field application a decrease of bacterial growth until the end of the experiment. At the end of the experiment after 24 hours a cfu/ml reduction of 36 % compared to reference could be observed (Figure 6B).

Exposing staphylococci suspensions to a sinusoidal electric field (470 mV/cm, 20 Hz), revealed an increase of cfu/ml compared to reference during exposure time intervals within the first 8 hours. Bacterial growth within the following 16 hours is delayed in comparison to reference. The application of a sinusoidal electric field reduces cfu/ml of 18 % compared to reference (Figure 6C).

The application of a constant electric field (588 mV/cm) on staphylococci in fluid medium showed an increase of microorganism concentration within the first 8 hours of treatment compared to untreated reference. In the following time period between eight and twenty four hours, a clear reduction of pathogen growth was detected resulting in a decrease of cfu/ml in a range of 37 % (Figure 6D).

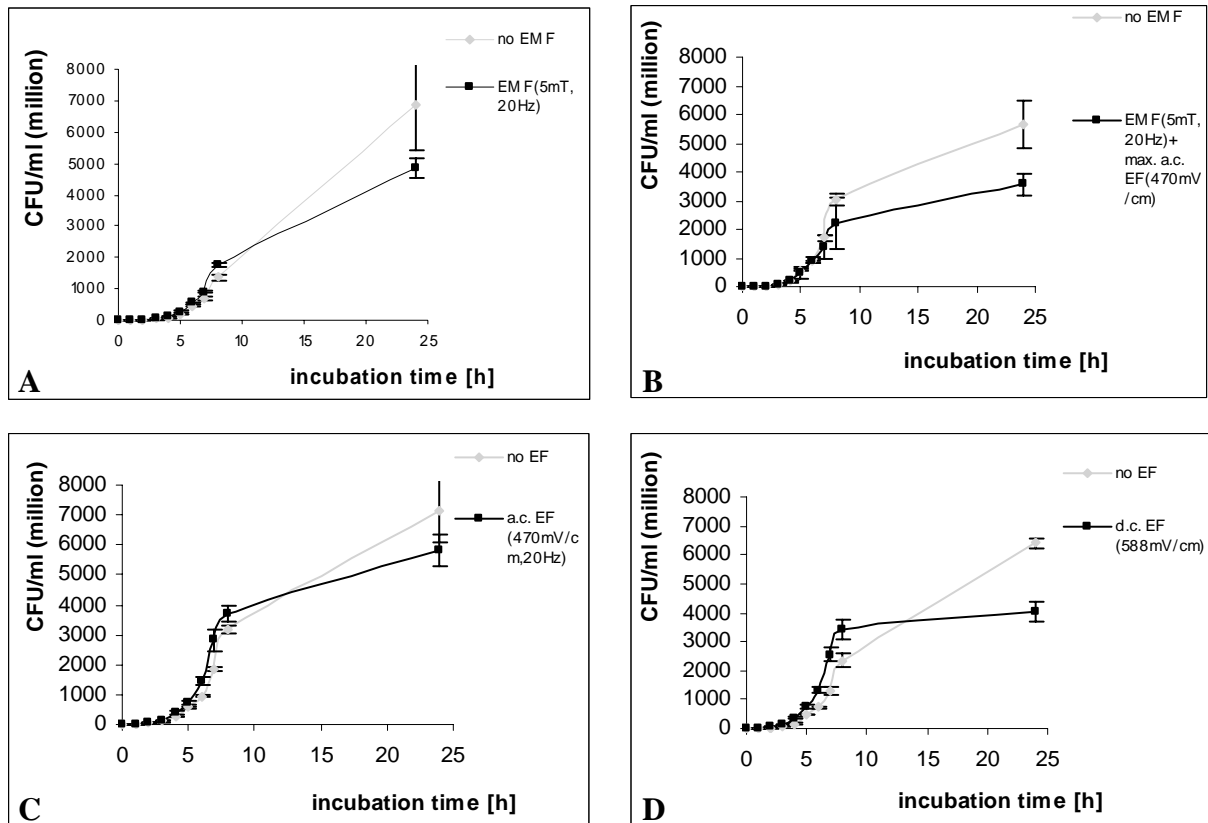


Figure 6. Fluid medium containing *S. aureus*: Influence of electric and electro-magnetic fields on bacterial concentration (cfu/ml). Mediumn cfu/ml of sample (n=4) and reference (n=4) from *S. aureus* cultured in sterile Mueller-Hinton broth under the influence of different electro-magnetic-fields. A) Low-frequency electro-magnetic field (5 mT, 20 Hz), B) Electro-magnetic field (5 mT, 20 Hz) combined with an additional electric field of 470 mV/cm, C) Sinusoidal electric alternating field (470 mV/cm, 20 Hz), D) Direct current field of 588 mV/cm.

EMF ^= electromagnetic field, a.c. EF ^= alternating electrical field, d.c. EF ^= direct current electrical field

4 Discussion

Medical implants like orthopaedic implants are highly susceptible to pathogens and therefore feature high infection rates. Common environmental and skin pathogens like *Staphylococcus aureus* and *Staphylococcus epidermidis* are the most frequently detected germs in device-related infection. These pathogens colonize the implant by adhering to the patients own proteins located on the surface of the graft and form a biofilm (1, 13, 14). The biofilm formation on biomaterials present challenging complications in the field of medical implants. In a biofilm bacteria are well protected from the host immune defence. The consequence is an

increase in antibiotic resistance so that even high local concentrations of antibiotics do not completely eradicate bacteria in biofilms (8, 9). A technology that offers considerable promise in the field of device-related infections is the application of weak electric and electromagnetic fields.

Several studies are focusing on the effect of electromagnetic fields on growth of bacteria like *S. aureus*. Strasak et al. report a decrease of optical densities for different bacteria strains exposing to a 50 Hz electro-magnetic field at room temperature (33). Fojt et al. observed a decrease of the number of viable bacteria by low-frequency electromagnetic fields at 50 Hz (11). Using sinusoidal low-frequency weak magnetic fields of 60 and 600 Hz at 3 mT for more than 50 hours, Ramon et al. could show an decrease of bacterial colonies of *E. coli* (28). The influence of static magnetic fields was also investigated. Gerencser et al. demonstrated reduced bacterial growth of staphylococci and *Serratia marcescens* by static magnetic fields (12). However, Kohno et al. could not detect any inhibition on *E. coli* exposed to static magnetic fields (18). Nevertheless, they observed a decreased growth rate and growth maximum number of *S. mutans* and *S. aureus* under anaerobic conditions. Grosman et al. detected no significant influence caused by a static magnetic field in the range of 0.5 to 4 Tesla on growth and biochemical activity on *S. aureus* and *E. coli* (15). These findings could not be corroborated by Zhang et al. investigating *E. coli* (37). Piatti et al. reported a growth inhibitory effect and a decrease of the pathogen virulence using *Serratia marcescens* in the presence of a static magnetic field (26). Studies of Pareilleux and Sicard about the influence of static electric fields on bacteria revealed a lethal activity of low-voltage alternating currents in the presence of chlorid ions in tested *E. coli* suspensions (23). An inactivation of microorganisms by strong pulsed electric fields in the range of 4.5 kV/cm is reported by Kermanshahi and Sailani (17). Recently Cellini et al. demonstrated that the exposure of *E. coli* to a 50 Hz electromagnetic field acts as a stressing factor leading to phenotypical and transcriptional changes (7).

In previous studies only one type of field was investigated. However, in this study we compared the effect of a low-frequency electromagnetic field, an electromagnetic field combined with an electric field, a sinusoidal electric field and a constant electric field on growth/growth inhibition of *S. aureus*. This germ was used as it is the predominating pathogen causing implant associated infections (9). These investigations admit results of the applied fields on fluid and gel-like medium under comparable conditions, conclusions about the mode of action can be drawn.

Our experiments with *S. aureus* on gel-like medium showed no significant influence of the applied electric and electromagnetic fields on bacterial growth. In contrast to these data all four applied fields revealed a significant effect on growth of *S. aureus* in fluid medium within the observation period of 24 hours. Depending on the applied field growth inhibition from 18 % using a sinusoidal electric field (470 mV/cm, 20 Hz) and 37 % using a constant electric field (588 mV/cm) could be observed (Table 1). These investigations demonstrated a reduction of *S. aureus* growth in fluid medium under field influence within 24 hours. Comparable effects could be shown by applying a direct current electric field and an electromagnetic field with additional electric field.

Table 1. Reduction of *S. aureus* growth in fluid medium after 24 hours under the influence of electric and electro-magnetic fields. A) Low-frequency electro-magnetic field (5 mT, 20 Hz), B) Electro-magnetic field (5 mT, 20 Hz) combined with an additional electric field of 470 mV/cm, C) Sinusoidal electric alternating field (470 mV/cm, 20 Hz), D) Direct current field of 588 mV/cm.

EMF ^= electromagnetic field, a.c. EF ^= alternating electrical field, d.c. EF ^= direct current electrical field

Reduction of staphylococci concentration after 24 hours compared to reference	electro-magnetic fields		electric fields	
	A) EMF (5 mT, 20 Hz)	B) EMF + a.c. EF (5 mT, 470 mV/cm, 20 Hz)	C) a.c. EF (470 mV/cm, 20 Hz)	D) d.c. EF (588 mV/cm)
	29.2 % (p = 0.0376)	36.9 % (p = 0.0044)	18.6 % (p = 0.0676)	37.3 % (p < 0.0001)

In case of the application of the low-frequency electro-magnetic field, the sinusoidal electric alternating field and the direct current field, growth reduction were considered to be significant ($P < 0.05$).

Observed growth inhibition effects in fluid medium and the fact that no impact of applied electric and magnetic field were assessed on gel-like medium are an indication that the unlimited mobility of ions is a basic requirement for field-induced effects.

Detected effects in fluid medium corroborate clinical observations in the magnetic field therapy of infected pseudarthrosis (20, 21). In those patients under the influence of low-frequency sinusoidal electromagnetic fields there is only in the beginning of the treatment an increase of the wound exudate which can be explained by our results in stimulating bacterial growth within the first eight hours of treatment. In clinical situation after 24 hours a

clarification of the exudate is observed corresponding to the decrease of bacterial growth as demonstrated in our experiments.

The different kinds of fields have an effect on the growth on *S. aureus* and the effect on other pathogens is under elucidation. Whilst electrochemical effects give reason for the impact of electric fields, the underlying biochemical effects of electromagnetic fields have not been clarified until today (7). One assumption is that there is a bactericidal effect under the influence of electromagnetic fields. During the field treatment, a number of bacteria colony forming units are reduced. Even a small reduction in the number of bacteria, at the beginning of the growth process, greatly affects the geometrical progression of the growth process (11, 32). Bacteriostatic effects induced by static magnetic fields may also be explained by radicals such as hydroxyl, chloride and hypochloride (18). The radical pair effect describes the generation of free radicals during high-energy photonic or electro-magnetic irradiation in biological systems due to the interaction of the magnetic field with unmatched electron spins. The formation of radicals leads to temporary damage of cell membranes and to a modification of the ionic channel conductivity which can result in cell death (24). Quantum electrodynamics predicts magnetic effects even with low energy stimulation as it occurs during the Kraus-Lechner procedure with frequencies between 10 and 30 Hz in the case that resonant stimulation conditions occur simultaneously (29).

The "Ion cyclotron resonance" (ICR), primarily considered by Liboff predicts effects by small ions involved in biological processes, that occur in definite frequency- and intensity ranges ("windows") of simultaneously impacting magnetic and electromagnetic fields related by a linear equation, which meanwhile is proven by a number of in vivo and in vitro experiments (22).

Experiments carried out by Binh have shown that frequencies to stimulate ion or ion-protein complex to "swing" in a static magnetic field agree particularly well with those predicted for the biologically relevant ions – such as Ca^{2+} , Mg^{2+} and Zn^{2+} – by means of the ion-cyclotron resonance formula (4). The resonance frequency for Ca^{2+} ions is in the range of extremely low-frequency fields which is an indication for a possible interaction of biological systems and applied electromagnetic fields.

Obviously an interaction of radicals and electromagnetic fields cause damage to bacteria and these effects needs further investigation.

Described methodologies offer new perspectives in the treatment of device-related infections with pronounced biofilm formation. In the literature recent studies assessed an inhibiting effect of electric and electromagnetic fields on biofilm formation.

Investigations by Perez-Roa et al. showed that low-voltage (0.5 V - 5 V) reduced the area of the electrodes covered by biofilm by 50 % (25). The exposure of bacterial biofilms to electrolysis resulted in killing (2.1-log reduction) and removal (4.0-log reduction) of viable cells within a few minutes (27). Van der Borden et al. described the advanced detachment and a decreased viability of staphylococci treated with 60 μ A and 100 μ A direct current (36). These in vitro investigations and the additional clinical observations show that there is high potential in the utilization of electric and electromagnetic fields to combat biofilms.

5 Conclusions

We conclude that a directed electromagnetic field to increase bone healing could offer new opportunities in the therapy of implant associated infections and infected non-unions.

6 Acknowledgements

We would like to thank V. Vatou for her great assistance in microbial testing. Furthermore we acknowledge H. Stephan and W. Kraus for their technical help, contributions and inspiring discussions. Part of this study was supported by funds of the “Bayerische Forschungsstiftung”. The authors did not receive any payments or benefits from a commercial party related directly or indirectly to the subject of this article.

7 Figure and Table Captions

Figure 1. Experimental equipment A) Solenoid with cooling jacket to generate a sinusoidal electro-magnetic field (5 mT, 20 Hz), B) Electric field applicator with rod-like electrodes to expose bacterial suspensions, C) Electric field applicator for standard Petri dishes, D) Secondary coil to induce an additional electric field.

Figure 2. Experimental setups to apply low-frequency electro-magnetic fields (20 Hz, 5 mT) and electro-magnetic fields with additional electric fields for *S. aureus* cultures on Mueller-HintonII agar and in suspensions.

Figure 3. Spatial distribution of the magnetic flux density inside the coil along the cross section beginning at the central axis. Measurements were carried out in each Petri dish layer to make sure that the cultures are exposed to a defined region of flux density.

Figure 4. Experimental setups to apply sinusoidal and direct current electric fields for *S. aureus* cultures on Mueller-HintonII agar and suspensions.

Figure 5. Gel-like medium containing *S. aureus*: Influence of electric and electro-magnetic fields on colony-forming units (cfu).

Figure 6. Fluid medium containing *S. aureus*: Influence of electric and electro-magnetic fields on bacterial concentration (cfu/ml).

Table 1. Reduction of *S. aureus* growth under the influence of electric and electro-magnetic fields. A) Low-frequency electro-magnetic field (5 mT, 20 Hz) in fluid medium, B) Electro-magnetic field (5 mT, 20 Hz) combined with an additional electric field of 470 mV/cm in fluid medium, C) Sinusoidal electric alternating field (470 mV/cm, 20 Hz) in fluid medium, D) Direct current field of 588 mV/cm in fluid medium.

8 References

1. **Barton, A. J., R. D. Sagers, and W. G. Pitt.** 1996. Bacterial adhesion to orthopedic implant polymers. *J Biomed Mater Res* **30**:403-10.
2. **Bassett, C. A.** 1988. Effects of a static magnetic field on fracture healing. *Clin Orthop Relat Res*:311-2.
3. **Bassett, C. A., S. N. Mitchell, and S. R. Gaston.** 1982. Pulsing electromagnetic field treatment in ununited fractures and failed arthrodeses. *Jama* **247**:623-8.
4. **Binhi, V. N., Y. D. Alipov, and I. Y. Belyaev.** 2001. Effect of static magnetic field on *E. coli* cells and individual rotations of ion-protein complexes. *Bioelectromagnetics* **22**:79-86.
5. **Borsalino, G., M. Bagnacani, E. Bettati, F. Fornaciari, R. Rocchi, S. Uluhogian, G. Ceccherelli, R. Cadossi, and G. C. Traina.** 1988. Electrical stimulation of human femoral intertrochanteric osteotomies. Double-blind study. *Clin Orthop Relat Res*:256-63.
6. **Capanna, R., D. Donati, C. Masetti, M. Manfrini, A. Panozzo, R. Cadossi, and M. Campanacci.** 1994. Effect of electromagnetic fields on patients undergoing massive bone graft following bone tumor resection. A double blind study. *Clin Orthop Relat Res*:213-21.
7. **Cellini, L., R. Grande, E. Di Campli, S. Di Bartolomeo, M. Di Giulio, I. Robuffo, O. Trubiani, and M. A. Mariggio.** 2008. Bacterial response to the exposure of 50 Hz electromagnetic fields. *Bioelectromagnetics* **29**:302-11.
8. **Costerton, J. W., B. Ellis, K. Lam, F. Johnson, and A. E. Khoury.** 1994. Mechanism of Electrical Enhancement of Efficacy of Antibiotics in Killing Biofilm Bacteria. *Antimicrobial Agents and Chemotherapy* **38**:2803-2809.
9. **Darouiche, R. O.** 2004. Treatment of infections associated with surgical implants. *N Engl J Med* **350**:1422-9.
10. **Ellner, P. D., C. J. Stoessel, E. Drakeford, and F. Vasi.** 1966. A new culture medium for medical bacteriology. *Am J Clin Pathol* **45**:502-4.
11. **Fojt L., Strašák L., Vetterl V., and S. J.** 2004. Comparison of the low-frequency magnetic field effects on bacteria *Escherichia coli*, *Leclercia adecarboxylata* and *Staphylococcus aureus*. *Bioelectrochemistry - Proceedings of the XVIIth International Symposium on Bioelectrochemistry and Bioenergetics* **63**:337-341.
12. **Gerencser, V. F., M. F. Barnothy, and J. M. Barnothy.** 1962. Inhibition of Bacterial Growth by Magnetic Fields. *Nature* **196**:539-541.
13. **Gotz, F.** 2002. *Staphylococcus* and biofilms. *Mol Microbiol* **43**:1367-78.
14. **Gristina, A. G., C. D. Hobgood, L. X. Webb, and Q. N. Myrvik.** 1987. Adhesive colonization of biomaterials and antibiotic resistance. *Biomaterials* **8**:423-6.
15. **Grosman, Z., M. Kolar, and E. Tesarikova.** 1992. Effects of static magnetic field on some pathogenic microorganisms. *Acta Univ Palacki Olomuc Fac Med* **134**:7-9.
16. **Heckman, J. D., A. J. Ingram, R. D. Loyd, J. V. Luck, Jr., and P. W. Mayer.** 1981. Nonunion treatment with pulsed electromagnetic fields. *Clin Orthop Relat Res*:58-66.
17. **Kermanshahi R.K., and Sailani M.R.** 2005. Effect of static electric field treatment on multiple antibiotic-resistant pathogenic strains of *Escherichia coli* and *Staphylococcus aureus*. *J Microbiol Immunol Infect* **38**:394-398.
18. **Kohn M., Yamazaki M., Kimura I. I., and W. M.** 2000. Effect of static magnetic fields on bacteria: *Streptococcus mutans*, *Staphylococcus aureus*, and *Escherichia coli*. *Pathophysiology* **7**:143-148.

19. **Kraus, W.** 1992. The Treatment of Pathological Bone Lesion with Nonthermal, Extremely Low-Frequency Electromagnetic-Fields. *Bioelectrochemistry and Bioenergetics* **27**:321-339.
20. **Lechner F., Ascherl R., and Uraus W.** 1981. Treatment of pseudarthroses with electrodynamic potentials of low frequency range. *Clin Orthop Relat Res*:71-81.
21. **Lechner F., Oeller G., and Ascherl R.** 1979. Treatment of infected pseudoarthroses with electrodynamic field therapy. *Fortschr Med* **97**:943-9.
22. **Liboff, A. R.** 1997. Electric-field ion cyclotron resonance. *Bioelectromagnetics* **18**:85-7.
23. **Pareilleux, A., and N. Sicard.** 1970. Lethal effects of electric current on *Escherichia coli*. *Appl Microbiol* **19**:421-4.
24. **Pazur, A.** 2004. Characterisation of weak magnetic field effects in an aqueous glutamic acid solution by nonlinear dielectric spectroscopy and voltammetry. *Biomagn Res Technol* **2**:8.
25. **Perez-Roa, R. E., D. T. Tompkins, M. Paulose, C. A. Grimes, M. A. Anderson, and D. R. Noguera.** 2006. Effects of localised, low-voltage pulsed electric fields on the development and inhibition of *Pseudomonas aeruginosa* biofilms. *Biofouling* **22**:383-90.
26. **Piatti E., Albertini M.C., and F. D. Baffone W., Citterio B., Piacentini M.P., Dacha M., Vetrano F., Accorsi A.** 2002. Antibacterial effect of a magnetic field on *Serratia marcescens* and related virulence to *Hordeum vulgare* and *Rubus fruticosus* callus cells. *Comp Biochem Physiol B Biochem Mol Biol* **132**:359-65.
27. **Rabinovitch, C., and P. S. Stewart.** 2006. Removal and inactivation of *Staphylococcus epidermidis* biofilms by electrolysis. *Appl Environ Microbiol* **72**:6364-6.
28. **Ramon C., Ayaz M., and S. D. D. Jr.** 1981. Inhibition of growth rate of *Escherichia coli* induced by extremely low-frequency weak magnetic fields. *Bioelectromagnetics* **2**:285-9.
29. **Schulten, K. a. W., A.** 1984. Magnetfeldeffekte in Chemie und Biologie. *Die Umschau* **25/26**:779-783.
30. **Sharrard, W. J.** 1990. A double-blind trial of pulsed electromagnetic fields for delayed union of tibial fractures. *J Bone Joint Surg Br* **72**:347-55.
31. **Stiller, M. J., G. H. Pak, J. L. Shupack, S. Thaler, C. Kenny, and L. Jondreau.** 1992. A portable pulsed electromagnetic field (PEMF) device to enhance healing of recalcitrant venous ulcers: a double-blind, placebo-controlled clinical trial. *Br J Dermatol* **127**:147-54.
32. **Strašák L., Vetterl V., and S. J.** 2002. Effects of low-frequency magnetic fields on bacteria *Escherichia coli*. *Bioelectrochemistry* **55**:161-164.
33. **Strašák L., Vetterl V., and F. L.** 2005. Effects of 50 Hz Magnetic Fields on the Viability of Different Bacterial Strains. *Electromagnetic Biology and Medicine (formerly Electro- and Magnetobiology)* **24**:293 - 300.
34. **Stuhler, T., G. Kaiser, O. Meffert, and D. Strache.** 1978. [The influence of low-frequency DC (system Kraus-Lechner) on bone growth (author's transl)]. *Arch Orthop Trauma Surg* **91**:297-303.
35. **Trock, D. H., A. J. Bollet, R. H. Dyer, Jr., L. P. Fielding, W. K. Miner, and R. Markoll.** 1993. A double-blind trial of the clinical effects of pulsed electromagnetic fields in osteoarthritis. *J Rheumatol* **20**:456-60.
36. **van der Borden, A. J., H. van der Werf, H. C. van der Mei, and H. J. Busscher.** 2004. Electric current-induced detachment of *Staphylococcus epidermidis* biofilms from surgical stainless steel. *Appl Environ Microbiol* **70**:6871-4.

37. **Zhang S., Wei W., and M. Y. Zhang J., Liu S.** 2002. Effect of static magnetic field on growth of *Escherichia coli* and relative response model of series piezoelectric quartz crystal. *Analyst* **127**:373-7.

Chapter 5

Augmentation of antibiotic efficacy by low-frequency electric and electro-magnetic fields examining *Staphylococcus aureus*

Abstract

Objectives: Systemic treatment of biomaterial-associated bacterial infections with high doses of antibiotics is an established therapeutic concept. Electro-magnetic fields provoke growth inhibition on *Staphylococcus aureus*. The purpose of this in vitro study was to determine the influence of different electric and electro-magnetic fields on antibiotic efficacy using gentamicin.

Methods: Cultures of *S. aureus* in fluid and gel-like media in presence of gentamicin were exposed to a low-frequency electro-magnetic field, an electro-magnetic field combined with an additional electric field, a sinusoidal alternating electric field and a direct current electric field.

Results: No significant difference between sample and reference was detected in gel-like media. In presence of gentamicin, each of the four applied fields showed an additional significant reduction of *S. aureus* concentration in fluid media after 24 hours of experiment. A direct current field decreased cfu/ml of over 91 percent.

Conclusions: An augmentation of antibiotic efficacy is a promising new way for anti-microbial chemotherapy. The application of electro-magnetic fields in the area of implant and bone infections could offer new perspectives in antibiotic treatment.

Keywords: Antibiotic efficacy, electro-magnetic fields, *Staphylococcus aureus*, gentamicin, infection

1 Introduction

Post-operative bone infections and biomaterial-associated infections are common and feared complications of bone fractures and artificial joint implantations (19). A treatment of bone and implant infections also means an administration of high systemic antibiotic concentrations as biofilms insulate pathogens from the host immune defence and antibiotic activity (5, 20). However, drug-induced side effects occur. In case of badly healing bone fractures like non-unions, low-frequency sinusoidal athermic electro-magnetic field therapy according to Kraus-Lechner is an established applied therapeutic procedure (10). This procedure is based on the interaction of sinusoidal electro-magnetic fields with bone and cartilage tissue. In case of infected non-unions, bone healing was observed with an infection palliation (11, 12). The purpose of this study was to investigate whether an application of different electro-magnetic fields could significantly improve antibiotic efficacy.

2 Materials and Methods

2.1 Test bacterium

For in vitro studies, a clinical isolate of *Staphylococcus aureus* (strain ATTC 49230) was used. The test strain was susceptible to gentamicin at a minimal inhibitory concentration MIC of 0.5 µg/ml and cultured on columbia agar plates (No. 254071, BD Diagnostic Systems, Heidelberg, Germany) at 37 °C for 18 hours before testing.

2.2 Growth curve

In order to correlate the optical density at 600 nm of a *S. aureus* suspension with the colony forming units of the microorganism, a calibration curve was recorded. A bacterial suspension was produced by resuspending about 100 colonies of *S. aureus* from columbia agar plates in 750 ml of sterile Mueller-Hinton broth (No. 275730, BD Diagnostic Systems, Difco™, Heidelberg, Germany). The homogeneous suspension was incubated at 37 °C for 24 hours. In time intervals of 60 minutes within the first eight hours and again after 24 hours both the optical density (GeneQuant pro, biochrom, Cambridge, UK) at 600 nm was measured and

different dilutions of each sample were plated on columbia agar plates. After incubating these agar plates for 24 hours at 37 °C the colony forming units were visually determined, extrapolated to the initial concentration in suspension and correlated to the measured value of optical density. This experiment was repeated three times and all values were combined as optical density values as well as cfu/ml can not be reproduced to defined values. A logarithmic regression curve with the formula $OD=0.0741 \ln(cfu)-0.2066$ and a correlation coefficient of 0.91 resulted.

2.3 Antibiotic

Gentamicin sulfate (No. FG0603020, Heraeus, Wehrheim, Germany) was used as antibiotic of choice. The minimal inhibitory concentration was determined according to the directive M7-A6-MIC Testing M100-S15 Vol. 25 No.1 (Rules of Clinical and Laboratory Standards Institute CLSI) at 0.5 µg/ml. For experiments on gel-like medium, three diffusion discs (CT0998B, Oxoid, Hampshire, UK) with gentamicin sulfate concentrations of 4 MIC, 2 MIC and 1 MIC corresponding to 2 µg, 1 µg and 0.5 µg were placed on each sample and reference bacterial lawn on Mueller-HintonII agar plate (No. 221177 BD Diagnostic System, Heidelberg, Germany). For fluid medium experiments, 1 ml of a 6.25 µg/ml gentamicin sulfate stock solution was added to each sample and reference tube, resulting in an end concentration in 50 ml volume of 0.125 µg/ml corresponding to 0.25 MIC.

2.4 Gentamicin test concentration

The optimal gentamicin concentration in conjunction with applied electric and electro-magnetic fields in fluid medium was elucidated in a preliminary experiment. 6 tubes were filled with 49 ml of bacterial suspension. In each tube 1 ml gentamicin sulfate solution of different concentrations was added, resulting in an end concentration of 0.125 MIC, 0.25 MIC, 0.5 MIC, 1 MIC, 2 MIC and 4 MIC. Saline was used as blank. A growth curve was determined by measuring the optical density of bacterial suspension at 600 nm every 60 minutes for 8 hours and again after 24 hours. Via a calibration curve, the optical density was converted in cfu/ml and correlated to time. The three different gentamicin concentrations of 4 MIC, 2 MIC and 1 MIC were used for experiments in gel-like medium.

2.5 Bacteria on gel-like medium

For experiments with pathogens on agar plates, bacterial cells were re-suspended in normal saline and adjusted to 1×10^8 cfu/ml by visual comparison with 0.5 McFarland standard. In each of the 7 sample and 7 reference Mueller-HintonII agar plates, 2 ml of this inoculum was added to receive a bacterial lawn. Three diffusion discs (CT0998B, Oxoid, Hampshire, UK) with gentamicin sulfate concentrations of 4 MIC, 2 MIC and 1 MIC were placed on each agar plate. Sample plates were then exposed to one of the four applied electro-magnetic fields in the sample incubator at 37 °C for 24 hours. The reference plates were placed in the reference incubator at 37 °C for 24 hours. After 24 hours the diameter of zones of inhibition between the corresponding diffusion plates of sample and reference were compared visually.

2.6 Bacteria in fluid medium

A *S. aureus* suspension as already described was produced for experiments in fluid medium. Four sterile 50 ml reference tubes and four sterile 50ml-sample tubes were filled with 49 ml of bacterial suspension. In each tube 1 ml of gentamicin sulfate solution was added, resulting in an end concentration of 0.25 MIC within the total volume of 50 ml in each tube. Samples were then exposed to one of the four applied electro-magnetic fields in the sample incubator at 37 °C within the first 8 hours. For that purpose, electro-magnetic fields were exposed in 40-minute intervals following a 20 minute break within the first 8 hours. After 8 hours, samples were incubated at 37 °C for 16 more hours. References were placed in the reference incubator at 37 °C for 24 hours. A bacterial growth curve of sample and reference was determined by measuring the optical density at 600 nm of bacterial suspension within the first eight hours in a time interval of 60 min and again at 24 hours of incubation at 37 °C. Bacterial concentrations of sample and reference at different investigation points were compared with the aid of the recorded calibration curve.

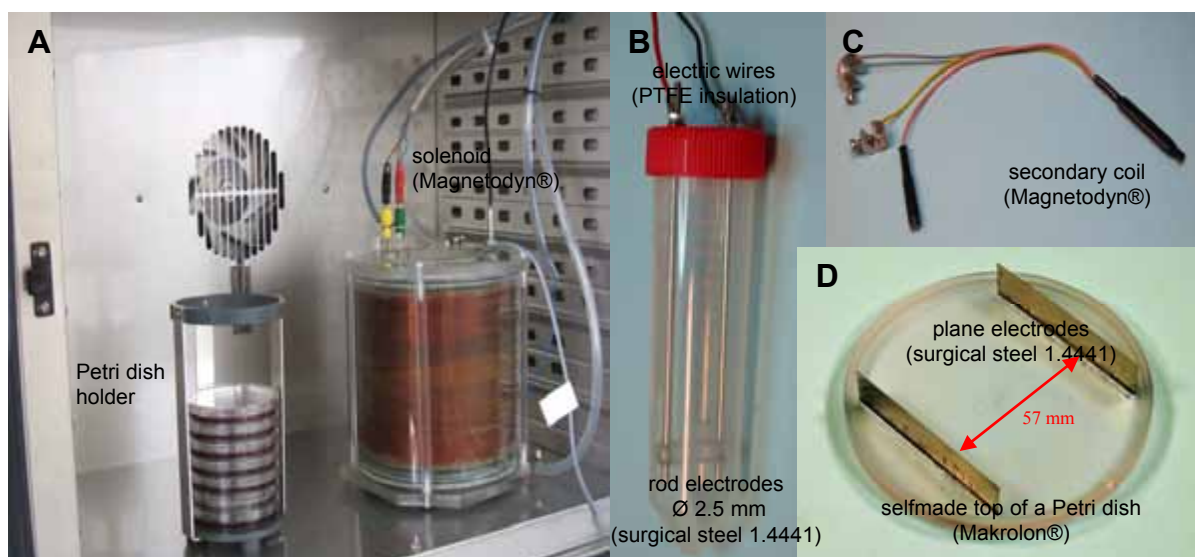


Figure 1. Instruments: A) Solenoid with cooling jacket to generate a sinusoidal electro-magnetic field (5 mT, 20 Hz) and Petri dish holder, B) Electric field applicator with rod-like electrodes to expose bacterial suspensions, C) Secondary coil to induce an additional electric field, D) Electric field applicator for standard Petri dishes.

2.7 Sinusoidal low-frequency electro-magnetic field

A low-frequency electro-magnetic field was generated by a solenoid (FA-P6-K, Neue Magnetodyn, Munich, Germany) (Figure 1A) supplied with a frequency generator (M80, Neue Magnetodyn, Munich, Germany). This set-up is clinically licensed for magnetic-field therapies in bone fracture healing. Frequencies between 10 Hz and 30 Hz and magnetic field strengths of 0.5 mT to 10 mT can be applied. Vials containing bacteria in fluid medium as well as agar plates inoculated with bacteria were placed inside the solenoid. While running experiments, the coil was prevented from overheating by the use of a cooling jacket constructed surrounding the coil. In order to ensure a stable incubation temperature of the bacteria at $37^{\circ} \pm 0.1^{\circ} \text{C}$, the coil was placed in an incubator (CB150, Binder, Tuttlingen, Germany). The cooling jacket was attached to a circulation water bath (F3, Haake, Vreden, Germany) including a thermostat to control the cooling liquid temperature. The temperature close to the bacterial culture was controlled by a calibrated temperature meter (VC306/K202, Conrad Electronic, Hirschau, Germany) and recorded online. To make sure that the reference incubator (CB150, Binder, Tuttlingen, Germany) was not influenced by the electro-magnetic field, the stray field of the coil was measured in x and z direction. The reference incubator was placed at a distance of 3 meters beyond the stray field. The homogeneity of the magnetic

field was assured by measuring the spatial distribution of the magnetic flux density inside the coil with a Gauss meter. A low-frequency electro-magnetic field with a frequency of 20 Hz and a flux density of 5 mT using a current of 1.2 A was examined for the following experiments (Figure 2A and 2 C).

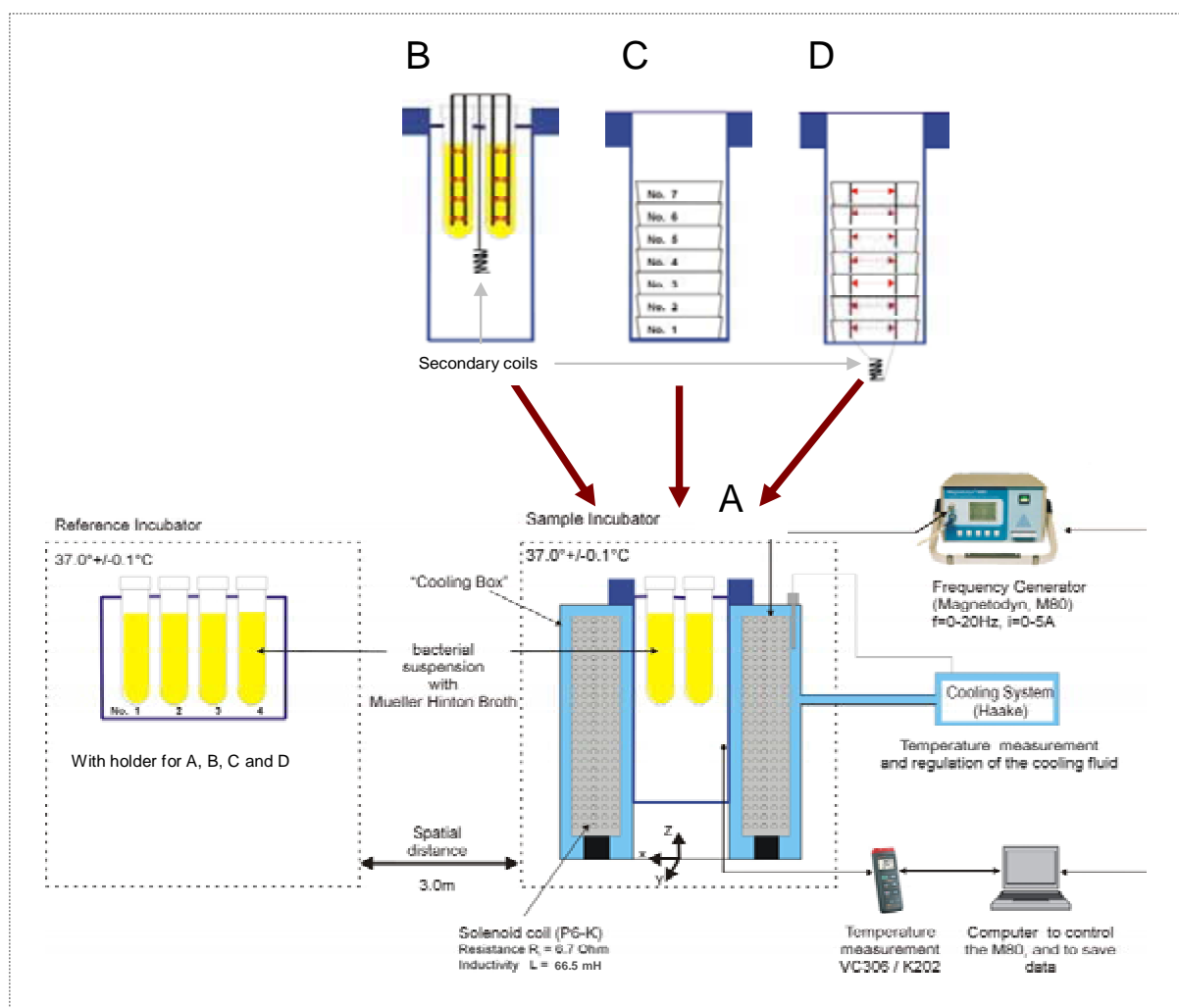


Figure 2. Scheme of experimental setups to apply low-frequency electro-magnetic fields (20 Hz, 5 mT: only Solenoid) and electro-magnetic fields with additional electric fields for *S. aureus* cultures on Mueller-HintonII agar and in suspensions. A sample incubator with a A) Low-frequency electro-magnetic field (5 mT, 20 Hz) in fluid medium, B) Electro-magnetic field (5 mT, 20 Hz) combined with an additional electric field of 470 mV/cm in fluid medium, C) Low-frequency electro-magnetic fields (5 mT, 20 Hz) exposed to gel-like medium and similar with D) Electro-magnetic field (5 mT, 20 Hz) combined with an additional electric field of 140 mV/cm on gel-like medium.

2.8 Electro-magnetic field combined with an additional electric alternating field

The experimental set-up already described for low-frequency electro-magnetic fields was applied for generating a low-frequency electro-magnetic field. In order to establish an additional electric field, secondary coils (Neue Magnetodyn, Munich, Germany) (Figure 1C) were placed inside the primary coil. For agar plates, the lids of Petri dishes contained two plane electrodes dipping inside the agar (Figure 1D). The alternating magnetic field generated from the primary coil induces an alternating voltage which can be picked off at the secondary coil. The secondary coils supply up to seven Petri dishes. Running the primary coil with 20 Hz and 5 mT, an additional voltage of 0.8 V_{eff} is induced in the secondary coils, resulting in an additional alternating electric field strength of 140 mV/cm. This voltage is applied on the electrodes of each Petri dish.

In fluid medium experiments, the secondary coils were made of surgical steel rods and placed inside the tubes attached to the lids (Figure 1B). A frequency of 20 Hz and a flux density of 5 mT lead to an additional voltage of 0.8 V_{eff}, resulting in an additional alternating electric field strength of 470 mV/cm (Figure 2B and 2D).

2.9 Sinusoidal electric alternating field

The effect of a sole sinusoidal alternating electric field on the number of bacterial colonies cultured on agar plates as well as in fluid medium was determined. For this, the electric field applicators already described as secondary coils were connected to a frequency generator (PM 5131, Phillips, Hamburg, Germany) to generate a pure alternating electric field without using a primary coil. A comparable sinusoidal voltage of 0.707 V_{eff} and a field density of 124 mV/cm effective in case of agar plates as well as a sinusoidal voltage of 0.8 V_{eff} and a field strength of 470 mV/cm in case of bacterial suspensions could be built up (Figure 1 and 3A, 3C).

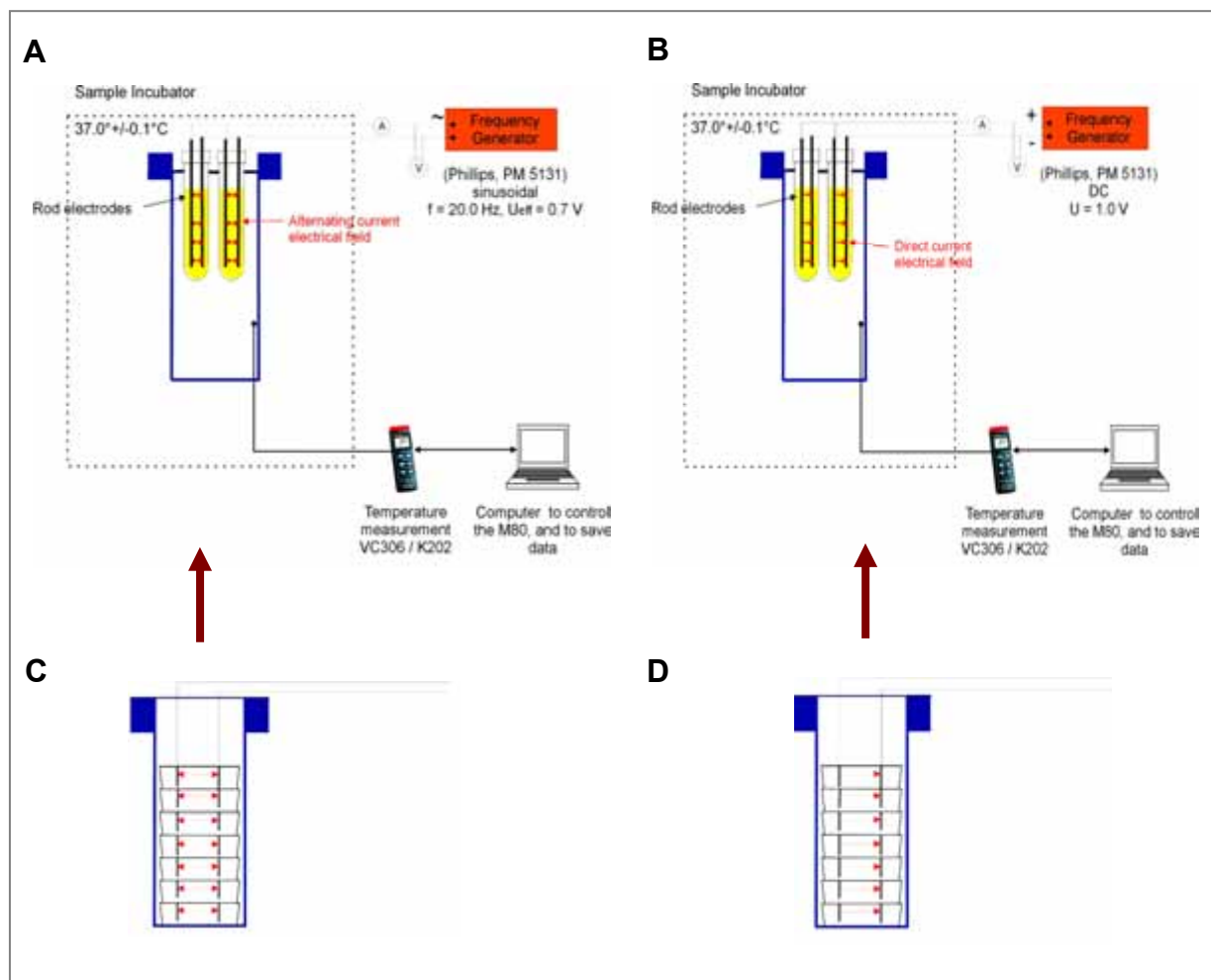


Figure 3. Scheme of experimental setups to apply sinusoidal and direct current electric fields for *S. aureus* cultures on Mueller-HintonII agar and suspensions: A) Sinusoidal alternating electric field (470 mV/cm, 20 Hz) in fluid medium, B) Direct current field of 588 mV/cm in fluid medium, C) Sinusoidal alternating electric field (124 mV/cm, 20 Hz) in gel-like medium, D) Direct current field of 175 mV/cm in gel-like medium.

2.10 Direct current field

Bacterial colonies on agar plates as well as in fluid medium were exposed to a direct current field by connecting the electrodes, as already described, to a frequency generator (PM 5131, Phillips, Hamburg, Germany). A direct current voltage of 1.0 V resulted in an electric field strength of 175 mV/cm affecting bacteria on agar plates and a field strength of 470 mV/cm affecting bacteria in fluid medium (Figure 1 and 3B, 3D).

2.11 Calculations and statistical methods

Data from bacterial growth studies were compared for statistical significance using the student t-test with $P < 0.05$ considered significant.

3 Results

3.1 Bacteria on gel-like medium

In gel-like medium, inhibition zones in the presence of gentamicin are shown to be dependent upon the MIC. However, the application of the four electric and electro-magnetic fields revealed no synergistic growth inhibitory effect, as seen in figure 4 for the application of the direct current field.

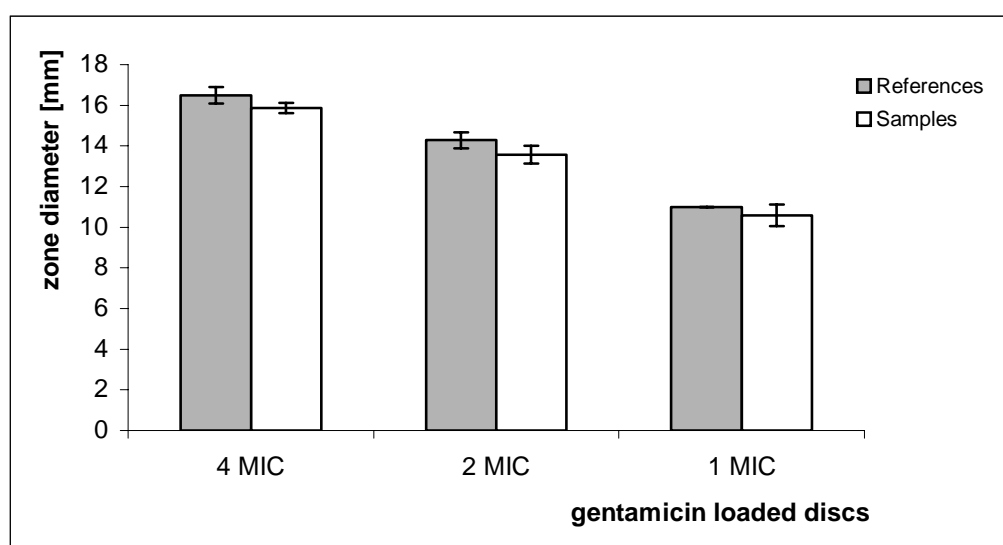


Figure 4. Median dimensions of inhibition zones [mm] of sample (n=7) and reference (n=7) from gentamicin loaded diffusion discs on *S. aureus* lawn cultured on Mueller-HintonII agar plate under the influence of a direct current fields of 175 mV/cm.

3.2 Bacteria in fluid medium

3.2.1 Gentamicin test concentration

In fluid medium growth, inhibition of the gentamicin concentrations chosen (0.125 MIC, 0.25 MIC, 0.5 MIC, 1 MIC, 2 MIC and 4 MIC) is demonstrated in figure 5. For the experimental set-ups with electro-magnetic fields in fluid medium, 0.25 MIC was chosen. This moderate inhibition is in a range allowing detection of synergistic influences induced by electric and electro-magnetic fields.

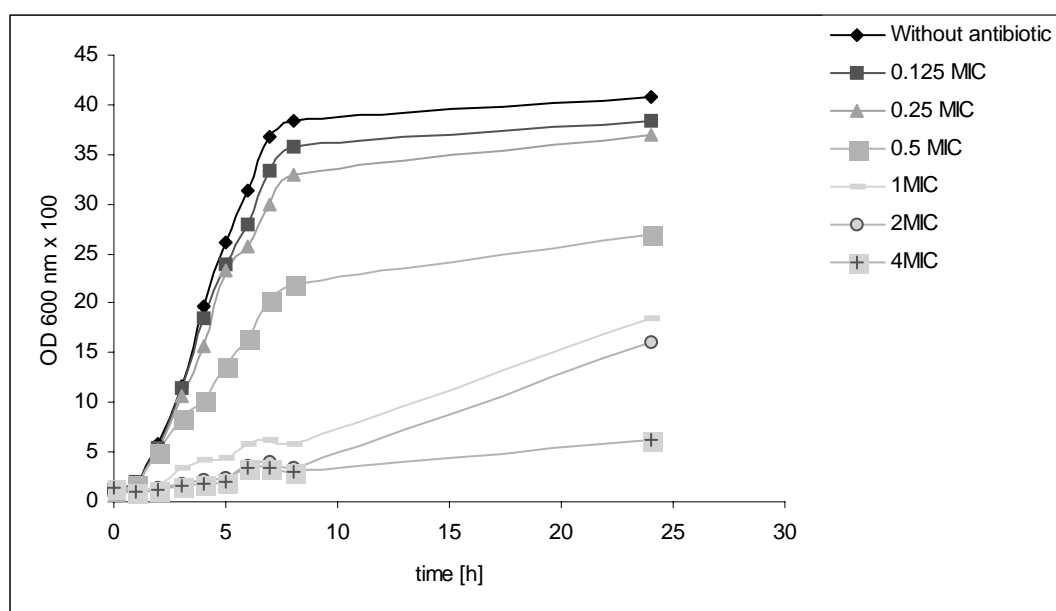


Figure 5. Growth inhibition of *S. aureus* by different MICs of gentamicin in fluid medium within 24 hours.

3.2.2 Low - frequent electromagnetic field

A marginal acceleration of bacterial growth within the first eight hours was detected when *S. aureus* suspensions in the presence of gentamicin (0.25 MIC) were exposed to a low frequent electromagnetic field (5 mT, 20 Hz). However, after 24 hours, the bacterial concentrations in the sample were significantly lower than in the reference. A significant reduction of *S. aureus* concentration of 32 % was demonstrated (Figure 6A).

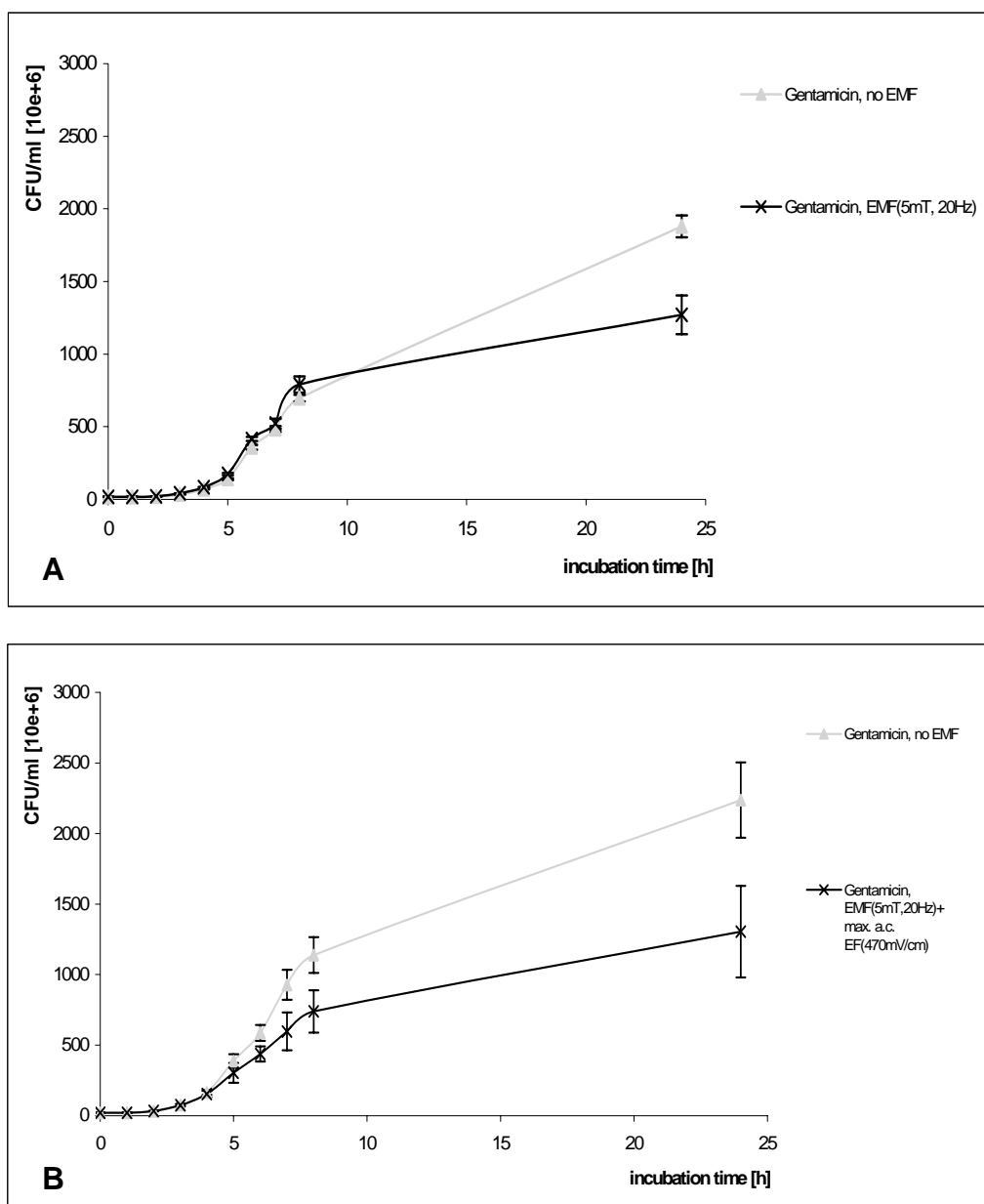


Figure 6 A/B. Median cfu/ml of sample (n=4) and reference (n=4) from *S. aureus* cultured in sterile Mueller-Hinton broth in presence of gentamicin (0.25 MIC) under the influence of different electromagnetic-fields. A) A low frequent electromagnetic field (5 mT, 20 Hz), B) An electromagnetic field (5 mT, 20 Hz) combined with an additional electric field of 470 mV/cm.

EMF ^= electromagnetic field, a.c. EF ^= alternating electrical field, d.c. EF ^= direct current electrical field

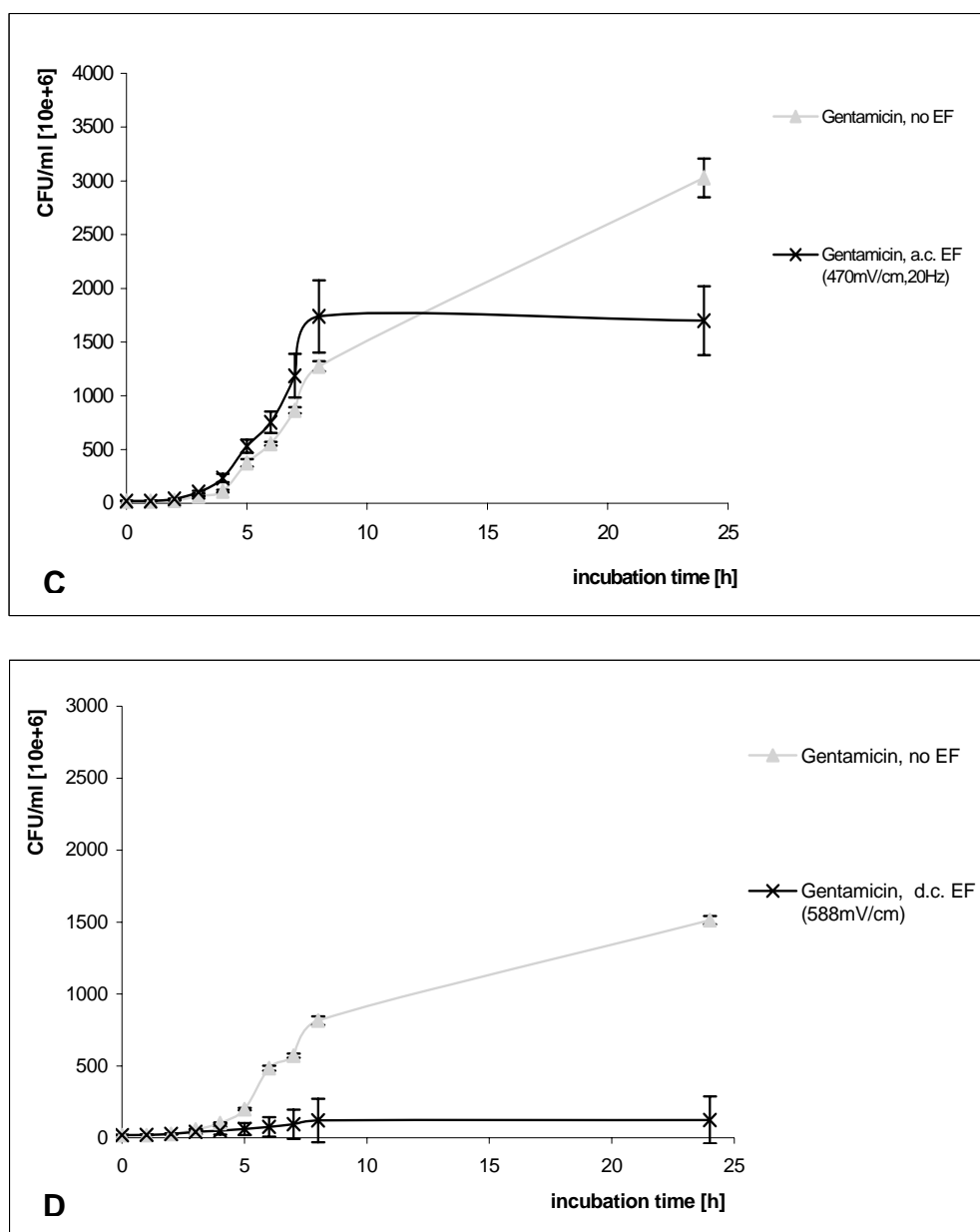


Figure 6 C/D. Median cfu/ml of sample (n=4) and reference (n=4) from *S. aureus* cultured in sterile Mueller-Hinton broth in presence of gentamicin (0.25 MIC) under the influence of different electric fields. C) A sinusoidal alternating electric field (470 mV/cm, 20 Hz), D) A direct current fields of 588 mV/cm.

EMF ^= electromagnetic field, a.c. EF ^= alternating electrical field, d.c. EF ^= direct current electrical field

3.2.3 Electro-magnetic field combined with an additional electric field

The application of an electromagnetic field (5 mT, 20 Hz) combined with an additional electric field (470 mV/cm) to *S. aureus* already showed a decrease of cfu/ml after 7 hours of field exposure. After 24 hours of the experiment, a statistically significant reduction of 41 % of cfu/ml as compared to the reference was determined (Figure 6B).

3.2.4 Sinusoidal alternating electric field

Treatment of *S. aureus* with a sinusoidal alternating electric field (470 mV/cm, 20 Hz) revealed an increase of bacterial concentration during the first 8 hours of exposure time. However, in the following 16 hours of incubation at 37 °C, germ growth reduction was observed. Compared to bacterial growth in the presence of 0.25 MIC of gentamicin in reference investigations, an application of a sinusoidal alternating electric field demonstrated a statistically significant reduction of 43 % of cfu/ml (Figure 6C).

3.2.5 Direct current field

The influence of a direct current field (588 mV/cm) on bacterial suspensions in the presence of gentamicin already showed a significant reduction of bacterial concentration after 6 hours. A statistically significant decrease of 91.8 % of cfu/ml was observed after 24 hours (Figure 6D).

4 Discussion

In the treatment of medical device infections, high concentrations of antibiotics are applied intravenously. Micro-organisms, mostly belonging to *S. aureus* and *S. epidermidis*, colonize implants and form a complex biofilm in conjunction with the patient's own proteins such as fibronectin or albumin (1, 17). This biofilm encloses pathogens against the host immune defence (14) and increases antibiotic resistance (6, 15). Therefore, higher doses of antibiotics have to be applied, although mandatory long-term application increases side-effects. In patients suffering from implant infections, the eradication of pathogens is an important clinical necessity which could be supported by electro-magnetic field therapy.

As a result, improvement of antibiotic efficacy is an important consideration and could be supported by the use of electro-magnetic fields.

Only few studies dealing with the enhancement of antibiotic activity by electric or electromagnetic fields are available in literature. Benson et al. (2) have investigated an enhancement of the activity of gentamicin against biofilm-forming *P. aeruginosa* adhered on different polymers by using magnetic fields between 5 and 20 Gauss. They report a reduction in the number of adhered bacteria when exposed to a 5 gauss magnetic field in the presence of gentamicin in a range of 86 %, independent of the colonized polymers. An improvement of antibiotic efficacy in orthopaedic implant infections has been found by Pickering et al. (16).

They observed that a pulsed electromagnetic field caused a reduction in the minimum biofilm concentration of gentamicin against five-day old biofilms of *S. epidermidis*. In contrast to this investigation, Stansell et al. (18) observed an increase of antibiotic resistance of *E. coli* when exposed to a static magnetic field. Grosman et al. (8) demonstrated no influence of a magnetic field on growth reduction of *E. coli* and *S. aureus* in a range of 0.5 to 4 Tesla. Data on the impact of electric current on the activity of antibiotics are hardly available in literature. Caubet et al. (3) report an enhancement of antibiotic activity against bacterial biofilms when radio frequency electric current is used. They detected a bioelectric effect with a radio frequency alternating electric current of 10 MHz applied to *E. coli* biofilms with simultaneous gentamicin and oxytetracycline treatment.

Our experimental set-up differs from previous studies. We have compared different types of electro-magnetic fields applied to a well-defined biofilm producing pathogen such as *S. aureus* (ATTC 49230) and simultaneous treatment with an antibiotic. Physical parameters of the applied fields were derived from the clinically established Magnetodyn[®] procedure to improve bone healing, as demonstrated in material and methods. Numerous data in literature concerning this magnetic field therapy are available as depicted by Kraus (9). A low-frequency electro-magnetic field, an electro-magnetic field combined with an additional electric field, a sinusoidal electric alternating field and a direct current field were used. Gentamicin was selected as a clinically approved antibiotic in the treatment of *S. aureus*-induced soft tissue, bone and implant-associated infection (7). Our experiments showed no influence of the four applied fields on growth inhibition in the presence of gentamicin tested on gel-like medium.

Low dose gentamicin application corresponding to 0.25 MIC under the influence of the four applied fields showed a statistically significant effect on growth inhibition in fluid medium. Depending on the type of field applied, an improvement of gentamicin efficacy from 32.4 %

using a clinically applied electromagnetic field (5 mT, 20 Hz) up to 91.8 % using a direct current field of 588 mV/cm was observed (Table 1).

Table 1. Overview of pathogen reduction in synergism with 0.25 MIC gentamicin caused by different electro-magnetic fields: A) Low-frequency electro-magnetic field (5 mT, 20 Hz) in fluid medium, B) Electro-magnetic field (5 mT, 20 Hz) combined with an additional electric field of 470 mV/cm in fluid medium, C) Sinusoidal alternating electric field (470 mV/cm, 20 Hz) in fluid medium, D) Direct current field of 588 mV/cm in fluid medium.

EMF ^= electromagnetic field, a.c. EF ^= alternating electrical field, d.c. EF ^= direct current electrical field

pathogen reduction after 24 h in [%] (relative to gentamicin without field-influence)	electro-magnetic field		electric field	
	A) EMF (5 mT, 20 Hz)	B) EMF + a.c. EF (5 mT, 470 mV/cm, 20 Hz)	C) a.c. EF (470 mV/cm, 20 Hz)	D) d.c. EF (588 mV/cm)
	32.4 % (p = 0.0002)	41.7 % (p = 0.0332)	43.9 % (p = 0.0004)	91.8 % (p < 0.0001)

In general, we have been able to demonstrate an additional statistically significant reduction of *S. aureus* growth in the presence of gentamicin under the influence of all applied fields in fluid medium. The strongest effect of augmented gentamicin efficacy could be shown by the application of the direct current field. We assume that this effect is caused by electrolysis-induced radicals. Formed hydroxyl and oxygen radicals are known to destroy cell membranes of bacteria. This so-called bioelectric effect (2, 4, 13, 16) may facilitate the penetration of antibiotic drugs and could be an explanation for the detected efficacy augmentation of gentamicin. The effect of various antibiotics and antiseptics depending on charged and non-charged compounds in the presence of the four fields are under investigation to shed light on the underlying mechanism.

5 Conclusions

In this study we have demonstrated that a combination of electro-magnetic fields with the antibiotic gentamicin improves efficacy against *S. aureus* in vitro. These results corroborate clinical observations that the application of electro-magnetic fields according to Kraus and Lechner in infected non-unions improves bone healing and induces infection palliation. We conclude that the combination of antibiotic treatment with low-frequency electro-magnetic fields could offer new opportunities in biomaterial-associated infection therapy.

6 Acknowledgements

We would like to thank V. Vatou for her great assistance in microbial testing. Furthermore, we acknowledge H. Stephan and W. Kraus for their technical help, contributions and inspiring discussions. The authors did not receive any payments or benefits from a commercial party related directly or indirectly related to the subject of this article. This work was partially funded by a grant from the “Bayerische Forschungsförderung”.

7 Figure and Table Captions

Figure 1. Instruments: A) Solenoid with cooling jacket to generate a sinusoidal electro-magnetic field (5 mT, 20 Hz) and Petri dish holder, B) Electric field applicator with rod-like electrodes to expose bacterial suspensions, C) Secondary coil to induce an additional electric field, D) Electric field applicator for standard Petri dishes.

Figure 2. Scheme of experimental setups to apply low-frequency electro-magnetic fields (20 Hz, 5 mT: only Solenoid) and electro-magnetic fields with additional electric fields for *S. aureus* cultures on Mueller-HintonII agar and in suspensions. A sample incubator with a A) Low-frequency electro-magnetic field (5 mT, 20 Hz) in fluid medium, B) Electro-magnetic field (5 mT, 20 Hz) combined with an additional electric field of 470 mV/cm in fluid medium, C) Low-frequency electro-magnetic fields (5 mT, 20 Hz) exposed to gel-like medium and similar with D) Electro-magnetic field (5 mT, 20 Hz) combined with an additional electric field of 140 mV/cm on gel-like medium.

Figure 3. Scheme of experimental setups to apply sinusoidal and direct current electric fields for *S. aureus* cultures on Mueller-HintonII agar and suspensions: A) Sinusoidal alternating electric field (470 mV/cm, 20 Hz) in fluid medium, B) Direct current field of 588 mV/cm in fluid medium, C) Sinusoidal electric alternating field (124 mV/cm, 20 Hz) in gel-like medium, D) Direct current field of 175 mV/cm in gel-like medium.

Figure 4. Median dimensions of inhibition zones of sample (n=7) and reference (n=7) from gentamicin-loaded diffusion discs on *S. aureus* lawn cultured on Mueller-HintonII agar plate under the influence of a direct current fields of 175 mV/cm.

Figure 5. Growth inhibition of *S. aureus* by different MICs of gentamicin in fluid medium within 24 hours.

Figure 6. Median cfu/ml of sample (n=4) and reference (n=4) from *S. aureus* cultured in sterile Mueller-Hinton broth in presence of gentamicin (0.25 MIC) under the influence of different electro-magnetic-fields.

Table 1. Overview of pathogen reduction in synergism with 0.25 MIC gentamicin caused by different electro-magnetic fields.

8 References

1. **Barton, A. J., R. D. Sagers, and W. G. Pitt.** 1996. Bacterial adhesion to orthopedic implant polymers. *J Biomed Mater Res* **30**:403-10.
2. **Benson, D. E., C. B. Grissom, G. L. Burns, and S. F. Mohammad.** 1994. Magnetic field enhancement of antibiotic activity in biofilm forming *Pseudomonas aeruginosa*. *Asaio J* **40**:M371-6.
3. **Caubet, R., F. Pedarros-Caubet, M. Chu, E. Freye, M. de Belem Rodrigues, J. M. Moreau, and W. J. Ellison.** 2004. A radio frequency electric current enhances antibiotic efficacy against bacterial biofilms. *Antimicrob Agents Chemother* **48**:4662-4.
4. **Costerton, J. W., B. Ellis, K. Lam, F. Johnson, and A. E. Khoury.** 1994. Mechanism of electrical enhancement of efficacy of antibiotics in killing biofilm bacteria. *Antimicrob Agents Chemother* **38**:2803-9.
5. **Davies, D.** 2003. Understanding biofilm resistance to antibacterial agents. *Nat Rev Drug Discov* **2**:114-22.
6. **Donlan, R. M.** 2000. Role of biofilms in antimicrobial resistance. *Asaio J* **46**:S47-52.
7. **Geipel, U., and M. Herrmann.** 2005. [The infected implant: bacteriology]. *Unfallchirurg* **108**:961-975; quiz 976-7.
8. **Grosman, Z., M. Kolar, and E. Tesarikova.** 1992. Effects of static magnetic field on some pathogenic microorganisms. *Acta Univ Palacki Olomuc Fac Med* **134**:7-9.
9. **Kraus, W.** 1992. Treatment of pathological bone lesion with non-thermal, extremely low frequency electromagnetic fields. *Bioelectrochemistry and Bioenergetics* **27**:321 - 339.
10. **Kraus, W., and F. Lechner.** 1972. [Healing of pseudoarthrosis and spontaneous fractures with structure-forming electrodynamic potentials]. *Munch Med Wochenschr* **114**:1814-9.
11. **Lechner, F., R. Ascherl, and W. Uraus.** 1981. Treatment of pseudarthroses with electrodynamic potentials of low frequency range. *Clin Orthop Relat Res*:71-81.
12. **Lechner, F., G. Oeller, and R. Ascherl.** 1979. [Treatment of infected pseudoarthroses with electrodynamic field therapy]. *Fortschr Med* **97**:943-9.
13. **McLeod, B. R., S. Fortun, J. W. Costerton, and P. S. Stewart.** 1999. Enhanced bacterial biofilm control using electromagnetic fields in combination with antibiotics. *Methods Enzymol* **310**:656-70.
14. **Pascual, A., D. T. Tsukayama, B. H. Wicklund, J. E. Bechtold, K. Merritt, P. K. Peterson, and R. B. Gustilo.** 1992. The effect of stainless steel, cobalt-chromium, titanium alloy, and titanium on the respiratory burst activity of human polymorphonuclear leukocytes. *Clin Orthop Relat Res*:281-8.
15. **Patel, R.** 2005. Biofilms and antimicrobial resistance. *Clin Orthop Relat Res*:41-7.
16. **Pickering, S. A., R. Bayston, and B. E. Scammell.** 2003. Electromagnetic augmentation of antibiotic efficacy in infection of orthopaedic implants. *J Bone Joint Surg Br* **85**:588-93.
17. **Schmitt, D. D., D. F. Bandyk, A. J. Pequet, and J. B. Towne.** 1986. Bacterial adherence to vascular prostheses. A determinant of graft infectivity. *J Vasc Surg* **3**:732-40.
18. **Stansell, M. J., W. D. Winters, R. H. Doe, and B. K. Dart.** 2001. Increased antibiotic resistance of *E. coli* exposed to static magnetic fields. *Bioelectromagnetics* **22**:129-37.

19. **Trampuz, A., and A. F. Widmer.** 2006. Infections associated with orthopedic implants. *Curr Opin Infect Dis* **19**:349-56.
20. **Trampuz, A., and W. Zimmerli.** 2006. Antimicrobial agents in orthopaedic surgery: Prophylaxis and treatment. *Drugs* **66**:1089-105.

Chapter 6

Magnetic drug targeting for biomaterial infections

Abstract

Objectives: Biomaterial-associated infections present a challenging problem in surgery. Increased antibiotic resistance of pathogens in biofilms requires high drug concentrations in the area of infection. The present work presents a novel strategy to concentrate high antibiotic doses at the surface of vascular grafts using newly developed antibiotic-functionalized nanoparticles directed by a magnetic drug targeting system.

Methods: Magnetic nanoparticles were ionically and covalently functionalized with gentamicin. Drug release kinetics within 90 minutes was studied in phosphate buffered saline at 37 °C. Anti-infective characteristics were determined by measuring the change in optical density of *Staphylococcus aureus* suspensions charged with coated ferrofluids within 24 hours. A cell proliferation assay was performed to assess the degree of cytotoxicity. The enrichment of ferrofluids at the surface of model tubes in circulatory experiments was investigated.

Results: A technology for the antimicrobially equipment of magnetic nanoparticles could be generated. All gentamicin-functionalized nanoparticles did not show drug release within 90 minutes. Selected coated nanoparticles reduced bacterial growth even beyond pathologically relevant concentrations within 24 hours. Excellent concentration-independent biocompatibility was assessed for ferrofluids of choice. Magnetic nanoparticles could be concentrated on the surface of model grafts.

Conclusions: The development and in vitro studies of described magnetic drug targeting system present a new perspective in the treatment of vascular graft infection. With the help of a strong external magnetic field drug-functionalized nanoparticles can be enriched at the surface of infected grafts ensuring high drug levels to fend off biofilm embedded pathogens.

Keywords: Magnetic nanoparticles, drug targeting, gentamicin, infection, *Staphylococcus aureus*

1 Introduction

Biomaterial-associated infections present a challenging problem for patients and surgeons (24, 27). Synthetic vascular grafts like PTFE prostheses are easily accessible to pathogens because of their porous structure (4). These pathogens, mostly belonging to *Staphylococcus aureus* and *Staphylococcus epidermidis*, colonize the implant by adhering to the patients own proteins located on the surface of the graft and forming a biofilm (9, 15, 19). Once a biofilm has established, there is an essential need for surgical intervention with the objective of vascular graft replacement because of a high risk of sepsis associated with a high amputation rate or mortality (6, 28). In many cases these life-essential replacements can not be performed because of the high risk of the surgical intervention itself due to the age structure of patients with vascular implants (29). A standard treatment with high doses of intravenous antibiotics is the result and mandatory long-term application increases side-effects (13). It is therefore essential to find new ways to locally concentrate antibiotics in the area of infected grafts, thereby minimizing side effects (25). In the last few years, nanotechnology moved into the focus of scientific interest (17, 18, 20). Drugs like chemotherapeutics can be ionically or covalently bound to magnetic nanoparticles and concentrated with the help of a magnetic drug targeting system in the target area (2, 21, 22). In the present study, a technology for the development of gentamicin-functionalized magnetic nanoparticles was generated (Figure 1), and developed particles were analyzed for drug release, antibacterial characteristics and biocompatibility. Furthermore, the enrichment of magnetic nanoparticles on the surface of modified model grafts in circulatory experiments in vitro was investigated with a magnetic drug targeting system.

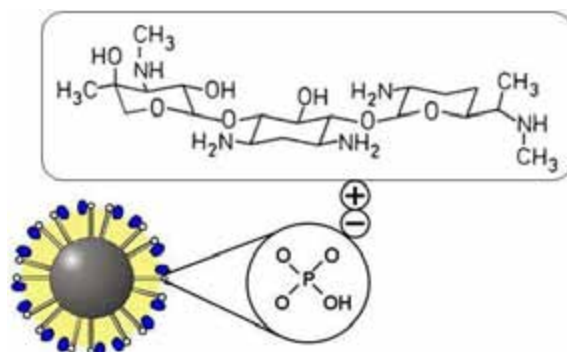


Figure 1. TargetMAG with ionically coupled gentamicin. The electrostatic attraction is based on the interaction between positively charged tertiary ammonium groups of gentamicin and negatively charged phosphate groups of the organic shell surrounding the magnetic iron core (Chemicell GmbH archives).

2 Materials and methods

2.1 Nanoparticles

Six different magnetic nanoparticle types consisting of a magnetite core and an organic shell were used for coating experiments (Table 1 A/B). Four different types of ferrofluids were chosen, that are potentially useful to prepare ionic adsorption complexes with the antibiotic gentamicin. S13, S21 and S26 were kindly provided by the University Hospital Munich (Klinikum r. d. Isar, Institut für Experimentelle Onkologie und Therapieforschung, Munich, Germany), TargetMAG was kindly provided by Chemicell (Chemicell GmbH, Berlin, Germany). The nanoparticle types FluidMAG and SiMAG (Chemicell GmbH, Berlin, Germany) were chosen for a covalent gentamicin binding (Table 1A/B).

Table 1A. Overview of individual nanoparticle types used for ionic or covalent gentamicin coupling.

	S13	S21	S26
Composition	Aqueous dispersion of palmitoyl-dextran -coated magnetic nanoparticles	Aqueous dispersion of palmitic acid -coated magnetic nanoparticles	Aqueous dispersion of dihexadecylphosphate -coated magnetic nanoparticles
functional group	Hydroxyl	Carboxyl	Phosphate
Binding type	ionic	ionic	Ionic
Particle Size hydrodynamic diameter [nm]	175	231	10
Mean magnetite crystallite size <d> (nm)	4,0	12,8	10,0
ξ-potential (mV)	-31.4	23.5	31.4
Iron concentration, mg Fe/ml	9,2	20,0	5,0

Table 1B. Overview of individual nanoparticle types used for ionic or covalent gentamicin coupling.

	TargetMAG	FluidMAG	SiMAG
Composition	Aqueous dispersion of starch polymer -coated magnetic nanoparticles particles	Aqueous dispersion of polysaccharide -coated magnetic nanoparticles	Aqueous dispersion of magnetic silicea particles
functional group	Phosphate	Glucuronic acid - Carboxyl	Carboxyl
Binding type	ionic	covalent	Covalent
Particle Size hydrodynamic diameter [nm]	250	250	500
Mean magnetite crystallite size <d> (nm)	60.0	60.0	60.0
ξ-potential (mV)	-35.1	-38.1	-40.9
Iron concentration, mg Fe/ml	30.0	25.0	50.0

2.2 Particle size and zeta potential

The median particle size as well as the zeta potential of individual nanoparticle types was determined by dynamic light scattering (Zetasizer Nano SZ, Malvern Instruments, Malvern UK) (Table 1A/B). Therefore nanoparticles were suspended in distilled water at 10 µg/ml.

2.3 Drug loading

For ionically bound gentamicin on magnetic nanoparticles the optimal ratio for coating procedure between gentamicin sulfate (Heraeus Kulzer GmbH, Werheim, Germany) and magnetic nanoparticles was assessed. Therefore different gentamicin concentrations were combined with a defined ferrofluid concentration. S13, S21 and S26 and TargetMAG nanoparticle suspensions were diluted with distilled water to a concentration of 1 mg Fe/ml. Gentamicin sulfate was dissolved at 1 mg/ml in distilled water and diluted to concentrations of 200 µg/ml, 100 µg/ml, 75 µg/ml, 50 µg/ml, 25 µg/ml and 10 µg/ml. 500 µl of the ferrofluid suspension (1mg/ml) was incubated with 500 µl gentamicin sulphate solution of the respective concentration at 37 °C for 30 minutes at 1400 rpm (Eppendorf Thermomixer, Eppendorf AG, Hamburg, Germany). Drug ferrofluid suspension was placed in a permanent

magnet field (NdFeB Magnet 80x40x10 mm, Neotexx, Berlin, Germany) for 30 minutes to achieve segregation between drug solution and nanoparticles. 500 μ l of the supernatant were removed. A reference was established by adding 500 μ l distilled water to 500 μ l of gentamicin sulfate solutions. Gentamicin was analyzed by the Innofluor Gentamicin assay system (Opus Diagnostics, Fort Lee, USA). Gentamicin concentrations assessed in the supernatant of respective ferrofluid suspensions were compared to reference gentamicin concentrations. The ratio between the difference of sample concentrations and the reference concentration is defined as the loading capacity.

2.4 Coating Technology

For further experiments S13, S21 and S26 were diluted with distilled water to a concentration of 1mg Fe/ml. Gentamicin sulfate was diluted to the optimal coating concentration of 100 μ g/ml. 500 μ l of the obtained ferrofluid suspension was then incubated with 500 μ l of 100 μ g/ml gentamicin sulfate at 37 °C for 30 minutes at 1400 rpm (Eppendorf Thermomixer, Eppendorf AG, Hamburg, Germany). A reference was established by adding 500 μ l distilled water to 500 μ l of 100 μ g/ml gentamicin sulfate solution. TargetMAG particles were coated with a one to five ratio between gentamicin and iron content. In order to assess the loading capacity, ferrofluid suspensions with covalently bound gentamicin were placed in a permanent magnetic field (NdFeB Magnet 80x40x10 mm, Neotexx, Berlin, Germany), for 30 minutes to achieve a segregation between drug solution and nanoparticles. 500 μ l of the supernatant were removed and analyzed for gentamicin concentration by the Innofluor Gentamicin assay system. Subsequently the loading capacity of used nanoparticles was assessed. Gentamicin was covalently coupled to FluidMAG and SiMAG nanoparticles by the carboiimide method (7, 8). Thereby, carboiimides react with the terminal carboxylate-groups from the magnetic beads to highly reactive O-acylisourea derivatives which bind the amino-groups of gentamicin via an amide bond.

2.5 Antibacterial characteristics

2.5.1 Test bacterium

For in vitro studies, a clinical isolate of *Staphylococcus aureus* (strain ATCC® 49230) was used. The test strain was susceptible to gentamicin (MIC 0.5 mg/l). *Staphylococcus aureus* was cultured on columbia agar plates (Becton Dickinson GmbH, Heidelberg, Germany) at 37 °C for 18 hours before testing.

2.5.2 Calibration curve

In order to correlate the optical density at 600 nm of a *S. aureus* suspension with the colony forming units of the microorganism, a calibration curve was recorded. A bacterial suspension was produced by resuspending about 100 colonies of *S. aureus* from columbia agar plates in 750 ml of sterile Mueller-Hinton broth (No. 275730, BD Diagnostic Systems, Difco™, Heidelberg, Germany). The homogeneous suspension was incubated at 37 °C for 24 hours. The optical density (GeneQuant pro, biochrom, Cambridge, UK) at 600 nm was measured at time intervals of 60 minutes within the first eight hours and again after 24 hours. Different dilutions of each sample were also plated on columbia agar plates. After incubating these agar plates for 24 hours at 37 °C the colony forming units were visually determined, extrapolated to the initial concentration in suspension and correlated to the measured value of optical density. This experiment was repeated three times and all values were combined since optical density values as well as cfu/ml can not be reproduced to defined values. A logarithmic regression curve with the formula $OD=0.0741 \ln(cfu)-0.2066$ and a correlation coefficient of 0.91 resulted.

2.5.3 Antimicrobial potential

In order to investigate the antimicrobial potential of drug-carrier-coated grafts, a hundredfold concentration of the commonly observed pathological concentration (1×10^4 cfu/ml) was chosen. Bacterial cells from columbia agar plates were resuspended in Müller-Hinton broth to form a bacterial suspension. 1 ml of gentamicin coated TargetMAG (TargetMAG-Genta) suspension (1 mg/ml) or 1 ml gentamicin coated S13 (S13-Genta) suspension (1 mg/ml) was

added to 49 ml of *Staphylococcus aureus* suspensions to determine their anti-infective efficiency. The optical density was measured after certain time intervals and plotted against time. With the aid of the calibration curve, bacteria concentrations of sample and reference at different points in time could be compared. A reference was established using TargetMAG and S13 suspensions.

2.5.4 Pathologically relevant bacterial concentrations

In order to assess antibiotic efficacy at pathologically relevant bacterial concentrations (12), bacterial suspensions with concentrations of 1×10^2 , 1×10^3 , 1×10^4 cfu/ml were prepared and incubated in partes aequales with gentamicin coated S13 and TargetMAG-Genta particles as well as non-coated S13 and TargetMAG particles of 2 mg/ml iron concentration suspended in NaCl 0.9 % for 24 hours in 37 °C. A reference was established by incubating individual bacterial suspensions with pure NaCl 0.9 %. 200 ml of each sample was plated out and colony forming units on blood agar plates were determined for each sample and reference.

2.5.5 Gentamicin efficacy

In a continuing experiment, the influence of individual gentamicin concentrations on *S. aureus* growth in fluid media was elucidated. Therefore, tubes filled with 49 ml of bacterial suspension were incubated with 1 ml gentamicin sulfate solution of different concentrations resulting in a gentamicin end concentration of 0.665 µg/ml, 1.330 µg/ml, 6.650 µg/ml and 66.500 µg/ml. Saline was used as a blank. A growth curve was determined by measuring the optical density of bacterial suspension at 600 nm every 60 minutes for 8 hours and again after 24 hours. Via a calibration curve, the optical density was converted in cfu/ml and correlated to time.

2.6 Gentamicin release from nanoparticles

The supernatant of coated S13 and TargetMAG ferrofluids was completely removed; particles were washed twice with purified water and 1ml PBS was added to nanoparticles. Drug ferrofluid suspensions were then placed in a permanent magnetic field and at time points

5, 10, 15, 30, 60 and 180 minutes 100 µl of supernatant were analyzed for gentamicin concentration by an Innofluor Gentamicin assay system. Released gentamicin concentrations were plotted against time in order to gain a release curve.

2.7 In vitro cytotoxicity studies

2.7.1 Cell culture

Human umbilical vein endothelial cells (HUVEC) were maintained in endothelial cell growth medium (PromoCell, Heidelberg, Germany) supplemented with SupplementMix, 10 % fetal bovine serum, penicillin and streptomycin (100 U/ml and 0.1 mg/ml, respectively), partricin (50 µg/ml) and stable glutamine at 37 °C in a humidified atmosphere containing 5 % CO₂. Cells were washed with PBS-Dulbecco (Biochrom AG, Berlin, Germany) and trypsinized with Trypsin/EDTA-Solution (Biochrom AG, Berlin, Germany).

2.7.2 Ferrofluid toxicity

Cytotoxicity tests were carried out with different concentrations of coated and uncoated magnetic nanoparticles. Human umbilical vein endothelial cells were cultured in a 96 well plate until subconfluence, TargetMAG, and S13 both blank and Gentamicin loaded ferrofluids were added in concentrations of 2000 µg/ml, 1000 µg/ml, 500 µg/ml, 100 µg/ml, 60 µg/ml and 10 µg/ml and cells were cultured for 10 hours at 37 °C. Resovist[®] served as reference, as it is an already established and licensed radiopaque material. After ferrofluid incubation cells were washed with PBS and metabolic activity of viable cells was measured with the Roche cell proliferation reagent WST-1 (Roche Diagnostics GmbH, Mannheim, Germany).

2.7.3 Gentamicin toxicity

In order to analyze the toxicity of gentamicin, cells were cultured in 96-well microplates in presence of different concentrations of gentamicin (1.33 µg/ml, 6.65 µg/ml, 33.25 µg/ml, 66.5 µg/ml, 133 µg/ml) until subconfluence followed by a Roche cell proliferation reagent WST-1 test.

2.8 Circulatory experiments

A closed circuit was built up as a model for bloodstream in a ratio of one to one hundred to physiological conditions (Figure 2). TargetMAG was chosen as a model ferrofluid. A flexible synthetic tube (target tube) of 8 mm diameter, 1.6 mm wall thickness and 10 cm length (Tygon® R3603, Ismatec Laboratoriumstechnik GmbH, Wertheim-Mondfeld, Germany) was placed between two plugs and placed in the centre of a Bruker Magnet (Bruker, Karlsruhe, Germany). Three different tip-target distances, the distance between the symmetry axis of the target tube and the magnet tip, at 0 mm, 15 mm and 30 mm were chosen. The plugs of the target tube were attached to two flexible tubes of 7 mm diameter (silicone tube, I:5 x A:7 mm, neoLab, Heidelberg, Germany). One tube was connected directly to a sealable reservoir containing 50 ml of an aqueous 1 mg/ml TargetMAG suspension, the second tube was directed via a peristaltic pump (VC380, ISMATEC Laboratoriumstechnik GmbH, Wertheim-Mondfeld, Germany) to the 50 ml ferrofluid reservoir. The peristaltic pump assured a flow rate of 260 ml/min, similar to physiological blood stream conditions for vascular grafts (in the range of 400 ml/min for sane veins and 150 ml/min to 200 ml/min for vascular grafts). Before starting the circulatory experiment, the ferrofluid suspension was shaken for 2 minutes until a homogenous distribution was achieved and 500 µl of the ferrofluid suspension were taken out for iron content analysis. The circulatory experiment was started by opening all valves in flow direction and starting the pump. At time points 15 min and 30 min, 500 µl samples were abstracted for further iron content analysis to allow ferrofluid saturation in the closed circuit. After ferrofluid saturation, the Bruker Magnet was operated for 30 minutes with a direct current of 30 A and 120 V creating a magnetic field strength of 1.7 Tesla at the vertex of the magnet (14). During magnetic field application after 15 minutes and 30 minutes 500 µl samples were abstracted for further iron content analysis. Ferrofluid agglomeration was studied with naked tubes as well as with tubes surrounded by a wire netting consisting of 0.8 mm nealed and oxidized Mumetal with a diameter of 0.8 mm, a length of 5 cm and a flank lead of 2 mm (Vacuum Schmelze Hanau, Germany). The wire netting was constructed in order to distort the field gradient and therefore the magnetic forces in a way that magnetic nanoparticles are forced to adsorb at the inner-surface of the PTFE graft as shear forces prevent particles from accumulating in the area of the graft.

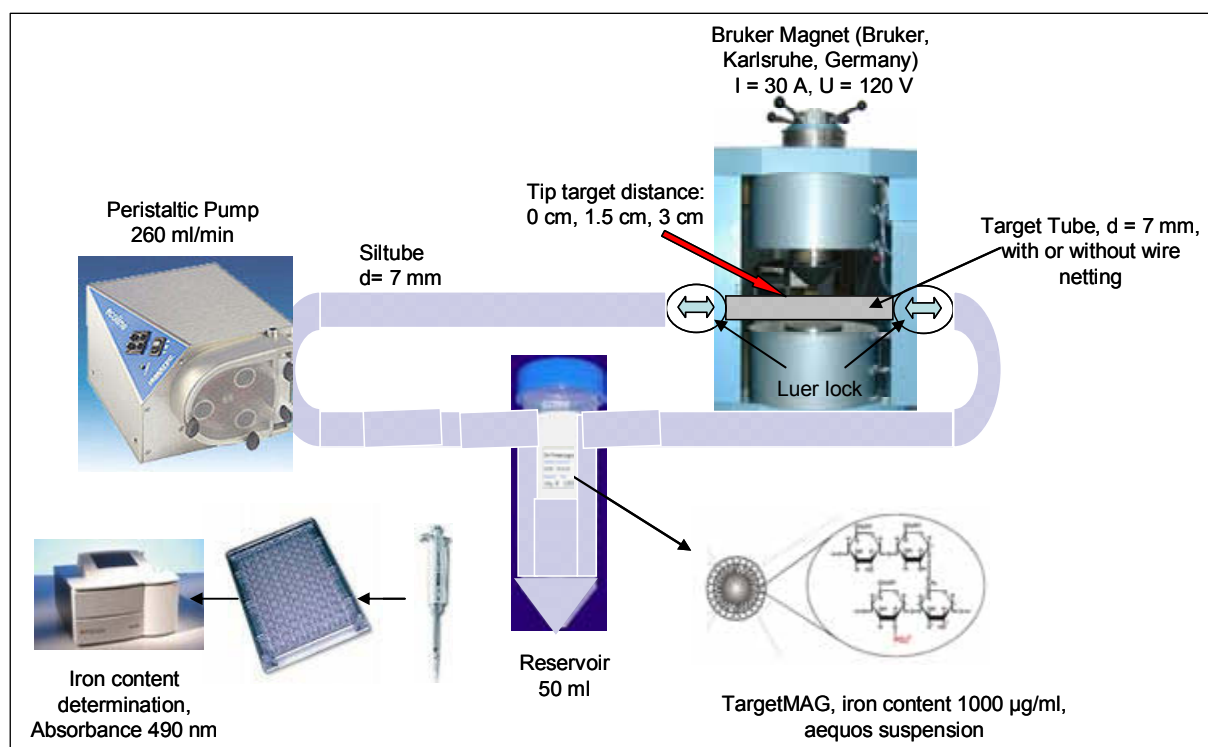


Figure 2. Closed circuit built up as a model for bloodstream in a ratio of one to one hundred to physiological conditions (total volume 50 ml ferrofluid suspension).

2.9 Iron content determination

Iron content analysis for determination of the nanoparticle concentration was based on turbidity measurements and was performed by visual spectroscopy (ELISA-reader sunrise, Tecan, Crailsheim, Germany). A calibration curve was recorded by correlating the optical density at 490 nm with iron concentrations between 5 µg/ml and 500 µg/ml. The iron content of samples for different time points was assessed and compared among each other.

3 Results

3.1 Loading of magnetic nanoparticles with gentamicin

For S13 and S26 loading curves could be generated, whereas for S21 particles, no difference between gentamicin concentrations in sample supernatant and reference supernatant during the loading process was observed indicating no particle loading. For S13 and S26 particles an increasing loading capacity with the application of higher gentamicin concentrations was observed (Figure 3A/B).

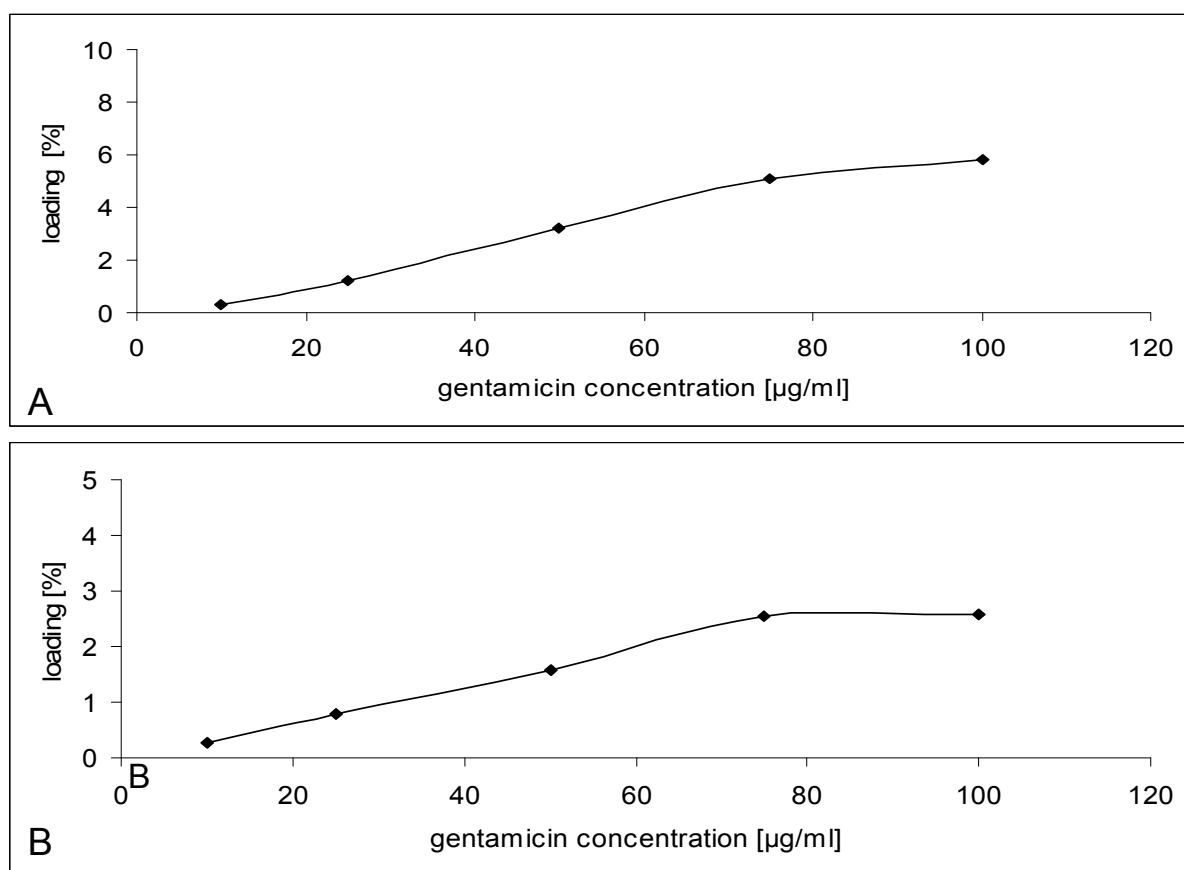


Figure 3 A/B. Loading of magnetic nanoparticles with gentamicin: A. S13 particles and B. S26 particles.

The maximal loading capacity of S13 ferrofluids was achieved at a gentamicin concentration of 10 % (c/c) referring to the total iron concentration resulting in 6.6 % (m/m) loading. For S26 particles, the maximal loading capacity was also achieved at the same gentamicin to iron ratio of 1:10 resulting in 1.4 % (m/m) antibiotic loading. For TargetMAG particles the

maximal loading capacity was achieved at an applied gentamicin concentration of 20 % of used iron concentration resulting in 15.0 % (m/m) drug loading.

The covalent equipment of FluidMAG and SiMAG with gentamicin was performed successfully, however the maximal loading capacity could not be determined. As S21 and S26 particles did not show enough drug loading at their surface, they were excluded from further experiments.

3.2 Antibacterial characteristics

Pathogen growth in suspensions at pathologically relevant bacterial concentrations ($10^2 - 10^4$ cfu/ml) incubated with gentamicin coated S13 and TargetMAG particles at 1 mg/ml was completely inhibited. Suspensions with uncoated nanoparticles or saline reference demonstrated the formation of bacterial lawns on agar plates. Bacterial growth in highly concentrated bacterial suspensions of 2×10^6 cfu/ml could be reduced by ionically bound gentamicin coated ferrofluids TargetMAG-Genta. In contrast, magnetic nanoparticles coated with covalent coupled gentamicin, like FluidMAG (FluidMAG-Genta) and SiMAG (SiMAG-Genta), showed a growth stimulating effect of *S. aureus* cultures in fluid media (Figure 4).

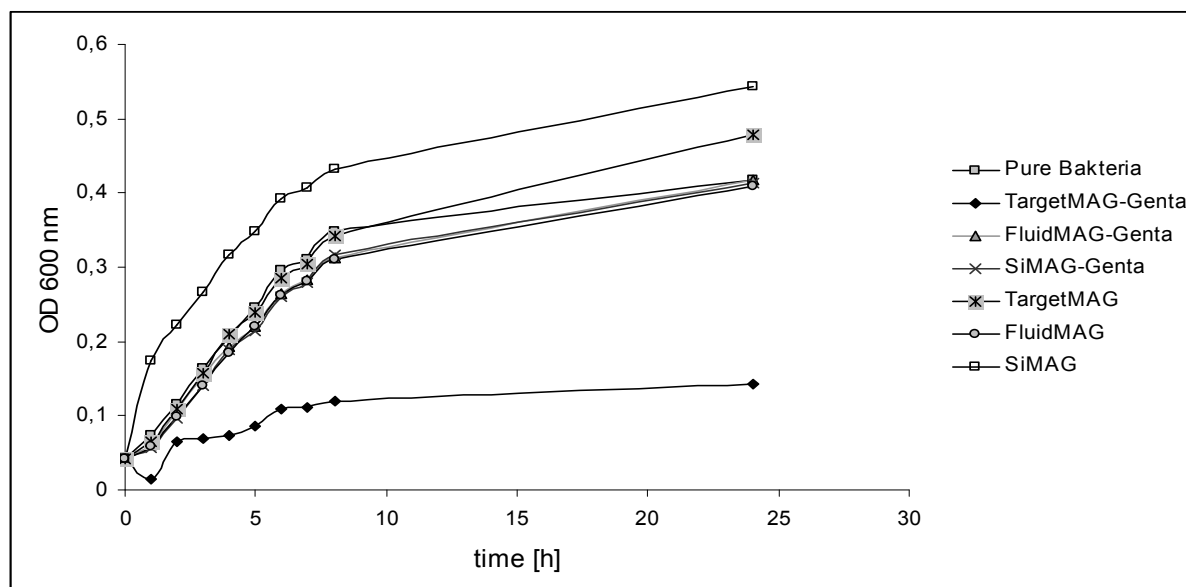


Figure 4. *Staphylococcus aureus* growth cultured in sterile Mueller-Hinton broth without adjuvant (pure bacteria), in presence of gentamicin coated nanoparticles (TargetMAG-Genta, FluidMAG-Genta, SiMAG-Genta), uncoated nanoparticles (TargetMAG, FluidMAG, SiMAG).

TargetMAG-Genta showed a *S. aureus* growth inhibition resulting in a colony reduction after 24 hours of over 99 % compared to reference (Figure 5). Coated S13 particles reduced bacterial growth by over 85 %, whereas the phenomena of a growth stimulating effect already observed for FluidMAG-Genta and SiMAG-Genta particles was also detected for uncoated S13 particles. Applying gentamicin concentrations between 0.665 $\mu\text{g/ml}$ up to 66.500 $\mu\text{g/ml}$ resulted in a *S. aureus* growth inhibiting effect of approximately 85 % to 88 % independent of concentration. As S21 and S26 particles did not show enough drug loading at their surface, they were excluded from experiments. As FluidMAG and SiMAG particles did not show antimicrobial potential, they were excluded from further experiments.

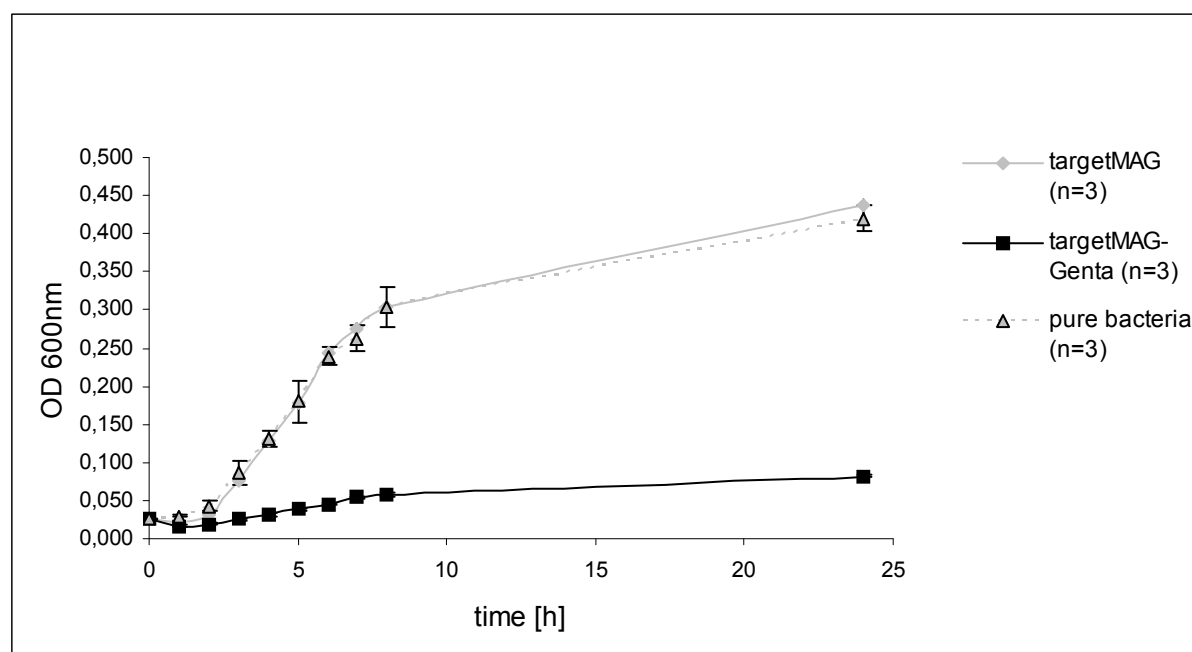


Figure 5. *Staphylococcus aureus* growth cultured in sterile Mueller-Hinton broth without adjuvant (pure bacteria), in presence of gentamicin coated nanoparticles (TargetMAG-Genta), uncoated nanoparticles (TargetMAG).

Analyses of drug release for all six coated nanoparticle types incubated in PBS at 37 °C and pH 7.4 for release showed no measurable gentamicin release from the surface of investigated magnetic nanoparticles.

3.3 Percent surface coverage

The percentage of S13 particle surface covered by gentamicin after the loading procedure can be estimated as performed. As 1 μg iron contains 7.9×10^{12} S13 particles and the gentamicin load per 1 μg iron averaged at 0.066 μg , 8.3×10^{-15} g gentamicin ($\approx 10.5 \times 10^6$ molecules) is bound per 1 S13 particle. Based on the fact that one particle has a surface area of $1.3 \times 10^{-15} \text{ m}^2$, 6.6 g gentamicin, corresponding to 13.8 mmol gentamicin, or 8.4×10^{21} gentamicin molecules are bound per one square meter particle surface. According to this calculation 8400 gentamicin molecules are bound to one square nanometer S13 surface.

3.4 In vitro cytotoxicity studies

The WST-1 assay shows high metabolic activity of HUVEC in the presence of magnetic nanoparticles at the concentration used in circulatory experiments of 1 mg/ml for Resovist[®] (150 % of reference cell proliferation), followed by TargetMAG-Genta particles (122 % of reference cell proliferation), and uncoated TargetMAG-NC particles (91 % of reference cell proliferation) (Figure 6A). Metabolic activity of HUVEC in presence of S13 particles was assessed at 95 % for S13-Genta and 101 % for S13 particles (Figure 6B). Under the influence of individual gentamicin concentrations, the metabolic activity ranged from 96 % up to 102 % compared to reference (Figure 6C).

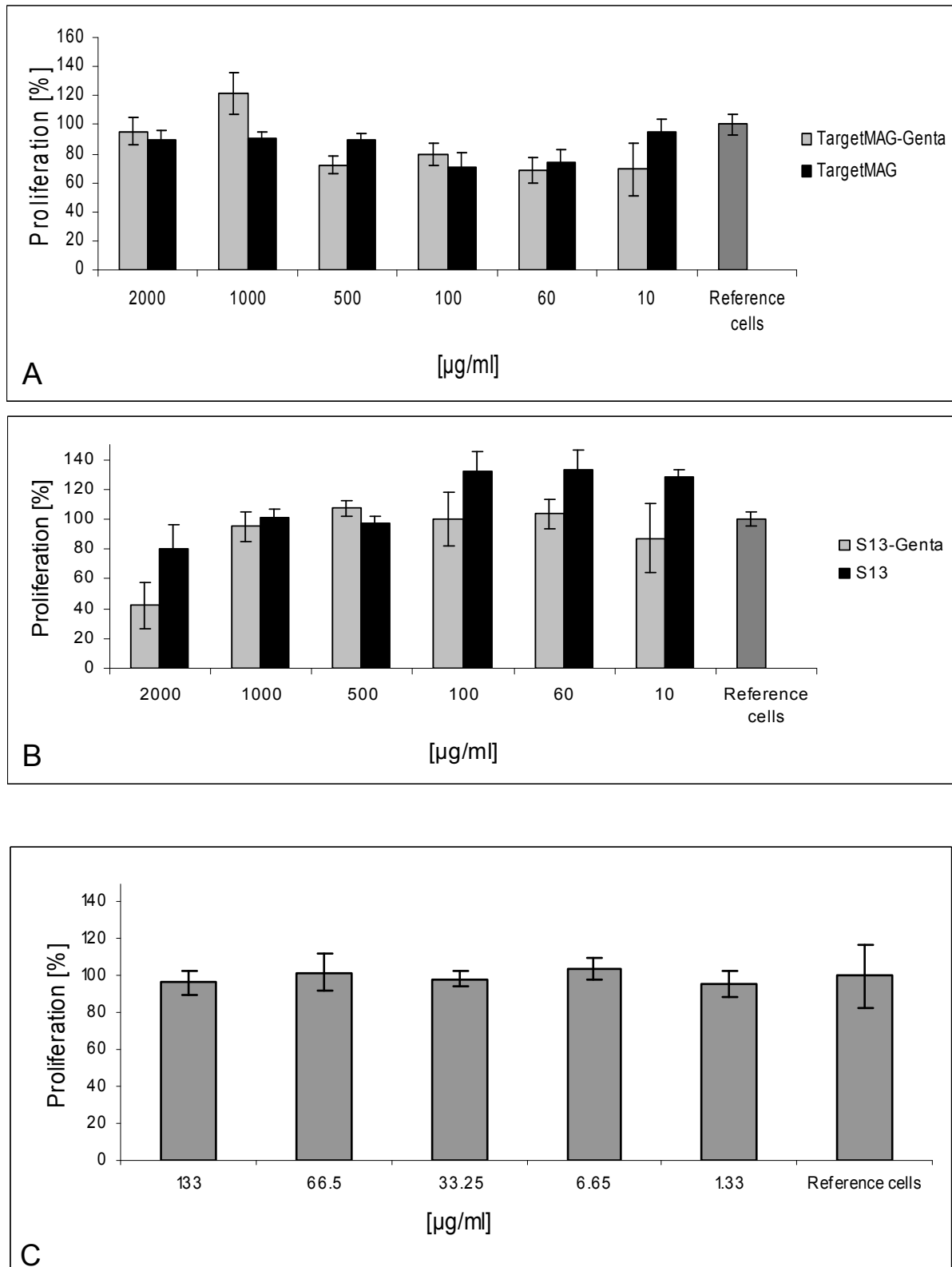


Figure 6 A-C. Metabolic activity of HUVEC incubated with different concentrations of A) TargetMAG and TargetMAG-Genta, B) S13 and S13-Genta and C) different gentamicin concentrations.

3.5 Circulatory experiments

The operation of the Bruker Magnet with 30 A and 120 V for 30 minutes resulted in an enrichment of the magnetic nanoparticles TargetMAG at the surface of the target tube when keeping a maximal tip-target distance of 15 mm, independent of the application of an additional wire netting. TargetMAG particles were used as they showed superior anti-infective and biocompatible characteristics towards all other developed nanoparticles. The nanoparticle fixation with indirect touch with the tip could already be visually observed. A setting with a tip-target distance larger than 15 mm did not result in any measurable ferrofluid agglomeration. The surface-adhered iron rate (RS) is defined as the ratio in percent between the iron content of adhered ferrofluids at the inner surface of the target tube after the magnetic field application of a certain time t and the total iron content in the circuit at $t = 0$. Differences between RS_{30} and RS_{15} values describing the influence of different application times of the magnetic field on the amount of ferrofluid accumulation were observed. RS_{15} values of experiments with a tip-target distance of 0 cm, with or without wire netting, ranged considerably below corresponding RS_{30} values. RS_{15} without wire netting averaged at $19.6 \% \pm 2.8 \%$ according to a total iron amount of $9.8 \text{ mg} \pm 1.4 \text{ mg}$, whereas under the influence of the wire netting RS_{15} averaged at $14.6 \% \pm 4.9 \%$ according to a total iron amount of $7.3 \text{ mg} \pm 2.5 \text{ mg}$. Increasing the tip-target distance to 15 mm showed an assimilation of corresponding RS_{15} and RS_{30} values. RS_{15} without wire netting averaged at $2.6 \% \pm 0.8 \%$ according to a total iron amount of $1.3 \text{ mg} \pm 0.4 \text{ mg}$, whereas under the influence of the wire netting RS_{15} averaged at $3.3 \% \pm 0.5 \%$ according to a total iron amount of $1.6 \text{ mg} \pm 0.2 \text{ mg}$. The highest amount of ferrofluids at the surface of the target tube after 30 minutes was assessed with a tip-target distance of 0 cm without the influence of the wire netting (Table 2). Thereby RS_{30} averaged at $31.5 \% \pm 3.3 \%$ according to a mean total iron amount of $15.8 \text{ mg} \pm 1.6 \text{ mg}$. The additional application of the wire netting at the same tip-target distance of 0 cm resulted in an average RS_{30} of $24.7 \% \pm 1.4 \%$ and an iron content of $12.4 \text{ mg} \pm 0.7 \text{ mg}$. Increasing the tip-target distance to 15 mm resulted in a decreased accumulation of ferrofluids at the inner surface of the target tube. RS_{30} in the presence of the wire netting averaged at $3.3 \% \pm 0.6 \%$ according to a total iron amount of $1.7 \text{ mg} \pm 0.2 \text{ mg}$, whereas without the influence of a wire netting RS_{30} averaged at $2.4 \% \pm 1.6 \%$ according to a total iron amount of $1.2 \text{ mg} \pm 0.8 \text{ mg}$.

Table 2 A/B. RS values/ absolute iron/ absolute gentamicin adhered on the target tube surface assessed A. without wire netting B. with wire netting.

A

Magnetic field application time	15 min	30 min	15 min	30 min
Tip-target distance	0 mm	0 mm	15 mm	15 mm
RS [%]	19.6 ± 2.8	31.5 ± 3.3	2.6 ± 0.8	2.4 ± 1.6
Absolute iron [µg]	9783.3 ± 1401.2	15766.7 ± 1635.8	1275.0 ± 388.9	1175.0 ± 813.2
Absolute gentamicin [µg]	1467.5 ± 210.2	2365.0 ± 245.4	191.3 ± 58.3	176.3 ± 122.0

B

Magnetic field application time	15 min	30 min	15 min	30 min
Tip-target distance	0 mm	0 mm	15 mm	15 mm
RS [%]	14.6 ± 4.9	24.7 ± 1.4	3.3 ± 0.5	3.1 ± 0.6
Absolute iron [µg]	7300.0 ± 2451.5	12350.0 ± 707.1	1625.0 ± 247.5	1650.0 ± 282.8
Absolute gentamicin [µg]	1095.0 ± 367.7	1852.5 ± 106.1	243.8 ± 37.1	247.5 ± 42.5

After magnetic field application, measured nanoparticle accumulations dispersed within several seconds and the ferrofluid concentration, represented by the iron content in the circuit, increased to the initial value (Figure 7).

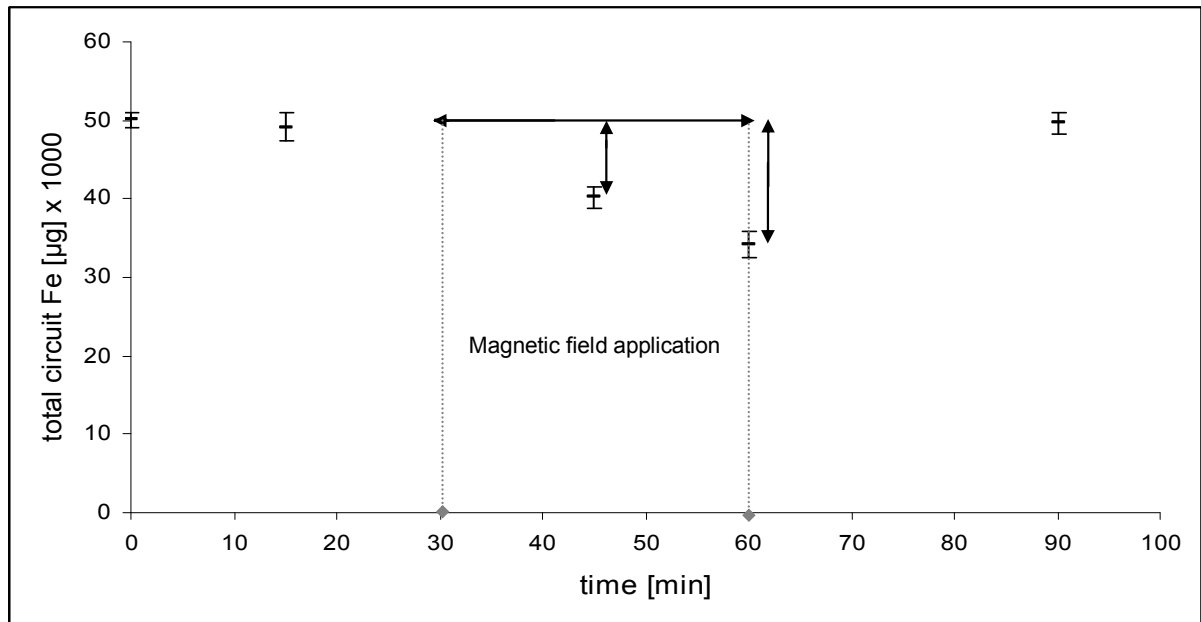


Figure 7. Change of the total iron content in μg over experimental time measured in the closed circuit using a tip-target distance 0 mm without wire netting.

4 Discussion

In the present work new antimicrobially equipped ultra-small superparamagnetic iron oxides were developed and studied. These particles usually consist of an iron oxide (Fe_3O_4) core surrounded by an organic shell consisting e.g. of dextrans, fatty acids or starch (11). The antibiotic gentamicin was ionically and covalently linked to the organic shell. The antimicrobial equipment of magnetic nanoparticles presents the possibility to accumulate high antibiotic concentrations on the surface of vascular grafts with the help of a magnetic drug targeting system.

Magnetic drug targeting has been performed in several *in vitro* and *in vivo* studies. Inada et al. applied urokinase-magnetide complexes for *in vitro* investigation of localized fibrinolysis (16). Viroonchaptan et al. showed that it is possible to release incorporated calcein from thermosensitive magnetoliposomes by temperature increase above 40°C (30). Mykhaylyk et al. reports the development and utilization of magnetic nanoparticles with high DNA binding capacity for high transfection efficiencies (23). Particularly in oncology, where the selective application of chemotherapeutics is an important column for a successful treatment, magnetic drug targeting systems moved into focus. Alexiou et al. demonstrated the *in vitro* accumulation of ferrofluids in the intracellular space of HeLa-cells by an external magnetic

field at room temperature (3). In the same study the treatment of VX2 tumor-bearing rabbits with mitoxantrone labelled magnetic nanoparticles revealed a higher chemotherapeutic concentration in the tumor region compared to systemic chemotherapy. The first clinical approach in human patients was performed with epirubicin-loaded ferrofluids for advanced and unsuccessfully pre-treated cancer or sarcoma (21). A successful accumulation of drug-loaded ferrofluids in one half of the patients was assessed. These successful advances show that the combination of drug-loaded magnetisable nanoparticles and a magnetic drug targeting system is not just a futuristic vision, but becomes an established method to obtain high drug levels in a target area of the body.

A major risk associated with implants like vascular grafts is the development of device-related infections (5, 10). The key events on the way to biomaterial infection are the adherence of pathogens and a subsequent biofilm formation as a consequence of a genetic switch and a change of the planktonic phenotype into the biofilm phenotype (26). This genetic switch leads to an increased host defence and antibiotic resistance which is the major barrier for a successful treatment. While post-operative infections can widely be avoided by anti-infective graft coatings, this time limited protection becomes less important in terms of infections caused years after surgical placement. An increase of the intravenous antibiotic application is also limited due to arising side-effects. The accumulation of high antibiotic concentrations in the area of infection on demand via a magnetic drug targeting system is therefore of high interest.

In the present work, gentamicin-functionalized nanoparticles were developed and studied in vitro for drug release, biocompatibility and anti-infective characteristics. The coverage of a broad spectrum of pathogens and the application for implant infection therapy were crucial factors for the choice of gentamicin (27). Loading capacity and anti-infective experiments demonstrated that only Target-MAG-Genta and S13-Genta meet the demands for applicable anti-infective nanoparticles. Loading capacities at 6.6 % (m/m) for S13 and 15 % (m/m) for TargetMAG particles showed that a successful coating technology was performed resulting in highly equipped nanoparticles concerning the drug amount on the nanoparticle surfaces.

The installation of a computer-aided model for a better understanding of the surface loading of nanoparticles with gentamicin was taken into consideration. However due to too many variables such as different gentamicin composition, individual conformations within one composition and various possible binding sites for one gentamicin molecule, this project was not pursued.

TargetMAG-Genta and S13-Genta demonstrated no drug release within 90 minutes, however high anti-infective characteristics were assessed. This phenomenon needs further prove as in previous works concerning magnetic drug targeting for tumor treatment, the release of chemotherapeutics from similar nanoparticles was the basic requirement for the effectiveness of developed particles. Alexiou et al. demonstrated a mitoxantrone release within 60 minutes (1) and based the effectiveness of developed particles on this drug release. We assume that a pH shifting of the bacterial growth medium Mueller-Hinton broth due to metabolic activity of bacteria from originally $\text{pH } 7.3 \pm 0.1$ to a lower pH might result in a drug release, however this requires further investigation.

In pathologically relevant bacterial concentrations, as demonstrated by Elek and Conen (12), TargetMAG-Genta and S13-Genta at a concentration of 1 mg/ml achieved a bacterial eradication rate of 100 %. This shows a highly effective potency against *S. aureus* growth. Even at a concentration hundredfolds beyond maximal pathologically relevant bacterial concentration, *S. aureus* growth could highly be reduced after 24 hours by TargetMAG-Genta and S13-Genta. Thereby TargetMAG-Genta showed a significantly higher growth inhibition effect than S13-Genta. TargetMAG, TargetMAG-Genta, S13 and S13-Genta, as well as in situ expected gentamicin concentrations, did not show cytotoxic potentials with regard to the metabolic activity of human umbilical vein endothelial cells. In circulatory experiments, the optimal parameters for a maximal iron accumulation, and therefore gentamicin concentrations, at the surface of the model tube were assessed. The magnetic field strength as well as the flow rate were held steady in consideration of the physiological blood flow at 150 ml/min up to 200 ml/min in a vascular graft of 7 mm diameter. The application time of the external magnetic field, the distance between target tube and magnet tip, and the utilization of an additional wire netting surrounding the target tube are important parameters that should be taken into consideration.

The application of an additional wire netting to distort the field gradient, which is meant to force nanoparticles to adsorb at the inner-surface of the PTFE graft, did not show the desired effects. A tip-target distance of 0 cm without a wire netting and 30 minutes field application represent the optimal choice of parameters resulting in an iron accumulation of $15767 \mu\text{g} \pm 1636 \mu\text{g}$ corresponding to $2365 \mu\text{g} \pm 245 \mu\text{g}$ gentamicin at the surface of the model graft. For in vivo experiments the tip-target distance has to be increased as replaceable vessels are situated at about 2 cm to 7 cm distance from the body surface. As shown in our experiments, nanoparticle enrichment on the tube surface with the described system is strongly reduced

with an increasing tip-target distance. The application of a stronger magnetic field and the influence of a higher viscosity of blood on the particle enrichment at a PTFE surface are the objectives of future investigations.

5 Conclusions

In this study we could demonstrate the development and selective enrichment of antibiotic-functionalized nanoparticles consisting of ultra-small superparamagnetic iron oxides surrounded by starch or palmitoyl-dextran with ionically bound gentamicin. Selected nanoparticles TargetMAG-Genta and S13-Genta completely inhibited the proliferation of *S. aureus* in pathologically relevant concentrations while preserving biocompatible characteristics. In in vitro circulatory experiments we further demonstrated that it is possible to accumulate high gentamicin concentrations on the surface of a model tube. If these results can be confirmed in vivo, developed magnetic drug targeting system could have be of high interest for the treatment of vascular graft infections.

6 Acknowledgements

We would like to thank Dr. B. Gleich (Institute of Medical Engineering, Technical University Munich, Germany) for his great assistance in technical questions. Furthermore we acknowledge H. Stephan and Dr. W. Kraus for their technical help, contributions and inspiring discussions. The authors did not receive any payments or benefits from a commercial party related directly or indirectly to the subject of this article. This study was supported by the Bayerische Forschungsförderung (BFS).

7 Figure and Table Captions

Figure 1. TargetMAG with ionically coupled gentamicin.

Figure 2. Closed circuit built up as a model for bloodstream in a ratio of one to one hundred to physiological conditions (total volume 50 ml ferrofluid suspension).

Figure 3A/B. Loading of magnetic nanoparticles with gentamicin: A. S13 particles and B. S26 particles.

Figure 4. *Staphylococcus aureus* growth cultured in sterile Mueller-Hinton broth without adjuvant (pure bacteria), in presence of gentamicin coated nanoparticles (TargetMAG-Genta, FluidMAG-Genta, SiMAG-Genta), uncoated nanoparticles (TargetMAG, FluidMAG, SiMAG).

Figure 5. *Staphylococcus aureus* growth cultured in sterile Mueller-Hinton broth without adjuvant (pure bacteria), in presence of gentamicin coated nanoparticles (TargetMAG-Genta), uncoated nanoparticles (TargetMAG).

Figure 6A-C. Metabolic activity of HUVEC incubated with different concentrations of A. TargetMAG and TargetMAG-Genta, B. S13 and S13-Genta and C. different gentamicin concentrations.

Figure 7. Change of the total iron content in μg over experimental time measured in the closed circuit.

Table 1A/B. Overview of individual nanoparticle types used for ionic or covalent gentamicin coupling.

Table 2A/B. RS values/ absolute iron/ absolute gentamicin adhered on the target tube surface assessed A. without wire netting, B. with wire netting.

8 References

1. **Alexiou, C., W. Arnold, R. J. Klein, F. G. Parak, P. Hulin, C. Bergemann, W. Erhardt, S. Wagenpfeil, and A. S. Lubbe.** 2000. Locoregional cancer treatment with magnetic drug targeting. *Cancer Res* **60**:6641-8.
2. **Alexiou, C., R. Jurgons, R. Schmid, W. Erhardt, F. Parak, C. Bergemann, and H. Iro.** 2005. [Magnetic Drug Targeting--a new approach in locoregional tumor therapy with chemotherapeutic agents. Experimental animal studies]. *Hno* **53**:618-22.
3. **Alexiou, C., R. Jurgons, R. Schmid, A. Hilpert, C. Bergemann, F. Parak, and H. Iro.** 2005. In vitro and in vivo investigations of targeted chemotherapy with magnetic nanoparticles. *Journal of Magnetism and Magnetic Materials* **293**:389-393.
4. **Anderson, J. E., A. S. Chang, and M. P. Anstadt.** 2000. Polytetrafluoroethylene hemoaccess site infections. *Asaio J* **46**:S18-21.
5. **Bunt, T. J.** 1983. Synthetic vascular graft infections. I. Graft infections. *Surgery* **93**:733-46.
6. **Chalmers, R. T., J. H. Wolfe, N. J. Cheshire, G. Stansby, A. N. Nicolaidis, A. O. Mansfield, and S. P. Barrett.** 1999. Improved management of infrainguinal bypass graft infection with methicillin-resistant *Staphylococcus aureus*. *Br J Surg* **86**:1433-6.
7. **Chemicell.** Coupling Protocol A1 SiMAG-Carboxyl 1.1.
8. **Chemicell.** Coupling Protocol fluidMAG-ARA 1.1.
9. **Costerton, J. W., L. Montanaro, and C. R. Arciola.** 2005. Biofilm in implant infections: its production and regulation. *Int J Artif Organs* **28**:1062-8.
10. **Darouiche, R. O.** 2004. Treatment of infections associated with surgical implants. *N Engl J Med* **350**:1422-9.
11. **Di Marco, M., C. Sadun, M. Port, I. Guilbert, P. Couvreur, and C. Dubernet.** 2007. Physicochemical characterization of ultrasmall superparamagnetic iron oxide particles (USPIO) for biomedical application as MRI contrast agents. *International Journal of Nanomedicine* **2**:609-622.
12. **Elek, S. D., and P. E. Conen.** 1957. The virulence of *Staphylococcus pyogenes* for man; a study of the problems of wound infection. *Br J Exp Pathol* **38**:573-86.
13. **Furuya, E. Y., and F. D. Lowy.** 2003. Antimicrobial strategies for the prevention and treatment of cardiovascular infections. *Curr Opin Pharmacol* **3**:464-9.
14. **Gleich, B.** 2007. Aktiver Wirkstofftransport mit magnetischen Feldern Magnetic Drug Targeting. Technische Universität München, München.
15. **Gristina, A. G., C. D. Hobgood, L. X. Webb, and Q. N. Myrvik.** 1987. Adhesive colonization of biomaterials and antibiotic resistance. *Biomaterials* **8**:423-6.
16. **Inada, Y., K. Ohwada, T. Yoshimoto, S. Kojima, K. Takahashi, Y. Kodera, A. Matsushima, and Y. Saito.** 1987. Fibrinolysis by urokinase endowed with magnetic property. *Biochem Biophys Res Commun* **148**:392-6.
17. **Iverson, N., N. Plourde, E. Chnari, G. B. Nackman, and P. V. Moghe.** 2008. Convergence of nanotechnology and cardiovascular medicine : progress and emerging prospects. *BioDrugs* **22**:1-10.
18. **Jain, K. K.** 2008. Nanomedicine: application of nanobiotechnology in medical practice. *Med Princ Pract* **17**:89-101.
19. **Khadori, N., and M. Yassien.** 1995. Biofilms in device-related infections. *J Ind Microbiol* **15**:141-7.
20. **Kingsley, J. D., H. Dou, J. Morehead, B. Rabinow, H. E. Gendelman, and C. J. Destache.** 2006. Nanotechnology: a focus on nanoparticles as a drug delivery system. *J Neuroimmune Pharmacol* **1**:340-50.

21. **Lubbe, A. S., C. Alexiou, and C. Bergemann.** 2001. Clinical applications of magnetic drug targeting. *J Surg Res* **95**:200-6.
22. **Lubbe, A. S., C. Bergemann, H. Riess, F. Schriever, P. Reichardt, K. Possinger, M. Matthias, B. Dorken, F. Herrmann, R. Gurtler, P. Hohenberger, N. Haas, R. Sohr, B. Sander, A. J. Lemke, D. Ohlendorf, W. Huhnt, and D. Huhn.** 1996. Clinical experiences with magnetic drug targeting: a phase I study with 4'-epidoxorubicin in 14 patients with advanced solid tumors. *Cancer Res* **56**:4686-93.
23. **Mykhaylyk, O., Y. S. Antequera, D. Vlaskou, and C. Plank.** 2007. Generation of magnetic nonviral gene transfer agents and magnetofection in vitro. *Nat Protoc* **2**:2391-411.
24. **Qiu, Y., N. Zhang, Y. H. An, and X. Wen.** 2007. Biomaterial strategies to reduce implant-associated infections. *Int J Artif Organs* **30**:828-41.
25. **Raschke, M. J., and G. Schmidmaier.** 2004. [Biological coating of implants in trauma and orthopedic surgery]. *Unfallchirurg* **107**:653-63.
26. **Sauer, K., A. K. Camper, G. D. Ehrlich, J. W. Costerton, and D. G. Davies.** 2002. *Pseudomonas aeruginosa* displays multiple phenotypes during development as a biofilm. *Journal of Bacteriology* **184**:1140-1154.
27. **Schmidmaier, G., M. Lucke, B. Wildemann, N. P. Haas, and M. Raschke.** 2006. Prophylaxis and treatment of implant-related infections by antibiotic-coated implants: a review. *Injury* **37 Suppl 2**:S105-12.
28. **Towne, J. B., G. R. Seabrook, D. Bandyk, J. A. Freischlag, and C. E. Edmiston.** 1994. In situ replacement of arterial prosthesis infected by bacterial biofilms: long-term follow-up. *J Vasc Surg* **19**:226-33; discussion 233-5.
29. **Tschantz, P., and Y. Tuchschnid.** 1995. [Risk factors in elderly surgical patients. A prospective study]. *Swiss Surg*:140-7.
30. **Viroonchatapan, E., M. Ueno, H. Sato, I. Adachi, H. Nagae, K. Tazawa, and I. Horikoshi.** 1995. Preparation and characterization of dextran magnetite-incorporated thermosensitive liposomes: an on-line flow system for quantifying magnetic responsiveness. *Pharm Res* **12**:1176-83.

Chapter 7

Functional neurotoxicity of individual antibiotics investigated with mammalian neuronal networks grown on microelectrode neuroarrays

Abstract

Objectives: The prevention of infections in the central nervous system demonstrates a life essential requirement in neurosurgery. In many cases antibiotics are locally applied and mingle directly with neuronal brain cells. The present work investigates the functional neurotoxicity of individual antibiotics using neuronal networks on microelectrode neuroarrays.

Methods: Penicillin G, streptomycin, penicillin/streptomycin, gentamicin and vancomycin were studied for functional neurotoxic effects. Compounds were added to mammalian frontal cortex networks cultivated on microelectrode neuroarray. Neuronal activity was recorded and suppression of action potential production regarding dose response curves and IC_{50} levels, the determination of different burst parameter and the drop out of individual cells were investigated and compared among each other.

Results: A step-wise activity decrease under the influence of studied antibiotics was observed. The IC_{50} averaged between 37 μM for streptomycin and 2371 μM for gentamicin. The investigation of burst parameters focusing on burst frequency, burst period and spikes in bursts corroborate the different characters of used antibiotics regarding functional toxicity. The drop out of individual cells and the comparison between active neurons and bursting neurons under compound influence unsheathe a higher loss of bursting neurons than active neurons under IC_{50} concentrations of streptomycin and vancomycin. IC_{50} concentrations of pen/strep and gentamicin caused a higher level of bursting neurons compared to the level of active neurons. The application of penicillin G in IC_{50} concentrations led to a slight loss of bursting neurons while the number of active neurons slightly increased.

Conclusions: The in vitro investigation of the impact of individual antibiotics on mammalian neuronal clusters cultured on microelectrode neuroarray provided useful data regarding the functional toxicity in particular the signal activity suppression, dose response and IC_{50} concentrations.

Keywords: Antibiotics, microelectrode neuroarray, neurosurgery, functional toxicity, frontal cortex

1 Introduction

In neurosurgery, antibiotics are locally applied in order to prevent or treat infection. Kala and Houdek evaluated patients treated with and without an antibiotic for cerebral abscess and demonstrated a beneficial effect of local antibiotic administration for cerebral abscess treatment (11). Kharitonova et al. described the preclinical and clinical application of gelatin sponges with kanamycin and gentamicin as a reliable anti-infective protection in neurosurgery (12). Broggi et al. achieved a recovery from deep brain abscesses in four patients by stereotactic implantation of a chronic intracavitary catheter connected to a subcutaneous reservoir to allow local antibiotic irrigations (1). Klein et al. applied neomycinsulfate intracerebral, epidural or intramuscular during neurosurgical operations and observed an infection rate below 1 % (10). In consideration of all these prosperities, very little data of neuronal toxicity of antibiotics is described in the literature. Side effects give a possible hint for toxic reactions in neuronal cells caused by antibiotics reaching from paralysis from neuromuscular blockage caused by streptomycin to irreversible ototoxicity occurring in patients treated with gentamicin (9, 14). Further studies are important in order to optimize as well as standardize applied doses to ensure a safer use of these drugs and to identify their influence on neuronal behaviour. Different in vitro models like microfluid techniques can be used for such investigations (8), however whole functional neuronal ensembles provide more physiologically relevant information (2, 4). Electrical signal patterns of a cluster of neurons on multielectrode neurochips were first described by Gross et al. (7). Different improvements in this technique lead to a stable and reliable method with the possibility to study the effects of transmitters, receptors, specific compounds, or drugs (3, 5, 15). The aim of this study was to test different antibiotics for their influence, used either for cell culture or in brain trauma surgery, on the electrical activity measured from neuronal networks on microelectrode arrays.

2 Materials and Methods

2.1 Compounds

The antibiotics penicillin G (1663 units penicillin G base per mg, Sigma Aldrich, St. Louis, USA), streptomycin (Sigma Aldrich, St. Louis, USA), pen/strep (GIBCO Laboratories, NY, USA), gentamicin (Sigma Aldrich, St. Louis, USA) and vancomycin (Sigma Aldrich, St. Louis, USA) were studied. Stock solutions were prepared for penicillin G (6.68 mg/ml), streptomycin (0.5 mg/ml), pen/strep (10000 units penicillin G and 10 mg streptomycin per ml), gentamicin (4.7 mg/ml) and vancomycin (14.49 mg/ml). Solutions were filtered with a 0.22 μm filter (Acrodisc[®] Syringe Filter, Pall Corporation, Ann Arbor, USA) under aseptic conditions and stored at 4 °C. Before compound application, solutions were brought to room temperature and a defined volume was added to the recording chamber with a pipette by lifting up the cap, adding the test solution in small droplets to the periphery of the medium in the chamber and mixing twice with a syringe through a Luer entry portal in the chamber.

2.2 Microelectrode Arrays (MEAs)

The MEAs were manufactured at the Center for Network Neuroscience (CNNS) at the University of North Texas. These are 50 · 50 x 1 mm glass plates with a 1 mm² central recording matrix containing 64 passive electrodes of thin film indium tin oxide conductors. The basic glass plate consists of a soda lime glass base and two films, a coating of sputtered silicon dioxide with 90 % optical transmission and a thickness of 1200 Å and a 1400 Å thick conductive coating of sputtered indium tin oxide (ITO). The glass is cut into plates, cleaned and baked at 200 °C for drying. Subsequently the ITO surface is coated with a thin layer of photoresist, which is softly baked (95 °C) to drive off excess solvent. In order to cover the areas that will later be electrodes, a clean chrome photo mask is fixed to the photoresist coated plate. Thereafter the plate is briefly exposed to UV light, which modifies the exposed photoresist in a way that it can be dissolved with solvents. Photoresist areas under the masked regions are protected against UV light and therefore stay intact during the following development and etching steps. After UV exposure, glass plates are developed in 0.8 % KOH solution, which leads to a removal of the UV light exposed photoresist revealing the ITO underneath. In order to increase the adhesion of the remaining photoresist, plates are “hard” baked (115 °C). Subsequently the plates are submerged in an acid etching solution comprised

of HCl, HNO₃ and H₂O, which etches the exposed ITO metal, but does not affect the ITO under the photoresist. Each plate is now cut into four individual MMEPs for further processing (6).

The edges of each MMEP need to be sanded to fit in the CNNS base plate with 0.5 mm total play at the top and bottom. Furthermore any ITO tool marks have to be sanded off to avoid a possible electrode coupling upon zebra strip attachment. Before the cleaning step, the MMEPs need to be checked for electrode coupling. If coupling occurs, electrodes have to be separated using a diamond- tipped engraver or a laser. The MMEPs are then first soaked in 100 % EtOH for three hours before being scrubbed in a 10 % Contrad solution with a camelhair brush. Subsequently, MMEPs are boiled for 30 minutes in a 10 % H₂O₂ solution, rinsed with ultra pure water and 100 % EtOH, finally stored in.

The following step in fabrication contains insulation and curing. Therefore part of the polysiloxane stock insulation must be evaporated at room temperature for 8 hours until a final volume of 50 % of the stock is obtained. The edge electrodes for the zebra strip contacts are now taped before the MMEPs are placed on the spinner which is started at a speed of 1500 – 2500 rotations per minute and approximately 2 ml of polysiloxane solution are applied on the center of the MMEP. The spinner is stopped thirty seconds later and MMEPs are cured at 150 °C for 8 minutes. For deinsulation, the electrode sites in the recording matrix are deinsulated separately with a near UV laser. After that, all 64 deinsulated electrodes are electroplated simultaneously with a citrate potassium gold cyanide (CPGC) solution, MMEPs are assembled on a non-conducting base plate with zebra conductors and a conducting top plate connected to a pulse generator. A gold wire anode is placed in the GPGC electroplating solution (3.1 g Au²⁺/l) which saturates the 64 ITO cathodes. The pulse generator supplies the system with 1200 mV at 1.0 µA for two minutes.

2.3 Cell culture

MMEPs were prepared for cell seeding by autoclaving for 25 minutes at 121 °C and exposing the hydrophobic polysiloxane insulation material to a butane flame to create a hydrophilic surface. After flaming, MMEPs are fitted with greased silicone gaskets and 50 µl of a sterile 5 mg/l poly-L-lysine solution (PLL, Sigma Aldrich, St. Louis, USA) is applied to the flamed matrices of each MMEP for 24 hours in an incubator under 10 % CO₂ and 95 % relative humidity. The PDL is then rinsed with ultra-pure water and removed with a sterile pipette.

Each MMEP is transferred to a Petri dish and each matrix is incubated with 60 µl of a 2 µg/ml laminin solution for 45 minutes.

Frontal cortex tissue is harvested from one time-pregnant ICR mouse (Harlan Sprague Dawley, Inc.) at embryonic day sixteen. After anesthesia with chloroform and sacrifice via cervical dislocation, the uterus is removed under sterile conditions. The obtained embryos in a usual quantity of twelve to fourteen are immediately immersed for further dissection in an anaesthetic bath of D1SGH at a pH of 7.35 and an osmolarity of 320 miliosmoles at 4 °C. With the aid of a pair of fine-tipped forceps and a stereoscopic microscope, embryos are decapitated and the skull revealed by removing skin and muscle tissue. The skull is carefully removed from the dorsal side working rostrally to caudally. The intact brain is then lifted from the skull cavity. In order to reveal the cerebral cortex, the meninges are removed from each brain and the frontal lobe is dissected in a trapezoidal pattern. After isolating the frontal cortex from each embryonic brain, it is stored in a separate bath of D1SGH. After aspirating the DSGH from the Petri dish, the frontal cortex tissue is minced with two sterile scalpel blades and enzymatically dissociated with the addition of 3 ml of 1:14 papain:DSGH solution. After 5 minutes incubation at 37 °C and 5 minutes at 22 °C, papain is removed via centrifugation with 50 µl DNase I in 5 ml DMEM5/5 at 900 rpm for four minutes. By adding DNase I, cell clumping during seeding induced by free DNA, released by proteolytic activity of papain is avoided (Huettnner & Baughman, 1986). The supernatant is removed and the cell pellet is suspended in 50 µL DNase I in 5 ml DMEM5/5 solution. With the help of a cytometer, the cell density is adjusted to 100000 cells/ml and cells are seeded onto the recording matrix area of each MMEP. Thereafter laminin is removed from the recording matrix area with a fine-bore plastic pipette and 100 µL cell suspension is seeded onto each matrix. After 2 hours of incubation at 38 °C, cell adhesion is evaluated and cells are fed with 1 ml of DMEM 5/5. A full medium change is performed after 24 hours with DMEM 5/5 in order to remove any DNase and non-adhered cells respectively cell debris. To eliminate remaining fetal bovine serum from the medium, a full medium change with DMEM 5 is performed three days later. Onto the matrix of each MMEP, a monolayer neuronal network atop a confluent glial carpet layer develops. Cell cultures could be maintained in an incubator at 37 °C under 10 % CO₂ and 95 % relative humidity for up to six months without addition of antibiotics or fungicides by bi-weekly half medium changes into DMEM 5. Cultures are ready for use usually three weeks to three months after seeding.

Networks developed from a mixture of different types of postmitotic neurons and glia cells. The glia cells have the important auxiliary function for metabolism and to supply neurons with ions and nutrients. They also influence synaptogenesis. By culturing neurons in combination with glia cells, stability over many months is ensured. After approximately two days in vitro spontaneous electrical activity develops (3). Random spiking at first stabilized after two weeks in culture into more coordinated activity. This activity is composed of coordinated main burst patterns and interburst spiking. These networks showed a high interculture repeatability (5) and remained spontaneously active and pharmacologically responsive for more than six months. For this study cultures between 25 and 40 days in vitro were used.

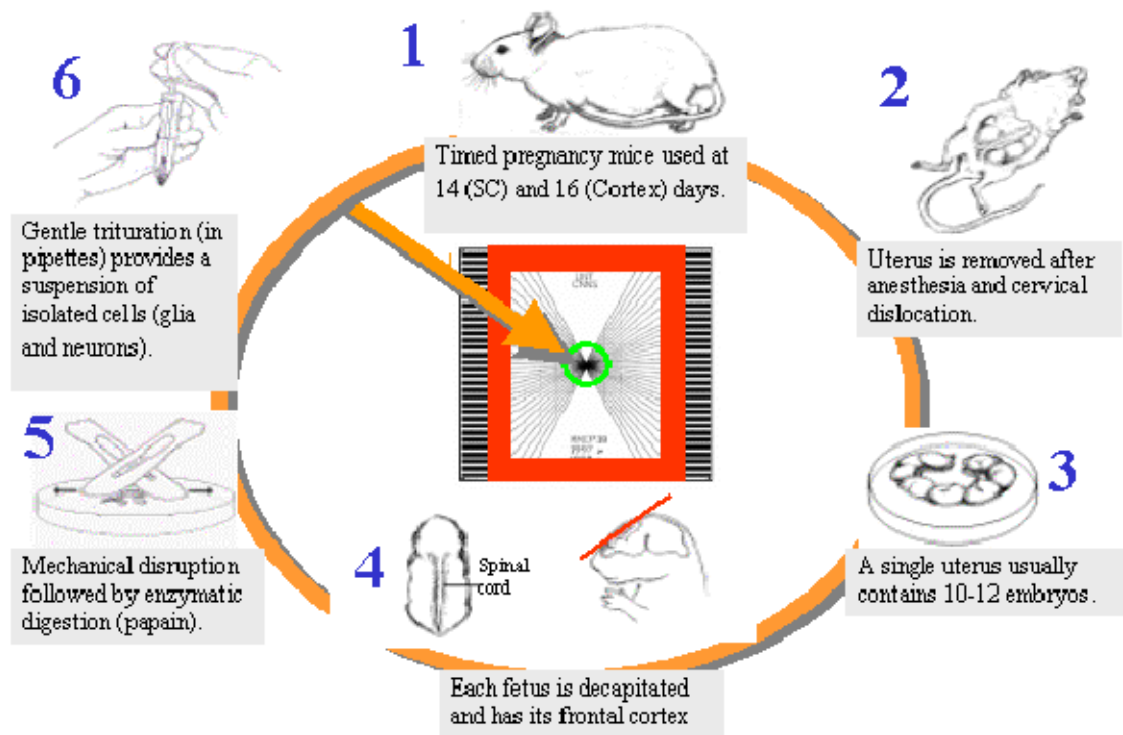


Figure 1. Preparation procedure of the neuronal cell cultures (CNNS archives).

2.4 Experimental Setup

2.4.1 Recording station

The signal amplifier systems at the CNNS are manufactured by Plexon Inc., Dallas, USA. The experimental setup consists of different parts described in the following. The edge connectors at either side of the MEA plate contact the matched preamplifier circuit board via flexible zebra strips. Thereby original signals of 50 – 800 μ V are amplified by a gain of 100. Any frequency components lower than 100 Hz and higher than 8000 Hz are filtered out. From the preamplifiers, signals are transferred to the MAP-box (Multichannel Acquisition Processor) and become amplified again (10x – 100x) and A/D converted. The DSP board contains four (32-channel board) digital signal processors. Each DSP receives eight channels of A/D converted data from a signal board. On each channel, up to four action potential waveforms can be discriminated in real time. From the DSP board, the signals are first transferred to a GPIB or MXI bus board and further to a workstation, where data analysing is performed. For a better differentiation between noise and real activity signals, two oscilloscopes (HM 407, HAMEG Instruments GmbH, Mainhausen, Germany) are attached to the MAP box showing the analog signal of the current channel and the signal of the last DSP selected in the Sortclient software (Plexon, Inc, Dallas, TX USA). For further control, selected analog signals are transferred to a loudspeaker array (CNNS, Denton, USA) of up to sixteen speakers, making selected signals audible.

2.4.2 Chamber Setup

A MMEP with a greased gasket and DMEM 5 for cell life supply was placed under aseptic conditions onto a base plate with a rubber separator as a spacer between glass and steel (Figure 2B). Part of the cell medium was removed with a syringe leaving behind a thin film of medium covering the matrix, the gasket was removed with forceps and a stainless steel chamber was fixed with set screws at the base plate in a way that the cell matrix was kept in the middle of the chamber. Removed cell medium was given into the chamber through a chamber entry portal and a cap (Figure 2B) was fixed on top of the chamber to create an enclosed system and connected to the chamber by a wire. The cell chamber was deposited on a microscope stage, connected to the preamplifiers of the recording station and grounded (Figure 3C). During experiment, osmolarity in the chamber was maintained constant at about

320 milliosmoles by adding ultra-pure water via a pump system (Pump 11, Harvard apparatus, Holliston, USA) through an entry portal in the chamber and controlling it with an osmometer (5500 vapor pressure osmometer, Wescor, Inc., Logan USA). In order to maintain the pH at 7.4, the chamber was supplied by a constant flow of a mixture of 10 % CO₂ and 90 % air (AFC 2600 Pro, Mass Flow Controller, Aalborg Instruments, USA) at 5–10 ml/min through a side entry portal in the cap that sat on top of the chamber. In order to maintain a constant temperature at 37 °C inside the cell chamber, two heating systems were used. A constant 12 V voltage source (Micronta Radio shack, Forth) was connected to four 3 Ω power resistors attached to the microscope stage (Axiovert 100, Zeiss, Göttingen, Germany) to heat up the plate to approximately 30 °C. The base plate contained a second set of power resistors. Temperature was controlled by a regulated heater (CN 9000 A, Omega Engineering, Inc., Stamford, USA) which was connected to the base plate (see Figure 2) and assured a stable temperature of 37 °C ± 1 °C.

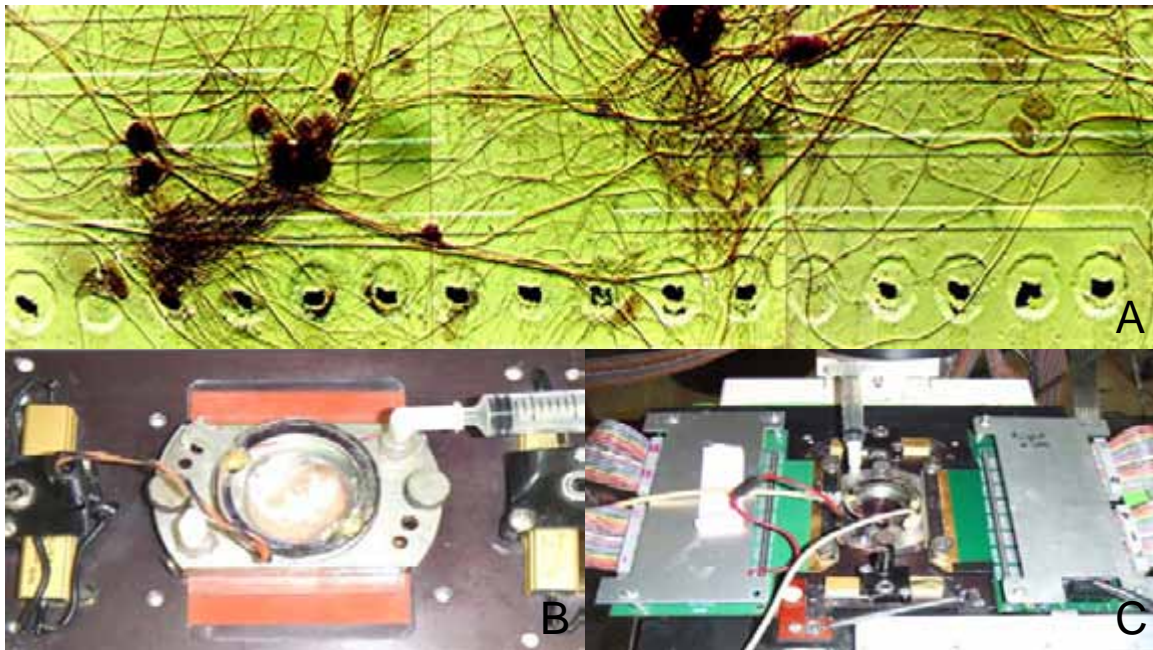


Figure 2. Experimental setup to study neuronal networks on microelectrode arrays: A) Segment of a frontal cortex network grown on an array for 21 days in vitro. B) Chamber setup: A MMEP with DMEM 5 for cell life supply is placed under aseptic conditions onto a base plate with a rubber cushion between glass and metal. C) Recording station. The edge connectors of the MMEPs are in contact with zebra strips, which make contact to the preamplifiers (CNNS archives).

2.4.3 Data recording

Recording was performed with a computer-controlled 64-channel amplifier system from Plexon, Inc., Dallas, USA, the so-called Multichannel Acquisition Processor System. This system provides programmable amplification, filtering, switching, and digital signal processing of multielectrode signals. A template-matching algorithm in real time provided spike identification and separation and delivered single neuron spike data online. For recording neuronal activity, the programs Sortclient (Plexon, Inc., Dallas, USA) and Vernac (CNNS, Denton, USA) were used. Vernac averages all sorted time stamps from the Sort client and plots minute mean values of the total spike and burst production in real time. It allows the user to get an overview of the previous and current conditions of the cell culture and the impact of compounds added. Data for further analysis is provided by the program Sortclient which records time stamps and waveforms of the selected units and provides values of different parameters describing the activity of identified action potentials (Figure 3).

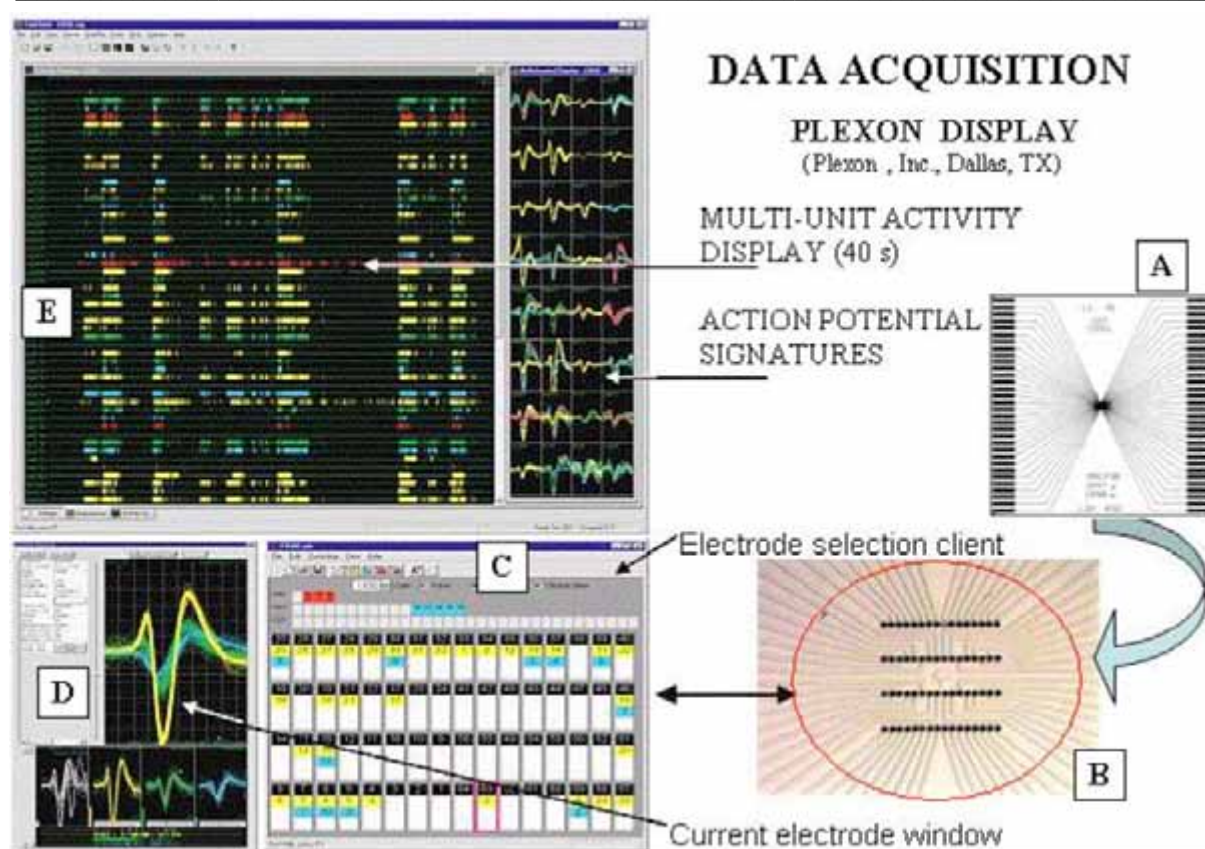


Figure 3. Summary of data acquisition and display: A) MEA showing 32 edge connectors on either side of the 5x5 cm glass plate. B) Central recording area with 64 microelectrodes. The network seeding area (red circle) is generally larger than the 1 mm² recording matrix. C) Computer display of electrode matrix geometry, showing assignment of DSPs to specific channels (yellow boxes) and assignment of speaker outputs (blue boxes). D) Selected channel display showing three action potentials recorded and separation via template matching. E. Raster plot of time stamps generated when discriminated action potentials cross threshold (40 s window). All discriminated action potentials (32 DSP system) are also shown to the right of the raster display.

2.4.4 Data analysis

Eight parameters were selected to describe the changes in activity in response to successively increasing concentrations of antibiotics. Most represent mean values from averaging all channels per minute (usually called “Minute Means”). In some cases “Total Activity” is plotted to eliminate artifactual increases at very low channel counts. All data was extracted from the Plexon time stamp files. The parameters are: (1) the spike and burst activity, (2) burst duration, (3) burst period (time between beginning on one burst to the beginning of the next burst), (4) the burst amplitude (integrated burst value representing maximum spike frequencies in a burst), (5) the number of spikes in a burst, (6) the mean spike frequency in a burst, (7) the number of bursting neurons. No universally accepted mathematical definitions

of bursts exist (16). Bursts were identified operationally by digital RC integration with rise time constants of 100-150 ms. A lower threshold was set to determine the start and stop times for the burst and a higher threshold served to confirm that the integrated profile was above the noise level (Figure 4). A gap rule of 100 ms devoid of spikes was used to separate burst events into two bursts (13). T1 and T2 were set by inspection during off line data analysis with the intent to capture major bursts and ignore singlets or doublets. Raster displays showing spiking and bursting were viewed with the Neuroexplorer program (NEX Technologies) and thresholds were set to mimic the burst count in initial segments of the native activity. If thresholds are not changed during one experiment, such an operational definition allows quantitative comparisons of burst patterns within the same culture.

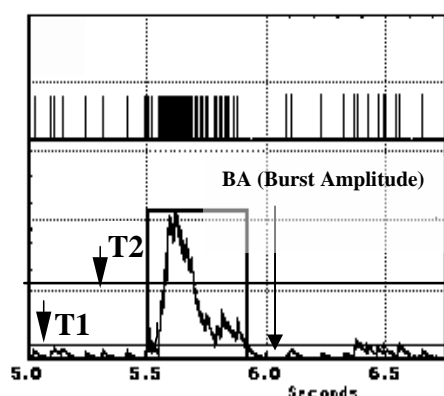


Figure 4. Time stamp sequence of a discriminated unit and mathematically simulated RC integration. Threshold 1 (T1) identifies start and stop times of bursts, whereas T2 is set to select only major bursts and eliminate noise.

For further statistical analysis activity was measured in bins of 60 seconds. That way minute mean values for action potential production and the significant burst parameters were calculated.

2.4.5 Dose Response curves

Changes in burst levels and spike levels were specific for each compound. Spike activity was plotted as a function of the log of test substance concentration and fitted with a sigmoidal function. Curve fitting, calculation of IC_{50} and fitting quality values were performed using Origin 6.0 software. IC_{50} values represent the concentration required for a 50 % inhibition of spike activity.

2.5 Experimental design

The aim of this study was to investigate the effect of different antibiotics on the spontaneous electrical activity of neuronal networks. Experiments were carried out as acute application of test substances to the 2 ml constant volume culture medium. The initial spontaneous activity of each network or a subsequent time period under bicuculline served as reference (baseline

activity) and was recorded at the beginning of each experiment for at least 30 minutes. This baseline activity was used as an absolute reference and all activity changes were determined as a percent change from this activity. Consequently, networks need to attain a stable reference state that was determined by a horizontal minute mean display in the VerNac window. A minute mean fluctuation of $\pm 10\%$ was preferred, although not always attained. Larger fluctuations were accepted as long as the minute-by-minute activity trace remained horizontal. For stabilization and activity increase 40 μM bicuculline was added to cultures. When such spike activity displayed by Vernac 0.6 was stable in time, compounds were applied in increasing concentrations approximately every 30 min. After each compound application, the network was allowed to seek a new stable state with relatively horizontal activity plateaus. Within each experiment, these stable activity plateaus were used for data analysis. The data set consisted of: For streptomycin and vancomycin three experiments and for pen/strep and gentamicin two experiments each were used for data analysis. For penicillin, three experiments under bicuculline and one experiment without bicuculline were performed and analysed.

3 Results

3.1 Suppression of action potential production

3.1.1 Dose-response curves

A step-wise decrease in action potentials (spikes) and bursts after compound addition was detected with each of the applied antibiotics. Figure 5 demonstrates the progression of minute mean spike and burst values of a neuronal network under increasing penicillin G/streptomycin (pen/strep) concentrations. Spike and burst rates showed an overall decrease in activity with increasing pen/strep concentrations. At the beginning of the experiment not under the influence of pen/strep, the mean activity was 52 spikes/min (S/min), the burst rate/min (B/min) was 2. By adding bicuculline, the mean activity was stabilized and raised to 80 S/min and 9 B/min, respectively (Figure 5). Adding pen/strep in nine concentration steps of 90 μM / 85 μM resulted in a decline of activity to a level of 10 S/min and 0 B/min at a final concentration of 2415 μM / 2320 μM pen/strep. A full medium change recovered the activity

of the neuronal network to 70 S/min and 2 B/min, respectively in the recorded window. From the high recovery and activity slope at 420 min, the pen/strep influence was considered reversible.

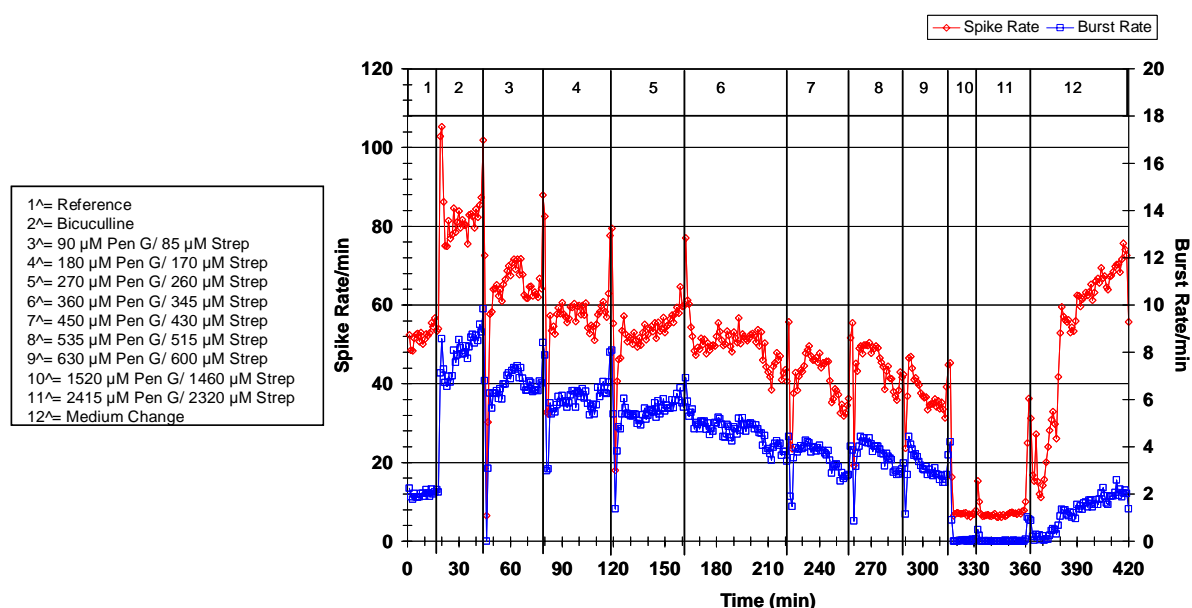


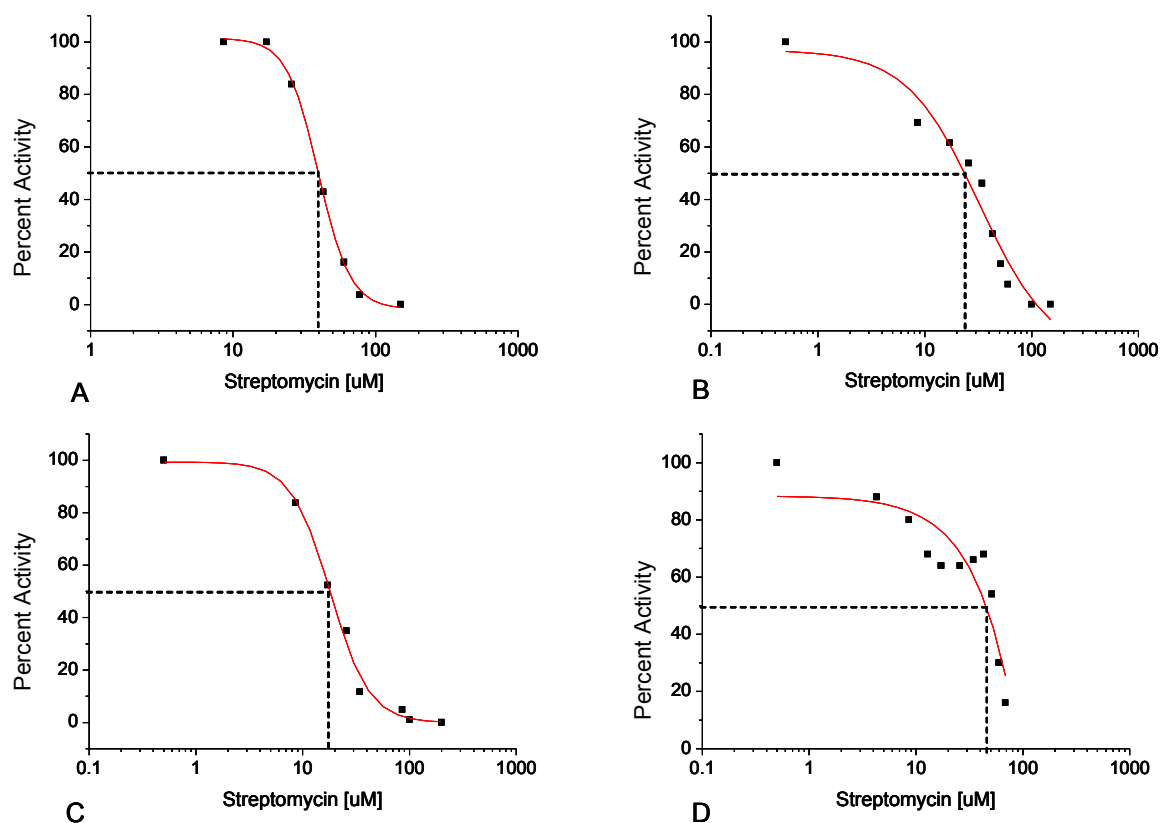
Figure 5. Step-wise decrease of spike rates and burst rates ($n = 69$ units) under increasing pen/strep concentrations with reversibility after medium change. Volume of pen/strep solutions added to a total bath volume of 2000 μl ranged from 20 μl to 100 μl .

3.1.2 IC_{50} Determination

Dose Response curves were developed resulting in different IC_{50} values for each test compound (Table 1). The IC_{50} for streptomycin (Figure 6) averaged $37 \mu\text{M} \pm 16 \mu\text{M}$ ($n=4$) and for pen/strep (Figure 7) $775 \mu\text{M}$ ($n=2$). Gentamicin (Figure 8) showed two differing IC_{50} values of $2371 \mu\text{M}$ ($n=2$). The IC_{50} value of vancomycin (Figure 9) averaged $1322 \mu\text{M} \pm 75 \mu\text{M}$ ($n=3$). In one experiment under vancomycin, an IC_{50} value of $2519 \mu\text{M}$ was assessed, however this experiment was regarded as unreliable. Under penicillin, cultures did not show a significant activity pattern change, and dose response curves could not be generated (Figure 10A - D). However in an internal control without bicuculline, an activity decrease caused by penicillin G was observed with an IC_{50} value of $1205 \mu\text{M}$ (Figure 10D). For further analysis of burst parameters this IC_{50} value is used.

Table 1. IC₅₀ values of individual antibiotics.

Antibiotic	IC ₅₀ Values [μM]
Streptomycin(n=3)	37 ± 16
Pen/Strep (n=2)	775
Gentamicin (n=2)	2371
Vancomycin (n=3)	1322 ± 75
Penicillin (n=1, without bicuculline)	1205

**Figure 6A – 6D. Dose response curves of streptomycin generated in four individual experiments.**

IC₅₀ values are: A) 40 μM, B) 32 μM, C) 18 μM, D) 57 μM.

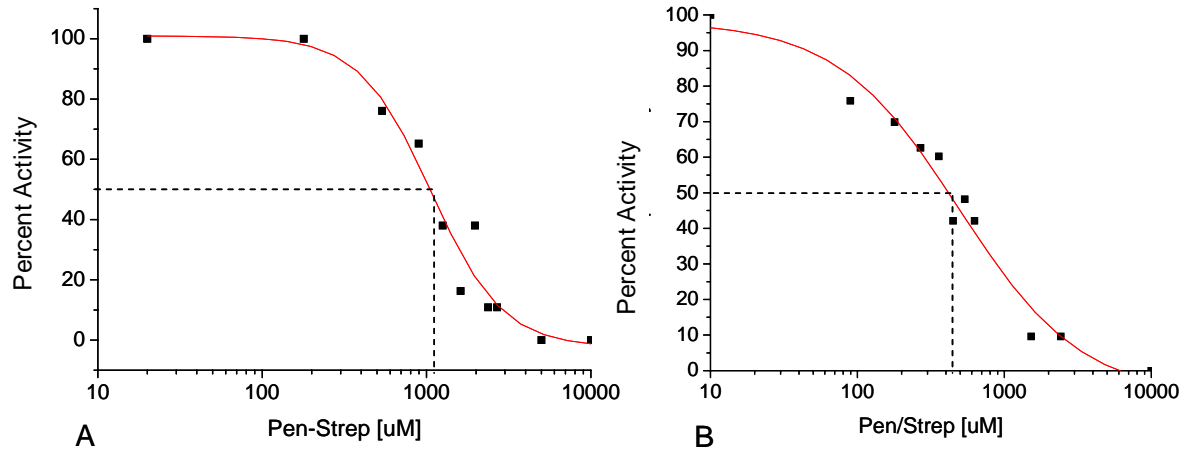


Figure 7 A/B. Dose response curves of pen/strep generated in two individual experiments.

IC_{50} values are: A) 1065 µM, B) 484 µM.

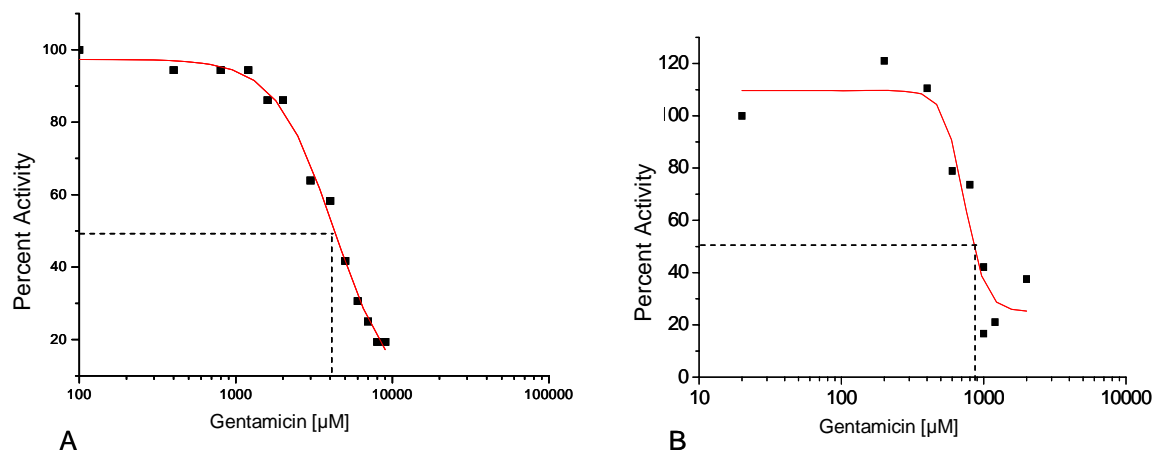


Figure 8 A/B. Dose response curves of gentamicin generated in two individual experiments.

IC_{50} values are: A) 4007 µM, B) 734 µM.

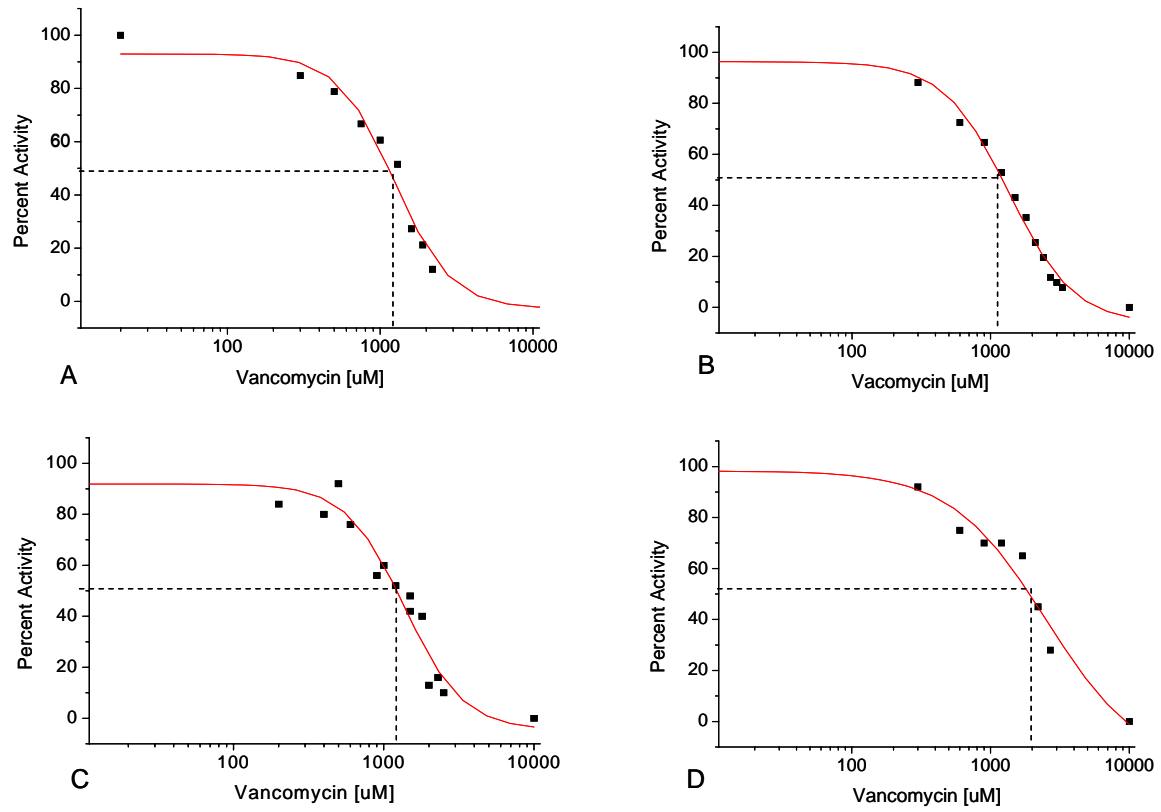


Figure 9A – 9D. Dose response curves of vancomycin generated in four individual experiments. IC_{50} values are: A) 1236 μ M, B) 1354 μ M, C) 1375 μ M, D) 2519 μ M.

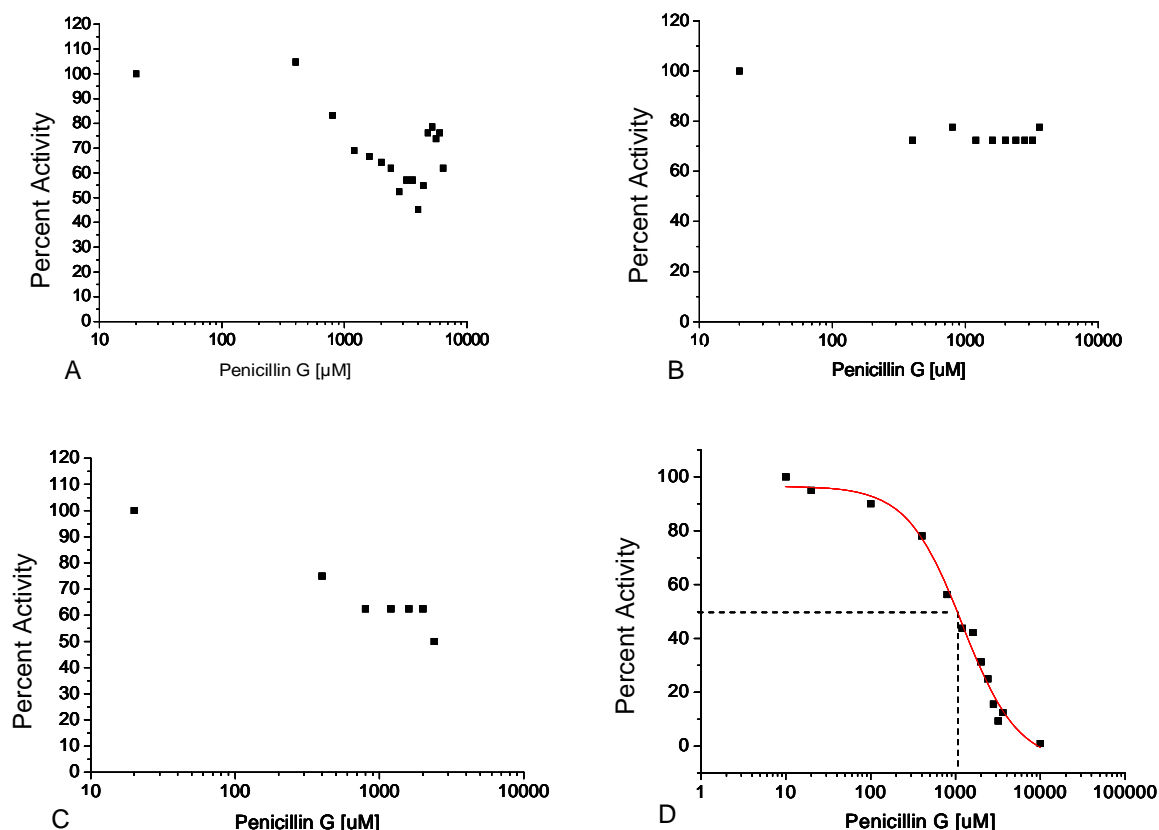


Figure 10A – 10D. Concentration/activity change dependence under penicillin G in four individual experiments: 10A) – 10C) under bicuculline, 10D) without bicuculline.

IC₅₀ value are: 10A) – 10C) no curve fitting, 10D) 1205 μM.

3.2 Burst Parameter

The influence of the five antibiotics on burst rate, burst period and number of spikes in bursts was quantified according to the following procedure. The values of the respective burst parameters at IC₅₀ concentration of each compound were divided by the values under native conditions and multiplied by 100 to obtain the percentage of change value (Table 2). The application of IC₅₀ concentrations to frontal cortex networks led to a slight increase of burst rate level under pen/strep to 103 % and under penicillin G to 101 %. A burst rate level decrease was observed under streptomycin to 86 % and gentamicin to 71 %. The application of vancomycin at IC₅₀ concentrations showed no change in burst rate values. Burst period levels showed an increase under the five tested compounds. The application of pen/strep raised the burst period level to 115 % while the application of gentamicin led to an average burst period level of 126 %. Streptomycin, penicillin G and vancomycin increased burst period

levels to 153 %, 160 % and 185 %, respectively. No change of spikes in burst level was detected under vancomycin while penicillin G and gentamicin decreased the spikes in burst level to 98 % and 70 % respectively. The application of streptomycin and pen/strep led to an increase of spikes in burst level to 104 % under streptomycin and 120 % under pen/strep.

Table 2. Levels of burst rate, burst period and spikes in burst of individual antibiotics defined as the ratio in percent under spike IC₅₀ concentrations and values under native DMEM 5 medium and bicuculline.

Antibiotic	Burst Rate Level [%]	Burst Period Level [%]	Spikes in Burst Level [%]
Penicillin G (n=3)	101 ± 2	160 ± 41	98 ± 4
Streptomycin (n=3)	86 ± 24	153 ± 53	104 ± 47
Pen/Strep (n=2)	103 (76/129)	115 (168/62)	120 (104/136)
Gentamicin (n=2)	71 (45/97)	126 (118/135)	70 (25/114)
Vancomycin (n=3)	100 ± 4	185 ± 55	100 ± 5

Figure 11 shows a typical development of spikes in burst rate under pen/strep. Values averaged under reference conditions at 160 Hz and increased after the addition of bicuculline to a level of 280 Hz. The step-wise addition of the compound pen/strep resulted in a decline of frequency to an average of 175 Hz under the influence of 626.5 µM/ 602 µM pen/strep. Higher drug concentrations caused an irregular frequency pattern which was stabilized at 90 Hz after full medium change.

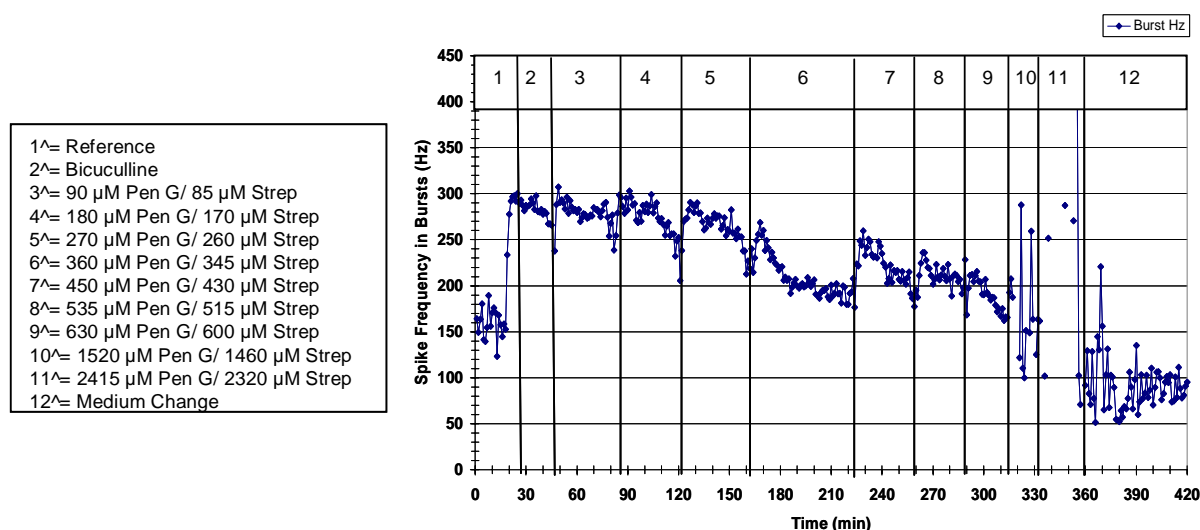


Figure 11. The change of mean spike frequencies in bursts values under the influence of pen/strep followed by a media change.

3.3 Drop out of individual cells

3.3.1 Bursting neurons

The application of individual antibiotics affected the amount of bursting and active neurons in frontal cortex neuronal networks. Table 3 shows the level of bursting neurons and active neurons defined as the ratio in percent of the measured values under IC₅₀ concentrations and the reference values under native DMEM 5 medium. While penicillin G, vancomycin and streptomycin in IC₅₀ concentrations caused a decrease in the number of bursting neurons ranging from 98 % for penicillin G to 73 % under streptomycin, gentamicin and pen/strep led to an increase in the number of bursting neurons to 106 % and 125 %, respectively.

Table 3. Levels of bursting neurons and active neurons of individual antibiotics defined as the ratio in percent of bursting neuron or active neuron values under IC₅₀ concentrations and values under native DMEM 5 medium and bicuculline.

Antibiotic	Level of bursting neurons [%]	Level of active neurons [%]
Penicillin G (n=3)	98 ± 6	102 ± 2
Streptomycin (n=3)	73 ± 4	89 ± 7
Pen/Strep (n=2)	125 (68/182)	104 (81/126)
Gentamicin (n=2)	106 (112/100)	100 (103/98)
Vancomycin (n=3)	87 ± 9	96 ± 7

3.3.2 Active neurons

A different tendency was observed investigating the number of active neurons. The level of active neurons defined as the ratio in percent of the measured values under IC₅₀ concentrations and the reference values under native DMEM 5 medium is demonstrated in Table 3. The application of gentamicin IC₅₀ concentrations did not change the level of active neurons while streptomycin and vancomycin lead to a decrease in the number of active neurons to 89 % under streptomycin and 96 % under vancomycin. Penicillin G and pen/strep in IC₅₀ concentrations led to a slight increase in the level of active neurons to 102 % under penicillin and 104 % under pen/strep.

3.3.3 Active neurons versus bursting neurons

A typical recording of the amount of bursting neurons and active neurons per minute is shown in Figure 12. After a medium change with DMEM 5, bicuculline was added to stabilize activity pattern in the culture. A continuous addition of streptomycin lead to a decrease of active and bursting neurons resulting in a nearly complete loss of burst activity at 77 μM streptomycin. Although burst had ceased, uncoordinated spike activity remained. After a medium change with DMEM 5 a recover of both parameters to a stable reference level was observed.

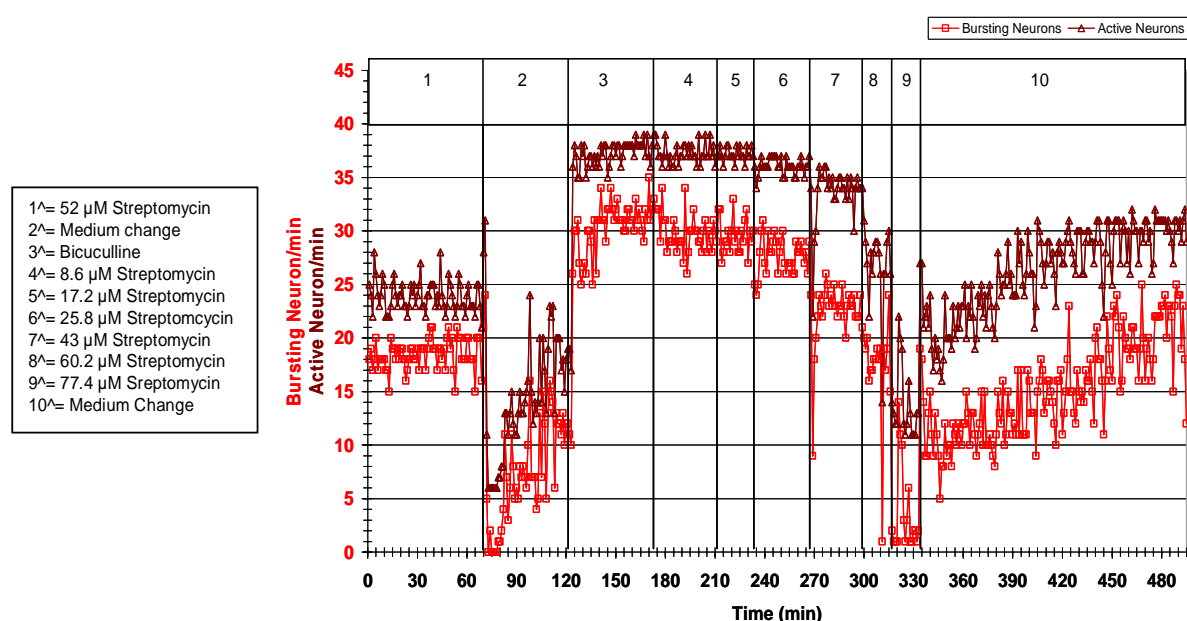


Figure 12. Number of active neurons versus bursting neurons per minute ($n=50$) under the influence of different streptomycin concentrations in μM and intermittent media changes. Volume of streptomycin solutions added ranged from 20 μl to 100 μl to a total bath volume of 2000 μl .

A comparison between the level of active neurons and the level of bursting neurons after addition of an antibiotic provided information about the grade of functional toxicity of applied compound. The application of streptomycin and vancomycin in IC_{50} concentrations showed a higher loss of bursting neurons than active neurons. IC_{50} concentrations of pen/strep and gentamicin caused a higher level of bursting neurons compared to the level of active neurons. The application of penicillin G in IC_{50} concentrations led to a slight loss of bursting neurons while the number of active neurons slightly increased (Table 3).

4 Discussion

The utilization of mammalian neuronal networks on microelectrode arrays is an emerging method to screen new compounds, investigate their impact on neuronal networks and define therapeutic windows in vitro, as a first step for further animal studies. An optimization and standardization of applied doses ensures a safer use of these drugs.

The screening of well-established compounds like antibiotics seems to be unessential at first glance as they are already widely applied in neurosurgery. Thereby the intravenous or local administration of antibiotics is part of the prophylactic, peri-operative and post-operative therapy. However a differentiation between cytotoxicity and functional toxicity has to be drawn. Neuronal networks only operate effectively when the inter-cellular transmittance of electrical signals is assured. Action potentials are generated in the axon hillock forwarded to the synaptic gap where released neurotransmitter result in a depolarization or hyperpolarization potential in the dendrite of the target cell. This simplified description is the basic mechanism for signal transmittance between neurons within a neuronal network and is the foundation for the maintenance of body functions. Cytotoxicity of drugs implicates the damage of cells and can be measured by, for instance, the MTT, WST or NRU-Test. Experiments with mammalian neuronal networks on microelectrode arrays have clearly shown that while the cytotoxic concentration of applied compounds is not yet reached, there is a concentration range where neurons loose their ability to generate action potentials and to transmit information within the network. This loss of neuronal functionality is a grey area which needs to be further investigated as the local application of antibiotics in neurosurgery is a common practice following therapeutic doses which are not neurotoxic yet, but might bear the risk of functional toxicity.

In the present work the antibiotics penicillin G, pen/strep, streptomycin, gentamicin and vancomycin were studied for functional toxicity on mammalian neurons being part of a neuronal network. These neuronal ensembles cultured on microelectrode arrays reflect more relevant physiological information than conventional in vitro pharmacological models. Studied antibiotics showed conformity in suppressing the action potential production during concentration increase observed by a step-wise decrease in spikes and bursts after compound addition. Obtained dose response curves corroborate this observation, demonstrating a decrease of percent mean spike activity under rising compound concentrations. Identified IC_{50} values demonstrated that a differentiation of applied antibiotics in terms of dose response has to be drawn. While the IC_{50} is already reached at 37 μM under streptomycin, gentamicin is well tolerated in terms of neuronal activity showing an IC_{50} value of 2371 μM . The average

IC₅₀ value of the combination of penicillin and streptomycin at 775 μ M corroborates the IC₅₀ value identification of the two separate studied compounds as penicillin G shows an IC₅₀ value at 1205 μ M. The expectation of an IC₅₀ value in the middle of those of streptomycin and penicillin was fulfilled. Vancomycin showed an average IC₅₀ value similar to penicillin G at 1322 μ M.

The impact of individual antibiotics on the burst parameters of cultures in particular the change of burst rate, burst period and spikes in burst under IC₅₀ concentrations compared to untreated cultures showed a complex pattern. An overall tendency of burst period increase and spikes in burst increase apart from gentamicin and penicillin G was observed whereas the burst rate apart from investigations under streptomycin and gentamicin maintained quite stable.

The gap between levels of active neurons and levels of bursting neurons is an important consideration when studying the functional toxicity of compounds. The number of neurons being active does not automatically give information about the condition of these neurons in regard to their functionality. The addition of compounds can rather lead to the loss of functionality in regard to information transmittance while conserving life functions. Common life/death assays do not provide information about this phenomenon. Concentrations considered to be non toxic may turn out to be suppressive against information transmittance within the neuronal network and therefore knock out important downstream body functions.

While streptomycin and vancomycin showed a higher gap under IC₅₀ concentrations between the level of bursting neurons maintained and the level of active neurons maintained, pen/strep and gentamicin demonstrated the opposite effect. By contrast penicillin G showed no explicit impact on the relation between the level of bursting neurons and the level of active neurons. Referred to individual IC₅₀ values, streptomycin and vancomycin showed the highest functional toxicity followed by penicillin G, gentamicin and pen/strep.

5 Conclusions

In this study we demonstrated an approach to in vitro characterize individual antibiotics for functional neurotoxicity. The utilization of mammalian neuronal networks on microelectrode arrays was therefore a good method for the investigation of compounds close to physiological conditions. New data on dose response, IC₅₀ concentrations and the impact on the neuronal activity pattern could be obtained for an advanced understanding of how antibiotics influence the information transmittance in neuronal ensembles. This in vitro microelectrode recording

system could be used for the investigation of the impact of analgesics, anaesthetic and narcotics on neuronal clusters, which is an interesting subject for future studies.

6 Acknowledgements

We would like to thank the University Hospital “Klinikum r. d. Isar München”, Institut für Experimentelle Onkologie und Therapieforschung” and the University of North Texas, Center for Neuronal Network Science for enabling this cooperation. The authors did not receive any payments or benefits from a commercial party related directly or indirectly related to the subject of this article. This work was partially funded by a grant from the “Bayerische Forschungsstiftung”.

7 Appendix

7.1 Activity pattern of antibiotics

7.1.1 Penicillin G

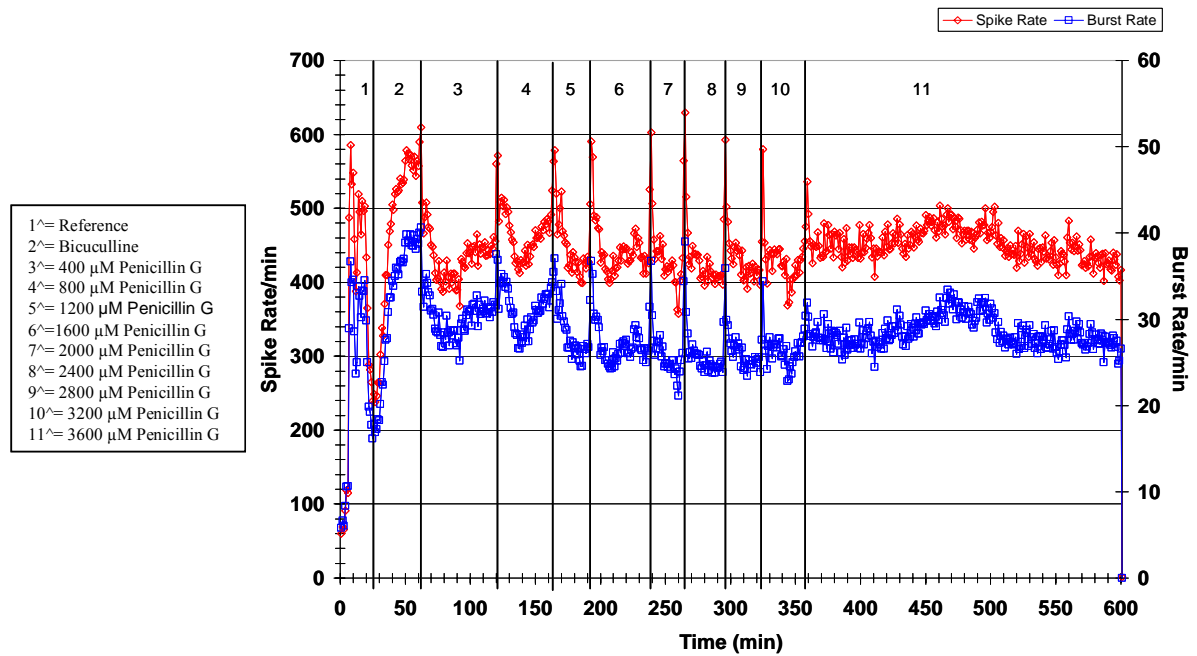


Figure 13. Change of spike rates and burst rates (n=68 units) under increasing penicillin G concentrations. Volume of penicillin G solutions added averaged for each step at 40 μ l to a total bath volume of 2000 μ l.

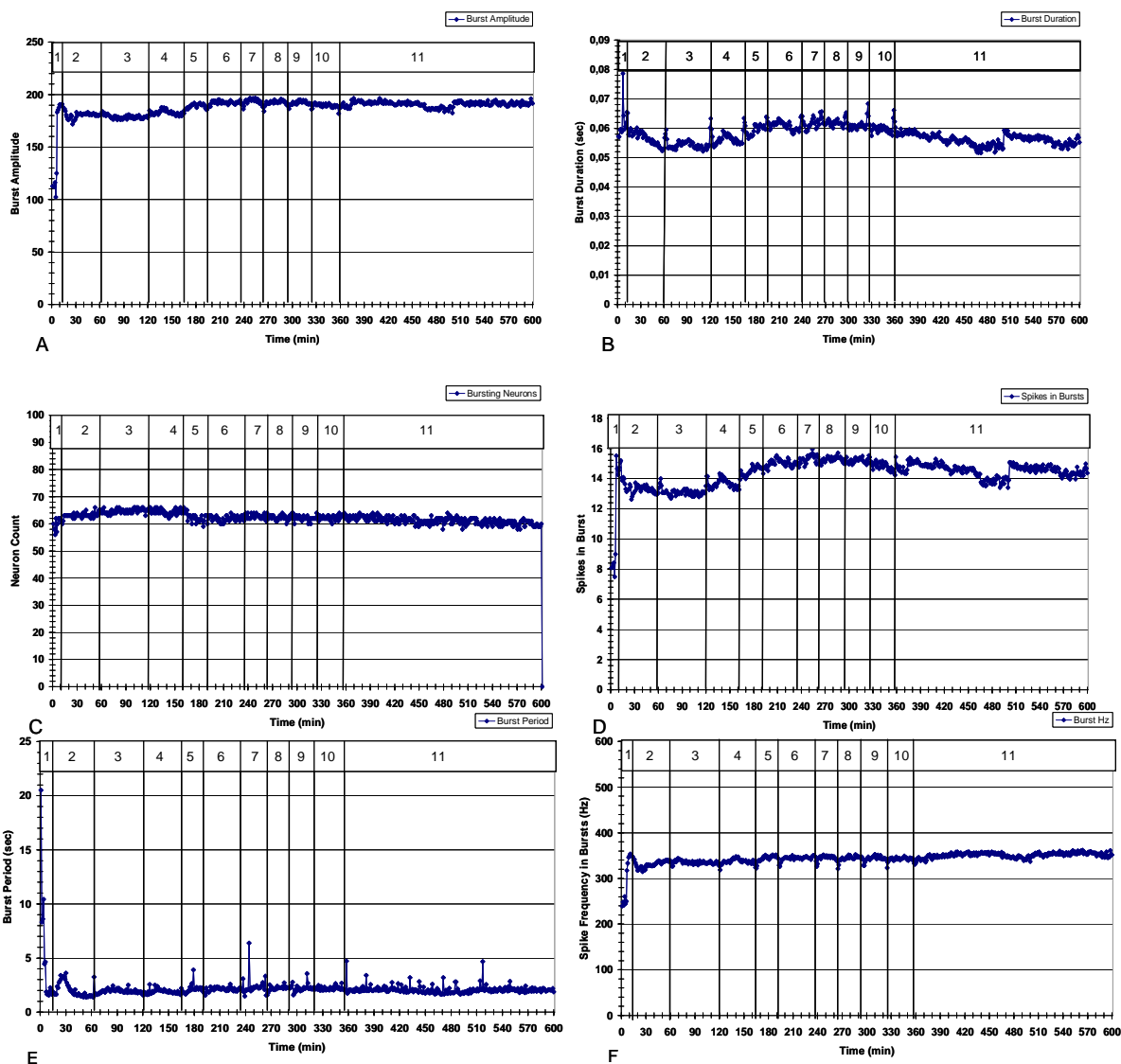


Figure 14A – 14F. Change of burst parameters: A) burst amplitude, B) burst duration, C) bursting neurons, D) spikes in bursts, E) burst period, F) Burst Hz - under the influence of penicillin G (n=68 units). Volume of penicillin G solutions added averaged for each step at 40 μ l to a total bath volume of 2000 μ l. All variables are mean values derived from averaging all burst measurement per minute across all units.

1[^]= reference, 2[^]= bicuculline, 3[^]= 400 μ M penicillin G, 4[^]= 800 μ M penicillin G, 5[^]= 1200 μ M penicillin G, 6[^]= 1600 μ M penicillin G, 7[^]= 2000 μ M penicillin G, 8[^]= 2400 μ M penicillin G, 9[^]= 2800 μ M penicillin G, 10[^]= 3200 μ M penicillin G, 11[^]= 3600 μ M penicillin G

7.1.2 Penicillin G/Streptomycin

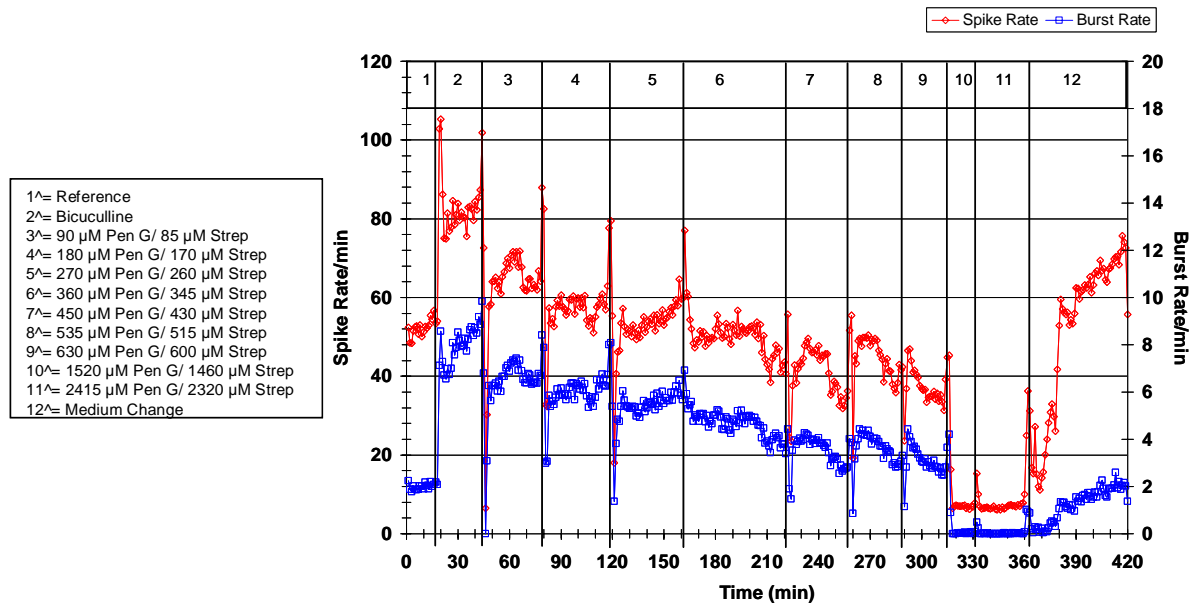
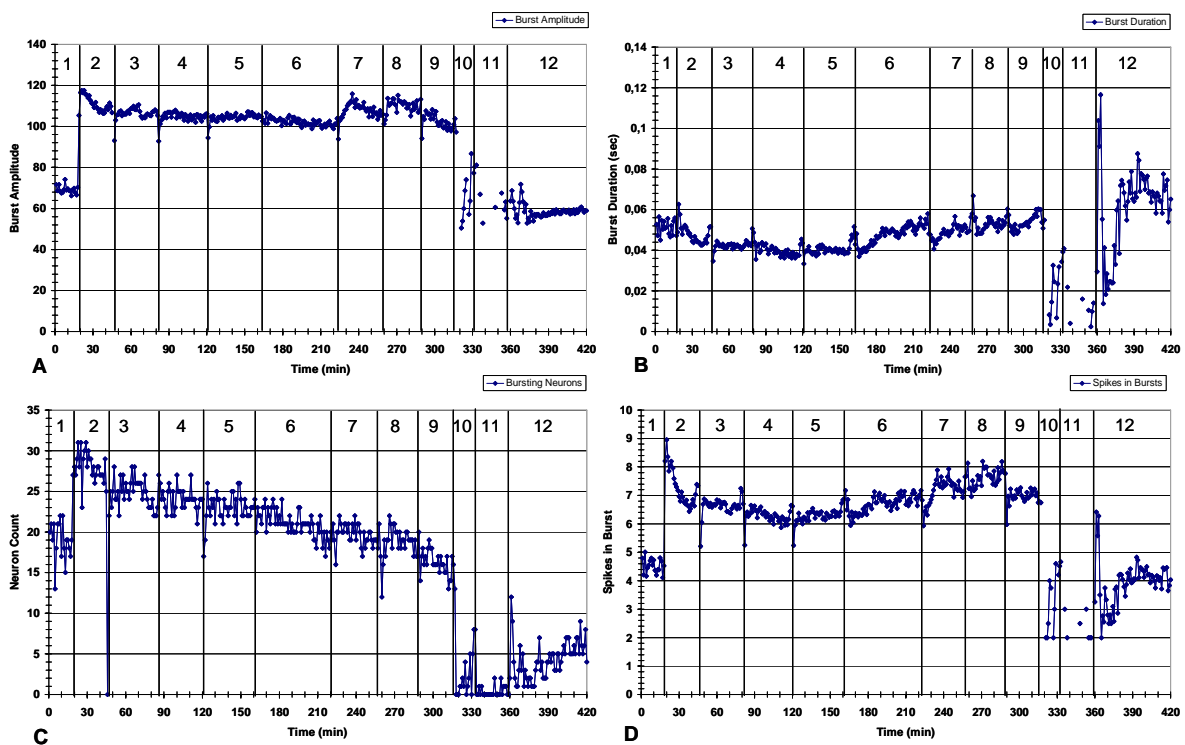


Figure 15. Step-wise decrease of spike rates and burst rates (n=69 units) under increasing pen/strep concentrations with reversibility after medium change. Volume of pen/strep solutions added ranged from 20 μ l to 100 μ l to a total bath volume of 2000 μ l.



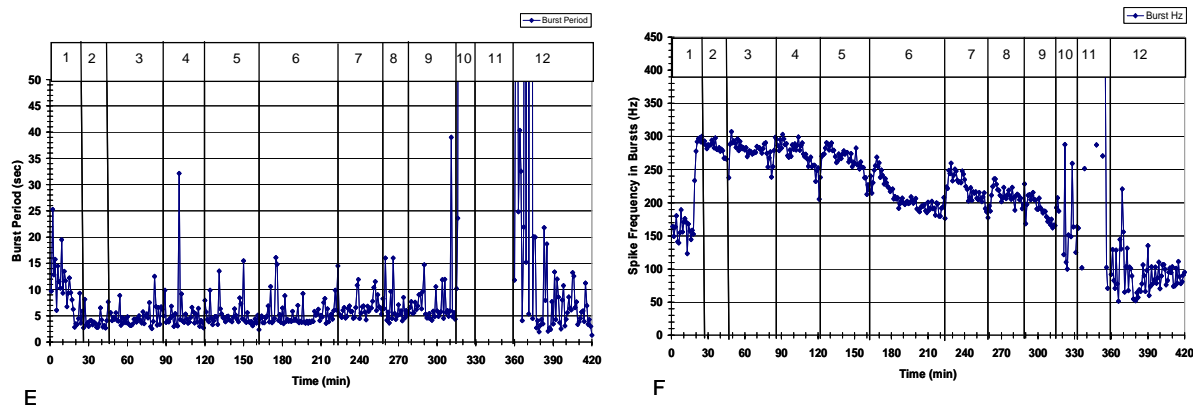


Figure 16A – 16F. Change of burst parameters: A) burst amplitude, B) burst duration, C) bursting neurons, D) spikes in bursts, E) burst period, F) Burst Hz - under the influence of pen/strep (n=69 units) followed by a medium change. Volume of pen/strep solutions added ranged from 20 μ l to 100 μ l to a total bath volume of 2000 μ l. All variables are mean values derived from averaging all burst measurement per minute across all units.

1 \wedge = 90 μ M pen G/ 85 μ M strep, 2 \wedge = 180 μ M pen G/ 170 μ M strep, 3 \wedge = 270 μ M pen G/ 260 μ M strep, 4 \wedge = 360 μ M pen G/ 345 μ M strep, 5 \wedge = 450 μ M pen G/ 430 μ M strep, 6 \wedge = 540 μ M pen G/ 515 μ M strep, 7 \wedge = 625 μ M pen G/ 600 μ M strep, 8 \wedge = 1520 μ M pen G/ 1460 μ M strep, 9 \wedge = 2415 μ M pen G/ 2320 μ M strep

7.1.3 Streptomycin

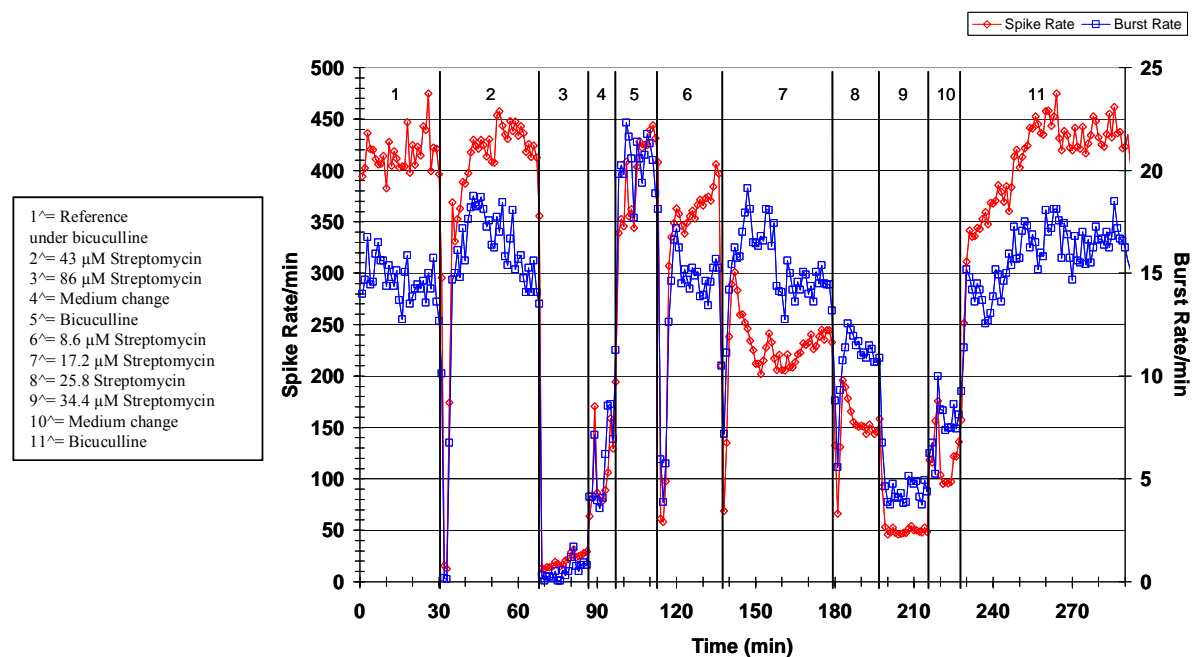


Figure 17. Change of spike rates and burst rates (n=16 units) under increasing streptomycin concentrations with reversibility after medium change. Volume of streptomycin solutions added ranged from 20 μ l to 100 μ l to a total bath volume of 2000 μ l.

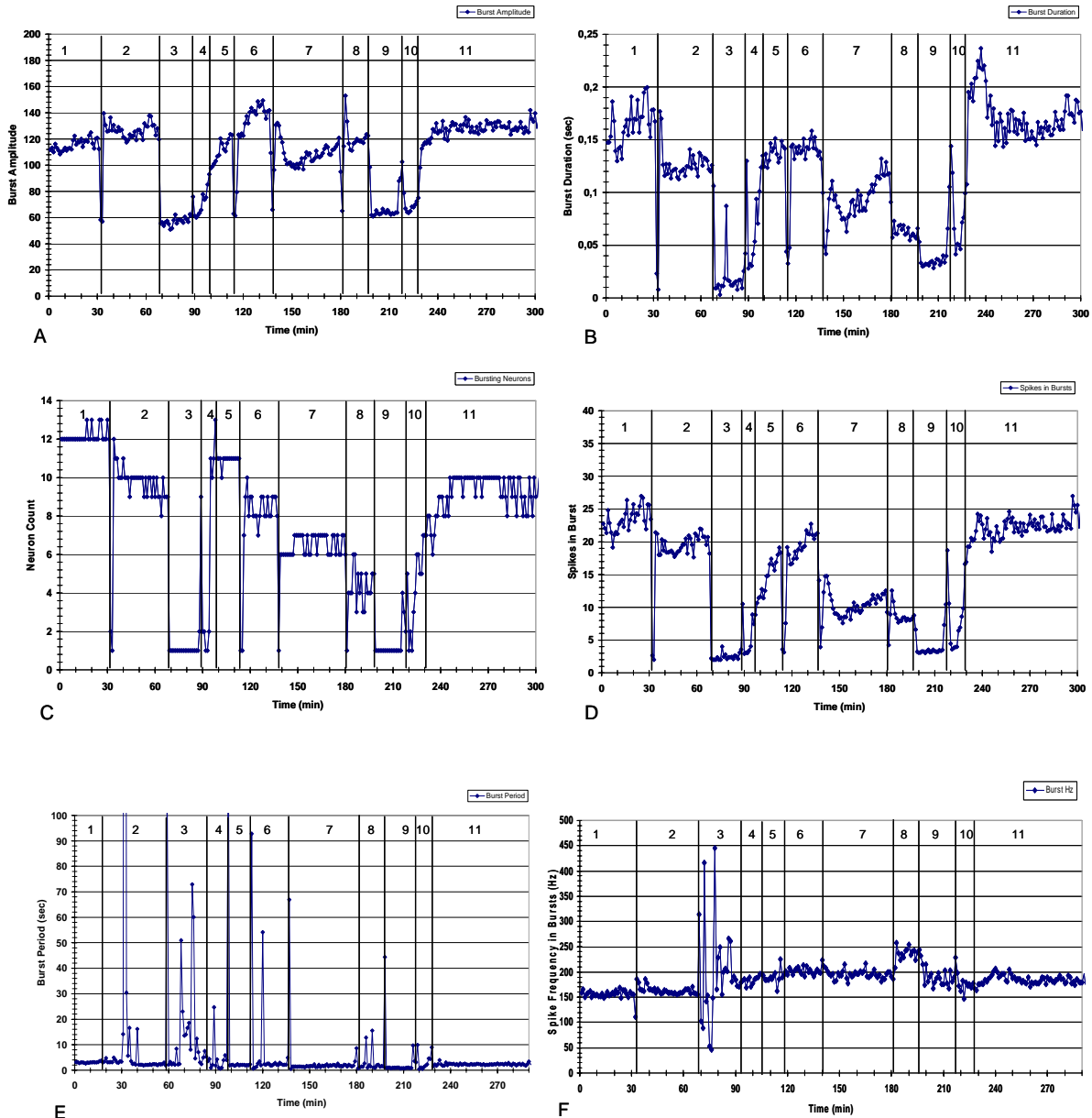


Figure 18A – 18F. Change of burst parameters: A) burst amplitude, B) burst duration, C) bursting neurons, D) spikes in bursts, E) burst period, F) Burst Hz - under the influence of streptomycin (n=16 units) followed by a medium change. Volume of streptomycin solutions added ranged from 20 μ l to 100 μ l to a total bath volume of 2000 μ l. All variables are mean values derived from averaging all burst measurement per minute across all units.

1^=reference under bicuculline, 2^= 43 μ M streptomycin, 3^= 86 μ M streptomycin, 4^= medium change, 5^= bicuculline, 6^= 8.6 μ M streptomycin, 7^= 17.2 μ M streptomycin, 8^= 25.8 μ M streptomycin, 9^= 34.4 μ M streptomycin, 10^= medium change, 11^= bicuculline

7.1.4 Gentamicin

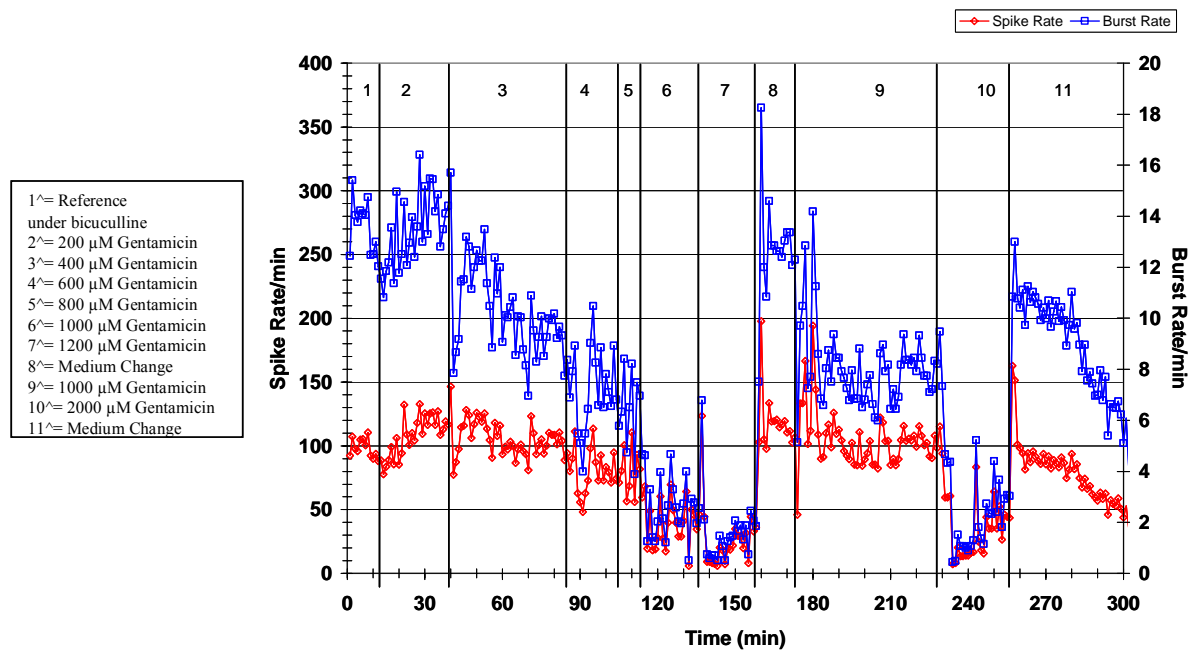
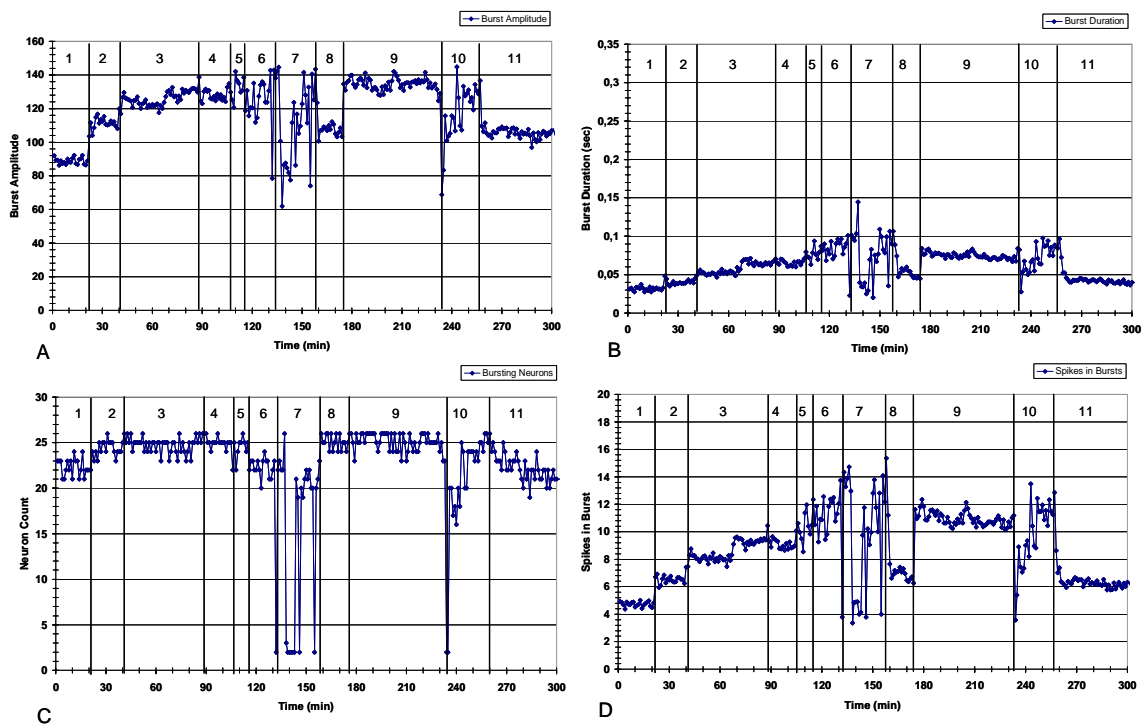


Figure 19. Change of spike rates and burst rates (n=27 units) under increasing gentamicin concentrations with reversibility after medium change. Volume of gentamicin solutions added ranged from 20 µl to 40 µl to a total bath volume of 2000 µl.



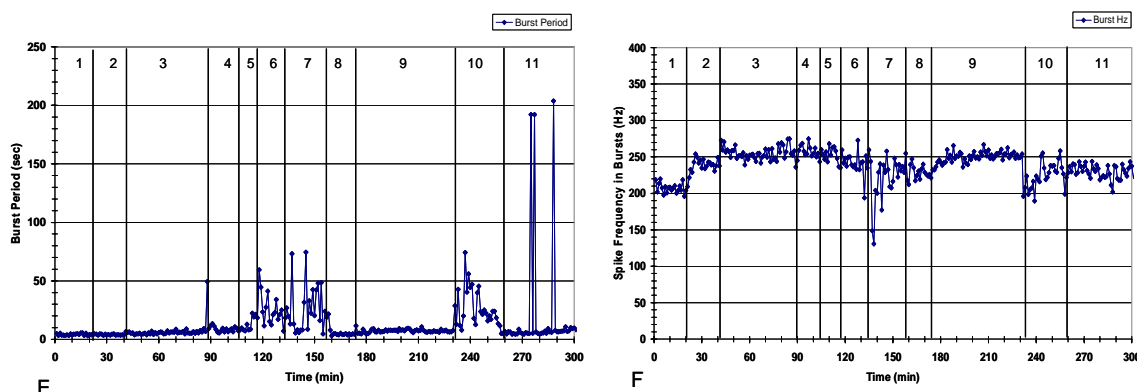


Figure 20A – 20F. Change of burst parameters: A) burst amplitude, B) burst duration, C) bursting neurons, D) spikes in bursts, E) burst period, F) Burst Hz - under the influence of pen/strep (n=27 units) followed by a medium change. Volume of gentamicin solutions added ranged from 20 μ l to 40 μ l to a total bath volume of 2000 μ l. All variables are mean values derived from averaging all burst measurement per minute across all units.

1 $^{\wedge}$ = reference under bicuculline, 2 $^{\wedge}$ = 200 μ M gentamicin, 3 $^{\wedge}$ = 400 μ M gentamicin, 4 $^{\wedge}$ = 600 μ M gentamicin, 5 $^{\wedge}$ = 800 μ M gentamicin, 6 $^{\wedge}$ = 1000 μ M gentamicin, 7 $^{\wedge}$ = 1200 μ M gentamicin, 8 $^{\wedge}$ = medium change, 9 $^{\wedge}$ =1000 μ M gentamicin, 10 $^{\wedge}$ = 2000 μ M gentamicin, 11 $^{\wedge}$ = medium change

7.1.5 Vancomycin

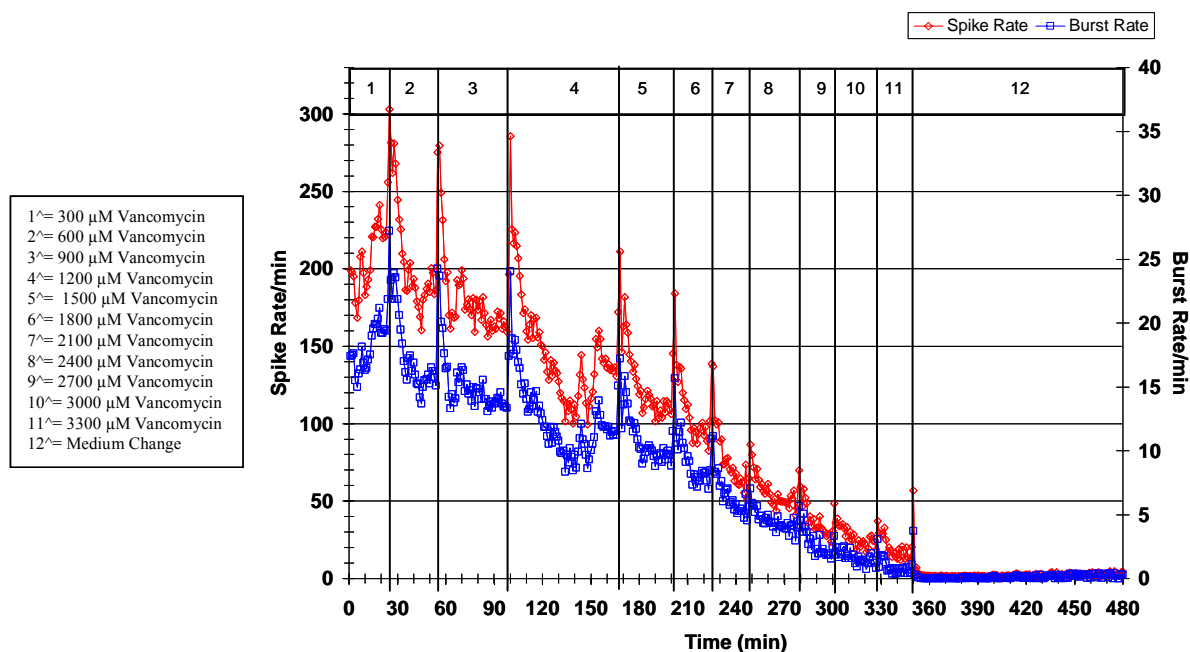


Figure 21. Change of spike rates and burst rates (n=23 units) under increasing vancomycin concentrations followed by a medium change. Volume of vancomycin solutions added averaged at 60 μ l to a total bath volume of 2000 μ l.

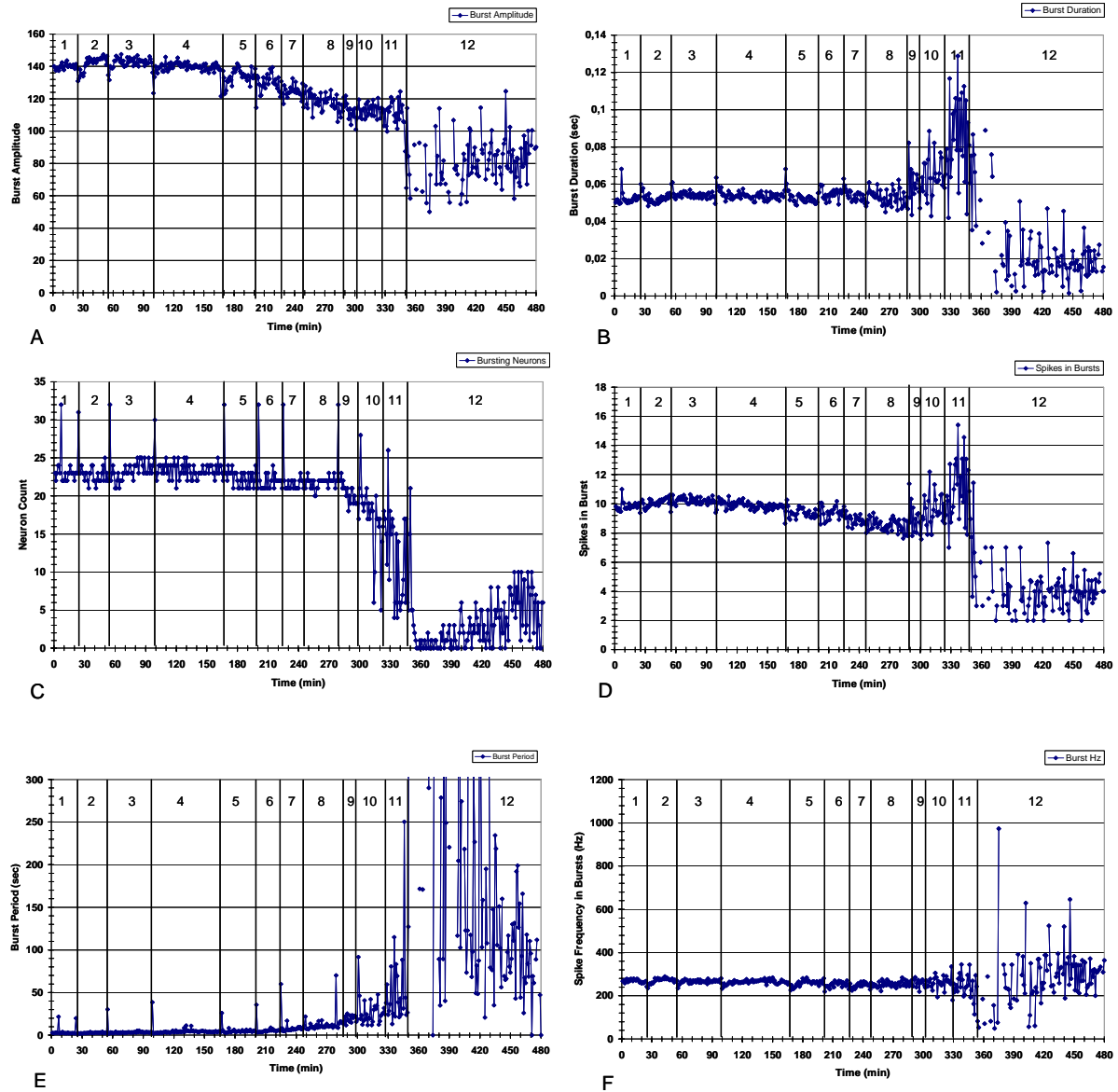


Figure 22A – 22F. Change of burst parameters: A) burst amplitude, B) burst duration, C) bursting neurons, D) spikes in bursts, E) burst period, F) Burst Hz - under the influence of vancomycin (n=23 units) followed by a medium change. Volume of vancomycin solutions added averaged at 60 μ l to a total bath volume of 2000 μ l. All variables are mean values derived from averaging all burst measurement per minute across all units.

1 \wedge = 300 μ M vancomycin, 2 \wedge = 600 μ M Strep, 3 \wedge = 900 μ M vancomycin, 4 \wedge = 1200 μ M vancomycin, 5 \wedge = 1500 μ M vancomycin, 6 \wedge = 1800 μ M vancomycin, 7 \wedge = 2100 μ M vancomycin, 8 \wedge = 2400 μ M vancomycin, 9 \wedge = 2700 μ M vancomycin, 10 \wedge = 3000 μ M vancomycin, 11 \wedge = 3300 vancomycin, 12 \wedge = medium change

8 Figure and Table Captions

Figure 1. Preparation procedure of the neuronal cell cultures

Figure 2. Experimental setup to study neuronal networks on multielectrode neurochips.

Figure 3. Activity pattern change of frontal cortex network. Each action potential is represented by a vertical tick. Several neurons can be recorded by one electrode and separated online by a software. Action potentials generated by a 64 electrode recording matrix 21 days in vitro.

Figure 4. Time stamp sequence of a discriminated unit and mathematically simulated RC integration.

Figure 5. Change of spike rates and burst rates ($n=68$ units) under increasing penicillin G concentrations. Volume of penicillin G solutions added averaged at 40 μl to a total bath volume of 2000 μl .

Figure 6A – 6C. Dose Response curves of streptomycin generated in three individual experiments.

Figure 7A/B. Dose Response curves of pen/strep generated in two individual experiments.

Figure 8A/B. Dose Response curves of gentamicin generated in two individual experiments.

Figure 9A – 9D. Dose Response curves of vancomycin generated in four individual experiments.

Figure 10A – 10D. Concentration/activity change dependence under penicillin in four individual experiments: 10 A) – 10 C) under bicuculline, 10 D) without bicuculline.

Figure 11. The change of burst frequency values under the influence of pen/strep followed by a media change.

Figure 12. Number of active neurons versus bursting neurons per minute (n=50) under the influence of different streptomycin concentrations in [μM] and intermittent media changes. Volume of streptomycin solutions added ranged from 20 μl to 100 μl to a total bath volume of 2000 μl .

Figure 13. Change of spike rates and burst rates (n= 68 units) under increasing penicillin G concentrations. Volume of penicillin G solutions added averaged at 40 μl to a total bath volume of 2000 μl .

Figure 14A – 14F. Change of burst parameters: A) burst amplitude, B) burst duration, C) bursting neurons, D) spikes in bursts, E) burst period, F) Burst Hz - under the influence of penicillin G (n= 68 units). Volume of penicillin G solutions added averaged at 40 μl to a total bath volume of 2000 μl . All variables are mean values derived from averaging all burst measurement per minute across all units.

Figure 15. Step-wise decrease of spike rates and burst rates (n= 69 units) under increasing pen/strep concentrations with reversibility after medium change. Volume of pen/strep solutions added ranged from 20 μl to 100 μl to a total bath volume of 2000 μl .

Figure 16A – 16F. Change of burst parameters: A) burst amplitude, B) burst duration, C) bursting neurons, D) spikes in bursts, E) burst period, F) Burst Hz - under the influence of pen/strep (n= 69 units) followed by a medium change. Volume of pen/strep solutions added ranged from 20 μl to 100 μl to a total bath volume of 2000 μl . All variables are mean values derived from averaging all burst measurement per minute across all units.

Figure 17. Change of spike rates and burst rates (n= 16 units) under increasing streptomycin concentrations with reversibility after medium change. Volume of streptomycin solutions added ranged from 20 μl to 100 μl to a total bath volume of 2000 μl .

Figure 18A – 18F. Change of burst parameters: A) burst amplitude, B) burst duration, C) bursting neurons, D) spikes in bursts, E) burst period, F) Burst Hz - under the influence of pen/strep (n= 16 units) followed by a medium change. Volume of pen/strep solutions added ranged from 20 μl to 100 μl to a total bath volume of 2000 μl . All variables are mean values derived from averaging all burst measurement per minute across all units.

Figure 19. Change of spike rates and burst rates (n= 27 units) under increasing gentamicin concentrations with reversibility after medium change. Volume of gentamicin solutions added ranged from 20 μ l to 40 μ l to a total bath volume of 2000 μ l.

Figure 20A – 20F. Change of burst parameters: A) burst amplitude, B) burst duration, C) bursting neurons, D) spikes in bursts, E) burst period, F) Burst Hz - under the influence of pen/strep (n= 27 units) followed by a medium change. Volume of gentamicin solutions added ranged from 20 μ l to 40 μ l to a total bath volume of 2000 μ l. All variables are mean values derived from averaging all burst measurement per minute across all units.

Figure 21. Change of spike rates and burst rates (n= 23 units) under increasing vancomycin concentrations followed by a medium change. Volume of vancomycin solutions added averaged at 60 μ l to a total bath volume of 2000 μ l.

Figure 22A – 22F. Change of burst parameters: A) burst amplitude, B) burst duration, C) bursting neurons, D) spikes in bursts, E) burst period, F) Burst Hz - under the influence of vancomycin (n= 23 units) followed by a medium change. Volume of vancomycin solutions added averaged at 60 μ l to a total bath volume of 2000 μ l. All variables are mean values derived from averaging all burst measurement per minute across all units.

Table 1. IC₅₀ values of individual antibiotics.

Table 2. Levels of burst rate, burst period and spikes in burst of individual antibiotics defined as the quotient between burst rate, burst period or spikes in burst values under IC₅₀ concentrations and values under medium change.

Table 3. Levels of bursting neurons and active neurons of individual antibiotics defined as the quotient between bursting neuron or active neuron values under IC₅₀ concentrations and values under medium change.

9 References

1. **Broggi, G., A. Franzini, D. Peluchetti, and D. Servello.** 1985. Treatment of deep brain abscesses by stereotactic implantation of an intracavitary device for evacuation and local application of antibiotics. *Acta Neurochir (Wien)* **76**:94-8.
2. **Gramowski, A., K. Jugelt, S. Stuwe, R. Schulze, G. P. McGregor, A. Wartenberg-Demand, J. Looock, O. Schroder, and D. G. Weiss.** 2006. Functional screening of traditional antidepressants with primary cortical neuronal networks grown on multielectrode neurochips. *Eur J Neurosci* **24**:455-65.
3. **Gramowski, A., K. Jugelt, D. G. Weiss, and G. W. Gross.** 2004. Substance identification by quantitative characterization of oscillatory activity in murine spinal cord networks on microelectrode arrays. *Eur J Neurosci* **19**:2815-25.
4. **Gross, G. W., A. Harsch, B. K. Rhoades, and W. Gopel.** 1997. Odor, drug and toxin analysis with neuronal networks in vitro: extracellular array recording of network responses. *Biosens Bioelectron* **12**:373-93.
5. **Gross, G. W., B. K. Rhoades, H. M. Azzazy, and M. C. Wu.** 1995. The use of neuronal networks on multielectrode arrays as biosensors. *Biosens Bioelectron* **10**:553-67.
6. **Gross, G. W., B. K. Rhoades, D. L. Reust, and F. U. Schwalm.** 1993. Stimulation of monolayer networks in culture through thin-film indium-tin oxide recording electrodes. *J Neurosci Methods* **50**:131-43.
7. **Gross, G. W., E. Rieske, G. W. Kreutzberg, and A. Meyer.** 1977. A new fixed-array multi-microelectrode system designed for long-term monitoring of extracellular single unit neuronal activity in vitro. *Neuroscience Letters* **6**:101-105.
8. **Gross, P. G., L. P. Weiner, E. P. Kartalov, and A. Scherer.** 2005. Microfluidic techniques for studying the nervous system. *Crit Rev Neurobiol* **17**:119-44.
9. **Holdiness, M. R.** 1987. Neurological manifestations and toxicities of the antituberculosis drugs. A review. *Med Toxicol* **2**:33-51.
10. **Holubar, J.** 1965. Mode of activation of the mirror focus initiated by local penicillin application to the contralateral cerebral cortex in rats. *Physiol Bohemoslov* **14**:509-14.
11. **Kala, M., and M. Houdek.** 1993. Local application of antibiotics in treatment of cerebral abscess. *Acta Univ Palacki Olomuc Fac Med* **136**:45-7.
12. **Kharitonova, K. I., E. N. Rodiukova, A. E. Simonovich, and V. V. Stupak.** 1990. [The experimental and clinical use of gelatin sponges with kanamycin and gentamycin for the prevention and treatment of suppurative complications in neurosurgery]. *Zh Vopr Neurokhir Im N N Burdenko*:9-11.
13. **Morefield, S. I., E. W. Keefer, K. D. Chapman, and G. W. Gross.** 2000. Drug evaluations using neuronal networks cultured on microelectrode arrays. *Biosens Bioelectron* **15**:383-96.
14. **Selimoglu, E.** 2007. Aminoglycoside-induced ototoxicity. *Curr Pharm Des* **13**:119-26.
15. **Selinger, J. V., J. J. Pancrazio, and G. W. Gross.** 2004. Measuring synchronization in neuronal networks for biosensor applications. *Biosens Bioelectron* **19**:675-83.
16. **Turnbull, L., E. Dian, and G. Gross.** 2005. The string method of burst identification in neuronal spike trains. *J Neurosci Methods* **145**:23-35.

Chapter 8

Summary of the thesis

1 General introduction

The objective of this thesis was to study new strategies to prevent post-operative medical device-associated infections and new concepts for the on demand treatment of already manifested medical device-associated infections. Chapter 1 provides a general introduction into the classification of biomaterials with the focus on vascular grafts and surgical sutures. The complex process of infection is highlighted and in particular, post-operative, neuronal and medical device-associated infections are discussed. The key events initiating biomaterial-associated infection are the adherence of pathogens like *Staphylococcus aureus* or *Staphylococcus epidermidis* on the surface of biomaterials and the subsequent biofilm formation triggered by quorum sensing signals controlling the complex structure of biofilm communities. Biofilm phenotypic pathogens show an increased antibiotic and host defence resistance presenting a major challenge for a successful treatment of device-related infections. Today graft explantation in combination with the pre-, peri and postoperative administration of antibiotics and antiseptics is surgical goldstandard.

2 The anti-infective equipment and characterization of PTFE grafts for the prevention of post-operative infection

In chapter 2 commercially available PTFE grafts were equipped with various biodegradable drug delivery systems and characterized for drug release, anti-infective potency, biocompatibility and haemocompatibility. PTFE grafts with a diameter of 6 mm were coated with gentamicin and teicoplanin incorporated in different lipid-like carriers under aseptic conditions with a dipping method. Poly-D, L-lactic acid, tocopherol acetate, the diglyceride Softisan[®] 649 and the triglyceride Dynasan[®] 118 were used as drug carriers. All coatings showed an initial drug burst followed by a low continuous drug release within 96 hours. Release kinetics depended on the carrier used. In pathologically relevant bacterial concentrations, the developed drug-carrier coatings achieved a bacterial eradication rate of 100 %. This shows a highly effective potency against *S. aureus* colonization. Even in a

concentration hundredfolds beyond maximal pathologically relevant bacterial concentration, *S. aureus* growth could strongly be reduced after 24 hours by each of the developed drug-carrier coatings. Coatings with incorporated teicoplanin showed an insignificant smaller growth inhibition effect than coatings with gentamicin. Bacterial adhesion after 24 hours of incubation in a 2×10^6 cfu/ml *S. aureus* suspension could effectively be reduced by drug-carrier-coated prostheses compared to uncoated ones. Different cytotoxic levels investigated with the cell proliferation assay WST 1 with fibroblasts L929 from mouse connective tissue could be observed bringing up tocopherol acetate as the most promising biocompatible carrier. Tests with oil red O reagent show that the diglyceride Softisan[®] 649 is incorporated in the cell soma which apparently leads to cell death. In order to assess haemocompatibility, tromboelastography studies, ELISA assays and an amidolytic substrate assay to detect markers of the activated coagulation and complement system were carried out. Excellent haemocompatible characteristics of all coatings were assessed. The development and in vitro studies of described biodegradable drug delivery systems highlighted the most important requirements for an effective as well as compatible anti-infective equipment of PTFE grafts. Through continuous local release, high drug levels can be obtained at only the targeted area, demonstrating that bacterial proliferation can completely be inhibited while at the same time biocompatibility as well as haemocompatibility can be ensured.

3 Anti-infective coatings of surgical sutures based on a combination of antiseptics and fatty acids

The anti-infective equipment of commercially available PGA surgical sutures was subject of chapter 3. Synthetic absorbable PGA surgical sutures were antimicrobially equipped with one type of chlorhexidine dipalmitate coating, two types of chlorhexidine dilaurate coatings and two types of octenidine hydrochloride coatings. For octenidine hydrochloride the fatty acid palmitic acid was used as drug carrier. Within one coating type, coatings differed only in the drug weight per unit length. Suture coating was performed by dip-coating procedures. Individual anti-infective coatings were characterized by drug release, anti-infective characteristics and biocompatibility studies. Drug release studies showed a continuous drug release in PBS at 37 °C within 96 hours which is a basic requirement for an effective anti-infective protection. The gap between the amount of released drug after 96 hours and the

remaining drug amount on the surface of developed sutures revealed a high potential for a long-term anti-infective protection in the body.

A reduction of the number of adhered pathogens on the suture surface as well as the inhibition of *S. aureus* growth in suspension was assessed by all investigated coating types. All chlorhexidine and octenidine coated sutures showed superior anti-infective characteristics in comparison to the clinically well-established Vicryl Plus[®]. Biocompatibility studies revealed a higher cytotoxic potential of developed suture coatings than Vicryl Plus[®].

We conclude that developed anti-infective suture coatings consisting of lipid based drug delivery systems in combination with antiseptics are highly effective against bacterial colonization in vitro, however antiseptic doses have to be adjusted to comply with biocompatibility.

4 Growth inhibition of *Staphylococcus aureus* induced by low-frequency electric and electro-magnetic fields

In many areas of medicine as for example in the magnet resonance tomography or the magnetic stimulation of brain areas strong magnetic fields are applied. In therapeutic procedures magnetic field therapy is often used for the improvement of bone fracture healing. The so-called Kraus-Lechner procedure is based on the interaction of low-frequency nonthermal sinusoidal electro-magnetic fields with bone and cartilage tissue and it is often applied to badly healing bone fractures of non-unions. Clinical observations have shown that in infected pseudarthrosis this technology improves bone healing and decreases bone infections. Nowadays there are no data of low-frequent electromagnetic fields based on the Kraus-Lechner techniques and similar electric fields on the influence on bacterial growth. Methodical investigations of the effect of different kinds of applied fields on bacterial growth have not been elucidated before as previous studies mostly focused on one specific electric or electromagnetic field effect.

The study of chapter 4 focused on the impact of different electric and electromagnetic fields on the growth of *S. aureus* by in vitro technologies as a new perspective for the treatment of device-associated infections. Cultures of *S. aureus* in fluid and gel-like media were exposed to a low-frequency electromagnetic field, an electromagnetic field combined with an additional electric field, a sinusoidal electric field and a static electric field.

In gel-like media no significant difference between colony-forming units of exposed samples and non-exposed references was detected. In contrast to these data, all four applied fields

revealed a significant effect on growth of *S. aureus* in fluid media within the observation period of 24 hours. Depending on the applied field growth inhibition from 18 % using a sinusoidal electric field (470 mV/cm, 20 Hz) and 37 % using a constant electric field (588 mV/cm) could be observed. These investigations demonstrated a reduction of *S. aureus* growth in fluid media under field influence within 24 hours. Observations about the influence of low-frequency electromagnetic fields on bacterial growth corroborate data in clinical situations of bone infections during magnetic field therapy and is of high interest for the treatment of medical device-associated infections.

5 The investigation of the influence of low-frequency electromagnetic fields on antibiotic susceptibility of *Staphylococcus aureus*

The aim of chapter 5 was to increase antibiotic susceptibility of *S. aureus* by the application of low-frequency electromagnetic fields as a new perspective for the on demand treatment of already manifested medical device-associated infections. Cultures of *S. aureus* in fluid and gel-like media in presence of gentamicin were exposed to a low-frequency electro-magnetic field, an electro-magnetic field combined with an additional electric field, a sinusoidal alternating electric field and a direct current electric field.

No significant difference between sample and reference was detected in gel-like media. Low dose gentamicin application corresponding to 0.25 MIC under the influence of the four applied fields showed a statistically significant bacterial growth inhibition effect in fluid media. Depending on the type of field applied, an improvement of gentamicin efficacy from 32 % using a clinically applied electromagnetic field (5 mT, 20 Hz) up to 92 % using a direct current field of 588 mV/cm was observed.

In general, we have been able to demonstrate an additional statistically significant reduction of *S. aureus* growth in the presence of gentamicin under the influence of all applied fields in fluid media. The strongest effect of augmented gentamicin efficacy could be shown by the application of the direct current field. We assume that this effect is caused by electrolysis-induced radicals. Formed hydroxyl and oxygen radicals are known to destroy cell membranes of bacteria. This so-called bioelectric effect may facilitate the penetration of antibiotic drugs and could be an explanation for the detected efficacy augmentation of gentamicin. We conclude that the combination of antibiotic treatment with low-frequency electro-magnetic fields could offer new therapeutic strategies in biomaterial-associated infection therapy.

6 Magnetic drug targeting for biomaterial infections

In chapter 6 new antimicrobially equipped ultra-small superparamagnetic iron oxides (USPIO) were developed and characterized. The antimicrobial equipment of USPIOs institutes the possibility to enrich high antibiotic concentrations on the surface of vascular grafts with the help of a magnetic drug targeting system. These USPIOs usually consist of an iron oxide (Fe_3O_4) core surrounded by an organic shell like dextrans, fatty acids or starch molecules. The antibiotic gentamicin was ionically and covalently linked to the organic shell. Individual USPIOs were characterized and compared among each other. All gentamicin-functionalized nanoparticles did not show drug release in PBS at 37 °C within 90 minutes. Selected coated nanoparticles reduced *S. aureus* growth even beyond pathologically relevant concentrations within 24 hours. Excellent concentration-independent biocompatibility was assessed for ferrofluids of choice. The enrichment of developed USPIOs at the surface of model tubes in circulatory experiments under physiologically comparable conditions was investigated. Magnetic nanoparticles could be concentrated on the surface of model grafts under optimized parameters. The development and in vitro studies of described magnetic drug targeting system presented a new perspective in the treatment of vascular graft infection. With the help of a strong external magnetic field drug-functionalized nanoparticles can be concentrated at the surface of infected grafts ensuring high drug levels to fend off biofilm embedded pathogens.

7 Functional neurotoxicity of individual antibiotics investigated with mammalian neuronal networks grown on microelectrode neuroarray

In order to elucidate the local application of antibiotics in combination with biomaterials used in brain surgery, the functional neurotoxicity of individual antibiotics applied in neurosurgery was investigated with mammalian neuronal networks grown on microelectrode neuroarrays. In chapter 7 frontal cortex tissue was harvested from time-pregnant ICR mice at embryonic day sixteen. Obtained embryos were decapitated and the frontal lobe of the extracted brains was dissected in a trapezoidal pattern. After various preparations, cells were seeded onto the recording matrix area of microelectrode neuroarrays. Cultures were ready for use usually three weeks to three months after seeding. Networks developed from a mixture of different types of postmitotic neurons and glia cells.

Penicillin G, streptomycin, penicillin/streptomycin, gentamicin and vancomycin were studied for functional neurotoxic effects. Compounds were added to mammalian frontal cortex neuronal networks cultivated on microelectrode neuroarrays. Neuronal activity was recorded and suppression of action potential production regarding dose response curves and IC_{50} levels, the determination of different burst parameter and the drop out of individual cells were investigated. A step-wise activity decrease under the influence of studied antibiotics was observed. The IC_{50} averaged between 37 μ M for streptomycin and 2371 μ M for gentamicin. The investigation of burst parameters focusing on burst frequency, burst period and spikes in bursts corroborate the different characters of used antibiotics regarding functional toxicity. The drop out of individual cells and the comparison between active neurons and bursting neurons under compound influence unsheathe a higher loss of active neurons than bursting neurons under streptomycin and vancomycin. A vice versa effect is observed under pen/strep and gentamicin while penicillin G does not influence this balance. In this study we demonstrated an approach to in vitro characterize individual antibiotics for functional neurotoxicity. The utilization of mammalian neuronal networks on microelectrode neuroarrays was therefore a good method for the investigation of compounds close to physiological conditions. New data on dose response, IC_{50} concentrations and the impact on the neuronal activity pattern could be obtained for an advanced understanding of how antibiotics influence the information transmittance in neuronal ensembles.

PROFESSIONAL EVENTS

Talks

07/2008	"Biomaterial infections", Internationale Biomechanik-und Biomaterialien Tage", Klinikum r. d. Isar, Munich, Germany
05/2008	"Infection of vascular implants - New ways of first-time intervention and on demand therapy", 8 th World Biomaterial Congress, Amsterdam, Netherlands
05/2008	"Infected vascular prosthesis - New Strategies for local anti-infectious Treatment, 34. Angiologisches Symposium, Frankfurter Arbeitskreis für Angiologie und Grenzgebiete, Kitzbühel, Austria
07/2007	"New anti-infective Coatings of Medical Implants", "Internationale Biomechanik-und Biomaterialien Tage", Klinikum r. d. Isar, Munich, Germany

Conferences

03/2008	10th International Essen Symposium on Biomaterials, Essen, Germany "Studies on the influence of electro-magnetic fields according to the Magnetodyn® procedure on Staphylococcus aureus growth and antibiotic efficacy", <i>poster presentation</i> "New ways in vascular implant infection", <i>poster presentation and brief talk</i>
11/2007	Jahrestagung der Deutschen Gesellschaft für Biomaterialien DGBM, Hannover, Germany "Studies on the influence of electro-magnetic fields according to the Magnetodyn® procedure on Staphylococcus aureus growth and antibiotic efficacy", <i>poster presentation</i> "New anti-infective graft coatings based on lipid-like formulations", <i>poster presentation</i>
11/2007	Neuroscience 2007, Society for Neuroscience, San Diego, California, USA, <i>guest visitor</i>
09/2007	3. Thüringer Grenz-und Oberflächentage, Erfurt, Germany "Comparison between different antiseptic formulations to achieve anti-infective suture coatings", <i>poster presentation</i>
08/2007	BIOSURF VII — Functional Interfaces for Directing Biological Response, Zürich, Switzerland "Haemocompatibility studies of novel anti-infective vascular grafts", <i>poster presentation</i>
07/2007	Internationale Biomechanik-und Biomaterialien Tage", Klinikum r. d. Isar, Munich, Germany "Investigation on the effect of electro-magnetic fields on the growth of Staphylococcus aureus and the increased effectiveness of gentamicin"
03/2007	German Chapter Annual Meeting, Freiburg, Germany "New Antibiotic Carriers in Surgery - Drug Delivery on PTFE Grafts", <i>poster presentation</i>

Journal Publications

- 03/2008 "New anti-infective coatings of medical implants based on lipid-like drug carriers", Vol. 52, No. 6, p. 1957-1963
Antimicrobial Agents and Chemotherapeutics,
F.D. Matl, S. Repmann, A. Obermeier, W. Friess, A. Stemberger and K.-D. Kuehn
- 02/2008 "Improvement of antibiotic efficacy by low-frequency electrical and electro-magnetic fields examining Staphylococcus aureus", Antimicrobial Agents and Chemotherapeutics, submitted
F.D. Matl, A. Obermeier, W. Friess and A. Stemberger
- 02/2008 "New Anti-infective coatings of surgical sutures", Journal of Biomaterials science, Polymer Edition, submitted
F.D. Matl, J. Zlotnyk, A. Obermeier, W. Friess and A. Stemberger
- 02/2008 "Growth inhibition of Staphylococcus aureus induced by low-frequency electrical and electro-magnetic fields", Bioelectromagnetics, submitted
A. Obermeier, **F. D. Matl**, W. Friess and A. Stemberger
- 02/2008 "Novel Antibiotic Coating for Vascular Prostheses", Journal of Materials Science: Materials in Medicine (JMSM), submitted
A. Stemberger, J. Schwabe, **F. D. Matl**, H. Büchner, S. Vogt, and K.-D. Kuehn
- 03/2007 "New Antibiotic Carriers and Coatings in Surgery", Local Antibiotics in Arthroplasty, Edited by Geert H.I.M. Walenkamp, Thieme Verlag, 2007
A. Stemberger, J. Schwabe, K. Ibrahim, **F. D. Matl**, M. Rössner, S. Vogt and K.-D. Kuehn

Florian Matl

CURRICULUM VITAE

PERSONAL DETAILS

Day of birth	11 th February 1978
Nationality	german
Address	Falkweg 49, 81243 Munich, Germany
Phone	+49 (0)89 82989735 (home) +49 (0)174 9376284 (mobile)
E-mail	florian.matl@lrz.tum.de

CAREER

08/2005-today	University Hospital, Klinikum r. d. Isar , Munich, Germany
The Universities	Technical University Munich Institute for Experimental Oncology and Institute of Medical Engineering Ludwig-Maximilians University, Munich Department of Pharmacy-Pharmaceutical Technology
The Position	PhD Student in the area of Biomaterials and Infections
Responsibility	Management of scientific projects in the interdisciplinary area of medical engineering
International	Visiting researcher for three months at the University of North Texas, Center for Network Neuroscience, Denton, Texas, USA Project: Neuronal toxicology of antibiotics
Key Achievements	<ul style="list-style-type: none">• Accomplishment of a dissertation about new strategies for vascular implant infections• Experience in the area of implants, degradable polymers, surface characterization, biocompatibility, haemocompatibility and magnetic drug targeting• Cell and bacterial culture experienced• Strong background in pharmaceutical technology, biopharmacy, pharmacokinetics and pharmacodynamics• Supervision of Master students and Bachelor students• Cooperations with Heraeus Kulzer GmbH, ITEM- the Biotooling Company, Neue Magnetodyn GmbH and different scientific groups of the Technical University Munich and the Ludwig-Maximilians University, Munich• Management of interdisciplinary projects between natural science, medicine and engineering• Several publications in international reputable journals• Performing talks and presentations at scientific conferences

08/2005 until 06/2006 **Wacker Chemie AG**, Munich, Germany

The Company International chemical company in the sector of semi-conductors, silicones and polymers

The Position **Temporary employee** in the head quarter, Department of Intellectual Property

Responsibility Supervision of the archive

Key Achievements

- Recording and archiving of contracts of nondisclosure
- Generating of claims
- Acquisition of patent literature
- Archiving of patent files
- Preliminary work for patent attorneys

11/2003 until 04/2004 **ALTANA Pharma AG**, Konstanz, Germany

The Company International pharmaceutical company meanwhile taken over by Nycomed, products in the area of respiratory disease and gastroenterology

The Position **Internship "Pharmaziepraktikant"** in the marketing division - Gastroenterology Medical Communication

Responsibility Updating of information about the competitor products in cooperation with the communication agency

Key Achievements

- Database generation of relevant competitor information
- Providing product information to subsidiaries
- Performance of literature research and literature ordering
- Actualising of the literature database
- Introduction of Reference Manager to the group
- Composing of picture material about an international scientific event in cooperation with an advertising company

PHARMACY WORK EXPERIENCES

2005 Rathaus Pharmacy, Rosenheim

2004 Zellertal-Pharmacy, Drachselsried

2003 Stern-Pharmacy, Germering

1999 Asam-Pharmacy, Munich

1999 Hospital-Pharmacy, Augsburg

HIGHER EDUCATION

Since 08/2005 **PhD Student**, University Hospital Munich

2005 **Postgraduate Certificate Degree** at the University of Otago,
Chair of Pharmaceutical Technology, New Zealand
Project: Qualitative and quantitative analysis of Leflunomide polymorphs

2004 **Approbation as licensed pharmacist**

1999-2003 Ludwig-Maximilians-University, Munich, Studies of pharmaceutical science
Second state examination: Pharmacist
First state examination

1986 until 1998 High school, Bad Koetzing

